Thermal Performance Analysis of ETFE-foil Panels and Spaces Enclosed with ETFE-foil Cushion Envelope

Submitted by

Sabrina Afrin

Doctoral Thesis

Submitted for the award of Doctor of Philosophy

of the University of Nottingham



Department of Architecture and Built Environment

University of Nottingham

Copyright © by Sabrina Afrin 2016

All rights reserved

Dedicated to my beloved Parents, my loving Husband and my beautiful Daughter …

Acknowledgement

Firstly, I would like to express my sincere gratitude to my supervisor Prof. John Chilton for his continuous and patient support throughout this research project, who also gave me the opportunity to work in this research project.

I would like to express my sincere gratitude to my supervisor Benson Lau. I am very much grateful for their support to complete this thesis. Without the encouragement of my supervisors, I would have not been able to finish my thesis.

I would like to thank Nottingham High School for allowing access to monitor the atrium. Particularly I am also grateful to Mr. Chris Scott, Estate Manager, Nottingham High School, who assisted in the installation of monitoring equipment, and facilitated access to the site as required; and the school technicians who were very supportive during the equipment installation and data collection. I also thank Architen Landrell Associates, for providing ETFE-foil samples, and Maber Architects who provided CAD drawings for the project. I am also grateful to Mr. Richard Mitchell, Energy Management Officer, Estate Office, University of Nottingham, for his support during data collection. Particularly without the help of Mr. Chris Scott and Mr. Richard Mitchell, I would not be able to collect valuable data for this research. I also like to thank all the technical staff of the Faculty of Engineering who assisted me throughout my research work.

At the end, my heartfelt appreciation to my beloved husband Shariful Shikder. The support he rendered during this process cannot be expressed in words. He was my guide throughout the study and I gained a lot of valuable knowledge from him on research. Without his enormous and continuous help and support it would be impossible for me to finish this PhD. Also I would like to mention my wonderful daughter Suzana. She occasionally seated by my side, draw pictures and waited for me when I would give her time to play or watch TV. She was born the year when I started my PhD in 2012; she and my research knowledge grew together, also within this time I did not realise when she grew bigger; she will be five-year-old soon. My special thanks to my beloved parents, my lovely sisters, nieces and all family members back home, for their encouragement to become ambitious and complete this thesis. Lastly, I would like to thank all of my friends in Loughborough and Nottingham for their presence around me and making my life beautiful.

Abstract

Ethylene-tetra-fluoro-ethylene (ETFE) is a synthetic fluoropolymer. In the form of ETFE-foil it is applied in building envelopes in a single layer or more commonly, as inflatable cushions composed of multiple layers. ETFE-foils are widely used as a lightweight building envelope where high translucency, low structural weight, and complex shape is essential. However, limited research in the field of thermal performance of ETFE-foil panels and spaces enclosed with it instigated this study. Therefore, this study investigated (I) the thermal behaviour of ETFE-foil materials and the thermal performance of spaces enclosed with ETFE cushion roofs, (II) used commercially available thermal simulation software to predict the thermal performance of spaces enclosed with ETFE cushion and glass roofs and compared this with actual monitored behaviour (III) identified strategies to improve the thermal performance of spaces enclosed with ETFE cushion roofs in current and projected climate scenarios; and finally (IV) proposed design recommendations of ETFE-foil panels/cushions as a building fabric components.

Material properties were investigated in laboratory based experiments. Further data were collected from two custom built outdoor test-rigs equipped with single-, two- and three-layer ETFE-foil panels. Environmental data were collected from two case study buildings to evaluate the thermal performance of the spaces enclosed with ETFE-foil cushion roofs. In addition, building simulation was conducted using EDSL TAS version 9.3.3.b to further analyse the indoor thermal environment and compare with monitored behaviour.

The study identified variable thermal-optical properties of ETFE foils caused by various percentages of fritted area and its pigment density. The results also identified that the thermal environment of the test-rigs was affected by the variations in the surface temperatures of ETFE-foils and the temperature of air volume between multiple ETFE-foils (in case of two and three layer panels) by convective and radiative heat transfer mechanisms. The results from the case study buildings identified that during hot summer days, indoor air temperature and temperature stratification was higher in the atrium space enclosed with three-layer ETFE-foil cushions compared to the space enclosed with two-layer ETFE-foil cushion covered with rain mesh. However, both of the spaces were overheated during the summer of 2015. To develop an accurate simulation model for ETFE cushion roofs, a novel approach of modelling was developed. The simulation model was validated and calibrated by comparing with measured data from test-rigs and case study buildings. A comparison of predicted

results of the spaces enclosed with a multi-layer ETFE-foil cushion roof and a glass roof showed that the extent of overheating was high when spaces were enclosed with glass roofs. Among two-and three-layer ETFE-foil cushion and glass roofs, two-layer ETFE-foil cushions with 75% fritting and rain mesh effectively reduced air temperature and cooling load during the peak summer period. The findings of this study will enable designers to select and develop design strategies for applying ETFE-foils in building envelopes on the basis of thermal and optical requirements. The study also suggested to change the view of current design practice that only focused on current conditions; such as the use of ETFE-foils may require more adaptive approach to mitigate overheating problems in projected climate.

Table of Contents

Abstract ..... **ii**

List of Figures ..... **xii**

List of Tables ..... **xix**

Chapter 1 ..... **1-1**

1 Introduction and Background **1-1**

1.1 Context of the research 1-1

1.2 Knowledge gap and Identification of research questions 1-3

1.3 Research aim, objectives, methods 1-5

1.4 Thesis Outline 1-5

Chapter 2 ..... **1-8**

2 Thermal behaviour of membrane envelopes and the spaces they enclose 2-8

2.1 Introduction 2-8

2.1.1 ETFE-foil 2-8

2.1.2 Colouring printing and coating in ETFE-foil 2-9

2.1.3 ETFE-foil cushion configurations 2-9

2.2 The thermal behaviour of fabric membranes 2-14

2.3 Heat transfer in membrane envelopes 2-15

2.3.1 Conduction 2-16

2.3.2 Convection 2-16

2.3.3 Radiation 2-17

2.4 The observed Thermal behaviour of space enclosed with membrane envelope 2-17

2.5 Impact of thermal behaviour of membrane envelope on thermal comfort 2-21

2.6 Indoor environment quality indicators 2-22

2.6.1 Thermal environment 2-22

2.6.2 Ventilation and air quality 2-23
2.6.3 Lighting 2-23
2.7 Thermal comfort environmental parameters 2-24
2.7.1 Temperature 2-24
2.7.2 Air movement 2-25
2.7.3 Relative humidity 2-25
2.8 Thermal environment assessment methods 2-26
2.8.1 Fanger's thermal comfort model 2-26
2.8.2 PMV-PPD model by ASHRAE 2-27
2.8.3 The concept of adaptive thermal comfort models 2-28
2.9 Comfort models 2-28
2.9.1 de Dear and Brager (1998) 2-28
2.9.2 ASHRAE Standard 55 2-29
2.9.3 BS 15251 2-29
2.10 Summary 2-30
Chapter 3 2-32
3 Methodology 3-32
3.1 Introduction 3-32
3.2 Background 3-32
3.3 The Pilot Studies 3-33
3.3.1 The purpose of the pilot studies 3-33
3.3.2 Method adopted for the pilot study 3-33
3.3.3 Equipment used for the pilot study 3-34
3.4 The results 3-36
3.5 Analysis of information acquired by the pilot study 3-37
3.6 Proposed methodology 3-38
3.6.1 Thermal performance evaluation of ETFE-foils 3-38
3.6.2 Thermal performance evaluation of ETFE-foil cushions and the spaces enclosed with an ETFE foil cushion envelope 3-39

3.7 Method to analyse thermal performance of spaces enclosed with ETFE-foil cushion roof 3-43
3.7.1 Criteria for selection of monitored buildings 3-43
3.8 Case Study A: Nottingham Boys High School, Nottingham, UK 3-44
3.8.1 Building information 3-44
3.8.2 Building usage pattern 3-45
3.8.3 Services 3-45
3.8.4 Installed monitoring equipment 3-45
3.8.5 Weather data 3-53
3.8.6 Data collection and synthesis 3-54
3.9 Case Study B: Engineering and Science Learning Centre (ESLC), Nottingham, UK 3-55
3.9.1 Building information 3-55
3.9.2 Building usage pattern 3-56
3.9.3 Services 3-56
3.9.4 Building regulation compliance 3-56
3.9.5 Post occupancy evaluation 3-57
3.9.6 Installed monitoring equipment 3-57
3.10 Thermal comfort assessment method 3-61
3.10.1 CIBSE Temperature benchmark 3-62
3.10.2 Building Bulletin 101 3-62
3.10.3 Adaptive comfort criteria to assess overheating 3-63
3.11 Building Simulation 3-66
3.11.1 Dynamic thermal simulation 3-66
3.11.2 Simulation 3-66
3.12 Summary 3-67
Chapter 4 3-69
4 Measuring thermal-optical properties of ETFE foil 4-69
4.1 Introduction 4-69

4.2 The Classification of Thermal Optical Properties 4-69
4.3 Methods used in previous studies 4-70
4.4 Justification 4-72
4.5 The thermal optical properties of ETFE foil 4-74
4.5.1 The selection of foil samples 4-74
4.5.2 Apparatus used to measure the Solar Optical Properties of the ETFE foil samples 4-78
4.5.3 Methods 4-80
4.5.4 The Results 4-81
4.6 Thermal transmittance 4-88
4.7 The thermal transmittance of ETFE foil/ cushion 4-89
4.7.1 Method 4-90
4.7.2 The Results 4-92
4.8 Summary 4-94
4.9 Limitation 4-96
Chapter 5 4-98
5 Thermal performance analysis of ETFE-foil panels 5-98
5.1 Introduction and Background 5-98
5.2 Objectives 5-101
5.3 Methodology 5-101
5.3.1 Description of the test rig 5-105
5.3.2 ETFE foil selection 5-111
5.3.3 Weather data 5-112
5.3.4 Timescale of the monitoring 5-114
5.4 Measurement of solar transmittance of ETFE-foil panels 5-116
5.5 Thermal performance analysis of ETFE-foil panels 5-122
5.5.1 Relationship between the surface temperature of ETFE-foil layers and test-rig internal condition 5-141

5.5.2 Impact of rain mesh on internal thermal condition of the experimental boxes 5-145

5.6 Summary 5-149

Chapter 6 5-151

6 Thermal performance of existing space enclosed with an ETFE- foil cushion envelope 6-151

6.1 Introduction 6-151

6.1.1 Outdoor weather 6-152

6.2 Case Study A: Nottingham High School 6-155

6.2.1 Analysis of monitored data and discussion 6-156

6.2.2 Indoor air temperature distribution 6-160

6.2.3 Overview of typical thermal behaviour of the ETFE-foil cushion roof ... 6-168

6.2.4 Effect of ETFE-foil surface temperature on thermal comfort 6-177

6.2.5 Impact of environmental variable on indoor thermal environment .. 6-178

6.2.6 Impact of atrium thermal environment to the adjacent spaces 6-179

6.3 Case Study B: Engineering and Science Learning Centre (ESLC) 6-182

6.3.1 Analysis of monitored data and discussion 6-182

6.3.2 Indoor air temperature distribution 6-185

6.3.3 Comparison of the thermal environment of the Nottingham High School and the Engineering and Science Learning Centre (ESLC) atrium 6-192

6.4 Thermal performance of atria enclosed with ETFE-foil cushion roof 6-193

6.4.1 CIBSE Temperature benchmark 6-195

6.4.2 Adaptive comfort 6-196

6.4.3 Building Bulletin 101 6-203

6.5 Comparison of the thermal behaviour of space enclosed with ETFE-foil cushion roof and fabric membrane roof 6-203

6.6 Summary 6-207

6.6.1 Summary of thermal behaviour of space enclosed with ETFE-foil cushion roof 6-207

6.6.2 Summary of thermal performance of space enclosed with ETFE-foil cushion roof 6-208
6.6.3 Challenges 6-209
6.6.4 Limitations 6-210
Chapter 7 6-211
7 Modelling thermal performance of ETFE foils and spaces enclosed with ETFE foil cushion roofs 7-211
7.1 Introduction 7-211
7.2 Calibration of the simulation model 7-212
7.3 Weather file 7-213
7.4 Properties of ETFE foil panels and glazing panels used in simulation 7-214
7.5 Simulation of test rig 7-214
7.5.1 Calibration 7-215
7.5.2 Simulation results 7-219
7.6 Simulation model of ETFE-foil cushion roofs in TAS 7-222
7.6.1 Approach adopted to model the ETFE cushion roof 7-224
7.6.2 Simulation model of Nottingham High School building and atrium ETFE-foil cushion roof 7-226
7.6.3 Simulation model of Engineering and Science Learning Centre and atrium ETFE-foil cushion roof 7-227
7.7 Zoning 7-228
7.7.1 Zone specification of Nottingham High School 7-228
7.7.2 Zone specification of Engineering and Science Learning Centre 7-231
7.8 Specifications of building fabrics in simulation models 7-232
7.8.1 Nottingham High School 7-232
7.8.2 Engineering and Science Learning Centre (ESLC) 7-233
7.9 Simulation parameters 7-234
7.9.1 Nottingham High School 7-234
7.9.2 Engineering and Science Learning Centre (ESLC) 7-238
7.10 Model Calibration 7-241

7.10.1 Calibration results for simulation mode of Nottingham High School7-242
7.10.2 Calibration results for ESLC simulation model 7-244
7.11 Strategies to improve thermal performance of space 7-247
7.11.1 Strategies applied for the Nottingham High School and ESLC simulation model 7-247
7.11.2 Results of implication of simulation criteria 7-251
7.12 Comparison with glass roof 7-257
7.12.1 Comparison of thermal performance of ETFE foil cushion and glass ... 7-257
7.12.2 Comparison of energy consumption of ETFE foil cushions, polycarbonate and glass 7-258
7.13 Future weather data 7-260
7.13.1 The result 7-260
7.14 Summary 7-261
Chapter 8 7-264
8 Discussion and Conclusions 8-264
8.1 Introduction 8-264
8.2 Summary of findings 8-264
8.2.1 Investigation of thermal-optical properties 8-264
8.2.2 Summary of findings from test-rig experiment 8-269
8.2.3 Summary of findings from on-site monitoring of actual buildings ... 8-270
8.2.4 Summary of findings from modelling and simulation 8-274
8.3 Evaluation of methodology 8-276
8.4 Recommendations 8-278
8.5 Conclusions and fulfillment of aim and objectives 8-281
8.5.1 Objective one 8-281
8.5.2 Objective two 8-282
8.5.3 Objective three 8-282
8.5.4 Objective four 8-283

8.5.5 Objective five 8-283
8.5.6 Objective six 8-284
8.5.7 Objective seven 8-285
8.6 Novelty and contribution to the knowledge 8-285
8.7 Limitations of the study 8-287
8.8 Future research 8-287
References 289
APPENDIX A: List of Publications 297
APPENDIX B: Figures and Tables 299

List of Figures

Figure 2-1: Construction types of ETFE-foil cushions (Schiemann and Moritz, 2010)2-11

Figure 2-2: Movable middle layer in ETFE-foil cushion 2-11

Figure 2-3: Moveable central layer with intelligent printing, (a) open, (b) closed (Knippers et al., 2011) 2-11

Figure 2-4: (a) Pattern open, (b) Pattern superimposed (LeCuyer, 2008) 2-12

Figure 2-5: Festo Technology centre atrium (LeCuyer, 2008) 2-12

Figure 2-6: Kingsdale School atrium (a) exterior view (top), interior view (bottom); (b) printed top layers (top), view of cushions (bottom) (LeCuyer, 2008) 2-13

Figure 2-7: Kingsdale School atrium solar gain controlled by (a) opening ETFE-foil cushion at clerestory level, (c) closing top two layers of cushion (LeCuyer, 2008) 2-13

Figure 2-8: Building physics aspects for polymer foil enclosure [reproduced from Knippers et al. (2011)] 2-22

Figure 3-1: Location of the data logger and the solar radiation sensor (top), location of the cushion where internal surface temperature was measured using thermal camera (bottom)- Pilot study [Plans (nts): Maber Architects] 3-35

Figure 3-2: Location of sensors in the School atrium [Section (nts): Maber Architects] 3-36

Figure 3-3: Data obtained from Pilot study during 22nd August 2013 (location- Nottingham High School atrium) 3-37

Figure 3-4: ETFE foil surface temperature measured in the middle (left) and at the edge (right) of the cushion at 14:11pm, 22nd August 2013 using thermal imaging (for location of cushion- see Figure 3-1) 3-37

Figure 3-5: Flow diagram of methodologies and associated objectives 3-41

Figure 3-6: Experimental and environmental data analysis, and modelling/ simulation process 3-42

Figure 3-7:(a) Location of High school [Source: Google map], (b) roof of atrium [photo: Sabrina Afrin], (c) atrium [photo: Sabrina Afrin] 3-45

Figure 3-8: Location of the data logger (a,b,c) and temperature sensors in (a) Ground floor, (b) First floor, (c) Second floor, (d) Level 4, Plan (nts)- drawing courtesy of Maber Architects, Photo -Sabrina Afrin 3-49

Figure 3-9: (a) Air temperature and mean radiant temperature sensors, (b) Thermometer (PCE-WB 20SD) 3-50

Figure 3-10: Plan (nts) showing ETFE-foil cushion roof and location of the monitored cushion, outlined in orange, surface temperature (both external and internal sensors

location pointed in red (Drawing courtesy of Maber Architects, Nottingham), Photo - Sabrina Afrin..... 3-51

Figure 3-11: Location of -(a) internal surface temperature sensors attached to cushion 1 & 2, solar radiation sensors placed on the internal roof, (b) external surface temperature sensors (cushion 1), solar radiation sensors adjacent to ETFE-foil cushion roof. Plan (nts)- drawing courtesy of Maber Architects, Photo -Sabrina Afrin..... 3-52

Figure 3-12: Weather station location on Nottingham High School roof..... 3-53

Figure 3-13: Data collection and synthesis..... 3-54

Figure 3-14: (a) Engineering and Science Learning Centre, University of Nottingham, (b) The atrium, (c) ETFE-foil cushion roof of ELSC [Photo- Sabrina Afrin]..... 3-55

Figure 3-15: (a) Installation of data logger and sensors on the lift roof, (b) location of data logger..... 3-58

Figure 3-16: Air temperature and mean radiant temperature sensors at different occupied levels of the atrium (Location a)..... 3-59

Figure 3-17: Air temperature sensors at different levels of the atrium (Location b) 3-60

Figure 3-18: Location of the external and internal solar radiation sensors with respect to ETFE-foil cushion roof..... 3-61

Figure 4-1: Electromagnetic wave spectrum [for radiation travelling through vacuum, refractive index ‘n=1’] (Incropera et al., 2013)..... 4-70

Figure 4-2: Angular transmittance of 100 μm ETFE sheet at various detector and sample angles (Robinson-Gayle, 2003)..... 4-71

Figure 4-3: Measurement of thermal optical properties using spectrometers- (a) IFS 66v/s, (b) Biochrom Libra S22..... 4-79

Figure 4-4: Spectral transmittance of ETFE foil and Glass measured using spectrometers..... 4-82

Figure 4-5: Solar Transmittance and Light Transmittance of transparent single layer ETFE foils of different thickness (ETFE-foil types are listed in Table 4-1)..... 4-83

Figure 4-6: Solar Transmittance of single layer fritted ETFE foil panel..... 4-84

Figure 4-7: Light Transmittance of single layer fritted ETFE foil panel..... 4-85

Figure 4-8: Solar Transmittance of two-layer ETFE foil panel..... 4-86

Figure 4-9: Light Transmittance of two-layer ETFE foil panel..... 4-86

Figure 4-10: Solar Transmittance of three-layer ETFE foil panel..... 4-87

Figure 4-11: Light Transmittance of three-layer ETFE foil panel..... 4-87

Figure 4-12: Comparison of measured thermal optical properties and the same values obtained from DETR (2003) for the Type 1 (100μm), Type 2 (150μm) and Type 3 (200μm) ETFE foil..... 4-88

Figure 4-13: Variation in U-value in a single cushion 4-92

Figure 4-14: Variation of thermal transmittance (U-value) in a single cushion with variation of air gap 4-93

Figure 4-15: Variation of U-value of Two layer ETFE foil cushion with variation in air gap and emissivity of internal surface 4-93

Figure 5-1: Temperature gradient recorded on ETFE-foil cushion roof and rain mesh using thermal image device. 5-99

Figure 5-2: Diagrammatic sectional drawings and position of pyranometer in test-rigs during phase 1 5-106

Figure 5-3: Diagrammatic sectional drawings and position of pyranometer in test-rigs during phase 2 5-107

Figure 5-4: (a) Pyranometer measuring incident total solar radiation, (b) DT85 Datalogger attached with temperature and radiation sensors and located inside equipment box 5-109

Figure 5-5: (a) Temperature sensors measuring mean radiant temperature and, air temperature, and solar radiation sensor measuring transmitted solar radiation, located just below ETFE-foil panel (b) Temperature sensors measuring internal surface temperature 5-109

Figure 5-6: Temperature sensors measuring external surface temperature and mesh surface temperature 5-109

Figure 5-7: Diagrammatic section of test-rigs (a) with single layer ETFE-foil panel, (b) with two-layer ETFE-foil panel and, (c) with three- layer ETFE panel during the Second phase experiment 5-111

Figure 5-8: (a) 200 μm transparent with 75% fritting, (b) 200 μm transparent with 25% fritting 5-112

Figure 5-9: (a) Temperature sensor measuring external ambient temperature and humidity, (b) steel frame around the sensor, (c) pyranometer measuring total horizontal solar radiation 5-113

Figure 5-10: Phase 1 test-rig experiment 5-117

Figure 5-11: Incident and Transmitted Solar Radiation comparison (Single layer panel with 75% fritted ETFE-foil) 5-119

Figure 5-12: Incident and Transmitted Solar Radiation comparison (Two-layer panel with 75% fritted top ETFE-foil) 5-119

Figure 5-13: Incident and Transmitted Solar Radiation comparison (Thee-layer panel with 75% fritted top ETFE-foil) 5-120

Figure 5-14: Incident and Transmitted Solar Radiation comparison (Single layer panel with 25% fritted top ETFE-foil) 5-120

Figure 5-15: Incident and Transmitted Solar Radiation comparison (Two-layer panel with 25% fritted top ETFE-foil) 5-121

Figure 5-16: Incident and Transmitted Solar Radiation comparison (Three-layer panel with 25% fritted top ETFE-foil) 5-121

Figure 5-17: Second phase test-rig investigation (without mesh) 5-122

Figure 5-18: Second phase test-rig investigation (with and without mesh) 5-123

Figure 5-19: Comparison of Test-rig 1 and Test-rig 2 air temperature, air volume air temperature and surface temperature recorded during 9th Sep 15 5-124

Figure 5-20: Comparison of Test-rig 1 and Test-rig 2 air temperature, air volume air temperature and surface temperature recorded during 19th Sep 15 5-124

Figure 5-21: Comparison of Test-rig 1 and Test-rig 2 air temperature, air volume air temperature and surface temperature recorded during 26th Sep 15 5-125

Figure 5-22: Relative condition of experimental Test-rig 1 and Test-rig 2 5-126

Figure 5-23: Relative internal condition of Test-rig 1 and Test-rig 2 5-127

Figure 5-24: Relative condition of Test-rig 1 and Test-rig 2..... 5-128

Figure 5-25: Test-rig 1 (two-layer 75% fritted top layer) and Test-rig 2 (three-layer 25% fritted top layer) internal air temperatures, air-volume air temperatures, relative to outdoor ambient temperatures..... 5-134

Figure 5-26: Test-rig 1 (two-layer 75% fritted top layer) and Test-rig 2 (three-layer 25% fritted top layer) ETFE-foil panel surface temperatures relative to outdoor ambient temperature..... 5-135

Figure 5-27: Test-rig 1 (three-layer 75% fritted top layer) and Test-rig 2 (three-layer 25% fritted top layer) internal air temperatures, air-volume air temperatures, relative to outdoor ambient temperatures..... 5-136

Figure 5-28: Test-rig 1 (three-layer 75% fritted top layer) and Test-rig 2 (three-layer 25% fritted top layer) ETFE-foil surface temperatures relative to outdoor ambient temperatures 5-137

Figure 5-29: Test-rig 1 (single layer 75% fritted) and Test-rig 2 (single layer 25% fritted) internal air temperatures, air-volume air temperatures, and ETFE-foil surface temperatures relative to outdoor ambient temperatures..... 5-138

Figure 5-30: Convective heat transfer between ETFE surface and air temperature adjacent to it in Test-rig 1 and Test-rig 2..... 5-144

Figure 5-31: Radiative heat transfer through ETFE-foil surface in Test-rig 1 and Test-rig 2 5-144

Figure 5-32: Relative condition of surface temperature, air volume air temperature and air temperature of Test-rig 1 and Test-rig 2 5-147

Figure 5-33: Comparison of Test-rig 1 and Test-rig 2 condition 13th Sep 15 5-148

Figure 6-1: OAT, daily mean temperature and ExIR recorded during summer 2014 . 6-153

Figure 6-2: OAT, daily mean temperature, and ExIR recorded during summer 2015 6-154

Figure 6-3: Outdoor air temperature recorded adjacent to Nottingham High School and ESLC 6-155

Figure 6-4: Indoor air temperatures and solar radiation recorded in Nottingham High School atrium between 29th June and 3rd July 2015 – clear sky conditions 6-158

Figure 6-5: Indoor air temperatures and solar radiation recorded in Nottingham High School atrium during 14th September 2015 – overcast sky conditions 6-159

Figure 6-6: Temperature differences between air temperatures of different atrium levels of Nottingham High School and outdoor air temperatures between 29th June and 3rd July 2015 6-162

Figure 6-7: Temperature differences between air temperatures of different atrium levels of Nottingham High School and outdoor air temperatures during 14th September 2015 6-163

Figure 6-8: Temperature difference between Nottingham High School atrium level 1, 2, 3 and 4, between 29th June and 3rd July 2015 6-166

Figure 6-9: Temperature difference between Nottingham High School atrium level 1, 2, 3 and 4 during 14th September 15 6-167

Figure 6-10: Internal and external cushion surface temperatures, occupied level 3 air temperatures, level 4 air and mean-radiant temperatures, incident and transmitted solar radiation, and outdoor air temperature recorded between 29th June and 3rd July 2015 6-169

Figure 6-11: Temperature difference between external surface temperature (ST Loc1)– internal surface temperature (ST Loc 4) [middle of the cushion]; internal surface temperature [ST Loc 4 (middle of the cushion)]- internal surface temperature [ST Loc 5 (edge of the cushion)]; external surface temperature (ST Loc 2) – internal surface temperature [ST Loc 5 (edge of the cushion)] 6-171

Figure 6-12: Temperature difference between external surface temperature (ST Loc 1) -outdoor air temperature; internal surface (ST Loc 4)- outdoor air temperature, internal surface temperature (ST Loc 4)- level 4 (adjacent to ETFE-foil cushion air temperature); internal surface temperature (ST Loc 4)- level 3 (second floor) between 29th June and 3rd July 6-174

Figure 6-13: Temperature difference between external surface temperature (ST Loc 1)-outdoor air temperature; internal surface (ST Loc 4)- outdoor air temperature, internal surface temperature (ST Loc 4)- level 4 (adjacent to ETFE-foil cushion air temperature); internal surface temperature (ST Loc 4)- level 3 (second floor) during 14th September 2015 6-175

Figure 6-14: Relationship between internal surface temperature (STLoc4_NH), air temperature [Tsi 4(a)_NH] and mean radiant temperature [MRTsi 4(a)_NH] 6-177

Figure 6-15: Location of temperature sensors in level 3 (second floor) [Plan (nts): drawing courtesy Maber architect] 6-180

Figure 6-16: Air temperatures of different vertical and horizontal positions in the atrium and space adjacent to atrium during 29th August and 30th August..... 6-181

Figure 6-17: Impact of atrium level 3 (Tsi (a)_NH) air temperature on internal space adjacent to it 6-181

Figure 6-18: Indoor air temperatures and solar radiation recorded in the ESLC atrium between 29th June and 3rd July 2015 – clear sky conditions..... 6-183

Figure 6-19: Indoor air temperatures and solar radiation recorded in the ESLC atrium between 14th September 15 – overcast sky 6-184

Figure 6-20: Temperature difference between ESLC atrium level 1, 2, 3 and 4, between 29th June and 3rd July 2015..... 6-186

Figure 6-21: Temperature difference between ESLC atrium level 1, 2, 3 and 4, during 14th September 2015 6-187

Figure 6-22: Temperature differences between air temperatures of atrium levels of ESLC and outdoor air temperatures between 29th June and 3rd July 2015 6-188

Figure 6-23: Temperature differences between air temperatures of atrium levels of ESLC and outdoor air temperatures during 14th September 2015 6-189

Figure 6-24: Internal surface temperatures variations of ETFE-foil cushion roof of Nottingham High School (fixed sensor) and ESLC (thermal imaging) atria (7th August 2014) 6-191

Figure 6-25: Temperature difference between occupied level 1, 2 and 3 of ESLC and Nottingham High School atrium between 29th June and 3rd July 2015..... 6-192

Figure 6-26: Percentage of occupied hours when Nottingham High School and ESLC atrium level 1, 2 and 3 were above 25°C, 26°C, 28°C, 30°C and 32°C 6-193

Figure 6-27: Air temperature of level 3 (second floor) of Nottingham High School atrium, CIBSE temperature benchmark, maximum and minimum acceptable temperature range for category II building, BB101 Criteria 1 & 3 temperature benchmark 6-198

Figure 6-28: Air temperature of level 3 (second floor) of ESLC atrium, CIBSE temperature benchmark, maximum and minimum acceptable temperature range for category II building 6-199

Figure 6-29: Air temperature of level 2 (first floor) of Nottingham High School atrium, CIBSE temperature benchmark, maximum and minimum acceptable temperature range for category II building 6-200

Figure 6-30: Air temperature of occupied level 2 (first floor) of ESLC atrium, CIBSE temperature benchmark, maximum and minimum acceptable temperature range for category II building 6-201

Figure 6-31: Atrium level 3 without (before) and wih (after) air conditioning system .. 6-209

Figure 7-1: Results obtained from model calibration of single layer ETFE panel roof with 75% fritted ETFE foil panel 7-216

Figure 7-2: Linear relationship between predicted (model 5) and measured data 7-217

Figure 7-3: Temperature differences between simulation model enclosed with glass roof and two-layer ETFE foil panel with 75% fritted top layer 7-220

Figure 7-4: Temperature differences between simulation model enclosed with glass roof and three-layer ETFE foil panel with 75% fritted top layer 7-221

Figure 7-5: ETFE cushion roof structure (two-way curve) of Nottingham High School (top), Engineering and Science Learning Centre (Bottom) 7-223

Figure 7-6: Representation of ETFE cushion roof in studied models (i) Roof model 1, (ii) Roof model 2, (iii) Roof model 3, (iv) Roof model 4 7-225

Figure 7-7: Simulation model of ETFE-foil cushion roof of Nottingham High School atrium 7-227

Figure 7-8: Simulation model of ETFE foil cushion roof of Engineering and Science Learning Centre atrium 7-228

Figure 7-9: Zoning of (a) Ground floor, (b) First floor, (c) Second floor of simulation model (Nottingham High School) 7-230

Figure 7-10: Zoning of (a) Ground floor, (b) First floor, (c) second floor of Engineering and Science Learning Centre 7-232

Figure 7-11: Base Case 1 air temperature relative to Base-Case 0 7-242

Figure 7-12: Simulated air temperatures of the second floor of the atrium with various window opening percentage and comparison with measured data 7-243

Figure 7-13: Base model 1 and Base model 2 air temperature relative to measured data 7-244

Figure 7-14: Base model 1 air temperature relative to Base model 0 7-245

Figure 7-15: Simulated air temperatures of the second floor of the atrium with various window opening percentage and comparison with measured data 7-245

Figure 7-16: Base model 1 and Base model 2 air temperature relative to measured data 7-246

Figure 7-17: Temperature differences between case 24, 25, 26 and Predicted model air temperatures during occupied hours (Nottingham High School) 7-252

Figure 7-18: Air temperatures of Predicted, Case 24, Case 25, Case 26 model; maximum, minimum and comfort temperature (Nottingham High School) 7-252

Figure 7-19: Temperature differences between case 24, 25, and 26 and predicted air temperatures during occupied hours (ESLC) 7-254

Figure 7-20: Air temperatures of Predicted, Case 24, Case 25, Case 26 model maximum, minimum and comfort temperature (ESLC) 7-254

Figure 7-21: Cooling load in Predicted model of Nottingham High School, roofed with two layer ETFE cushion and Glass type 1, 2, 3 7-259

Figure 7-22: Cooling load in Predicted model of ESLC, roofed with three layer ETFE cushion and Glass type 1, 2, 3 7-260

Figure 8-2: Design and evaluation stages for building performance analysis 8-280

List of Tables

Table 2-1: Summary of results obtained from previous studies on thermal behaviour of space enclosed with membrane envelope 2-19

Table 2.2: Surface temperatures necessary to avoid condensation assuming internal air temperature of 20 °C and different RH (CIBSE, 2006) 2-26

Table 2-3: ASHRAE thermal sensation scale (ASHRAE 2013) 2-27

Table 3-1: Sensors identification and location -Pilot Study 3-34

Table 3-2: Research objectives and associated methodologies 3-40

Table 3-3: Summary of salient features of monitored ETFE-foil cushion enclosures. 3-44

Table 3-4: Location of air temperature sensors 3-46

Table 3-5: Location of surface temperature sensors 3-47

Table 3-6: U-value of the building fabric (Estate, University of Nottingham) 3-57

Table 3-7: Location of temperature sensors 3-58

Table 3-8: Suggested applicability of the categories and their associated acceptable temperature range for free running buildings (Standards, 2008) 3-65

Table 4-1: List of ETFE foil samples used to measure solar transmittance and Light transmittance 4-75

Table 4-2: List of combination of Two layer ETFE foils 4-76

Table 4-3: List of combination of Three layer ETFE foils 4-77

Table 4-4: Direct solar and light transmittance of ETFE foil and glass 4-82

Table 4-5: Total solar energy transmittance (g-value) of single layer ETFE foil 4-83

Table 4-6: U-value of ETFE foil cushion 4-89

Table 4-7: Gas conductance in variable air gap 4-92

Table 5-1: Description of measurement sensors 5-108

Table 5-2: List of parameters measured on the test-rigs (First phase) 5-108

Table 5-3: List of parameters measured on the test-rigs (Second phase) 5-108

Table 5-4: Description of measurement sensors 5-113

Table 5-5: Measured environmental parameters and identifications 5-113

Table 5-6: Different combinations of ETFE-foil in Test-rig 1 (First phase) 5-115

Table 5-7: Different combination of ETFE-foil in Test-rig 1 and Test-rig 2 (Phase 2). 5-116

Table 5-8: Comparison of measured and calculated transmittance of ETFE-foil panel with that of test-rig experiment 5-118

Table 5-9:Average transmitted solar radiation recorded during daylight hours 5-130

Table 5-10:Temperature differences between Test-rig 1 and Test-rig 2 air temperatures and air-volume air temperatures 5-131

Table 6-1: Identification of environmental parameters 6-156

Table 6-2: correlation between air temperature at different occupied level and incident, transmitted solar radiation and outdoor ambient temperature 1st July 15 6-179

Table 6-3: Summary of occupied periods in summer 2014, 2015 6-194

Table 6-4: Criteria for assessing internal temperature in naturally ventilated atrium space 6-194

Table 6-5: Total occupied hours above 28°C for summer 2014 and 2015..... 6-196

Table 6-6: TM52 Overheating assessment of the Nottingham High School and the ESLC atria 6-202

Table 6-7: BB101 Overheating assessment of the Nottingham High School atrium .. 6-203

Table 6-8: Summary of results obtained for research on thermal behaviour of space enclosed with membrane envelope 6-205

Table 7-1: Weather file parameters used in simulation 7-213

Table 7-2: Glazing types used in the Predicted model (EDLS TAS Version 9.3.3.b) . 7-214

Table 7-3: Construction of simulation model 7-215

Table 7-4: Thermal Properties of ETFE foil used in simulation model 7-215

Table 7-5: Input parameters in simulation 7-215

Table 7-6: Pearson Correlation of measured and predicted result with variable infiltration rate 7-216

Table 7-7: Input parameters in simulation 7-218

Table 7-8: Properties of ETFE-foil panels (single layer) and glazed panels 7-218

Table 7-9: Properties of ETFE-foil (two-layer) panels and glazed panels 7-219

Table 7-10: Properties of ETFE foil panels (three-layer) 7-219

Table 7-11: Selection of model 7-226

Table 7-12: Properties of ETFE foil cushion 7-233

Table 7-13: U-value of building fabrics 7-233

Table 7-14: Properties of ETFE foil 7-233

Table 7-15: U-value of building fabrics 7-234

Table 7-16: NCM Activities_v5.2.4 (Part L 2010) followed (EDLS TAS Version 9.3.3.b) 7-236

Table 7-17: Window opening details, function used in analysis model and TAS building simulator 7-236

Table 7-18: Occupancy, lighting and equipment schedule 7-237

Table 7-19: NCM Activities_v5.2.4 (Part L 2010) followed (EDLS TAS Version 9.3.3.b) 7-239

Table 7-20: Window opening details, function used in analysis model and TAS building simulator 7-239

Table 7-21: Occupancy, lighting and equipment schedule 7-240

Table 7-22: Model description and parameter 7-241

Table 7-23: Thermal optical properties of the external layer of ETFE foil cushion 7-248

Table 7-24: Thermal optical properties of external and internal layer of ETFE foil cushion 7-249

Table 7-25: Emissivity of ETFE foil 7-250

Table 7-26: Window opening and associated air temperature of atrium second floor, Nottingham High School 7-250

Table 7-27: Window opening and associated air temperature of atrium second floor, Engineering and Science Learning Centre 7-251

Table 7-28: Period selected for simulation in summer 2015 7-251

Table 7-29: Results and remarks on simulation criteria 7-255

Table 7-30: Percentage of Hours air temperature of Predicted simulation models enclosed with ETFE cushion roof and different type of glazing above T_{max} during Peak period 7-257

Table 7-31: Percentage of Hours air temperature of Predicted simulation models enclosed with ETFE cushion roof and different type of glazing above T_{max} during Peak period 7-258

Table 7-32: Projected Scenario of the predicted model of the Nottingham High School and ESLC 7-261

Table 8-1: List of properties, and combination of single, two and three-layer ETFE-foils 8-266

Table 8-2: Thermal optical properties of single, two- and three-layer ETFE-foils 8-268

Table 8-3: Summary of air temperature (°C) at different levels of the atria on 1st July 2015 8-271

Table 8-4: Comparison of extreme temperature differences (thermal stratification) between different levels in the monitored atria (1st July 2015) 8-272

Table 8-5: Comparison of temperature difference (°C) between individual atrium levels and outdoor air temperature 8-272

Chapter 1

1 Introduction and Background

1.1 Context of the research

In recent decades, scientific evidence of climate change and environmental impact of greenhouse gas emissions have made it essential to reduce energy use in buildings, as buildings account for a significant amount of energy consumption globally (Pérez-Lombard et al., 2008, Harvie, 2015, Knippers et al., 2011). As a consequence, growing concern and interest in building performance is evident in the building design domain. Emphasis is given to improving environmental performance to compensate the overall energy consumption and it is also expected that new buildings will have minimum impact on the environment.

Building envelope plays an important role to moderate the impact of the external environment. This comprises the outer elements of a building and consists of walls, roof, windows, doors, etc. The major function of a building envelope is to create a comfortable environment for the occupants by ensuring thermal and solar control, indoor air quality, sufficient daylight, fire resistance, acoustic control, and creating the visible links between indoor and outdoor environment.

Materials like brick, wood, concrete, glass, stone etc. are conventional materials used to construct building envelopes. Other than these conventional materials, flexible fabrics or foil materials known as membranes are also used to construct building envelopes. In contrast to conventional materials, membranes are extremely light weight. Different types of fibrous materials and polymers are used as membranes. They can be transparent or opaque. Membrane materials for building application include – PVC (polyvinyl chloride) coated polyester woven fabric, PTFE (polytetrafluoroethylene) coated glass fibre woven fabric, fluorine polymer coated glass fibre woven fabric, polyester blend woven fabric, PVC foil, ETFE (Ethylene tetrafluoroethylene) foil, THV (a polymer of tetrafluoroethylene, hexafluoropropylene and vinylidene fluoride) foil etc. (Milwich, 2010).

Among different polymers suitable for building integration, ETFE (ethylene-tetra-flouro-ethylene) is a synthetic fluoropolymer, that has been used commercially since the 1970s. The first large-scale use of extruded ETFE-foil in inflated cushions was for the roof of the Mangrove Hall at Burgers' Zoo, in Arnhem, The Netherlands, constructed

in 1982 (LeCuyer, 2008). Since then there have been developments of its material properties, technology, and installation systems. These have increased ETFE-foil's use in architectural applications (Chilton, 2013), such that the material is now widely used as a lightweight building envelope where high translucency, low structural weight, and complex shape is essential. ETFE-foil (typically 100μm to 300μm in thickness) is typically applied in building envelopes in the form of inflatable cushions and can consist of single and multiple layers of ETFE-foils.

Evidence showed that the application of ETFE-foil in building envelopes is increasing in frequency. Moritz (2007), conducted an extensive survey on the application of ETFE-foil and documented 200 projects constructed with ETFE-foil cushions in different countries. From the outcomes, it can be stated that building integration of ETFE-foils is increasing throughout the world and widely applied in Germany (59%) and Great Britain (18.9%). This is also evident in the study of Gómez-González et al. (2011). Moreover, application of ETFE-foil cushions in building envelopes of impressive large-scale projects, for example the Eden Project in Cornwall (built in 2000), the Allianz Arena in Munich (built in 2005), Olympic stadium and swimming pool in Beijing (built for Beijing Olympics 2008), moved this material and its construction method into the focus of architectural and engineering interest.

ETFE-foil differs fundamentally from coated fabric membranes in terms of thermal as well as building physics behaviour. The thermal optical characteristics of ETFE-foils are significantly advantageous over other fabric membranes because of its transparency (Knippers et al., 2011, Schiemann and Moritz, 2010). ETFE-foils are virtually transparent to short-wave (solar radiation) and long wave radiation (Poirazis et al., 2009). This transmittance depends on the membrane construction properties such as number of foil layers, thickness, colour or fritting of the foils. It transmits about 90% of daylight in the visible light spectrum. For that reason, ETFE-foils are in direct competition with other materials such as glass, fibre reinforced plastics or textile membranes. The major difference between ETFE-foil and glass is that in ETFE-foil envelopes spectral distribution of the visible light spectrum is almost constant with hardly any refraction so the intensity and quality of colours retained inside the building but for glass this intensity and quality of colour altered by refraction (Moritz, 2007, Schiemann and Moritz, 2010). Another significant difference between ETFE-foil and glass or polycarbonates is the high transmission of the ultraviolet spectrum (Moritz, 2007, Schiemann and Moritz, 2010). Different thermoplastics used for building envelopes other than ETFE-foil e.g. polyethylmethacrylate, polystyrene, polytetrafluoroethylene (PTFE), polyethylene (PE) were examined by Callister (2011)

and Minamisawa et al. (2007), as an alternative to glass. But the results found to be unsuitable as a replacement material. The reason stated is that their visual performance, material and energy performance are not similar to glass (Baille et al., 2006, Callister, 2011)

The purpose of the advancement of ETFE-foil in the building industry was to reduce material costs at the same time confirming benefits in terms of comfort, aesthetics, and safety. Integration of this reduces embodied energy by reducing supporting structures in comparison to glass (Monticelli et al., 2009, EPD, 2014, Chilton et al., 2013a). Moreover, as a transparent foil material ETFE-foil allows flexibility in building geometry, reduce fragility and weight of the building components while providing sufficient access to light and heat (Robinson-Gayle et al., 2001, DETR, 2003). Thus, ETFE-foil cushions are now widely used as an alternative to glass when building complex structures.

1.2 Knowledge gap and Identification of research questions

Review of the existing body of knowledge on ETFE-foil used in cushions showed that aspects of their application, fabrication, and structural modification have been investigated substantially (LeCuyer, 2008, Knippers et al., 2011, Chilton, 2013, Harvie, 2015, Robinson-Gayle et al., 2001, Wu et al., 2011, Cremers, 2010) . Robinson-Gayle (2003), DETR (2003), Knippers et al. (2011), Mainini et al. (2014) stated thermal-optical properties of ETFE-foil (e.g. transparent and white foil of different thickness). However, they did not specify optical properties of fritted ETFE-foils of different coverage. These types of fritted foils are now applied widely to control solar gain into the enclosed space. Antretter et al. (2008), carried out a test-cell investigation and CFD simulation (transient and steady state) to examine heat transfer through airflow inside the ETFE-foil cushion. In a different test-cell investigation Dimitriadou (2015), determined and compared the energy consumption of glass and ETFE-foil panels. Using a hot-box, Max et al. (2012), investigated a novel greenhouse glazing system composed of glazed unit and ETFE-foil. While Mainini et al. (2014) measured thermal transmittance of vertical ETFE-foil panel using a test-rig experiment in an environmental chamber. But no study measured and compared the thermal condition of an enclosure covered with single, two and three layers ETFE-foil panel. Toyoda and Takahashi (2013), Schöne (2007) investigated a solution for rain noise control of ETFE-foil cushion using silicone-gel layers and non-woven fabric (mesh). Although Desmarais et al. (1999) indicated that mesh with smaller holes decreases solar radiation, its actual impact on internal air temperature was not investigated. Poirazis et al. (2009), carried out a study on energy transmission properties of ETFE-foil to

determine thermal and optical performance on the basis of a mathematical model. He pointed towards the limitations of dynamic simulation software in that available software in current use does not provide material templates for ETFE-foil unlike for other glazing materials. Turrin et al. (2010), developed a parametric model to identify the structural behaviour of a large roof and its effect on thermal comfort and daylighting of the space underneath. In a different study Turrin et al. (2012), investigated performance oriented design of a large roof structure for semi-outdoor space. Dimitriadou (2015), performed simulations to predict thermal conditions and energy consumption of an ETFE-foil cushion enclosure.

It is evident that the above studies neither focused on the actual thermal performance of the space enclosed with an ETFE-foil cushion envelope nor compared this thermal performance with predicted behaviour. Moreover, the impact of ETFE-foil cushion envelope on the internal thermal environment of a building remained unexplored yet. The increasing frequency of building integration of ETFE-foil cushions in more complex and permanent enclosures has made it necessary to identify the relevant thermal properties of the material.

A transparent/ translucent ETFE-foil cushion envelope can be considered as a passive environmental filter that moderates the outdoor environment e.g. outdoor air temperature, solar radiation, glare etc. But on a hot day, continuous transmittance of solar radiation through ransparent/ translucent ETFE-foil can result in overheating. Furthermore, the double curved geometry of this envelope, its thermal-optical properties etc., make it different from conventional envelope systems. Additionally, existing standards available for conventional materials and construction systems cannot be applied directly for ETFE-foil cushions (Antretter et al., 2008). So thermal performance analysis of ETFE-foil cushion building envelopes is essential to prove its construction complies with the user requirements.

Considering these gaps in existing knowledge, the following key research questions emerged and were established as the focus of this research.

- What are the current barriers to the accurate prediction of the thermal performance of ETFE-foil panels and spaces enclosed with ETFE-foil cushion envelopes?
- What approach is necessary to predict the thermal performance of ETFE-foil panels and spaces enclosed with ETFE-foil cushion envelopes?

- How thermal performance of ETFE cushions affect the thermal performance of spaces enclosed by ETFE-foil cushion envelope?
- What is the overall implication of this research for the future development of the area?

1.3 Research aim, objectives, methods

The overall aim of the research is to evaluate the thermal performance of ETFE-foil panels and spaces enclosed with ETFE-foil cushion envelopes.

Objectives of the research:

Objective 1: Develop knowledge base on properties of ETFE-foils and ETFE-foil cushion construction; identify the thermal behaviour of fabric membranes and spaces enclosed with fabric membrane envelope (method: literature review).

Objective 2: Determine thermal-optical properties of ETFE-foils (methods: Lab experiment, British Standard).

Objective 3: Evaluate the thermal performance of single, two and three layers ETFE-foil panels (methods: Test cell monitoring).

Objective 4: Evaluate the thermal performance of occupied spaces enclosed with ETFE-foil cushion envelope (method: Monitoring existing building).

Objective 5: Evaluate and compare the thermal performance of spaces enclosed with ETFE-foil cushion and glass roofs (method: computer simulation).

Objective 6: Identify strategies to improve the thermal performance (overheating) of spaces enclosed with ETFE-foil cushion in current and projected climate scenarios (method: Data analysis and computer simulation)

Objective 7: Identify implications of the research for designers and develop design recommendations of ETFE-foil panels and spaces enclosed with ETFE-foil cushion envelope (Result analysis).

1.4 Thesis Outline

This thesis consisted of eight chapters. The structure of the thesis and contents of each chapter are discussed in this section.

Chapter 1: This chapter presents a synopsis of the thesis. At the beginning, it discusses the context of the research, identifies knowledge gaps and states research aim and objectives. Lastly, the chapter provides an outline to the rest of the thesis.

Chapter 2: This chapter presents a review of the properties of ETFE-foil and configurations of ETFE-foil in cushion construction used to enhance the thermal performance of the space it encloses; and thermal behaviour of fabric membrane and spaces enclosed with fabric membrane envelope. It also describes the impact of this thermal behaviour on the thermal comfort of occupants and identifies thermal comfort assessment methods to evaluate indoor thermal performance.

Chapter 3: This chapter provides an overview of the research methodologies used to achieve the research aim and objectives. The criteria to identify the research methods were initially gathered by reviewing relevant research articles, books, guides, standards, etc. Subsequently, the chapter prescribed detailed methods adopted to conduct the empirical research. The chapter includes detailed descriptions of the case study buildings, data collection and analysis techniques, environmental performance analysis methods, and selection of building simulation tools.

Chapter 4: This chapter presents thermal-optical properties of single, two- and three-layer ETFE-foils. To achieve the objective, this chapter reviews methods adopted by previous studies to determine thermal-optical properties of ETFE-foils. It also discusses justification of selection of the methods adopted to measure the thermal-optical properties of ETFE-foils. The methods applied to obtain these properties are also discussed.

Chapter 5: This chapter presents the results and analysis of the thermal performance of single-layer, two-layer and three-layer ETFE-foil panels. This is completed in two phases: the first phase determined solar transmittance of single-layer, two-layer and three-layer ETFE-foil panels, and the second phase evaluated the thermal performance of single-layer, two-layer and three-layer ETFE-foil panels. This chapter discusses the methods adopted in previous studies and justification of selection of methods applied in the study to analyse the thermal performance of ETFE-foil panels.

Chapter 6: This chapter presents the results and analysis of the thermal performance of occupied spaces enclosed with ETFE-foil cushion envelope. The chapter discusses details of data collection procedures for the case study buildings. The indoor thermal environment of both of the buildings is critically analysed with adopted methodology.

Chapter 7: This chapter presents simulation based analysis to evaluate and compare the thermal performance of spaces enclosed with ETFE-foil cushion roofs and glass roofs. It also identifies strategies to improve the thermal performance (overheating) of spaces in current and projected climate scenarios. At the beginning, simulation models are calibrated by comparing with the measured data. Further simulations are conducted to estimate and compare buildings energy consumption when enclosed with ETFE-foil roofs and glass roofs.

Chapter 8: This chapter presents the summary of findings from the research study and then critically evaluates the methodologies adopted to conduct the research. On the basis of theoretical knowledge and findings obtained from the empirical studies, design recommendations are proposed. Finally, the chapter discusses the fulfillment of research aim and objectives. The novelty of the study and contribution to the knowledge are discussed with limitations and proposals for future research.

Chapter 2

2 Thermal behaviour of membrane envelopes and the spaces they enclose

2.1 Introduction

This chapter introduces ETFE-foil, its properties and various configurations of ETFE-foil in cushion construction that can be used to enhance the thermal performance of enclosed spaces. From the previous chapter, it was apparent that research in the area of the thermal performance of ETFE-foil cushion and space enclosed with it is limited. Therefore, a review of the typical thermal behaviour of the membrane and thermal behaviour of space enclosed with a membrane envelope was attempted and discussed in this chapter. This review particularly focused on the results obtained in previous research on the thermal behaviour of spaces enclosed with membrane envelopes. Even though ETFE-foil's characteristics are different from that of other fabric membranes, its application and functional purposes are similar. Thus, it was assumed that similar thermal conditions might exist in the spaces enclosed with an ETFE-foil cushion envelope. This chapter also describes the impact of this thermal condition (which is likely to be encountered in the space enclosed with ETFE-foil cushions) on thermal comfort of occupants and thermal comfort assessment methods that can be used to assess indoor thermal performance.

2.1.1 ETFE-foil

Ethylene-tetra-fluoro-ethylene (ETFE) is a synthetic fluoropolymer. Although patented by DuPont in 1940, it was not used commercially until the 1970s. In the form of ETFE-foil (typically 100µm to 300µm in thickness) it is applied in building envelopes in a single layer or, more commonly, as inflatable cushions composed of multiple layers. Because of their high light transmission and transparency, ETFE-foil cushions are now widely used as an alternative to glass as a cladding for complex structures (Moritz, 2007, Schiemann and Moritz, 2010). ETFE foil is very resistant to environmental influence where the material is exposed to a diverse range of aggressive actions e.g. ultraviolet (UV) radiation, acids, alkalis etc., and it exhibits excellent long-term resistance to soiling. Thus, this material neither changes its colour nor becomes brittle. With all these advantages, in the recent times ETFE-foil has become one of the most popular materials that is ideal for membrane envelopes and tensile structures (LeCuyer, 2008, Knippers et al., 2011).

2.1.2 Colouring printing and coating in ETFE-foil

Transparent ETFE-foils are commonly used in building envelopes e.g. façades, roofs etc. Nevertheless, ETFE-foil can also be found in silver, white and different other colours e.g. blue, green, pink etc. Among these different colour, white ETFE-foil reduces radiation transmission in the UV range considerably (Knippers et al., 2011). ETFE foils can be printed also, however, because of its anti-adhesive behaviour, pre-treatment is necessary before printing. For printing, silver or white ink is used to reflect light and heat in particular. Moreover, the degree of transmittance of these inks can be controlled during printing. Thus, it is possible to print a variety of motifs, patterns (e.g. dot, honeycomb, chequer board etc.) by varying the transmittance of ink accordingly. While printing, using repetitive pattern, it is possible to vary the degree of coverage of the printed part e.g. dots of various size and degree of coverage. By using sputtering techniques foils can be coated with metallic, ceramic or organic coating. Furthermore, printed or coated foils can be laminated using transparent foil layers. This lamination of multiple foils is considered as a single ply that improves the strength of the foil layer and also protects printed motifs and coatings (Knippers et al., 2011). Nowofol developed a selective coating using Ultra-Violet and Infra-red filter. This helps to improve thermal properties of ETFE-foil by selectively transmitting or reflecting different wavelengths in the solar spectrum (Vector-foiltec, 2013).

2.1.3 ETFE-foil cushion configurations

In ETFE-foil cushion systems, foil layers' form part of the load bearing structure, which is integrated into the form as pneumatically prestressed layers with their edge clamped to extruded aluminium framing. Moreover, construction of ETFE-foil cushion varies with regards to load bearing and building physics characteristics (Schiemann and Moritz, 2010). In a cushion, the middle layer can be much thinner because it is subjected to low pressure. However, by creating a dual chamber system, the middle layer improves heat insulation properties. Therefore, it is possible to enhance insulation properties of ETFE-foil cushions by increasing the number of air chambers (LeCuyer, 2008). Furthermore, fritting and printing of foil layers increases opportunities to improve the thermal performance of ETFE-foil cushion by controlling solar gain into the enclosure. Depending on the functional requirements, fritting can be reflective or absorbtive. Highly reflective frit is more efficient to moderate indoor thermal conditions than highly absorbing frit. In a cushion system with highly absorbing frit the temperature of the middle layer is increased (Poirazis et al., 2009). As a result, transmission of long wave radiation towards the interior and exterior is increased. Moreover, reflective frit

acts as a screen for longwave radiation exchange. Thus incorporation of frit reduces the possibilities of overheating and excessive cooling (Poirazis et al., 2009). Besides, low-emissivity coating of the ETFE-foil layer can reduce solar gain as well as longwave radiation exchange. Therefore, it is possible to alter the thermal performance of the envelope system. Heat and light transmission of ETFE-foil cushions can also be manipulated by the following procedures (Knippers et al., 2011, LeCuyer, 2008, Moritz and Hafner, 2010).

- Separating individual foil layers at anchoring profiles e.g. Figure 2-1(e).
- Separate pressure control for two air chambers and moving the middle layer by repositioning and elastic elongation while changing pressure (see Figure 2-2). In this type of system the outer and middle layer can be printed or fritted in an inverse pattern motif known as intelligent printing (see Figure 2-3, Figure 2-4).
- Use of different colours in the middle layer.
- Incorporating aluminium and ETFE lamellae, mobile textile membranes.

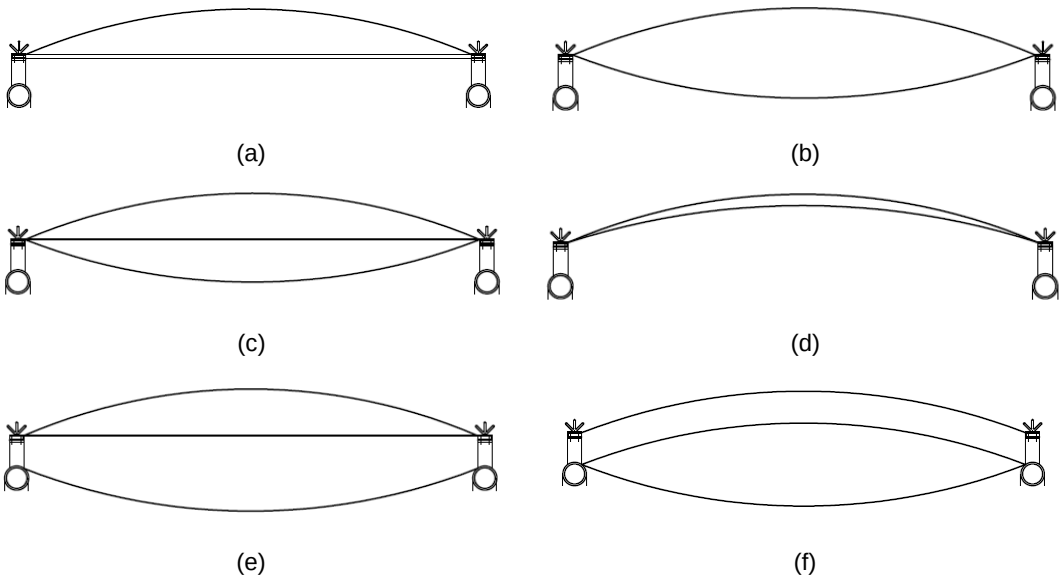


Figure 2-1: Construction types of ETFE-foil cushions (Schiemann and Moritz, 2010)

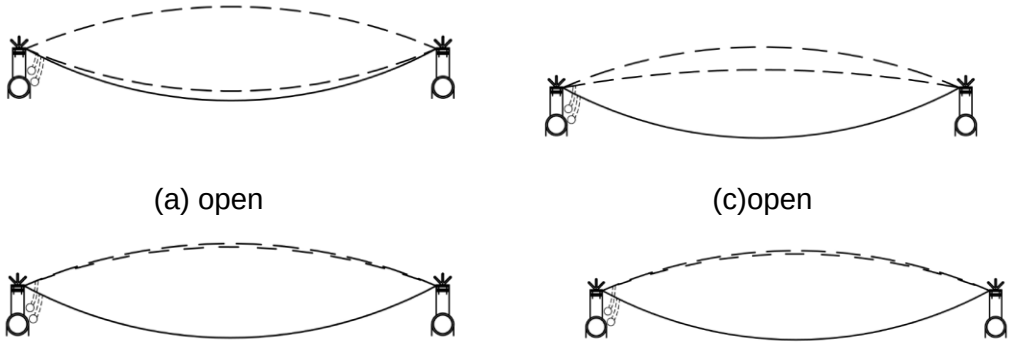


Figure 2-2: Movable middle layer in ETFE-foil cushion

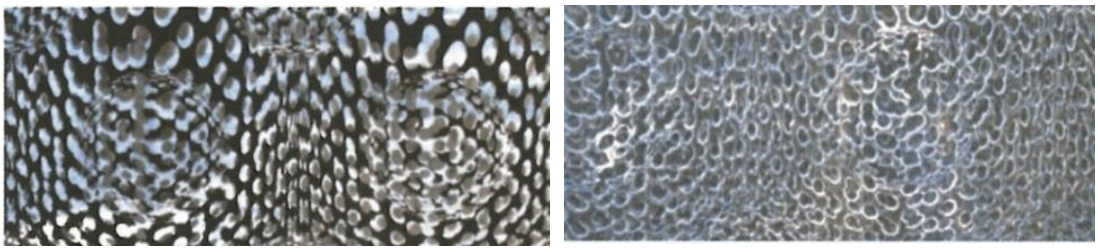
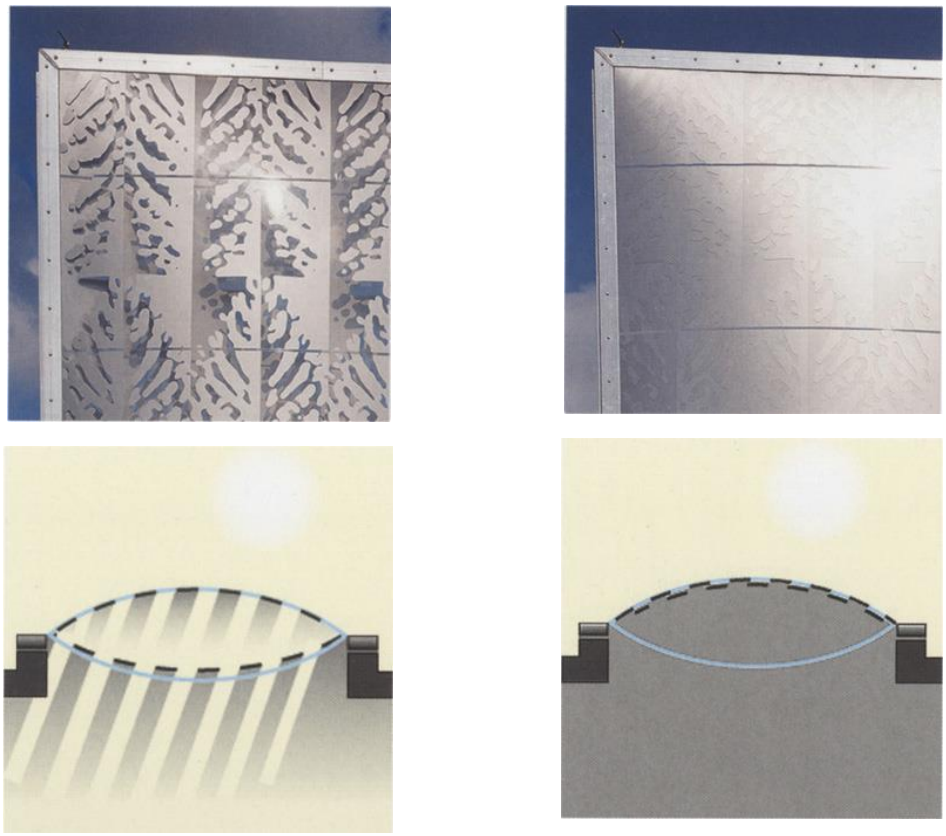


Figure 2-3: Moveable central layer with intelligent printing, (a) open, (b) closed (Knippers et al., 2011)



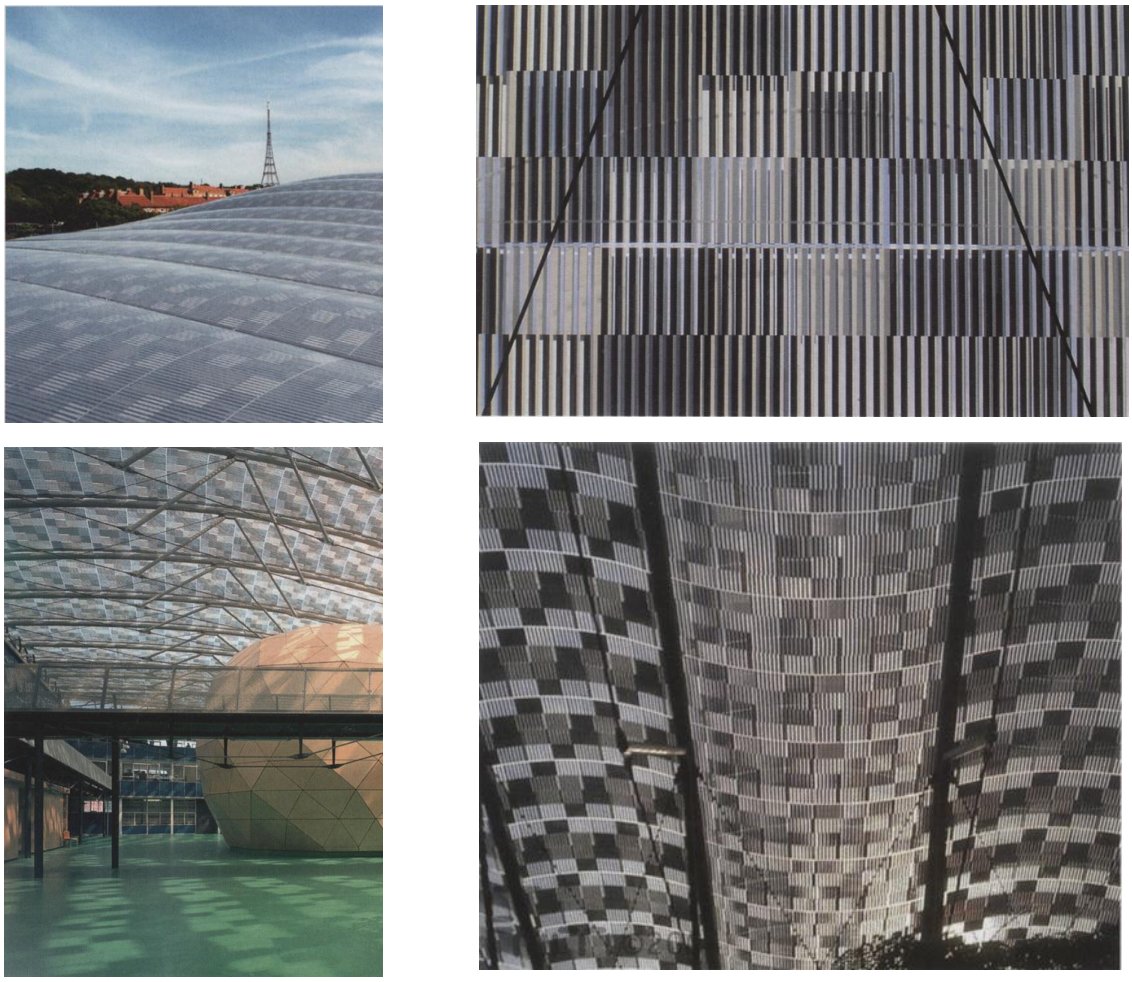
(a) (b)

Figure 2-4: (a) Pattern open, (b) Pattern superimposed (LeCuyer, 2008)

Figure 2-5, Figure 2-6 and Figure 2-7 present the different configurations of ETFE-foil cushion and control strategies that were applied in the Festo Technology and Kingsdale School building envelopes to improve the indoor thermal environment.

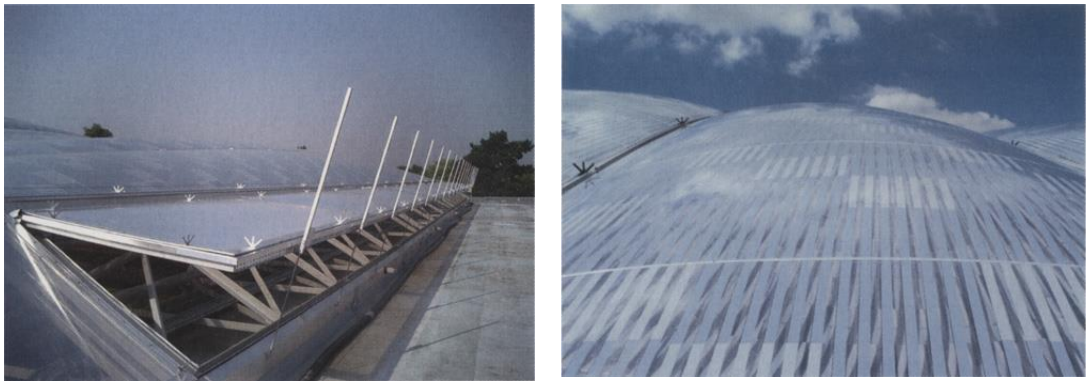


Figure 2-5: Festo Technology centre atrium (LeCuyer, 2008)



(a) (b)

Figure 2-6: Kingsdale School atrium (a) exterior view (top), interior view (bottom); (b) printed top layers (top), view of cushions (bottom) (LeCuyer, 2008)



(a) (b)

Figure 2-7: Kingsdale School atrium solar gain controlled by (a) opening ETFE-foil cushion at clerestory level, (c) closing top two layers of cushion (LeCuyer, 2008)

2.2 The thermal behaviour of fabric membranes

Typical fabric membranes used in building envelopes are around 1 mm thick and have a weight of around or less than 1kg/m^2. According to Harvie (2015), this type of membrane envelope can change temperature by 5°C within a minute just because of cloud moving in front of the sun. On a sunny day in summer it may become 20°C hotter than the ambient external air temperature during the day yet become 3.5°C cooler than external ambient temperature under a clear night sky (Harvie, 1996). It is also apparent that the surface temperature of this type of envelope can be raised to 40°C to 50°C on hot days (Croome and Moseley, 1984a, Harvie, 1996). Moreover, membrane envelopes are usually used to cover large facade or roof areas, which respond quickly to the exterior conditions. Because, unlike for thicker and heavier materials, there is no significant time lag between a temperature change on their outside surface and the resulting change in their inside surface, a rapid change of surface condition means it has an impact on indoor thermal conditions.

However, in ETFE-foil cushions, particularly with multiple air chambers, a temperature gradient exists between the external and internal surface. This was evident in a test rig experiment carried by Antretter et al. (2008), where the study found in a two layer cushion that the internal layer was a maximum 13.3°C hotter than the external layer when transmitted solar radiation inside the test rig recorded was 219 W/m^2. Whereas in the three-layer cushion, the middle layer was found to be hotter than both the internal and external layer while the internal layer was also 8°C hotter than the external layer (Poirazis et al., 2009, Hu et al., 2016). However, these results were obtained using test-rig experiment and mathematical modelling. Therefore, from this finding, it can only be assumed that surface temperature will vary in two and three-layer cushion, but the extent of this in an actual building envelope is not known yet. Besides similar to coated fabric membranes, ETFE-foil cushions might interact with the external conditions. Nevertheless, how quickly an ETFE-foil cushion responds to the change in outdoor conditions in the presence of an air layer between foils, which provides insulation is still relatively unexplored. Variation in surface temperatures of ETFE-foil in a cushion system might have an impact on the internal air temperature, but this is yet to be examined under actual condition.

Although membrane envelopes behave unconventionally but the underlying heat transfer mechanisms such as conductive, convective and radiative heat transfer is the same as for any other conventional building materials. Again, this heat transfer depends on material properties e.g. thermal optical properties, thermal transmittance

etc. Thus, it is important to examine actual properties that might have an impact on their performance as well as the thermal performance of spaces they enclose. Therefore, in order to better understand the thermal performance of materials like ETFE-foils, it is necessary to measure the following.

- Solar transmittance - indicates the amount of solar radiation transmitted through ETFE-foils.
- Solar absorbtance and reflectance - indicates the amount of solar radiation absorbed and reflected.
- Longwave infrared heat transfer - it is a function of the surface temperature of the ETFE-foil, the emissivity of foil as well as the emissivity of the surrounding building fabric and their surface temperatures.
- Emissivity - is a measure of longwave infrared radiation that a surface emits to its surroundings.
- Thermal transmittance - heat flux through ETFE-foil cushion which depends on temperature difference between indoor and outdoor.

2.3 Heat transfer in membrane envelopes

It was already mentioned in section 2.2 that the heat transfer mechanism will be identical for unconventional membrane envelopes those constructed of materials like ETFE-foil, PVC coated polyester fabric etc., as well as conventional construction e.g. brick wall, concrete floor etc., (Knippers et al., 2011, Harvie, 2015, Devulder 2004). Poirazis et al. (2009) applied the principles of heat transfer mechanism in the mathematical model to determine heat flux on ETFE-foil cushion surface. Antretter et al. (2008), also suggested considering basic principles of heat transfer while analysing the performance of ETFE-foil.

According to Incropera et al. (2013), “Heat transfer is thermal energy in transit due to a spatial temperature difference”.

“Any layer in a component, the quantity of energy transmitted per unit of time depends on the temperature differences between two sides of layer, the distance covered by the energy flow (the thickness of the material) and thermal conductivity of the material forming that layer’’.

However, the process of heat exchange in a translucent envelope system is a complex phenomenon and is discussed in the following sections.

2.3.1 Conduction

In conductive heat transfer, a temperature gradient exists in a static medium that may be either solid or fluid. It takes place in solid bodies and fluids at rest. It is transfer of energy from more energetic to less energetic particles of a substance due to the interaction between particles with the presence of temperature gradient and in the direction of decrease of temperature. An appropriate rate equation can be used to quantify the amount of energy transferred per unit time through conduction. For conduction, the rate equation is known as Fourier's law (Incropera et al., 2013).

2.3.1.1 Conduction heat transfer of a membrane surface

For membrane materials, it is important to quantify intra-surface conduction, in order to assess the rate at which variations in conditions occurs between the surfaces of multi-layer membranes (Harvie, 1996). However, transient conductivity depends on material density, specific heat capacity and conductivity. These properties are related with thermal diffusivity. In materials with little thermal mass, heat conducts very rapidly and is said to have thermal diffusivity. From material diffusivity, it is possible to calculate time lag. However, the limited range of conductivities, specific heat capacities and densities of membranes resulted in very low time delay that is less than a minute. So it is adequate to represent thermal conductivity of membranes by using steady state methods (Clarke, 1985) however for accuracy it is not necessary to measure specific heat capacities and densities for membranes (Harvie, 1996).

2.3.2 Convection

In convective heat transfer, two mechanisms are associated. Energy is transferred by random molecular motion as well as bulk or macroscopic motion of a fluid. This type of motion contributes to heat transfer in the presence of a temperature gradient (Incropera et al., 2013).

2.3.2.1 Convection heat transfer of a surface

One material property that significantly affects the rate of convective heat transfer is the surface roughness. Building materials with smooth surface finishes are considered to have a roughness of zero (McAdams, 1954). Therefore a membrane with a surface thickness less than a millimetre and smooth surface coating would be considered to have surface roughness zero and no convective heat transfer will occur on it's surface (Harvie, 1996). However, this phenomenon is not real in the case of ETFE- foil. This is one of the heat transfer mechanism that impact surface temperature of ETFE-foil in a cushion, even though the foils are smooth. This was evident in the investigation results

obtained by Antretter et al. (2008). Thus surface roughness might accelerate heat transfer rate but convective heat transfer also occurs on the smooth membrane surface.

2.3.3 Radiation

Thermal radiation is the energy emitted by a substance that is at nonzero temperature. Heat radiation emits in a range of frequencies specific to this temperature region (Knippers et al., 2011). Emission occurs from solid surface as well as liquids and gases. Here energy transported by electromagnetic waves. Although conduction and convection process requires the presence of a material medium for energy transfer but radiation do not. Thus radiative heat transfer occurs most efficiently in vacuum (Incropera et al., 2013).

2.3.3.1 Radiative heat transfer of a surface

Radiation can also be incident on a surface from its surroundings, from a sources e.g. sun or from another surface to which the surface is exposed. The rate at which all such radiation is incident on a unit area of the surface is known as irradiation and expressed as 'G'. A part or all of the irradiation can be absorbed or emit by the surface, thus modify the thermal energy of the material (Incropera et al., 2013). The rate at which radiant energy is absorbed or emit per unit area of a surface termed as absorptivity or emissivity. These are the radiative property of the surface and depend on surface finishes. The thermal energy of a matter increased and decreased by absorbed and emitted radiation whereas reflected and transmitted radiation has no effect on this energy.

Radiative heat transfer affects the thermal condition of ETFE-foil cushion. However this heat transfer depends on emissivity, thus can be reduced by the application of low-E coating on ETFE-foil surface (Antretter et al., 2008, Poirazis et al., 2009).

2.4 The observed Thermal behaviour of space enclosed with membrane envelope

It was discussed in section 2.2 that membrane envelopes are repond rapidly to outdoor weather conditions e.g. solar radiation. However, buildings constructed with this type of membrane roof often also consist of thermally massive walls, floors etc which barely change their condition during the day and tend to preserve indoor thermal conditions as preferred by the occupants. Therefore, thermal conditions vary depending on

proximity to the membrane roof or close to the ground. This is the result of variation in air temperature and radiant temperature.

It was already discussed in chapter 1 that no study had investigated thermal behaviour of space enclosed with an ETFE-foil cushion envelope. Therefore, an attempt was made to acquire information from previous research that investigated thermal behaviour of spaces enclosed with coated fabric membrane envelopes. The results obtained in previous research are presented briefly in Table 2-1. The purpose was to see the extent of variation in thermal condition.

Table 2-1: Summary of results obtained from previous studies on thermal behaviour of space enclosed with membrane envelope

Study	Space type, location, weather	HVAC system	Envelope type	Surface temperature	Temperature difference between air close to membrane and outdoor air	Temperature difference between air close to membrane and near to the floor
Wu et al. (1984)	Stadium moderately cold climate	Air conditioned (seating area of a stadium only)	air-supported roof, composed of single and double layer membrane		3°C above outdoor temperature	On warm summer day- 9°C (without AC) 11°C (with AC operating in the seating area)
Croome and Moseley (1984a)	Air house, The University of Bath	Inflation fans	air-supported structure with PVC-coated polyamide skin	40°C	8°C above outdoor temperature during day, 1°C below outdoor air temperature at night	4°C
Harvie (1996)	Factory, Chepstow, UK	Air conditioning system, destratification fans, natural ventilation through the apex of the roof	Double membrane composed of PVC coated polyester membrane and permeable proban treated cotton calico	31°C		8°C (free running period)

(Table 2-1 continued)

Harvie (1996)	Arena, Llangollen, Clwyd.	Apex extract fans, low level natural ventilation is provided by small openings	Single layer, PVC coated polyester	33°C (maximum 40°C)	12.5°C above outdoor temperature during day	10°C (positive stratification during the day) 1.1°C (negative stratification during the night)
	Lawn Tennis and Croquet Club Wimbledon, London.	Louvres provide natural ventilation, ventilators to extract air from occupied space, infra-red heaters	PVC coated polyester membrane	45°C (maximum 50°C)		5.6°C (positive stratification during the day)
Devulder (2004)	New Inland Revenue Amenity Building (IRAB), Nottingham, UK	Electric radiant heaters	Single skin PTFE/glass		15°C above outdoor temperature during day	6°C to 12°C (positive stratification during the day) 3°C (negative stratification during the night)

On the basis of findings of previous research (presented in Table 2-1) the thermal environment enclosed within a membrane envelope can be characterised by non-uniformity and high responsiveness. Both indoor and outdoor air temperature, and membrane surface temperature are key to the creation of this non-uniform behaviour. It can be anticipated that similar conditions might exist in spaces enclosed with ETFE-foil cushions, although this was unexplored. In order to investigate thermal performance of ETFE-foil covered enclosures it is necessary to focus on the following:

- impact of external environmental stimuli e.g. solar radiation, external ambient temperature on thermal state of ETFE-foil cushion surface
- impact of surface temperature of ETFE-foil on the adjacent air temperature
- solar radiation transmission through ETFE-foil cushion and its impact on the enclosed space
- impact of external ambient temperature on the enclosed space
- identify whether temperature stratification exists and the extent of this stratification
- impact of this stratification on thermal comfort of the users of the space
- selection of a space which can be used to represent above phenomenon e.g. enclosed space with large internal height

2.5 Impact of thermal behaviour of membrane envelope on thermal comfort

Results obtained from previous studies presented in Table 2-1 indicates that the temperature difference between the space enclosed, the membrane envelope and close to the ground is significant. This variation in thermal condition might have considerable impact on the thermal comfort of the occupants of the spaces adjacent to membrane roof in particular due to overheating. Thus, the primary significance of the thermal behaviour of space enclosed by membranes, e.g. ETFE-foil cushions, is the way it affects the comfort of the occupants of that space. Although thermal comfort depends on various parameters e.g. physical activity, clothing type, air temperature, mean radiant temperature etc, but it may primarily be affected by the permeable heat transfer of the membrane envelope (Harvie, 1996). Permeable heat transfer in an ETFE-foil cushion envelope is specified by Knippers et al. (2011) and illustrated in Figure 2-8.

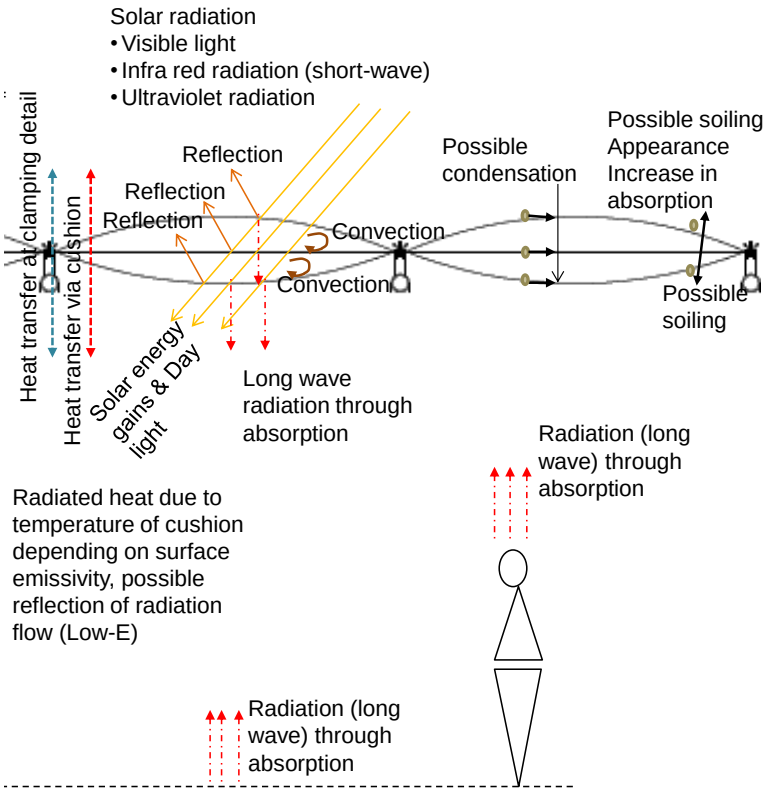


Figure 2-8: Building physics aspects for polymer foil enclosure [reproduced from Knippers et al. (2011)]

Thus, to assess the environmental quality of an enclosed space, whether it is comfortable, uncomfortable or overheated, it is important to establish appropriate environmental quality indicators. This is discussed in the following section.

2.6 Indoor environment quality indicators

A well-tempered indoor environment is considered to be necessary to ensure health, safety and comfort of its occupants. The quality of the indoor environment is dependent on various inter-related aspects in a building. Among many factors thermal, ventilation and lighting are three key environmental aspects that need to be considered to determine the indoor environmental quality (CIBSE, 2006, CIBSE, 2015b). The following section describes briefly the importance of these indicators in a building design.

2.6.1 Thermal environment

Thermal environment is one of the key contributors in ensuring environmental comfort and is essential to satisfy the state of mind and body. Poor thermal comfort brings discomfort to occupants and extreme thermal environment can bring health hazards (ASHRAE, 2009). Thermal comfort is dependent on various design features of a

building such as envelope type e.g. brick wall, membrane roof, etc, window configuration, ventilation strategies, etc.

The transparent building envelope e.g. ETFE-foil cushions, incorporated into a large high interior space (e.g. atrium) allows deeper penetration of high levels of natural light and strong solar radiation. This can create either a pleasant thermal environment or if designed incorrectly, adverse factors such as glare and poor thermal comfort.

The issue of thermal environment is a growing concern due to extreme climatic conditions (too cold or too hot) in recent years around the world as well as in the UK and other European countries.

2.6.2 Ventilation and air quality

Ventilation is a widely used technique, that is used for cooling, for reducing the amount of undesired components in the air (e.g. carbon dioxide concentration) and to control moisture and/or humidity in the air. It is essential to provide fresh air to keep occupants active and healthy. Buildings can be ventilated either naturally using windows, vents etc. or mechanically by means of a heating ventilation and air-conditioning (HVAC) system.

In a building with transparent/ translucent roof e.g. ETFE-foil cushions and large interior space, ventilation plays an important role in providing optimum quality of indoor air circulation within the space and maintaining acceptable level of thermal comfort. People spend most of their time indoors, however, poor ventilation can cause discomfort and health hazard.

2.6.3 Lighting

Lighting (natural or artificial) defines the visual environment including definition of colour and texture. Availability of daylight is essential to define the visual relationship between the outdoor and indoor environment. A sufficient amount of daylight helps to eliminate the need for artificial lighting; thus, saves energy.

Lighting quality and availability is a complex task to measure as light levels can vary widely within a space. Moreover, perceived lighting quality in a space is dependent on illumination level, distribution of illumination, and glare.

Other than visual parameters, there are non-visual parameters that can influence the overall environmental comfort such as heat emission from the light sources and their energy consumption.

In large spaces such as in atria, transparent/ translucent roofs are incorporated to admit high levels of daylight and create a visual link between indoor and outdoor. However, without proper control, significant access of daylight can cause discomfort.

2.7 Thermal comfort environmental parameters

According to CIBSE guide A (CIBSE, 2006, CIBSE, 2015b) the environmental parameters that affect thermal comfort are as discussed in the following sections.

2.7.1 Temperature

The temperature is the most important environmental parameter affecting thermal comfort. Indoor air temperature is the dry-bulb temperature of the air.

Mean radiant temperature (MRT) is an important variable of the environment that defines people's thermal comfort. This can be measured by a uniform black enclosure in which an occupant exchanges the same amount of thermal radiation as in the actual the non-uniform enclosure. There are various approaches of gathering or calculating MRT. Mean radiant temperature is dependent on the surface temperatures of the space and position of the person in relation to the surfaces.

MRT can be calculated or estimated by measuring globe temperature, air temperature and air velocity (ASHRAE, 2009). The accuracy of estimating MRT is dependent on the type of environment and the accuracy of the measurement device used. Another way of measuring mean radiant temperature can be by measuring area weighted mean temperature of all the objects surrounding the body and the respective position of the person. Detail of this method is stated in ASHRAE (2013).

Operative temperature combines the air and radiant temperature in a single index. This includes combined effect of convective and radiative heat exchange. This is a weighted mean temperature between the air and radiant temperature (CIBSE, 2006, CIBSE, 2015b). In well-designed buildings during winter air temperature can often be equal to the operative temperature. A realistic assessment of operative temperatures within a space under normal occupant behaviour is important. The operative temperature in summer can be calculated using Equation 2.1.

$$T_{op} = HT_a + (1 - H)T_r \qquad \text{……(2.1)}$$

Where, T_a (°C) = indoor air temperature

T_r(°C) = mean radiant temperature

$H = h_c/(h_c + h_r)$ and $1 - H = h_r/(h_c + h_r)$

h_c ($Wm^{-2}K^{-1}$) = surface heat transfer co-efficient by convection,

h_r ($Wm^{-2}K^{-1}$) = surface heat transfer co-efficient by radiation

CIBSE guide A (CIBSE, 2006), $\frac{h_c}{h_r} = \sqrt{(10v)}$, where v is the air velocity (ms^{-1})

$$T_{op} = \frac{Ta\ \sqrt{(10v)} + Tr}{1 + \sqrt{(10V)}} \quad \text{.....(2.2)}$$

At very low indoor air velocity (below 0.1 ms^{-1}) natural convection (v) is assumed to be 0.1, and Equation 2.1 becomes,

$$T_{op} = \frac{1}{2}\ T_a + \frac{1}{2}\ T_r \quad \text{.....(2.3)}$$

2.7.2 Air movement

Air movement provides a cooling effect. However, if cooling is not desired then it may cause discomfort by creating a draught. The air temperature of this moving air should be in between room temperature and air temperature of ventilation.

2.7.3 Relative humidity

According to CIBSE (2006), relative humidity (RH) has an influence on thermal comfort and overall environmental perception. Low relative humidity can cause dryness and irritation feeling in the eyes and adversely affect respiration. In a building with mechanical ventilation, this can happen during winter when external air is preheated to vent (Kuchen & Fisch 2009). Medium humidity has lower impact; however, high humidity restricts evaporation from the skin and respiration, and can cause thermal discomfort (Szokolay 2008). In naturally ventilated buildings RH can be influenced by interior equipment, ventilation, configuration of the space, etc.

In a moderate thermal environment, 40-70% RH is acceptable but perception of humidity increases at higher temperatures (above 26-28°C). At design temperature, particularly for sedentary occupancy, humidity should be above 40%, although for short periods humidity below 30% is acceptable. It was also suggested that in heated only buildings in the UK during cold weather humidity can remain below 40% (CIBSE, 2006). But in this condition moisture control is important to reduce condensation risk. Surface temperatures of building envelope necessary to avoid condensation are listed in Table 2.2.

Table 2.2: Surface temperatures necessary to avoid condensation assuming internal air temperature of 20 °C and different RH (CIBSE, 2006)

Internal relative humidity (%)	Surface temperature to avoid condensation (°C)
40	6
50	9.3
60	12
70	14.4

2.8 Thermal environment assessment methods

The thermal sensation of people is the basis for the development of the thermal environment assessment methods. With the continuous improvement of the knowledge in the thermal sensation of people, various methods evolved over time. At the early stage, this knowledge in thermal sensation principles were developed through extensive lab-based studies. However, in the later stage, data were collected from actual buildings. This procedure provided more realistic evidence about the thermal comfort preference of the occupants. Based on these findings, a range of thermal comfort models have been proposed to date. The following sections present a review of existing thermal comfort models and assessment methods.

2.8.1 Fanger's thermal comfort model

Fanger (1967), determined a thermal comfort model. The model was developed from extensive data collection and analysis with the participation of approximately 1300 college-age students and 128 older adults in a climate chamber based experimental setting (Fanger, 1967).

Equation 2.4 describes Fanger's thermal comfort model:

$$F(M, Icl, v, tr, ta, Pw) = 0 \qquad \text{.....(2.4)}$$

Where, M = metabolic rate, met

Icl = cloth index, clo

v = air velocity, m/s

tr = mean radiant temperature, C°

ta = ambient air temperature, C°

Pw = vapour pressure of water in ambient air, Pa

The equation indicates that the thermal comfort is not only determined by the air temperature but includes a range of other environmental parameters such as air velocity, mean radiant temperature. Ambient air temperature is the direct environmental index obtained from the dry bulb temperature. Mean radiant temperature (MRT) is derived from a uniform black body temperature which would result in the same radiant energy exchange as in the actual environment. Air velocity and water vapour pressure is also obtained directly from the environment.

However, it is not only the physical environment that determines the thermal comfort, but also the individual's physiological condition. Various physiological variables influence thermal perception such as skin temperature, core or Internal temperature, sweat rate, skin wetness, thermal conductance between the core body and the skin, etc.

2.8.2 PMV-PPD model by ASHRAE

Based on the Fanger's heat balance theory, ASHRAE initiated the Predicted Mean Vote (PMV) method of identifying thermal comfort using the experimental setting where people are exposed to various temperatures for a long period of time. The PMV model is based on the heat balance model of the human body (originally initiated by Fanger), which includes four physical parameters: air temperature, mean radiant temperature, relative humidity and air flow-velocity, and two user related parameters, the person's activities (known as 'met', "metabolic equivalents of task") and clothing insulation (known as 'clo').

The PMV method has been determined by extensive field studies in the American and European countries. Details of the PMV and PPD calculation procedure is available in ASHRAE 55 (ASHRAE, 2013) or BS EN ISO 7730 (BSI, 2005). ASHRAE thermal sensation scale defines thermal comfort level on a seven-point scale (see Table 2-3).

Table 2-3: ASHRAE thermal sensation scale (ASHRAE 2013)

Scale	Sensation
+3	Hot
+2	Warm
+1	Slightly warm
0	Neutral
-1	Slightly cool
-2	Cool
-3	Cold

2.8.3 The concept of adaptive thermal comfort models

The bases for adaptive comfort models were established from early studies in the 1970s which specified the relationship between outdoor temperature and human thermal comfort. The attempt to include adaptive comfort models in the standards are found from ASHRAE. de Dear et al. (1998) conducted a study within the project known as ASHRAE RP-884 to identify adaptive thermal comfort indices. The authors conducted an extensive analysis of previously collected data from all over the world. Their analysis was based on 21,000 individual data collected from 160 countries around the world. According to the authors, three clearly distinguished broad categories of thermal adaption are - behavioural adjustments, and occupants' physiological and psychological condition. Among these three, behavioural adjustment of the body's heat balance probably plays the most dynamic role in maintaining people's comfort. Clothing control is one of the most active adaptive approaches used to control the heat balance associated with behavioural adjustments.

2.9 Comfort models

2.9.1 de Dear and Brager (1998)

The following equation is presented in the publication by de Dear and Brager (1998) for the adaptive comfort calculation for a centralized HVAC building. The authors also proposed 80% and 90% comfort criteria based on percentage dissatisfied.

$$T_{co} = 22.6 + 0.04.ET^{*}_{out} \quad \text{.....(2.5)}$$

Equation 2.5 was derived after accounting the effects of semantic artefacts in comfort criteria as described in de Dear et al. (1998), analysing the field data (described in section 2.8.3). Here T_{co} is the comfort temperature.

The upper (+) and lower (-) limit for 80% acceptability criteria can be defined by:

$$T_{co} = 22.6 + 0.04.ET^{*} \pm 1.91 \quad \text{.....(2.6)}$$

And the upper (+) and lower (-) limit for 90% acceptability criteria can be defined by:

$$T_{co} = 0.04\ x\ ET^{*} + 22.6 \pm 1.12 \quad \text{.....(2.7)}$$

For naturally ventilated buildings, the comfort criteria are described by the following equation:

$$T_{co} = 18.9 + 0.255 \text{ x } ET^{*}_{out} \quad \text{.....(2.8)}$$

ET* is defined by the arithmetic mean of the outdoor temperature for 6am (considering minimum) and 3pm (considering) maximum for previous one month.

2.9.2 ASHRAE Standard 55

Based on the findings from the RP884 project (de Dear et al., 1998), the ASHRAE standard 55 incorporated some of its adaptive thermal comfort criteria in the ASHRAE 55 (Standard 2004) and the following equation was included:

$$T_{co} = 0.31.T_{ext,ref} + 17.8 \quad \text{.....(2.9)}$$

The equation is valid for following conditions,

- for summer season, particularly when the outdoor temperature ranges from 10°C to 33.5°C,
- for buildings where occupants have the direct ability to operate windows, and
- in the case of buildings where the occupants perform low metabolic rate activity (<1.3 MET).

In this case $T_{ext,ref}$ is the arithmetic monthly average temperature, which is characterized by the mean daily minimum and daily maximum temperature of the month in question.

2.9.3 BS 15251

BS EN 15251 (2007) proposed an adaptive thermal comfort standard with the following regression equation,

$$T_{co} = 0.33 \text{ x } T_{ext,ref} + 18.8 \quad \text{.....(2.10)}$$

Here $T_{ext,ref}$ is derived by the running mean temperature (T_{rm}) for past 7 days using the following equation,

$$T_{rm} = (1-\alpha).\{T_{ed-1} + \alpha.T_{ed-2} + \alpha^2.T_{ed-3} \ldots\ldots\} \quad \text{.....(2.11)}$$

This equation can be simplified to,

$$T_{rm} = (1-\alpha).T_{ed-1} + \alpha.T_{rm-1} \quad \text{.....(2.12)}$$

Where,

T_{rm} = Running mean temperature for today

T_{rm-1} = Running mean temperature for previous day

T_{ed-1} = Daily mean external temperature for the previous day

T_{ed-2} = Daily mean external temperature for the day before and so on

α is a constant between 0 to 1, and recommended to use 0.8.

The guide also proposes that running mean temperature can be derived using following approximate equation,

$$T_{rm} = (T_{ed-1} + 0.8\,T_{ed-2} + 0.6T_{ed-3} + 0.5T_{ed-4} + 0.4T_{ed-5} + 0.3T_{ed-6} + 0.2T_{ed-7}) / 3.8 \quad \text{……(2.13)}$$

According to BS EN 15251 (BSI, 2007), the risk of overheating relates to comfort temperature, along with the categories of building and its users. Acceptable temperature ranges for different categories of the buildings are listed in Table 3-8.

2.10 Summary

This chapter presents properties of ETFE-foil and various alternatives to modify properties of ETFE foils those can be used to enhance thermal performance ETFE-foil cushion. It also discusses the results obtained on previous studies which shows that air in-between foil layers in a cushion creates a temperature gradient across the air chamber that in turn affects surface temperature of the ETFE-foil, particularly in two and three-layer cushion systems. Both convective and radiative heat transfer results in this temperature gradient. Therefore, in order to better understand the thermal performance of membranes like ETFE-foil, it is necessary to focus on following properties.

- Solar transmittance
- Solar absorptance
- Reflectance
- Emissivity
- Thermal transmittance

On the basis of findings of previous research, the thermal behaviour of space enclosed with a membrane envelope can be characterised by non-uniformity and responsive. Both air temperature, and surface temperature results in this non-uniform behaviour. It can be assumed that similar conditions might exist in spaces enclosed with ETFE cushions which is unexplored. Thus in order to investigate the thermal condition of a spaces enclosed with ETFE cushion, it is necessary to focus on following aspects.

- Influence of external environmental stimuli e.g. solar radiation, outdoor temperature on thermal state of ETFE-foil cushion surface
- Influence of surface temperature of ETFE-foil on the air temperature
- Identify whether temperature stratification exists and the extent of this stratification
- Impact of this stratification on occupant's thermal comfort
- Selection of a space which can be used to represent above phenomenon e.g. enclosed space with large internal height

This chapter also reviewed thermal comfort models presented in different standards such as CIBSE, ASHRAE and British Standard. The basic principles of these comfort models are identical and applicable for naturally ventilated buildings. In order to identify comfort band, outdoor temperature is the key along with occupant's activity, physiological condition etc. On the basis of the category of the building (e.g. category II of BS 15251) and outdoor temperature, it is possible to identify the temperature benchmark that can be used to assess the thermal performance of existing space enclosed with ETFE-foil cushion.

Chapter 3

3 Methodology

3.1 Introduction

This chapter outlines the research methodologies used to achieve the research aim and objectives. The bases to identify the research methods were initially gathered by reviewing relevant research articles and books. Also guides and standards were reviewed to identify thermal performance standards and specific methods for material performance analysis. A pilot study was conducted to verify the data collection approach for occupied buildings, which provided the basis to finalise the approach for collecting long term environmental data.

At the beginning, this chapter discusses the context of the research and establishes the wider research approach. Then the chapter presents the procedure followed to conduct the pilot study and results obtained from this study. Subsequently the chapter describes detailed methods adopted to evaluate the thermal performance of ETFE foil cushions and spaces enclosed with them. A detailed description of the case study buildings, data collection and analysis techniques and environmental performance analysis methods is provided, and the selection of building simulation tools is discussed.

3.2 Background

In Chapter 2 the existing body of knowledge on the thermal perfromance of ETFE foil and space enclosed by it was critically reviewed. It was apparent that, limited research had investigated thermal performance of ETFE foil cushions whereas no research was focused on actual thermal performance of a space enclosed with an ETFE cushion enclosure. Although ETFE foil's thermal-optical properties, structural properties, thermal characteristics etc., were different from other fabric membranes e.g. PVC coated polyester, PTFE coated glass etc., their application and functional purposes were similar. Therefore, the methodology adopted by different researchers to analyse environmental performance of lightweight envelope were reviewed here, e.g. Harvie (1996), Devulder et al. (2007), He and Hoyano (2010), He and Hoyano (2010), Croome and Moseley (1984b), Wu et al. (1984) etc. It was evident from their studies that fabric membranes are extremely responsive to the external weather conditions. Besides, Harvie (1996) and Devulder (2004) found that thermal behaviour of spaces enclosed

by light-weight envelopes was unconventional. However, heat transfer mechanisms that caused this type of behaviour were similar to those found within any other type of enclosures constructed of conventional building materials. Nevertheless, the thermal performance of ETFE foil cushions and the space they enclose would need to be quantified. This could only be explained on the basis of knowledge of individual heat transfer mechanisms that occur on the ETFE foil cushion envelope.

Moreover, appropriate analytical techniques developed through empirical knowledge would require to evaluate the thermal performance of ETFE foil and the spaces enclosed by it. Therefore, this subject would require long-term research that would include investigation on thermal-optical properties of ETFE foil, evaluation, and prediction of thermal performance of ETFE foil and spaces enclosed by ETFE cushion envelope.

Because of the complexity of the subject, it was thought to be necessary to undertake simple pilot studies at the beginning. The fundamental aim was to provide basic information about the thermal performance of space enclosed by ETFE foil cushions and to recognize difficulties that were likely to be encountered while investigating that performance more precisely.

3.3 The Pilot Studies

3.3.1 The purpose of the pilot studies

Because no existing research has analysed the thermal performance of actual spaces enclosed with an ETFE cushion roof, a pilot study was carried out. The pilot study conducted limited monitoring of an existing space enclosed with an ETFE cushion envelope. The objectives of this study was:

- to gain an overall impression of the thermal performance of space enclosed by ETFE foil cushions,
- to reveal how thermal performance could best be studied for a more comprehensive monitoring programme,
- to identify what information would be required if an attempt was made to predict that performance.

3.3.2 Method adopted for the pilot study

An in-situ method was adopted for the pilot study. This was conducted between 21st August 2013 and 26th August 2013. For this study only one building was available, the Nottingham High School. The Nottingham High School has a three-storey atrium which

was enclosed with a two-layer, 25 cushion ETFE foil cushion roof, in 2009. The rationale of selection of the building and detailed description of this can be found in Section 3.7.1.

The screened thermocouples continuously recorded diurnal variations of air temperature at various levels in the atrium, at 1 minute intervals to give a clear impression of how quickly the thermal condition of the space responded to the climatic variation. Site weather data was collected from a weather station located on an adjacent roof of the school which was close to the ETFE cushion roof (see Figure 3-12). This weather station recorded data at 5 minute intervals. Thus, to see the impact of outdoor weather (e.g. outdoor temperature) on indoor thermal conditions data recorded at 5 minute intervals was extracted, plotted and analysed.

3.3.3 Equipment used for the pilot study

During the pilot study, internal air temperature of various levels of the atrium and transmitted solar radiation through the ETFE cushions was monitored with available equipment. Table 3-1, Figure 3-1 and Figure 3-2 present sensor identifications and locations in the atrium. Figure 3-1 also presents location of the cushion in which surface temperature was measured using thermal imaging.

The equipment used in the pilot study were:

- ϕ0.1 mm K-type thermocouple (screened) to measure internal air temperature
- Data Taker DT80 data logger to record data
- Kipp & Zonen CMP1 Pyranometer (spectral range: 0.3-2.8μm) to measure internal transmitted solar radiation
- Internal surface temperature of cushion measured using thermal imaging camera (FLIR T900)

Table 3-1: Sensors identification and location -Pilot Study

Sensor identification	Location
H1	First floor air temperature
H2, H3	Second floor air temperature
InIR	Internal transmitted solar radiation
OAT	Outdoor air temperature

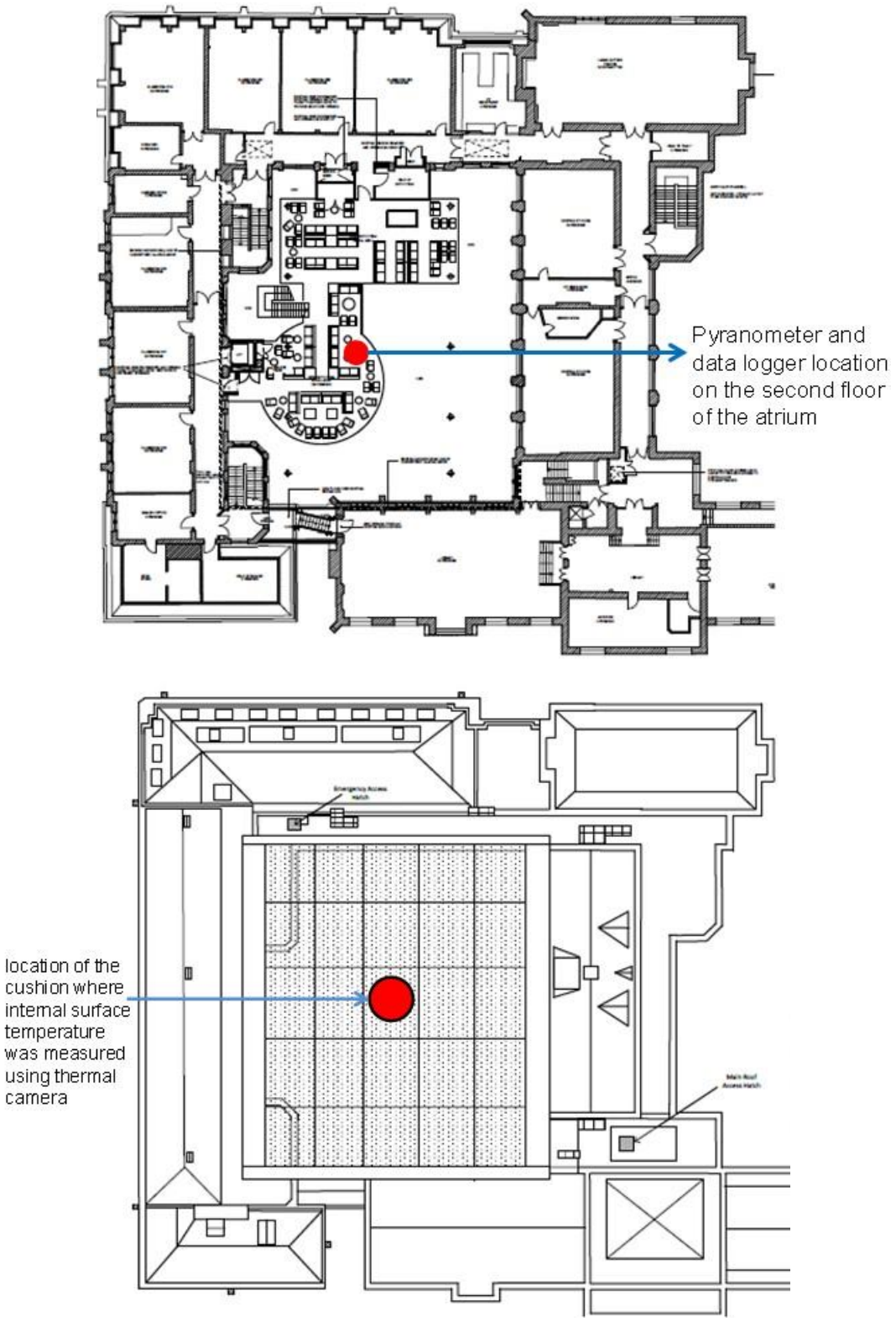


Figure 3-1: Location of the data logger and the solar radiation sensor (top), location of the cushion where internal surface temperature was measured using thermal camera (bottom)- Pilot study [Plans (nts): Maber Architects]

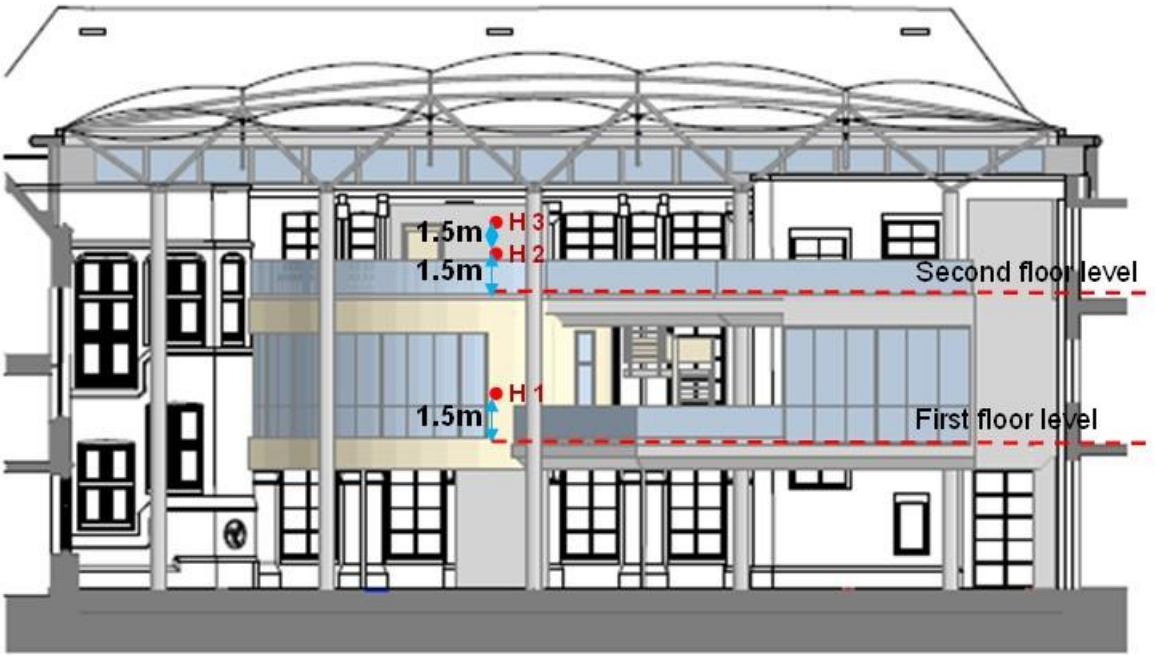


Figure 3-2: Location of sensors in the School atrium [Section (nts): Maber Architects]

The selected time for the pilot study was a school holiday period. Therefore, the atrium was not occupied by students and the HVAC system was not operating during that period. Besides during the study period, it was possible to access to the school atrium on 22nd August 13 to acquire thermal images of the ETFE cushion roof.

3.4 The results

Second floor (H2) and first floor (H1) air temperature was on average 3.8°C and 3°C hotter than that of outdoor air temperature respectively. Besides, temperature differences recorded at two different positions apart by 1.5m on the second floor (H2 and H3) varied between 0.37°C to 1.98°C during the day but coincided at night and morning. Figure 3-3 presents internal air temperatures of the atrium, outdoor air temperature and transmitted solar radiation on 22nd August 2013. From Figure 3-3 it can be seen that during the day air temperature of second floor (H2, H3) stayed 1°C to 4.5°C hotter than that of the first floor (H1). However, at night the first floor air temperature was 0.5°C above the air temperature recorded on the second floor (H2, H3). Therefore, this variation in air temperature indicates existence of positive and negative stratification during the day and night respectively. Moreover, during the day air temperature of the second floor (H2, H3), followed a similar trend to outdoor air temperature and transmitted solar radiation. This indicated the impact of outdoor weather parameter (OAT, InIR) on the second floor thermal condtions during both day and night.

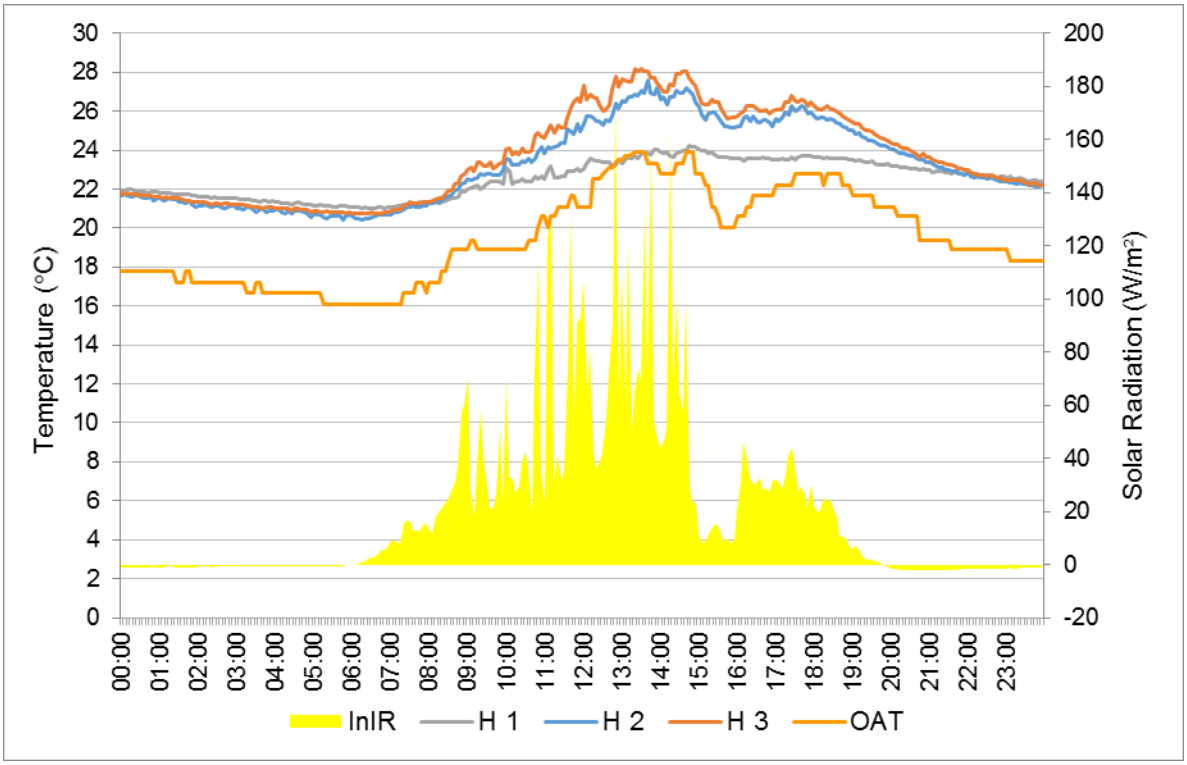


Figure 3-3: Data obtained from Pilot study during 22nd August 2013 (location- Nottingham High School atrium)

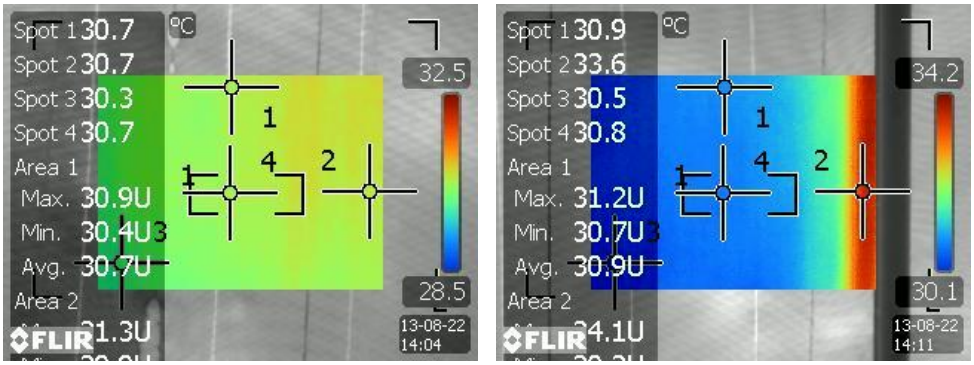


Figure 3-4: ETFE foil surface temperature measured in the middle (left) and at the edge (right) of the cushion at 14:11pm, 22nd August 2013 using thermal imaging (for location of cushion- see Figure 3-1)

3.5 Analysis of information acquired by the pilot study

Short term observation from the pilot study showed that internal thermal conditions of the atrium were very responsive to external weather (e.g. OAT, InIR). This phenomenon was apparent on the second floor which was adjacent to the ETFE cushion roof. This responsiveness appeared to be the result of the direct transmission of solar radiation through the translucent ETFE roof as well as the low thermal resistance of the ETFE cushion envelope that allowed quick transmission of the external thermal conditions into indoor spaces. In a long-term monitoring, it would be important to record this quick response of the indoor spaces. It would require appropriate temperature sensors because any delay might affect the accuracy of the

data recorded. Besides, solar transmittance of the translucent ETFE cushion envelope seemed to be responsible for the frequent change in internal conditions of the atrium. Thus, it was essential to determine these two properties of ETFE foil cushion.

Conditions recorded at different vertical positions within the atrium were found to be different as a result of their proximity to the ETFE cushion roof. Observation of the pilot study also suggested that during periods of bright sunshine significant thermal stratification exist in the atrium. Therefore, it is important to establish an appropriate strategy while positioning internal temperature sensors for long-term monitoring.

On the other hand, along with monitoring of indoor spaces, it would be important to monitor the thermal condition of the ETFE cushion envelope e.g. surface temperature of the ETFE foil. This would demonstrate the impact of the thermal condition of ETFE foil envelope on the thermal performance of the actual enclosures.

However, the environmental conditions of the actual enclosures were uncontrolled. Moreover, these conditions were also influenced by the HVAC system, occupancy, internal gains etc. During the monitoring, it would be difficult to clearly identify the effect of the ETFE foil cushion roof on the overall performance of the environment it enclosed. Therefore, to see the actual impact of ETFE foil on the enclosed spaces, it would be necessary to investigate this separately under controlled and known environment.

3.6 Proposed methodology

On the basis of analysis of the results obtained from the pilot study it was decided to investigate two elements separately. These were:

- thermal performance evaluation of ETFE foil, and
- thermal performance evaluation of spaces enclosed with a ETFE foil cushion envelope

The following section presents the objectives and methods to investigate this two element separately.

3.6.1 Thermal performance evaluation of ETFE-foils

The thermal performance of single, two and three layer ETFE-foil panels were evaluated and compared in a test rig investigation. This was completed to achieve objective 3 and the method is discussed thoroughly in Chapter 5. This test rig experiment was also applied to measure the solar transmittance of single, two- and three-layer ETFE-foil panels. Results were validated by comparing these with values

obtained using lab-based experiment and BS EN 410: 2011 (BSI, 2011). In order to achieve objective 5 thermal modelling and simulation was done. Here predicted models represented a similar configuration to that of the test rig. Using the same model thermal conditions of ETFE foil panels and glass panels were simulated and compared. The results were validated by comparison with values measured in the test rig experiment. Detailed description of this method is presented in Chapter 7. The environmental data and simulation data were analysed adopting the similar procedure.

3.6.2 Thermal performance evaluation of ETFE-foil cushions and the spaces enclosed with an ETFE foil cushion envelope

In order to evaluate the thermal performance of ETFE foil cushions and the spaces enclosed, two different buildings were selected. These were the Nottingham High school, and the Engineering and Science Learning Centre (ESLC) at the University of Nottingham. Both are institutional buildings. Selected case study buildings can be considered to represent the desired sample and data obtained from these buildings were expected to fulfil the research objectives. The rationale for selection of the case study buildings are presented in section 3.7; building information, usage pattern, services etc. of the Nottingham High School and the ESLC are stated in section 3.8 and section 3.9 respectively. Detailed methods are discussed in Chapter 6. Modelling and simulation were applied to predict the performance of case study buildings in current time and according to the UKCP09 climate change scenarios (the 2050s, 2100s). Thermal conditions and energy consumption of predictive models enclosed with an ETFE foil cushion roof and glass roof were analysed and compared. Detailed methods are stated in Chapter 7. The method adopted for environmental assessment of actual buildings and predictive models were identical. Similar guides and standards were used to assess overheating and indoor thermal performance.

Table 3-2 presents objectives and associated methodologies adopted in this research. Figure 3-5 presents the flow diagram showing methodologies and associated objectives. Figure 3-6 shows the methods adopted to obtain and analyse data obtained from the experimental investigation, environmental monitoring and simulation and modelling process.

Table 3-2: Research objectives and associated methodologies

No.	Objectives	Method
1	Develop knowledge base on properties of ETFE-foils and ETFE-foil cushion construction; identify the thermal behaviour of fabric membranes and spaces enclosed with fabric membrane envelope	Literature review
2	Determine thermal-optical properties of ETFE-foils	Lab experiment, British Standard
3	Evaluate the thermal performance of single, two and three layers ETFE-foil panels	Test rig experiment
4	Evaluate the thermal performance of occupied spaces enclosed with ETFE-foil cushion envelope	Monitoring existing buildings
5	Evaluate and compare the thermal performance of spaces enclosed with ETFE-foil cushion and glass roof	Computer simulation
6	Identify strategies to improve the thermal performance (overheating) of spaces enclosed with ETFE-foil cushion in current and projected climate scenarios	Data analysis and computer simulation
7	Identify implication of the research and develop design recommendations of ETFE-foil panels and spaces enclosed with ETFE-foil cushion envelope	Result analysis

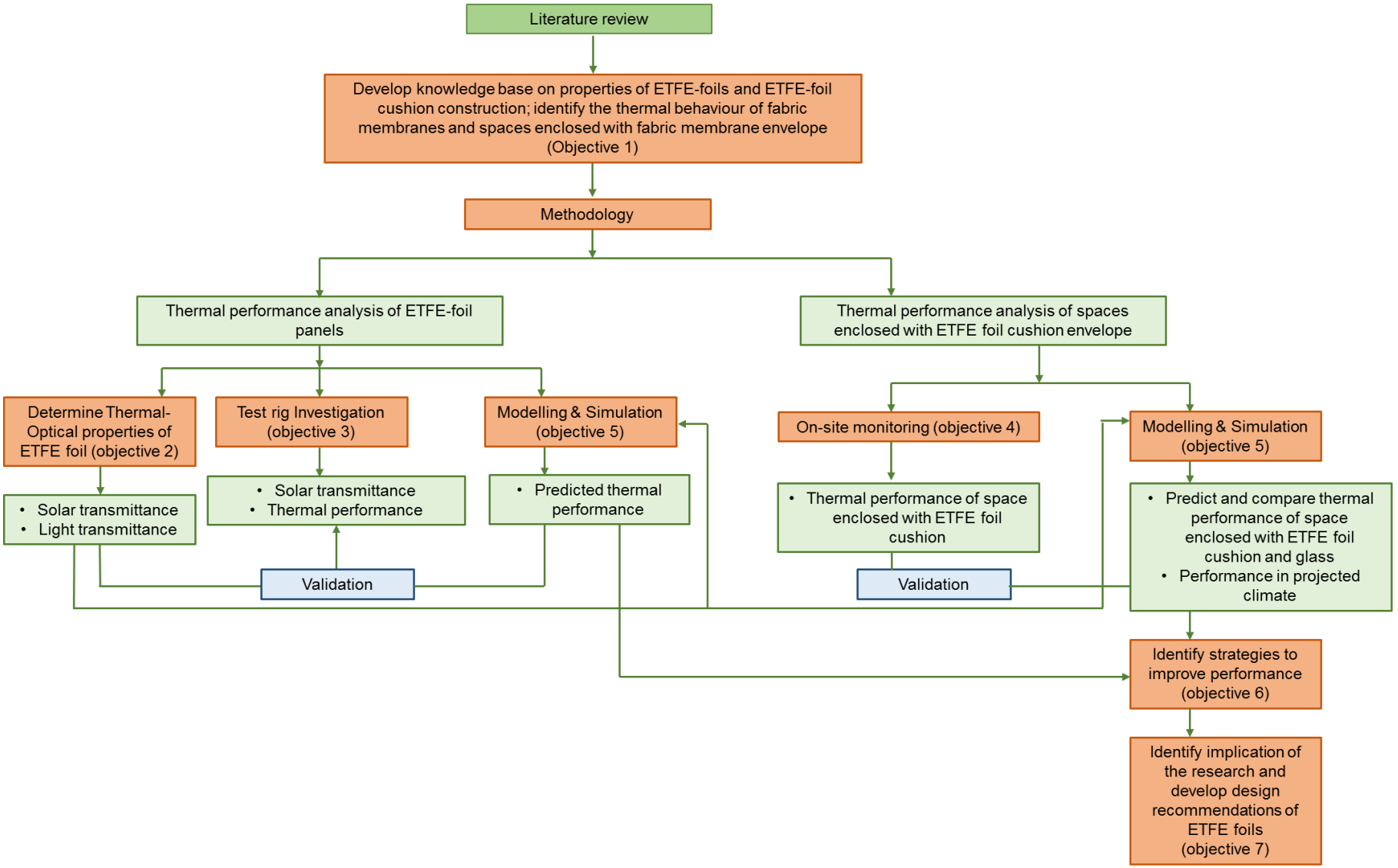


Figure 3-5: Flow diagram of methodologies and associated objectives

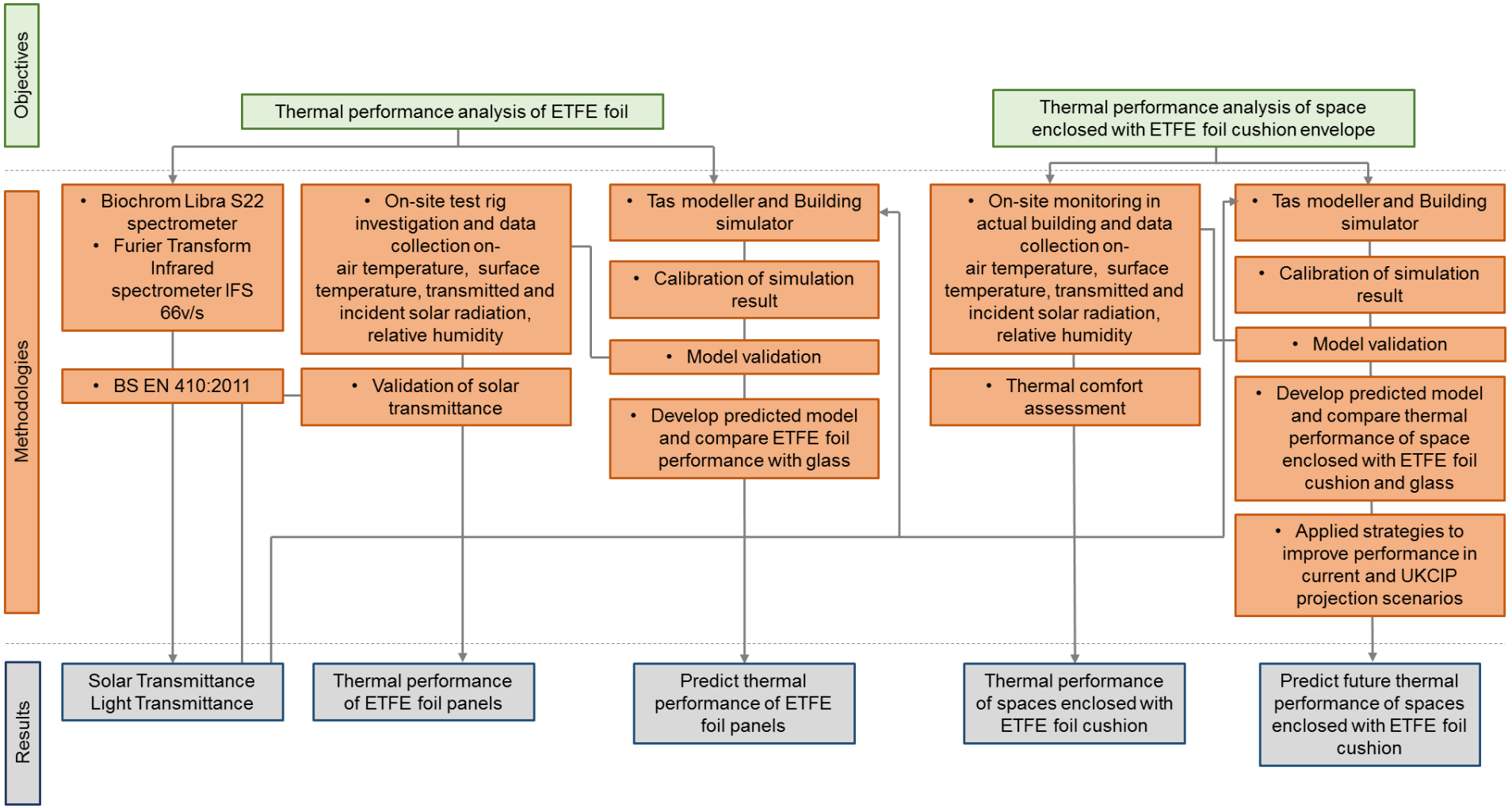


Figure 3-6: Experimental and environmental data analysis, and modelling/ simulation process

3.7 Method to analyse thermal performance of spaces enclosed with ETFE-foil cushion roof

Following sections describes the rationale for selection of the type of buildings for long-term monitoring.

3.7.1 Criteria for selection of monitored buildings

Two buildings were selected to measure the performance of ETFE-foil cushions. Summary of salient features of case study buildings are presented in Table 3-3. The rationale for selection of these buildings is described in the following sections.

3.7.1.1 Scale

For the purpose of this study spaces covered with ETFE-foil cushion were necessary, however, to observe the full range of thermal stratification it was necessary that space is large enough, such as an atrium. Thermal stratification that also impacts thermal comfort is also a common phenomenon to evaluate thermal performance. It was also considered to select a building with an atrium mostly used for functional purposes. The selection was also based on buildings that were compliant with recent building regulations on energy efficiency. Therefore, results obtain could serve as a basis for establishing the typical thermal behaviour of ETFE-foil enclosures to assist designers and architects in the decision making process while applying ETFE-foil cushion envelopes in building design.

3.7.1.2 Location

Available resources for the data collection and on-site monitoring were limited. Therefore, existing buildings situated within reasonable traveling distance were given priority.

3.7.1.3 Occupancy

Occupancy profile and internal gains affect a building's indoor thermal performance. However, monitoring user behaviour requires complex equipment, which was not available during the monitoring. Therefore, preference was given to select moderate occupancy building with fixed user behaviour patterns.

3.7.1.4 ETFE-foil cushion construction

Building envelopes that were constructed with two- or three-layer ETFE-foil cushion systems were given priority.

Table 3-3: Summary of salient features of monitored ETFE-foil cushion enclosures

Description	Case Study 1: Nottingham Boys High School	Case Study 2: Engineering and Science Learning centre (ESLC)
Built year	1860-1960 (renovated in 2009)	2011
Atrium Total Floor area	1297m^2 (approx.)	615m^2 (approx.)
Number of floor	3	3
Type of space (ETFE-foil cushion roofing system was used)	Atrium	Atrium
Occupancy	Continuous High	Intermittent Moderate
ETFE-foil cushion type	Double layer Top layer: 200 microns (75% fritted) Bottom layer: 200 microns (transparent) Covered with rain noise suppression mesh externally	Triple layer Top layer: 200 microns with 4.2mm standard dot matrix pattern (65% coverage) Middle layer: 150 microns clear Bottom layer: 150 microns clear
Monitored period	November 2013- September 2015	August 2014 to September 2015
Roof area	625m^2	396m^2
Location	Nottingham, UK	Nottingham, UK

3.8 Case Study A: Nottingham Boys High School, Nottingham, UK

3.8.1 Building information

The three-storey school building, located in Nottingham, was originally built in 1860. It has a central courtyard, which was renovated during 2009 to form an enclosed atrium. The three-storey high atrium contains a dining hall and cafeteria at ground floor and first floor respectively, and a study space for students on the second floor. The atrium roof consists of two–layer ETFE-foil cushions with fritted top layer and clear bottom layer both of 200μm covered with a rain noise suppression mesh. This roof, see Figure 3-7 (b), is complete with aluminum framing, inflation and air management equipment with associated air handling pipework and connections. In turn, these are supported by steel trusses and columns so that the atrium roof structure does not bear on the existing school buildings.



(a) (b) (c)

Figure 3-7:(a) Location of High school [Source: Google map], (b) roof of atrium [photo: Sabrina Afrin], (c) atrium [photo: Sabrina Afrin]

3.8.2 Building usage pattern

The school building and its system operate between 8am and 6pm with most activities take place in the atrium between 8am and 3pm, which are the usual school hours. During school holidays, the ground floor of the atrium is generally used by the holiday club for particular times and rest of the floors remain unoccupied.

3.8.3 Services

The atrium space heating system consists of fan coil units, fan convectors, under floor heating systems and mechanical ventilation, controlled by a Building Management System (BMS). It operates on a global time zone set from 08.00 to 18.00, Monday-Friday, and is turned off at weekends. Natural ventilation operates automatically through windows at high level (located on the west side only) in conjunction with dampers located above north and south entrance doors at the ground floor. Under floor heating systems operates throughout the year when average air temperature of the atrium dropped below 18°C.

Later in August 2015, four wall mounted air conditioning units were installed in the second floor of the atrium. But according to the school management, this air conditioning system was not operating until the end of September 2015.

3.8.4 Installed monitoring equipment

The on-site monitoring started from November 2013 and was completed in September 2015. The detailed monitoring protocol is described in the following sections.

3.8.4.1 Data logger

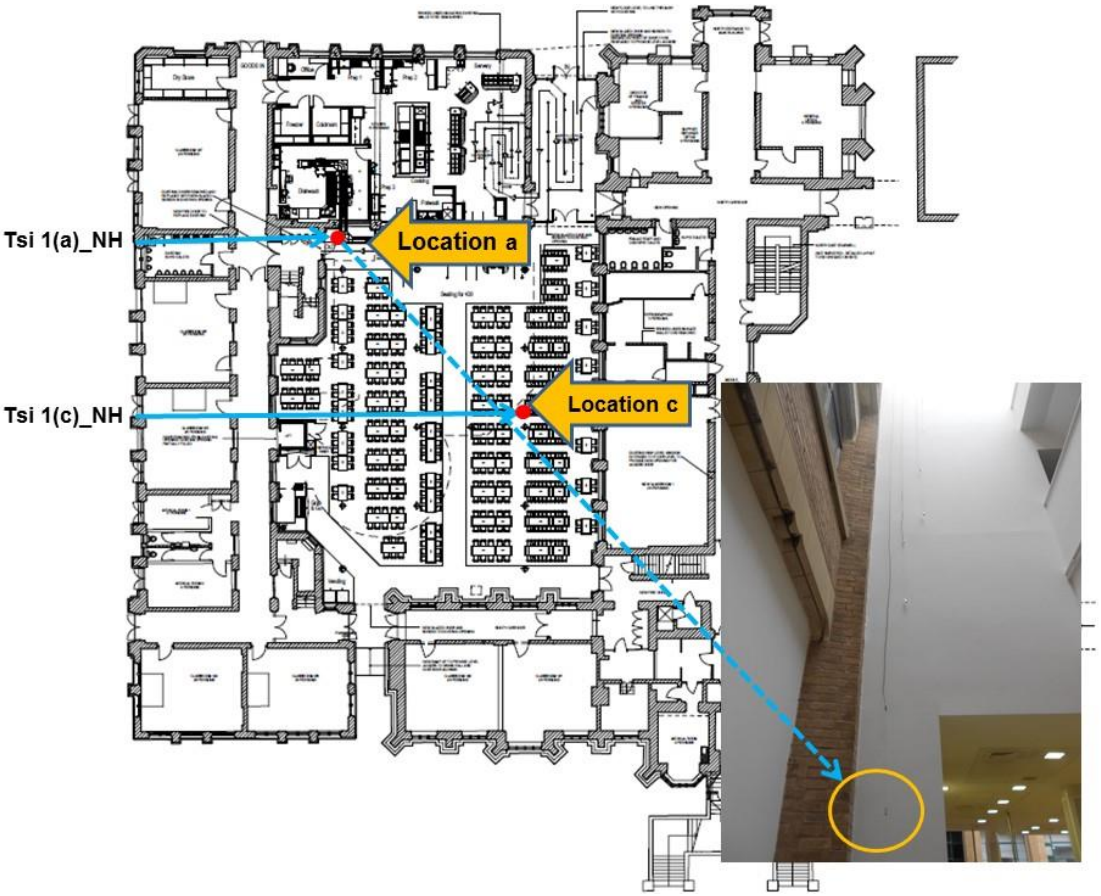
Two different roof spaces were selected to place the data loggers and sensors on the basis of agreement with the estate manager. These roofs were internal flat roofs near to the ETFE-foil cushion roof of the atrium. For clarity, roof locations were considered as location a and location b. A DT85 data logger (location a) and a DT 80 data logger (location b) were placed on these roofs. In total 18 and 12 number of thermocouples were connected to the DT 85 (location a) and the DT 80 (location b) data loggers respectively. Sensors connected with the data loggers were attached to the ETFE-foil cushion surface (both internal and external) and suspended through the voids to reach to each floor below. Location of these sensors is illustrated in Figure 3-8. These temperature sensors were wired in a shared output configuration and their electromagnetic shields were connected to the appropriate input of the data loggers. These data loggers measured and recorded data at 1 minute intervals. Air temperature and surface temperature sensor identification and location is presented in Table 3-4 and Table 3-5.

Table 3-4: Location of air temperature sensors

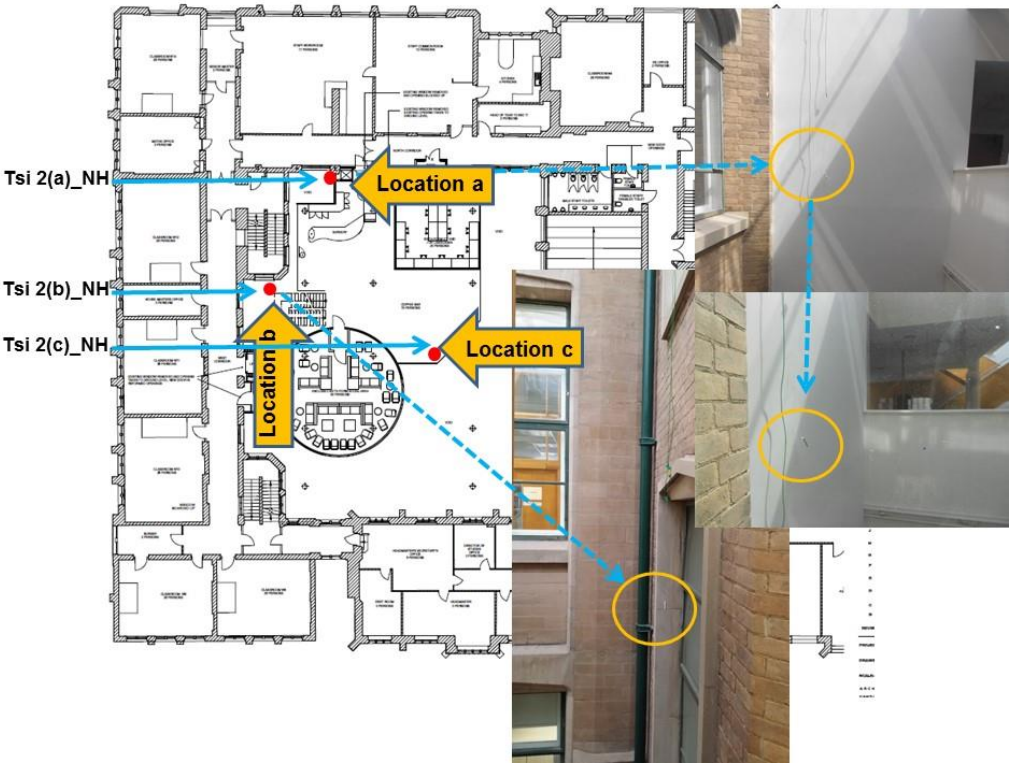
Sensor Identification	Location	Measured thermal conditions represent
Tsi 1(a)_NH	Ground floor (Level 1)	Part of the atrium adjacent to classroom, circulation space
Tsi 2(a)_NH	First floor (Level 2)	
Tsi 3(a)_NH	Second floor (Level 3)	
Tsi 4(a)_NH	Adjacent to ETFE-foil cushion 1 surface (Level 4)	
Tsi 2(b)_NH	First floor (Level 2)	
Tsi 3(b)_NH	Second floor (Level 3)	
Tsi 4(b)_NH	Adjacent to ETFE-foil cushion 2 surface (Level 4)	
Tsi 1(c)_NH	Ground floor (Level 1)	Middle of the atrium
Tsi 2(c)_NH	First floor (Level 2)	
Tsi 3(c)_NH	Second floor (Level 3)	

Table 3-5: Location of surface temperature sensors

Sensor Identification		Location	Measured temperatures represent
ST_Loc 1_NH	Cushion 1	External	Middle of the cushion
ST_Loc 2_NH			Edge of the cushion
ST_Loc 3_NH		Internal	Middle of the cushion
ST_Loc 4_NH			Middle of the cushion
ST_Loc 5_NH			Edge of the cushion
ST_Loc 7_NH	Cushion 2	Internal	Middle of the cushion



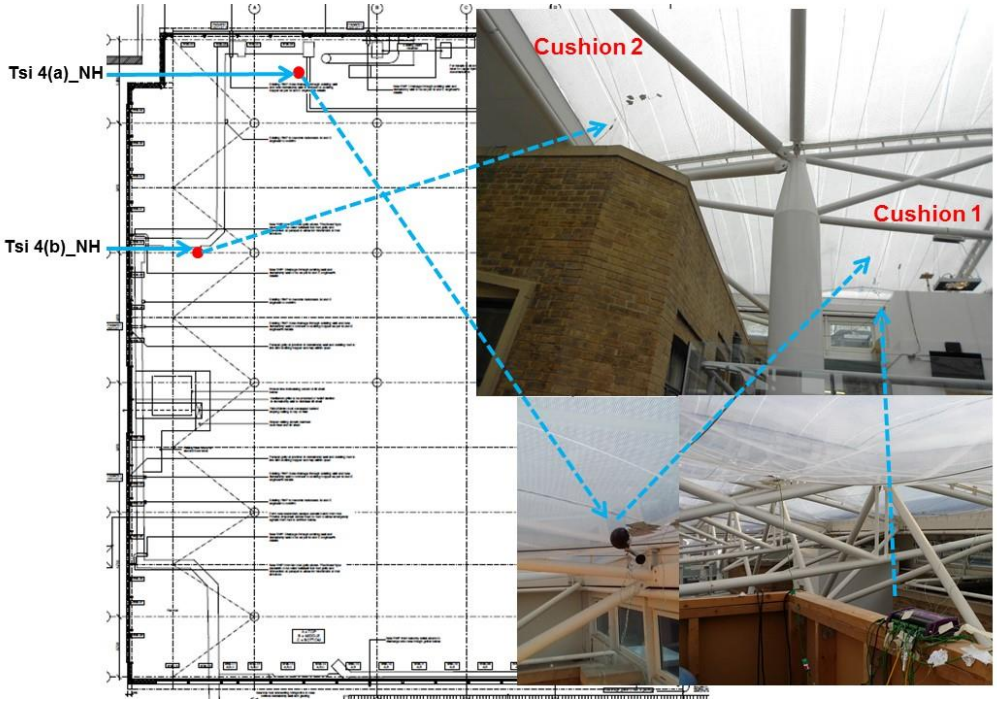
(a) Ground floor (Occupied level 1) [Figure 3-8 continued to the next page]



(b) First floor (Occupied level 2)



(c) Second floor (Occupied level 3) [Figure 3-8 continued to the next page]



(d) Below ETFE-foil cushion roof (Level 4)

Figure 3-8: Location of the data logger (a,b,c) and temperature sensors in (a) Ground floor, (b) First floor, (c) Second floor, (d) Level 4, Plan (nts)- drawing courtesy of Maber Architects, Photo - Sabrina Afrin

3.8.4.2 Air temperature sensors

Thermocouples (ϕ0.1 mm, K-type) were distributed vertically and horizontally in various plan position inside the atrium. Figure 3-8 shows location of these temperature sensors located at the ground floor, first floor and second floor of the atrium. While placing these sensors, it was considered that sensors would not interfere with school activities which was also advised by school management. Thermocouple tips were shielded in lightweight thin aluminium tubes to minimise influence of incident radiation and moisture on measured air temperatures. During the school holiday period between 21st August and 1st September 2015, the air temperatures in the middle of the atrium were measured using Tiny tag data loggers. This location was described as Location c in Figure 3-8.

3.8.4.3 Mean radiant temperature sensors

Harvie (1996), suggested that CIBSE (CIBSE, 2006, CIBSE, 2015b) method for measuring mean radiant temperature using blackened globe might not be appropriate for monitoring the thermal performance of fast response spaces enclosed by membranes. Because this sort of globe could take up to 20 minutes to reach equilibrium temperature (Parsons, 2003). Therefore the thick black globe recommended by CIBSE (CIBSE, 2006, CIBSE, 2015b) was also considered

inappropriate for this study. However, it was also necessary to ensure safety of school students. Thus, light weight black balls with diameter 40mm were selected in order to measure mean-radiant temperature. Thermocouples were placed inside the black globe which was sealed to make it airtight. These sensors were calibrated comparing measured mean radiant temperature with a hand-held thermometer (PCE-WB 20SD) before and after installation. Temperature data recorded using both type of sensors varied within (+/-) 0.25˚C ~ 0.4˚C. Figure 3-9 presents air temperature and mean radiant temperature sensors located near to the ETFE-foil cushion roof, and hand-held thermometer (PCE-WB 20SD).



(a) (b)

Figure 3-9: (a) Air temperature and mean radiant temperature sensors, (b) Thermometer (PCE-WB 20SD)

3.8.4.4 Surface temperature sensors

Thermocouples (K-type) were attached to external and the internal surface of ETFE-foil cushion using 3M Silver Tape.

From the Pilot study, it was evident that surface temperature varies in different locations of a cushion. Therefore, to see this temperature variation, sensors were attached at four locations internally and two locations externally in Cushion 1. A temperature sensor was also attached to Cushion 2 but internally only. Figure 3-10 presents location of the cushions where sensors were attached whereas the location of temperature sensors attached to the Cushion 1 and Cushion 2 surfaces are illustrated in Figure 3-11. The Estate Manager agreed to drill a hole in the roof parapet to establish a connection between external surface temperature sensors, external pyranometer and internal data logger.

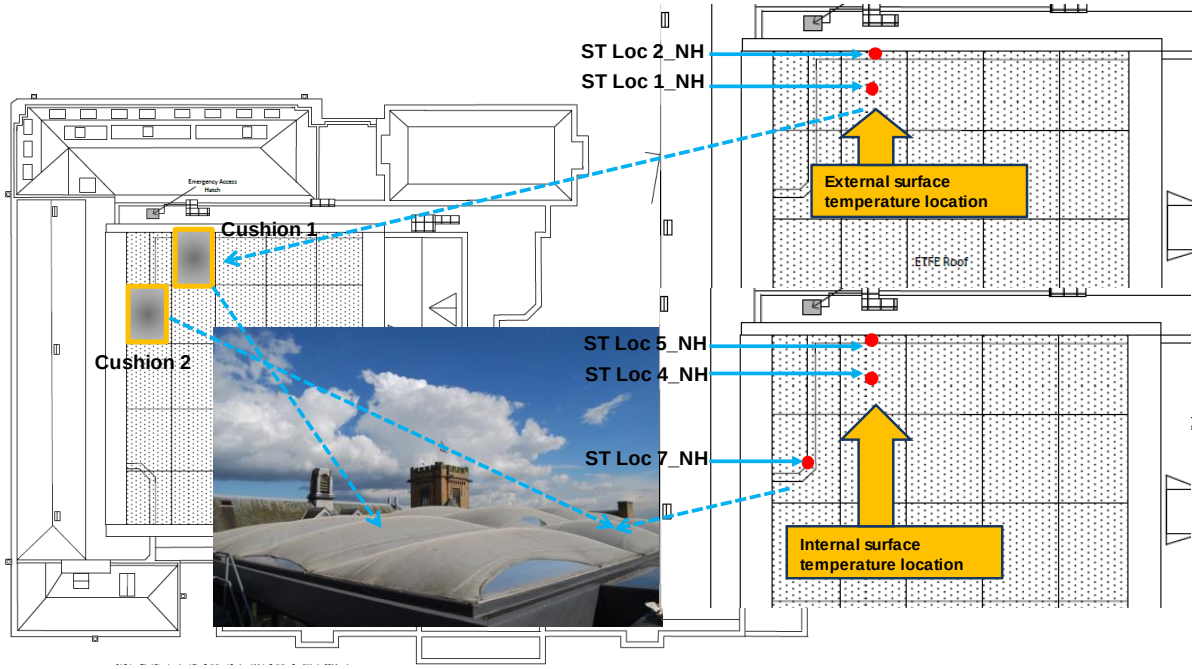
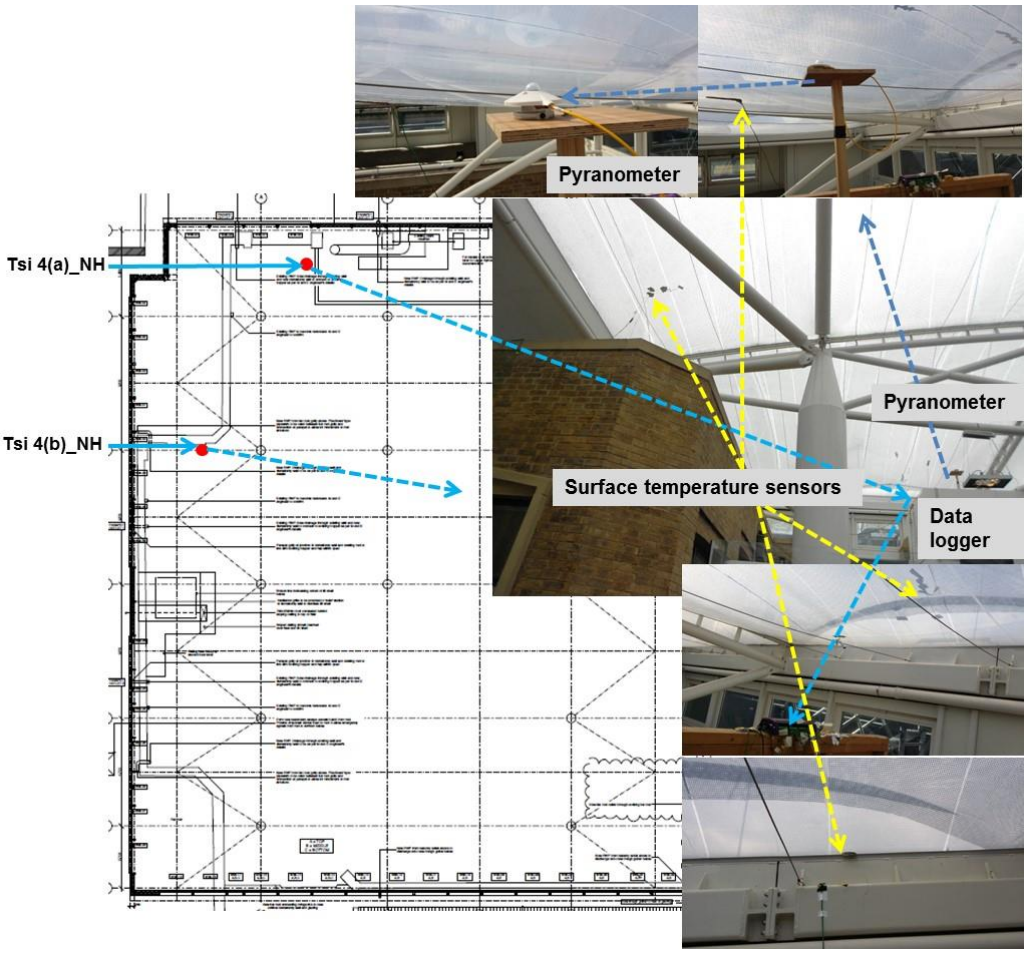


Figure 3-10: Plan (nts) showing ETFE-foil cushion roof and location of the monitored cushion, outlined in orange, surface temperature (both external and internal sensors location pointed in red (Drawing courtesy of Maber Architects, Nottingham), Photo -Sabrina Afrin



(a) Internal roof plan (nts) [Figure 3-11 continued to the next pages]



(b) External surface temperature sensors

Figure 3-11: Location of -(a) internal surface temperature sensors attached to cushion 1 & 2, solar radiation sensors placed on the internal roof, (b) external surface temperature sensors (cushion 1), solar radiation sensors adjacent to ETFE-foil cushion roof. Plan (nts)- drawing courtesy of Maber Architects, Photo -Sabrina Afrin

3.8.4.5 Indoor and outdoor irradiance

Two Kipp&Zonen CMP3 Pyranometer (sensitive wavelength band: 0.3-2.8µm) were positioned adjacent to the ETFE-foil Cushion 1. One was positioned internally to measure transmitted total solar radiation and the other one was positioned externally to measure incident total solar radiation. The internal pyranometer was positioned just below the Cushion 1, and the external pyranometer was placed on the external roof, adjacent to the Cushion 1. The distance between the internal and external pyranometers were two metres (approx.). These solar radiation sensors were not used to provide accurate tracking of the sun inside the space because the position of the sensors and obvious shading created by the supporting structures would render difficulties in the accuracy. The fundamental aim of measuring incident and transmitted radiation via the ETFE-foil cushion roof was to identify its impact on the internal thermal environment. It was observed that internal pyranometer was shaded by supporting and surrounding structures, therefore a frame was mounted around the external pyranometer to provide approximately similar shading characteristics. It was also considered that this measurement could highlight short-term phenomenon experienced on the site, e.g. passage of an isolated cloud in front of the sun, clear sky radiation blocked by moving cloud, diffuse radiation in the absence of direct radiation during the overcast day etc. Because of limited resources, it was only possible to measure transmitted radiation through Cushion 1. Furthermore, external radiation

sensors were placed adjacent to Cushion 1 because the area adjacent to Cushion 2 was shaded by adjacent structures.

3.8.4.6 Relative humidity

During the monitoring period, internal relative humidity was recorded both in winter and summer period. In winter this was done by placing Tiny Tag Plus 2- TGP-4017 data logger near to the ETFE-foil cushion to examine the risk of condensation. In summer, it was measured to observe the extent of variation in humidity in different occupied levels.

3.8.5 Weather data

Weather data was collected at a regular interval from the weather station placed at a distance of 30 metres (approx.) from the southeast part of the ETFE-foil cushion roof (marked in red in Figure 3-12). This weather station records external ambient temperature, relative humidity, wind speed, wind direction, and rainfall at five minute intervals. However, for a limited period (May 2014 to July 2014) a sensor was placed near to the ETFE-foil cushion roof (location marked in yellow in Figure 3-12) to record outdoor ambient temperature and humidity at five minute intervals.



Figure 3-12: Weather station location on Nottingham High School roof

3.8.6 Data collection and synthesis

In order to see the actual impact of outdoor conditions on the indoor thermal condition, it was necessary to combine indoor parameters recorded using the equipment described in section 3.8.4 with outdoor weather data. The data collection and synthesis process used in this research are presented in Figure 3-13.

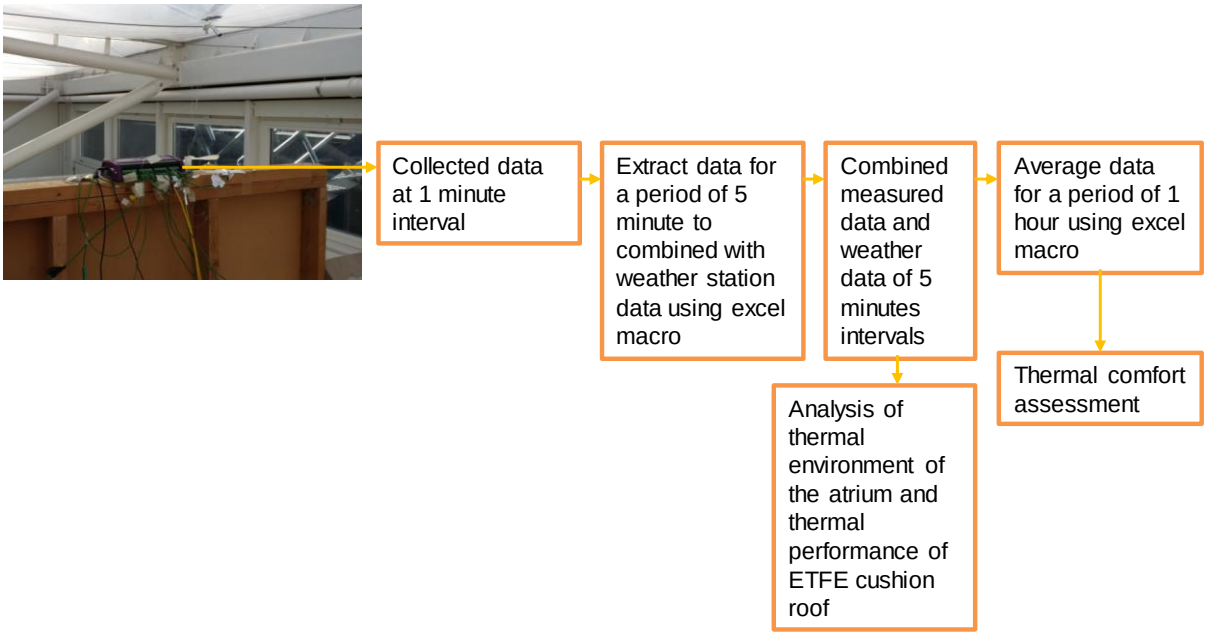


Figure 3-13: Data collection and synthesis

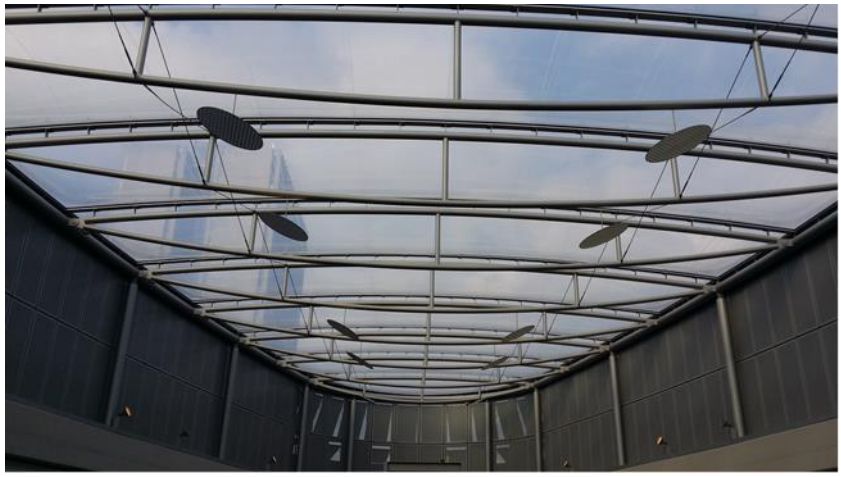
3.9 Case Study B: Engineering and Science Learning Centre (ESLC), Nottingham, UK

3.9.1 Building information

The Engineering & Science Learning Centre at the University of Nottingham is located at the University Park Campus. This three-storey building was built during 2011. This building contains support centre, graduate centre, learning and teaching space, seminar rooms, computer rooms, seating spaces and a central atrium [see Figure 3-14 (b)] used for multipurpose activities. According to the designer, this large atrium is the heart of the building and varying capacity rooms are arranged off the atrium on all three floors. The main purpose of using ETFE-foil cushion roof was to gain natural light through a lightweight roof.



(a) **(b)**



(c)

Figure 3-14: (a) Engineering and Science Learning Centre, University of Nottingham, (b) The atrium, (c) ETFE-foil cushion roof of ELSC [Photo- Sabrina Afrin]

The atrium roof consists of three–layer, ETFE-foil cushions with fritted top layer (200μm), transparent middle (150μm) and the bottom layer (150μm), complete with aluminum framing, inflation and air management equipment with associated air handling pipework and connections. In turn, these are supported by steel trusses and peripheral structure.

3.9.2 Building usage pattern

The ground floor of the atrium is mostly used for multi-purpose activities e.g. fair, research activities, social gathering etc. whereas there is open seating arrangement on the first and second floor of the atrium which is mostly used by the students. Graduate centre and computer rooms located at second floor are also occupied by students. Moreover, office space at ground floor is occupied throughout the year. Timetabled rooms and seminar spaces on the first floor and second floor are mainly occupied during term time when the university operates.

3.9.3 Services

The building and its system operate between 8am to 8pm with most activities taking place in the building between 9am and 5pm. The primary heating system in the atrium consists of the ground source heat pump, district heating, under floor heating system with BMS controlled heating/cooling. Glazed motorised louvre windows are provided at both low and high level of the atrium to maintain the temperature and CO_2 levels at comfortable levels. This ventilation system operates if the temperature exceeds 21°C during weekdays or 25°C at the weekend. An atrium under floor heating system operates throughout the year when the average atrium air temperature drops below 20°C.

3.9.4 Building regulation compliance

The building achieved a BREEAM (Building Research Establishment Environmental Assessment Method) excellent rating with energy performance rating of 35 (B: 26-50). The U-value of the building fabric according to BRUKL output document, in compliance with England and Wales Building Regulation Part L are listed in Table 3-6.

Table 3-6: U-value of the building fabric (Estate, University of Nottingham)

Element	U- value (calculated)
Wall	0.23 W/m^{2}K
Floor	0.2 W/m^{2}K
Roof	0.2 W/m^{2}K
Windows, roof windows and roof lights	1.98 W/m^{2}K
Doors	2.19 W/m^{2}K

3.9.5 Post occupancy evaluation

A post occupancy evaluation of the ESLC was carried out in 2012 by the university Estates Department. Various issues were identified by the users of the building. According to the office space users at ground floor, the hot air from the atrium caused discomfort as ventilation of the atrium ground floor was through the automatic windows of this office space. Later window setting was changed from automatic to manual operation, so that users of the office can operate windows when required. Office and seminar room users raised another issue related to the rain noise generated from the ETFE-foil cushion roof during heavy rain.

3.9.6 Installed monitoring equipment

The on-site monitoring started from July 2014 and ended in September 2015. The detailed monitoring procedure is described in the following sections.

3.9.6.1 Data logger

In the ESLC building's atrium, the ETFE-foil cushion roof was not accessible. Therefore, similar to the previous case study it was not possible to position the sensors close to the ETFE-foil cushion roof. However, there was a lift in the atrium and the lift shaft roof was the highest accessible position close to the ETFE-foil cushion roof. A DT 80 data logger was placed on this roof (see Figure 3-15). Sensors positioned (Location a) at the different levels of the atrium were connected with this Data logger (DT 80).



(a) (b)

Figure 3-15: (a) Installation of data logger and sensors on the lift roof, (b) location of data logger

Table 3-7: Location of temperature sensors

Sensor Identification	Location	Measured thermal conditions represent
Tsi 1(a)_ESLC	Ground floor (Level 1)	Part of the atrium adjacent to class rooms, circulation space
Tsi 2(a)_ ESLC	First floor (Level 2)	
Tsi 3(a)_ ESLC	Second floor (Level 3)	
Tsi 4(a)_ ESLC	Adjacent to ETFE-foil cushion 1 surface (Level 4)	
Tsi 1 (b)_ ESLC	Ground floor (Level 1)	
Tsi 2 (b)_ ESLC	First floor (Level 2)	
Tsi 3 (b)_ ESLC	Second floor (Level 3)	

3.9.6.2 Air temperature sensors

Thermocouples (ϕ0.1 mm, K-type) were distributed vertically from the top of the lift shaft roof towards the ground floor of the atrium. In total 10no. thermocouples were used to measure air temperature of the atrium. Thermocouple tips were shielded in lightweight thin aluminium tubes to minimise the influence of incident radiation and moisture on measured air temperature. Location of these sensors are specified as Location a and illustrated in Figure 3-16. Through personal communication with University of Nottingham Estate, it was possible to collect air temperature data from the building management system. The temperature sensors associated with the BMS system were placed 8 metres away from Location a. These temperature sensors are

located at each occupied level of the atrium and recorded data at 15 minute intervals. Location of these sensors are specified as Location b (see Figure 3-17). Sensor identification and location in the atrium is specified in Table 3-7.

.

3.9.6.3 Mean radiant temperature sensors

Similar to the previous case study mean-radiant temperature was measured by using lightweight black balls (diameter 40mm). Thermocouples were placed inside the black globe which was sealed to make it airtight. Figure 3-16 presents the location of these mean radiant sensors at various occupied levels of the atrium.

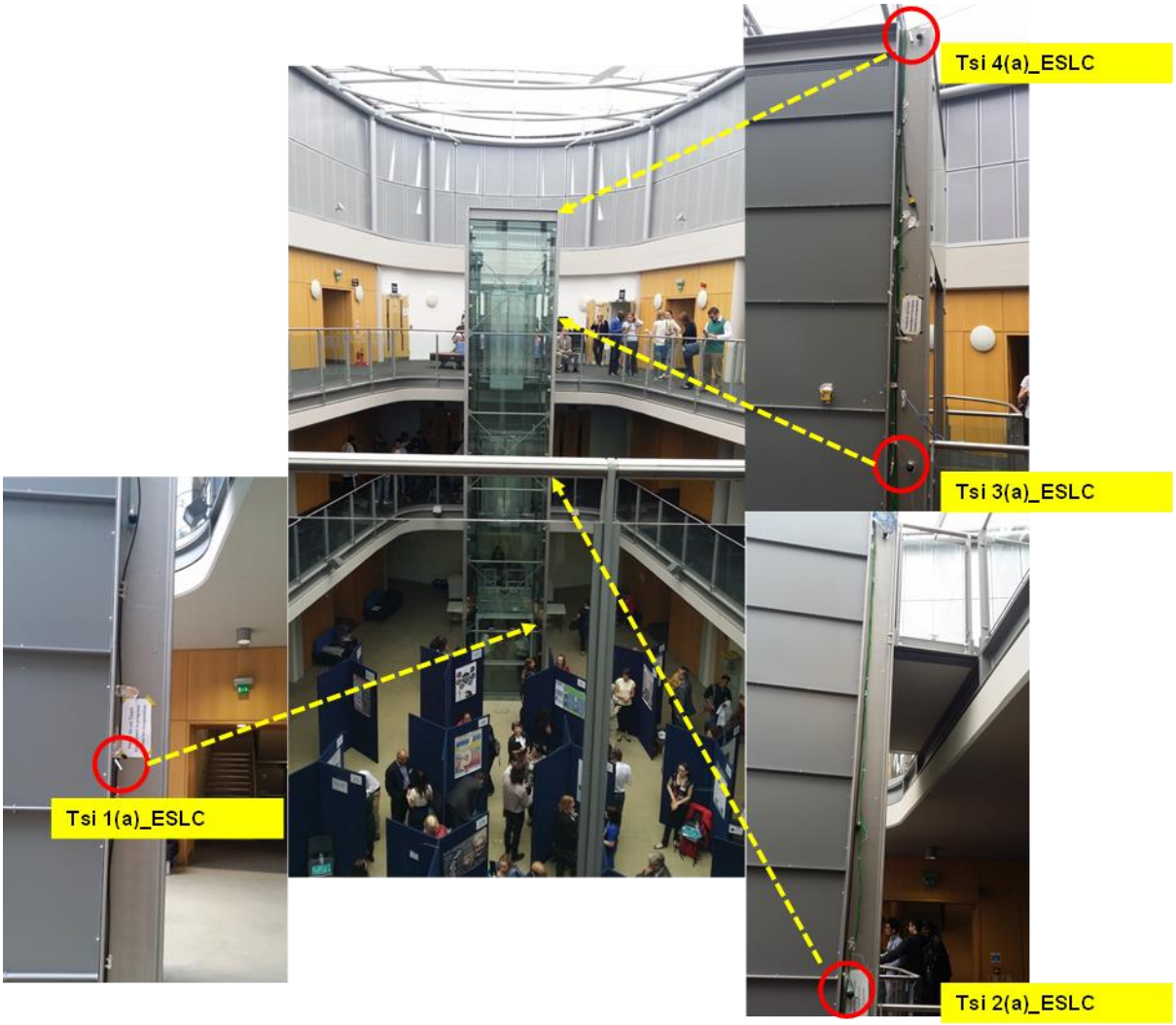


Figure 3-16: Air temperature and mean radiant temperature sensors at different occupied levels of the atrium (Location a)

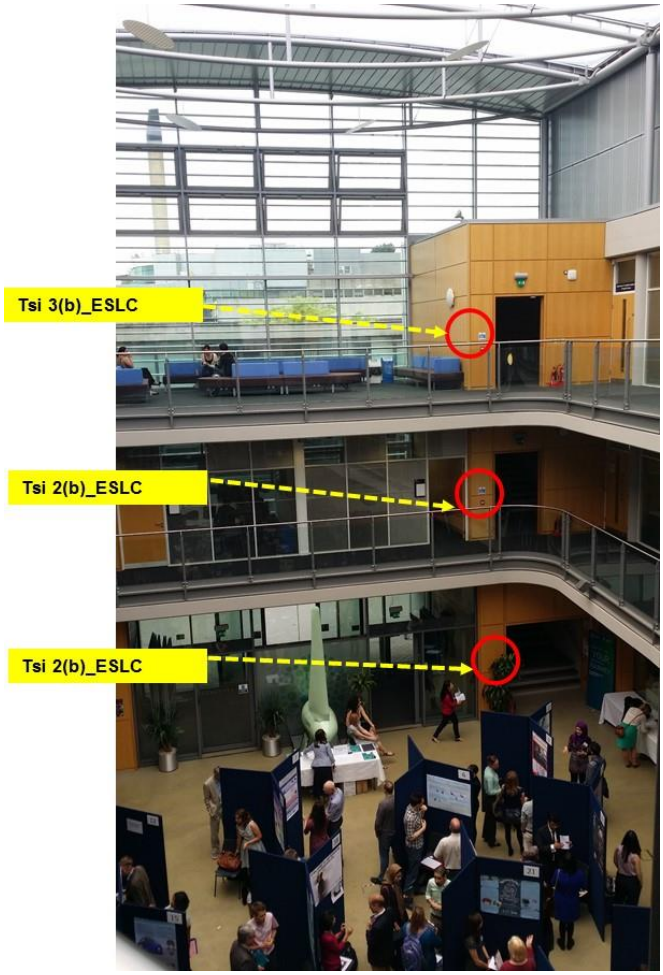


Figure 3-17: Air temperature sensors at different levels of the atrium (Location b)

3.9.6.4 Surface temperature sensors

It was mentioned earlier that the ETFE-foil cushion roof was not accessible in the ESLC building. Therefore, it was not possible to attached sensors to the ETFE-foil cushion surface.

3.9.6.5 Indoor irradiance

Transmitted solar radiation was measured by Kipp & Zonen CMP3 Pyranometer (sensitive wavelength band: 0.3-2.8µm). This pyranometer was positioned internally on top of the lift roof. Figure 3-18 shows location of the internal pyranometer.



Figure 3-18: Location of the external and internal solar radiation sensors with respect to ETFE-foil cushion roof

3.9.6.6 Relative humidity

Indoor relative humidity of the occupied level 3 in summer was recorded using Tiny Tag Plus 2- TGP-4017 data logger. The purpose was to examine its variability particularly in the level that was exposed to the ETFE-foil cushion roof.

3.9.6.7 Weather data

Outdoor air temperature and relative humidity was recorded using Tiny Tag Plus 2-TGP-4017 data logger. External total solar radiation was measured by Kipp & Zonen CMP3 Pyranometer, (sensitive wavelength band: 0.3-2.8µm) which was placed externally on a different roof 10 metres (approx.) apart from the ETFE-foil cushion roof of ESLC (Figure 3-18). Weather data was also collected from weather station positioned on top of the EoN house, which is located near the School of Architecture and Built-Environment, University of Nottingham. This weather station is located approximately 0.7 miles away from the Engineering and Science Learning Centre building.

3.10 Thermal comfort assessment method

This section discusses the thermal comfort assessment methods that were applied to evaluate the thermal performance of Nottingham High School and Engineering and Science Leaning Centre atria.

3.10.1 CIBSE Temperature benchmark

The Chartered Institution of Building Services Engineers (CIBSE) has published several guides on environmental design of buildings. CIBSE Environmental Guide A (CIBSE, 2006, CIBSE, 2015b) provides temperature benchmarks or thresholds to identify buildings' overheating performance. This temperature threshold remains the same, irrespective of the time of year and geographical location. CIBSE guide A states the following criteria to assess overheating.

I. Criterion: The building will be overheated when peak temperature exceeds more than 1% of annual occupied hours above 28°C.

3.10.2 Building Bulletin 101

Approved document Part L2A (HMGovernment, 2010b) and Part F1 (HMGovernment, 2010a) referred Building Bulletin 101 (UKGOV, 2014) as a source of guidance for assessing overheating risk in educational buildings. According to The Building Bulletin 101 the performance standards for summertime overheating in compliance with the Approved Document Part L2 are following:

1) Criterion 1: There should be no more than 120 hours when the air temperature in the teaching and learning space rises above 28°C
2) Criterion 2: The average internal air temperature should no more than 5°C above the outdoor air temperature
3) Criterion 3: The internal air temperature should not exceed 32°C during the occupied hours

The Approved Document also stated that proposed school buildings should meet at least two of the above criteria in order to comply with the performance standard and demonstrate that teaching and learning spaces will not suffer from overheating. Although BB101 considers external conditions by limiting temperature difference between outdoor and indoor air temperature it does not consider occupant's vulnerabilities. Because during the summer period, it allows air temperature of 28°C for the duration up to 120 hours (22% of the occupied hours). Acceptable temperature and percentage of occupied hours both are quite high, the relationship between outdoor and the indoor temperature is not realistic also. As a result, many schools designed according to BB101 suffered from a number of difficulties e.g. overheating, excessive energy use for heating, draught etc.(CIBSE, 2015c).

3.10.3 Adaptive comfort criteria to assess overheating

Thermal comfort range is influenced by the outside temperature and people can adapt to a wider range of temperatures depending on their thermal experience of outdoor temperatures of previous days (de Dear et al. 1998; de Dear & Brager 2002; Nicol & Humphreys 2002). Thus, this provides a wider range of acceptable temperatures specifically for naturally ventilated buildings. This concept is adopted in later standards known as adaptive thermal comfort models and included in ASHRAE, BS EN and CIBSE guides (BSEN15251, 2007, ASHRAE, 2013, CIBSE, 2013a).

The CIBSE overheating task force has considered adaptive thermal comfort models and decided that it is no longer suitable to have a fixed indoor temperature regardless of the outdoor conditions. This task force also suggested the application of an adaptive approach for overheating assessment of free-running buildings, where the target indoor temperature should reflect the outdoor temperature at that time (Nicol et al., 2012). Lomas and Giridharan (2012) recommended using an adaptive approach while analysing comfort conditions of the occupant in current and future UK climate. However, in free running buildings occupant discomfort is related to the temperature difference between the operative temperature and the comfort temperature whereas comfort temperature changes with outdoor temperature.

CIBSE TM57 (CIBSE, 2015d) is the latest guide for integrated school design, which specifies a temperature benchmark similar to that stated in BS EN 15251 (2007) and CIBSE TM52 (CIBSE, 2013b). CIBSE TM52 (CIBSE, 2013b) gives specific guidance on thermal comfort and overheating analysis for the UK. This guide provides various thermal comfort and overheating criteria and summarises their use based on building/usage types. The adaptive comfort criteria for free running - naturally ventilated buildings are primarily based on BS EN 15251 (2007) adaptive comfort models. The CIBSE TM52 specified three criteria to evaluate overheating in free-running buildings. These criteria are presented in the following:

a) Criterion 1: Hours of exceedance (He)

The number of hours (He) during which ΔT (difference between maximum acceptable temperature and operative temperature) is greater than or equal to one degree (K) during the period between May and September inclusive shall not be more than three per cent of occupied hours.

b) Criterion 2: Daily weighted exceedance (We)

To allow for the severity of overheating on any individual day weighted exceedance (We) shall be less than or equal to 6 in any one day. The following equation can be used to calculate this weighted exceedance:

$$We = \sum[(h\_e\ )\times WF] \quad \text{.....(3.1)}$$

$$= (h\_e0\times 0) + (h\_e1\times 1) + (h\_e2\times 2) + (h\_e3\times 3) \quad \text{.....(3.2)}$$

Where the weighting factor $WF = 0$, if ΔT ≤ 0, otherwise $WF = \Delta T$, and h_{ey} is the time (h) when $WF = y$. Further details are available on CIBSE TM52 guide (CIBSE 2013).

c) Criterion 3: Upper limit temperature (T_{upp})

The difference between operative temperature and maximum acceptable temperature (ΔT) should not be more than 4K.

A free-running building that fails to meet any two of the above criteria would be classified as overheated.

- Running mean temperature (T_{rm})

The calculation of acceptable temperature limits is based on running mean temperature, which is the weighted average of outdoor mean temperatures for the previous seven days. According to BS EN 15251 (2007), running mean temperature can be calculated using the following formula:

$$T_{rm} = (1-\alpha).(T_{ed-1} + \alpha.T_{ed-2} + \alpha 2.T_{ed-3} \ldots) \quad \text{.....(3.3)}$$

Where,

T_{rm} = running mean temperature;

T_{ed-1} = Daily mean outdoor temperature for the previous day;

T_{ed-2} = Daily mean outdoor temperature for the day before and so on;

α is a constant between 0 and 1 (recommended to use 0.8).

Adaptive comfort upper and lower limit temperatures determine the thermal comfort band, means people will be satisfied when the indoor operative temperature is within

this limit. Upper and lower limit temperatures can be calculated by following Equation 3.5 and Equation 3.6 respectively, when running mean temperatures are known:

$$T_{comf} = 0.33\,T_{rm} + 18.8 \quad \text{.....(3.4)}$$

$$T_{max} = 0.33\,T_{rm} + 21.8 \quad \text{.....(3.5)}$$

$$T_{min} = 0.33\,T_{rm} + 15.8 \quad \text{.....(3.6)}$$

Where, T_{comf} (˚C) is the comfort temperature, T_{max} (˚C) is the maximum acceptable temperature and T_{min} (˚C) is the minimum acceptable temperature.

Equation 3.3 was used in most of the previous studies to calculate running mean temperatures (Lomas & R Giridharan 2012; Ferrari & Zanotto 2012; Sameni et al. 2015).

According to BS EN 15251 (BSEN15251, 2007) the risk of overheating relates to comfort temperature, along with the categories of building and its users. Acceptable temperature ranges for different categories of the building are listed in Table 3-8. Here CIBSE (2013a), (CIBSE, 2015d) suggested that designers should aim to remain within Category II limits.

Table 3-8: Suggested applicability of the categories and their associated acceptable temperature range for free running buildings (Standards, 2008)

Category	Description	Acceptable range (K)
I	Spaces occupied by very sensitive and fragile persons	+/-2
II	Normal expectation (for new and renovated building)	+/-3
III	A moderate expectation (used for existing building)	+/-4
IV	Values outside the criteria for the above categories (only acceptable for limited periods)	>4

This study applied overheating assessment methods - CIBSE temperature benchmark and adaptive comfort criteria to assess overheating in the Nottingham High School and Engineering and Science Learning Centre atrium. Overheating criterion specified in Building Bulletin 101 were also applied to assess the thermal condition of Nottingham High School atrium. This was considered because the school atrium was built in 2009 when BB101 was the benchmark to assess comfort conditions of renovated and new school buildings. A number of case studies of schools presented in CIBSE (2015d),

also used BB101 to assess overheating in recent times. On the basis of overheating analysis methods thermal performance of both atria enclosed with ETFE-foil cushion roof were evaluated. This is presented in Chapter 6.

3.11 Building Simulation

3.11.1 Dynamic thermal simulation

Models are abstract representations of buildings. In the case of environmental performance simulation, the model presents a three dimensional geometric representation of the building with essential elements (such as doors, windows, ventilation, occupancy, internal gains, climate, etc.). The dynamic thermal simulation (DTS) is the process of simulating a building's thermal performance on an hourly basis using specific climate data with the range of input variables. The flexibility of loading various climate data in the same model made the process suitable to evaluate thermal performance using projected climate scenarios.

3.11.2 Simulation

The use of simulation software has escalated in the building performance domain because of the increased computing power by desktop computers and improvement of calculation algorithms. The process and standards of building performance modelling is provided by CIBSE AM11 (CIBSE, 2015a) in the UK. The guides provide methods of calculation and guidance on modelling procedure for thermal, ventilation, lighting and energy performance of buildings. Among various software Design Builder, TRNSYS, Tas, IES-VE and Hevacomp are widely used packages which provide CIBSE AM11 recommended calculation ability. The simulation engine EnergyPlus (NREL, 2015) is a software developed by US Department of Energy (DOE) and used as a background calculation engine in Design Builder and Hevacomp packages. EnergyPlus also allows to import geometry from Google SketchUp using the OpenStudio Plug-in (NREL, 2016). Design Builder can be used in association with TRNSYS to simulate the behaviour of transient systems to assess performance of thermal and electrical energy systems (TRNSYS, 2016). IES-VE is integrated with an integrated DTS engine called ApacheSim, which is capable to perform detailed simulation with the ability to handle complex inputs and geometric shapes.

According to Byrn and Schiefloe (1996), selection of software packages for simulation depends on the type of work (e.g. simplified design tools are used in the early design stage while detailed simulation tools are used when design evolves and details are available etc.), accuracy of software and individual preferences. Gilbert (2006),

reviewed different software that were used for simulation, assessments and design purposes. He investigated the capability, usability, level of integration of different software packages. On the basis of the investigation, his study recommended to use Tas for thermal simulation. This was because, according to the investigation, Tas has the best workflow methodology and also provides flexibility to model complex systems and simulation results will be as accurate as any other competitive software. An investigation carried by Rodrigues (2009) also used Tas for thermal performance analysis. This study also used Environmental Design Solutions Limited (EDSL) Tas Version 9.3.3.b. Tas simulates the thermal performance using dynamic calculations based on the response factor method (EDSL, 2016). The dynamic simulation tool EDSL Tas consists of two parts, the Tas 3D modeller and Tas building simulator. The building geometry is modelled in the Tas modeller which is then exported to the Building simulator. The functions of the software are:

- The assessment of the environmental performance of the building
- Prediction of energy consumption
- Natural ventilation analysis (basic level)
- Day light factor (basic level)

3.12 Summary

This chapter presented the detailed methodologies required to obtain the objectives of the research. The chapter also presented the findings of a pilot study, which defined the detailed methodologies adopted to investigate the thermal performance of the ETFE-foil cushions. The pilot study was conducted by collecting physical environmental data (air temperature and solar radiation) from Nottingham High School atrium between 21st August 2013 and 25th August 2013. A summary of findings from the pilot study is:

- The space enclosed with ETFE-foil cushion envelope is very responsive to external weather conditions e.g. solar radiation, outdoor ambient temperature.
- Significant variation of indoor air temperature was apparent between different vertical levels of the atrium.
- During the day the surface of the ETFE-foil cushion was hotter than indoor air temperatures of the floor adjacent to the roof.
- There might be an effect of heat transfer between the ETFE-foil cushion surface and the space adjacent to it.

- The surface temperature of the ETFE-foil varies in a single cushion (identified by thermal imaging).

On the basis of the above observation it was decided to investigate the thermal performance of ETFE-foil, and the space enclosed with the ETFE-foil cushion envelope separately.

It was proposed that the thermal performance of the ETFE-foil should be investigated by adopting the following methods:

- measurement of thermal-optical properties of ETFE-foil,
- test rig investigation, and
- modelling and simulation.

Thermal-optical properties of the ETFE-foil are to be measured using spectrometers and analysed using BSEN 410 (BSI, 2011). A test rig investigation is to be conducted by collecting data from simplified test rigs equipped with ETFE-foil panels of different configuration (single-layer, two-layer, and three-layer); the test rigs are to be placed on a roof terrace and directly exposed to outdoor conditions to obtain unobstructed solar radiation. Modelling and simulation are to be conducted to validate the measured data and compare the test rig results against glass panels. Detailed descriptions are discussed in Chapter 5 and 7.

Thermal performance of the space enclosed with ETFE-foil cushions was investigated in a pilot study. Further studies are proposed adopting the following methods:

- On-site monitoring of the actual spaces: Air temperature, mean radiant temperature, incident and transmitted solar radiation, and relative humidity were measured using sensors and data loggers within the space. Temperature sensors were placed in each levels at varying heights to identify stratification (Figure 3-8, Figure 3-16 and Figure 3-17). Further details of the data collection and analysis are presented in Chapter 6.
- Modelling and simulation: To estimate predicted thermal performance of spaces enclosed with ETFE-foil cushions using dynamic simulation Tas version 9.3.3.b.
- Assessment of htermal comfort of actual buildings and predicted model using criteria described in section 3.10.

Chapter 4

4 Measuring thermal-optical properties of ETFE foil

4.1 Introduction

This chapter investigates thermal optical properties of ETFE foils. It initially reviews the methods adopted in previous studies to determine the thermal-optical properties of ETFE-foils. Subsequently it discusses the justification of selection of the methods and finally presents thermal-optical properties of single, two- and three-layer ETFE-foil panels. Findings of this chapter address Objective 2, which is to independently determine thermal-optical properties of ETFE-foil.

4.2 The Classification of Thermal Optical Properties

The thermal optical properties of a material define its typical radiant behaviour within the thermal spectrum (Bauer, 1965). These properties are considered as a function of three fundamental parameters, they are: transmittance, reflectance and absorptance. These parameters describe the ratio of the transmitted, reflected and, absorbed radiant flux, to the incident radiant flux (ASTM, 1986b) and sum to 1.0.

The Earth receives electromagnetic as well as corpuscular radiation from the sun. The electromagnetic radiation emits from the sun is known as the solar radiation. The solar radiation, incident on the upper boundary of the terrestrial atmosphere is known as extra-terrestrial solar radiation. The extra-terrestrial solar radiation varies with time of the year because the distance from the sun to the earth varies due to the elliptical orbit, on which earth moves round the sun (Badescu., 2008).

Solar radiation is attenuated by scattering and absorption by the molecules of the air, aerosol particles suspended in the air, water droplets and, ice crystals etc., on its path through the atmosphere. Direct solar radiation is the part of the extra-terrestrial solar radiation that reaches the Earth's surface. The solar radiation incident on a surface being normal to the solar beam is called direct normal solar radiation. The part of solar radiation scattered in the atmosphere and reaches to the earth surface is known as diffuse solar radiation. The sum of direct and diffuse solar radiation on a horizontal plane at the Earth's surface is called global solar radiation (Kasten et al., 1989).

Around 97% of solar radiation reaching the Earth's surface is within the range between 0.3 µm and 2.3 µm, however, 97% of the radiation emerging from a hot surface will be

within 3µm and 50µm (ASTM, 1982). The latter varies with temperature and occurs within the longwave infrared waveband. Fundamentally the higher the temperature of a surface, it emits radiation at a lower wavelength.

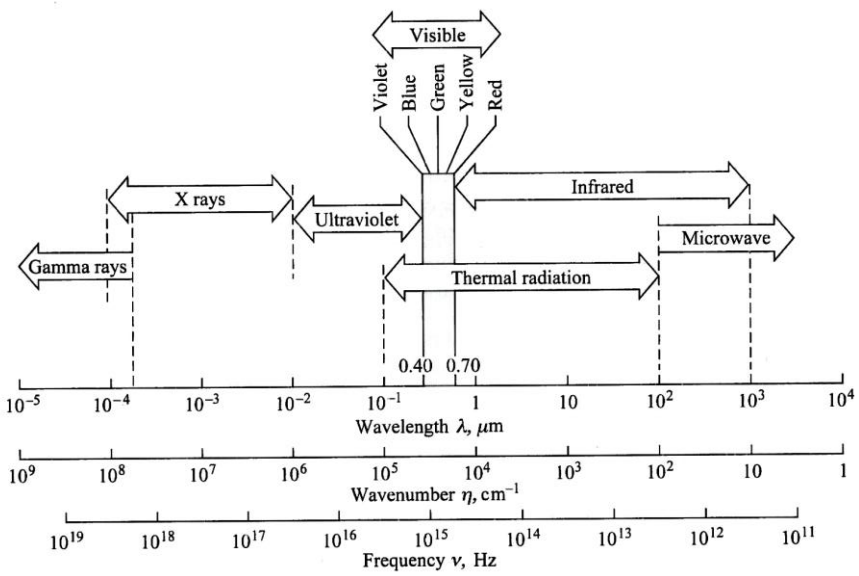


Figure 4-1: Electromagnetic wave spectrum [for radiation travelling through vacuum, refractive index 'n=1'] (Incropera et al., 2013)

The range of radiation wavebands of different wavelength is stated in Figure 4-1, where thermal radiation is the part that ranges from 0.1µm (ultraviolet) to 100µm (mid infra-red). Hence thermal radiation includes the waveband of solar radiation (short-wave) and longwave infra-red radiation. Thus, knowledge of the spectral properties of ETFE-foil covering this entire thermal spectrum would be advantageous because this will determine the amount of solar radiation and longwave radiation exchange through the ETFE-foil envelope. That in turn will effect the thermal performance of ETFE-foils and spaces enclosed with ETFE-foil cushion envelope.

4.3 Methods used in previous studies

Robinson-Gayle (2003), carried out an investigation on the normal and angular transmittance of ETFE foil samples. A calibrated Perkin Elmer PE883 spectrometer was used to measure the spectral transmittance of ETFE-foils for wavelength between 295nm and 2500nm. The results obtained from the spectrometer were then used to calculate solar and light transmittance of ETFE foils by using methods described in ISO 9050:2003 (ISO, 2003). The results obtained on solar and light transmittance of ETFE foils showed that clear foils had high solar (91%-94%) and light transmission (90%-93%). Robinson-Gayle (2003) also, investigated angular transmittance of ETFE foil samples, which was carried out in the National Physical Laboratory (NPL). The results (see Figure 4-2) revealed that transmittance through the ETFE sample was

insensitive to the angle of incidence. It was found during the experiment that, 80% of the light transmitted through ETFE-foil sample was at 180° to the angle of incidence, which was similar to the total transmittance through the sample. The study also stated that even at low solar angles the majority of sunlight would be transmitted through ETFE foil into the space enclosed with it.

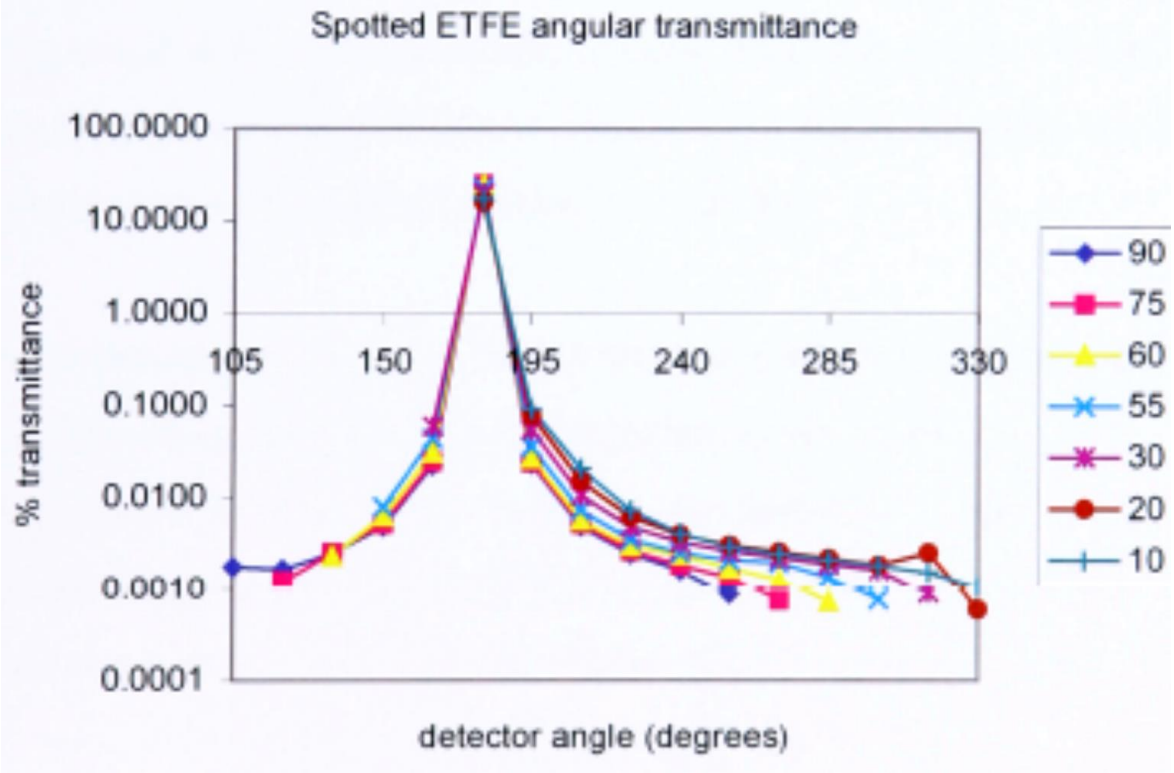


Figure 4-2: Angular transmittance of 100 µm ETFE sheet at various detector and sample angles (Robinson-Gayle, 2003)

Thus, it can be assumed that normal, as well as the angular transmittance of transparent ETFE foil samples for the entire spectrum, would be similar. The reason behind this can be the thinness and transparency of ETFE foils which makes it different from fabric membranes, those were investigated by Harvie (1996) and Devulder (2004). However, for ETFE-foils of different colour and fritting, this phenomenon could be different because of the scattering of light on ETFE-foil surface.

Dimitriadou (2015), carried out transmittance test of different types of ETFE-foil using a Fourier Transform Infra-Red Perkin Elmer Spectrum 100 spectrometer. The ETFE-foil samples were examined between wavelength 2500nm and 16,667nm. The study discussed and compared transmittance of different types of ETFE-foil samples at different wavelengths where light and solar transmittance were based on average transmittance between wavelength 2500nm and 16,667nm. BS EN 410: 2011 (updated version of ISO 9050:2003) specified methods to calculate thermal optical

properties of single, two- and three-layer glazing systems. However, Dimitriadou (2015), did not consider any particular method to determine transmittance of ETFE-foils. Information provided on the transmittance of ETFE-foil samples seemed unreliable. Therefore results determined by Dimitriadou (2015) was not considered in this study while comparing measured results with previous research.

Mainini et al. (2014), measured spectral transmittance and reflectance of ETFE-foil samples with a UV-Vis-NIR Spectrophotometer Perkin Elmer Lambda 950. On the basis of result acquired from the spectrophotometer, actual transmittance and reflectance of single layer foil were calculated according to ISO 9050:2003.

Methods adopted by Robinson-Gayle (2003) and Mainini et al. (2014), to determine spectral properties of ETFE-foils were similar. Both used a spectrometer to measure spectral transmittance and reflectance, while overall transmittance of ETFE foils were calculated based on the method stated in ISO 9050:2003. These methods applied in previous studies are found suitable to determine solar and light transmittance of ETFE-foil samples for this study.

4.4 Justification

The thermal optical properties of transparent/ translucent building envelopes impact the thermal environment of enclosed spaces by allowing access of external environmental stimuli such as solar radiation, outdoor temperature, etc. This phenomenon was evident in the previous chapter, where the results of the pilot study demonstrated that an ETFE foil cushion transmits a significant amount of solar radiation affecting the thermal performance of the space it encloses. Therefore, it was thought to be necessary to obtain the overall solar transmittance and light transmittance of a selection of ETFE-foils. Collectively these properties are known as thermal optical properties (Bauer, 1965).

On the other hand, the knowledge of the thermal transmittance (U-value) of building envelope is necessary for the quantification of heat losses and (or) gain through it. Thus, it was necessary to determine thermal transmittance of the ETFE-foil cushion envelope also.

According to Harvie (2015), it can be difficult to obtain thermal optical properties of architectural fabrics and foils (e.g. PVC coated polyester, PTFE coated glass, ETFE foil, etc.), because manufacturers are more used to supplying information about structural performance. Moreover, the specification sheet of manufacturers reflects the priorities of the designers which tend to be as follows:

- Structural properties
- Behaviour in fire
- Colour and degradation
- Transmittance of visual light

However, an attempt was made to compile data available from the manufacturers on the thermal optical properties of ETFE-foils. From the acquired information, it was also evident that the available information tended to concentrate on structural rather than environmental properties. The standard information on the thermal properties included solar transmittance and reflectance, and U-value of single layer foil etc. The limited available information on the thermal properties of ETFE-foils might be due to that, in most countries, there are regulatory requirements for the maximum thermal transmittance or a minimum thermal resistance, while no regulations impose any strict value for optical properties of glazing material to limit solar gain. Thus, the information on material properties tended to fulfil regulatory requirements and priorities of the designers. As a result, the environmental properties obtained from the manufacturer's information were incomplete, unsubstantiated and also entirely inadequate.

It also proved difficult while collecting information on these properties from previous research work carried by Robinson-Gayle (2003), Mainini et al. (2014), DETR (2003), Dimitriadou (2015). Poirazis et al. (2009), also found difficulties while obtaining information on the thermal optical properties of ETFE foils, particularly in the longwave spectrum. His research suggested that detailed knowledge on this area is essential to predict the impact of longwave radiation on the thermal performance of space enclosed by an ETFE-foil cushion envelope. He also stated that as ETFE-foil is not entirely opaque to longwave radiation, considering ETFE-foil as glass while simulating building's performance might result in significant error. Besides Harvie (2015), suggested that accurate modelling of architectural fabrics requires specification on optical thermal properties which can be developed based on either a specific request to the manufacturers, measurements or assumption made on the known properties of similar materials. Therefore, measurement and documentation of thermal optical properties of different types of ETFE-foils are important to determine their impact on the thermal performance of spaces.

It was apparent from the above discussion that the most appropriate way to acquire the appropriate information necessary for this research would be to measure the thermal optical properties of ETFE foils. The following sections describe the experimental techniques that were carried out to measure the thermal optical

properties of different types of ETFE foils. Information obtained by these procedures was used to develop the simulation model used to predict the thermal performance of ETFE foils and spaces enclosed with it, which is presented in Chapter 7.

4.5 The thermal optical properties of ETFE foil

Thermal optical properties of materials are measured by shining a beam of radiation of known wavelength on to the surface of a material sample and comparing the intensity of the incident beam to that of transmitted, reflected and absorbed radiation. Because of the smoothness of the surface of thin (100μm- 500 μm), transparent ETFE foils it is more likely that it will transmit the major part of incident radiation. However, for fritted ETFE-foils the radiation they transmit and reflect, is likely to be partially diffuse. Diffusely transmitted radiation can be measured by placing material samples in front of a standard integrating sphere which will collect all the transmitted radiation (Harvie, 1996).

The equipment required to measure solar optical properties are sensitive and not commonly available. Therefore, with available equipment in the Engineering lab of the University of Nottingham, it was possible to measure *near normal* spectral properties of foil samples between wavelengths of 0.2μm and 2.7μm. This range covered ultra-violet, visible, infrared and mid-infrared range. The term *near normal* refers to the beam of radiation which strikes a sample at an angle of incidence close to its surface normal.

4.5.1 The selection of foil samples

ETFE-foil samples were obtained from Architen Landrell and Vector foiltec, both of them being ETFE-foil enclosure fabricator. These samples included different thicknesses of transparent ETFE-foils, silver foils with different density of pigment and foils with different coverage of fritting. These fritted samples were printed on one side. Fritting or printing on the ETFE-foil surface is generally done by using different colour pigments of different density, using different patterns and motifs with different coverage. Among different patterns, dots of varying degree of coverage and honey comb pattern, etc. are commonly applied in ETFE-foil cushions. Foils with different coverage of fritting refer to the foils printed with different percentage of fritting coverage, such as foil with 75% fritting comprised of 75% fritted area (can be printed with different density of pigments) and 25% transparent area.

Fritted foils examined in this study were categorised by the percentage of fritting and density of pigment used in printing. The pigment colour consisted of silver. Due to the variation in density of pigment in fritting, foils were classified with 25% translucent silver

(light silver), 50% translucent silver (medium silver) and 100% opaque silver (dark silver). Sample types are listed below in Table 4-1. Among the listed samples, Type 3 and Type 6.4 were similar to the foil that was used to construct the ETFE-foil cushion roof of Nottingham High School, which is one of the case study buildings presented in Chapter 6. In this study, solar and light transmittance of different combinations of two- and three-layer ETFE-foils were determined. These properties were applied in the simulation models of existing buildings covered with ETFE cushion roofs and presented in Chapter 7.

Table 4-1: List of ETFE foil samples used to measure solar transmittance and Light transmittance

Type	Thickness	Transparent percentage	Fritted percentage	Colour of fritting	Pigment type
Type 1	100μm	100%			
Type 2	150μm	100%			
Type 3	200μm	100%			
Type 4	300μm	100%			
Type 5	500μm	100%			
Type 6.1	200μm	75%	25%	25% silver (translucent)	Light silver
Type 6.2	200μm	50%	50%	25% silver (translucent)	Light silver
Type 6.3	200μm	35%	65%	25% silver (translucent)	Light silver
Type 6.4	200μm	25%	75%	25% silver (translucent)	Light silver
Type 6.5	200μm	11%	89%	25% silver (translucent)	Light silver
Type 7.1	200μm	75%	25%	50% silver (translucent)	Medium silver
Type 7.2	200μm	50%	50%	50% silver (translucent)	Medium silver
Type 7.3	200μm	35%	65%	50% silver (translucent)	Medium silver
Type 7.4	200μm	25%	75%	50% silver (translucent)	Medium silver
Type 7.5	200μm	11%	89%	50% silver (translucent)	Medium silver
Type 8.1	200μm	75%	25%	100% silver (opaque)	Dark silver
Type 8.2	200μm	50%	50%	100% silver (opaque)	Dark silver
Type 8.3	200μm	35%	65%	100% silver (opaque)	Dark silver
Type 8.4	200μm	25%	75%	100% silver (opaque)	Dark silver
Type 8.5	200μm	11%	89%	100% silver (opaque)	Dark silver

This study also determined solar and light transmittance of two and three layer ETFE-foil panels. Foil combinations used in this process are listed in Table 4-2 and

Table **4-3**.

Table 4-2: List of combination of Two layer ETFE foils

Two layer ETFE foil combinations		
Combination	**Type**	**Layer description**
Combination 1	Type 3	Layer 1: 200 µm Transparent
	Type 6.1	Layer 2: 200 µm 25% Light silver
Combination 2	Type 3	Layer 1: 200 µm Transparent
	Type 6.2	Layer 2: 200 µm 50% Light silver
Combination 3	Type 3	Layer 1: 200 µm Transparent
	Type 6.3	Layer 2: 200 µm 65% Light silver
Combination 4	Type 3	Layer 1: 200 µm Transparent
	Type 6.4	Layer 2: 200 µm 75% Light silver
Combination 5	Type 3	Layer 1: 200 µm Transparent
	Type 6.5	Layer 2: 200 µm 89% Light silver
Combination 6	Type 3	Layer 1: 200 µm Transparent
	Type 7.1	Layer 2: 200 µm 25% Mid silver
Combination 7	Type 3	Layer 1: 200 µm Transparent
	Type 7.2	Layer 2: 200 µm 50% Mid silver
Combination 8	Type 3	Layer 1: 200 µm Transparent
	Type 7.3	Layer 2: 200 µm 65% Mid silver
Combination 9	Type 3	Layer 1: 200 µm Transparent
	Type 7.4	Layer 2: 200 µm 75% Mid silver
Combination 10	Type 3	Layer 1: 200 µm Transparent
	Type 7.5	Layer 2: 200 µm 89% Mid silver
Combination 11	Type 3	Layer 1: 200 µm Transparent
	Type 8.1	Layer 2: 200 µm 25% Dark silver
Combination 12	Type 3	Layer 1: 200 µm Transparent
	Type 8.2	Layer 2: 200 µm 50% Dark silver
Combination 13	Type 3	Layer 1: 200 µm Transparent
	Type 8.3	Layer 2: 200 µm 65% Dark silver
Combination 14	Type 3	Layer 1: 200 µm Transparent
	Type 8.4	Layer 2: 200 µm 75% Dark silver
Combination 15	Type 3	Layer 1: 200 µm Transparent
	Type 8.5	Layer 2: 200 µm 89% Dark silver

Table 4-3: List of combination of Three layer ETFE foils

Three layer ETFE foil combinations		
Combination	**Type**	**Layer description**
	Type 3	Layer 1: 200 µm Transparent
	Type 1	Layer 2: 100 µm Transparent
Combination 16	Type 6.1	Layer 3: 200 µm 25% Light silver
	Type 3	Layer 1: 200 µm Transparent
	Type 1	Layer 2: 100 µm Transparent
Combination 17	Type 6.2	Layer 3: 200 µm 50% Light silver
	Type 3	Layer 1: 200 µm Transparent
	Type 1	Layer 2: 100 µm Transparent
Combination 18	Type 6.3	Layer 3: 200 µm 65% Light silver
	Type 3	Layer 1: 200 µm Transparent
	Type 1	Layer 2: 100 µm Transparent
Combination 19	Type 6.4	Layer 3: 200 µm 75% Light silver
	Type 3	Layer 1: 200 µm Transparent
	Type 1	Layer 2: 100 µm Transparent
Combination 20	Type 6.5	Layer 3: 200 µm 89% Light silver
	Type 3	Layer 1: 200 µm Transparent
	Type 1	Layer 2: 100 µm Transparent
Combination 21	Type 7.1	Layer 3: 200 µm 25% Mid silver
	Type 3	Layer 1: 200 µm Transparent
	Type 1	Layer 2: 100 µm Transparent
Combination 22	Type 7.2	Layer 3: 200 µm 50% Mid silver
	Type 3	Layer 1: 200 µm Transparent
	Type 1	Layer 2: 100 µm Transparent
Combination 23	Type 7.3	Layer 3: 200 µm 65% Mid silver
	Type 3	Layer 1: 200 µm Transparent
	Type 1	Layer 2: 100 µm Transparent
Combination 24	Type 7.4	Layer 3: 200 µm 75% Mid silver
	Type 3	Layer 1: 200 µm Transparent
	Type 1	Layer 2: 100 µm Transparent
Combination 25	Type 7.5	Layer 3: 200 µm 89% Mid silver
	Type 3	Layer 1: 200 µm Transparent
	Type 1	Layer 2: 100 µm Transparent
Combination 26	Type 8.1	Layer 3: 200 µm 25% Dark silver

(

Table 4-3 continued)

Combination	Type	Layer description
	Type 3	Layer 1: 200 µm Transparent
	Type 1	Layer 2: 100 µm Transparent
Combination 27	Type 8.2	Layer 3: 200 µm 50% Dark silver
	Type 3	Layer 1: 200 µm Transparent
	Type 1	Layer 2: 100 µm Transparent
Combination 28	Type 8.3	Layer 3: 200 µm 65% Dark silver
	Type 3	Layer 1: 200 µm Transparent
	Type 1	Layer 2: 100 µm Transparent
Combination 29	Type 8.4	Layer 3: 200 µm 75% Dark silver
	Type 3	Layer 1: 200 µm Transparent
	Type 1	Layer 2: 100 µm Transparent
Combination 30	Type 8.5	Layer 3: 200 µm 89% Dark silver

To compare the thermal optical properties of ETFE-foil with that of glass, the transmittance of different glass samples was determined using the same procedure. Glass samples were obtained from Pilkington glass and included 4mm thick K glass and Opti-float clear glass.

4.5.2 Apparatus used to measure the Solar Optical Properties of the ETFE foil samples

A Biochrom Libra S22 spectrometer [Figure 4-3 (b)] was used to measure the transmittance of foil samples for the wavelengths ranging from 0.2µm to 0.9 µm, which cover ultra violet, visible and near infra-red waveband. During the measurement, the scan step was 1nm and scan speed was 750nm/min.

A Fourier Transform Infrared spectrometer IFS 66v/s [Figure 4-3 (a)] was used to measure spectral transmission for the wavelengths ranging from 0.9 µm to 27 µm, covering near to mid-infrared waveband. Two different setups of the spectrometer were employed to measure the transmittance of ETFE-foil samples. For the first setup, the light source covered wavelengths from 0.869 µm to 1.6 µm (near and, mid-infrared waveband) and the second setup covered wavelength from 1.33 µm to 27 µm (near-infrared and mid-infrared waveband).

The spectrometer had two options to measure transmittance, they are step-scan and rapid-scan mood. During the experiment step-scan option was used because this technique allows the resolution of very weak signals which cannot be detected in the rapid-scan mode. Using step-scan mood, in total 32 scans were acquired at each step. The Fourier transformation was performed for the sum of all these steps.



(a)



(b)

Figure 4-3: Measurement of thermal optical properties using spectrometers- (a) IFS 66v/s, (b) Biochrom Libra S22

Before the experiment, samples were cleaned with lens cleaning fluid to remove dust and particles as much as possible, because the presence of dust might impact the accuracy of measurements. At the beginning of the experiment, an initial spectrometer scan was done without any sample, to calibrate the equipment. If the results showed 100% transmittance, then the sample was positioned in a sample holder, which was placed in between the light source and detector in an air tight box.

In the experiment, a nearly parallel direct beam of light (6mm diameter light source) of known wavelength strikes a sample at an angle of incidence close to its surface normal, passes through the sample and then onto the detector, which measures the

transmitted part of light through the sample. In this process, any scattering of the light beam was interpreted as loss. The transmittance of 8 to 9 pieces of each type of ETFE foil samples (size: 10mm x 10mm) was measured and results obtained from the average values.

The transmittance of silver foil was tested using the printed surface facing opposite the light source, to avoid incident light simply reflecting off the sample, straight back along the path from which it came.

Both spectrometers- Biochrom Libra S22 and IFS 66v/s were operated in a vacuum and air-tight condition, therefore the recorded spectra were free from water vapour, floating particles in the air etc.

4.5.3 Methods

The transmittance of foil samples for the spectral wavelength ranging from 0.2µm to 0.9 µm (ultra violet, visible and near infra-red waveband) was measured using the Biochrom Libra S22 spectrometer. While the Fourier Transform Infrared spectrometer IFS 66v/s was used to measure spectral transmission for the wavelength ranging 0.8 µm to 27 µm (near to mid-infrared waveband). The results obtained from this experiment were used to calculate direct solar and light transmittance of single, two- and three-layer ETFE foils, on the basis of the procedure described in BS EN 410: 2011 (BSI, 2011). Based on calculated direct solar transmittance, total solar energy transmittance (g-value or solar factor) of ETFE samples was obtained using the method stated in BS EN 410: 2011 (BSI, 2011).

Using two different spectrometers: Biochrom Libra S22 and IFS 66v/s, the experiment covered the entire range of wavelengths necessary to calculate the actual light and solar transmittance of single, two and three layers of ETFE foil as described in BS EN 410: 2011 (updated version of ISO 9050:2003). This method is applicable for solar optical properties measured at quasi-parallel, near normal angle of incidence using radiation distribution of illuminant. Importantly it presents the formulae for exact calculation of luminous and solar characteristics of transparent and coated material (BSI, 2011).

Results obtained on the transmittance of foil samples were then used to determine absorptance using Equation 4.1 and reflectance was calculated using Kirchoff relationship (Equation 4.2).

. Absorptance = 2- log (%T) …...(4.1)

$$\text{Transmittance} + \text{Reflectance} + \text{Absorptance} = 1 \qquad \ldots\ldots(4.2)$$

Fritted foils usually consist of the transparent and translucent (printed) part. Therefore, difficulties arose particularly to identify which part the light passed through during the experiment. Because the experiment operated in an air tight box.

Thus, the transmittance of fritted foils was estimated using the transmittance of the transparent part and translucent (printed) part. For example, to determine solar and light transmittance of transparent foil fritted with silver fritting and 25% fritting coverage, the transmittance of transparent foil and silver foil was determined separately. Then the average transmittance for the fritted sample was estimated using the ratio of the fritted part (e.g. 25%) and transparent part (e.g. 75%).

4.5.4 The Results

The results obtained from the experiment are presented and discussed in the following sections.

4.5.4.1 Solar and light transmittance of single layer ETFE foil panel

The solar optical properties of ETFE-foil and glass samples can be characterised as high transmittance up to wavelength 3.0μm. However, transmittance began to decrease at higher wavelengths particularly for glass, while spectral transmittance of ETFE-foils was still high even above a wavelength of 5.0μm. The spectral transmittance of 100 μm, 200 μm and 300μm transparent ETFE-foils and, opti-float and K-glass measured using the spectrometers is presented in Figure 4-4. Solar and, light transmittance, calculated according to BS EN 410: 2011 (BSI, 2011) is presented in Table 4-4. ETFE-foil types are listed in Table 4-1. The results presented in Figure 4-4, showed that in the visible spectrum and infra-red spectrum, the transmittance of ETFE foil was generally higher than that of opti-float glass and k-glass. The spectral transmittance of ETFE-foil reduces as its thickness increases. This is evident from Table 4-4, where the light and solar transmittance of 100μm transparent ETFE foil, according to the method of BS EN 410, was 0.905 and 0.91 respectively, while these values reduce correspondingly to 0.76 and 0.72 for 500μm transparent foil (Figure 4-5). At a wavelength of 5μm and beyond, the spectral transmittance of both glass samples decreased to nearly 0% while ETFE-foil samples still transmitted significant levels of spectral light. This waveband partially includes the longwave range. Therefore, it can be stated that in the longwave range transparent ETFE foils will transmit radiation, while glasses will be effectively opaque for this waveband.

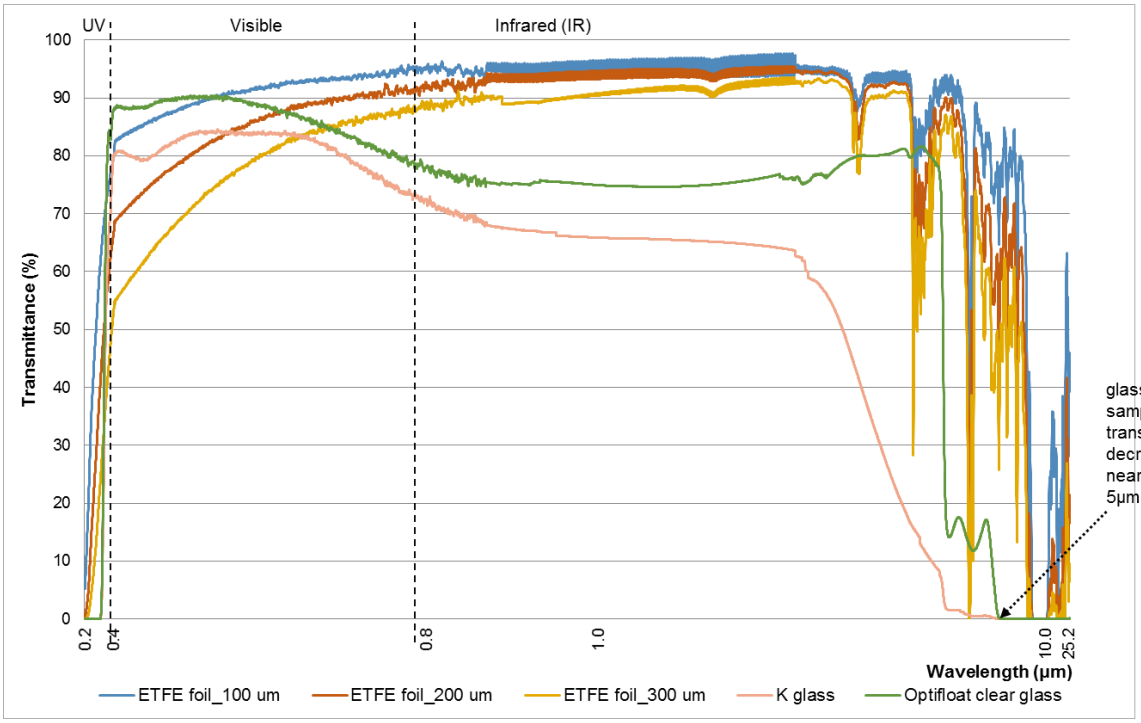


Figure 4-4: Spectral transmittance of ETFE foil and Glass measured using spectrometers

Table 4-4: Direct solar and light transmittance of ETFE foil and glass

Materials	Light transmittance	Light reflectance	Solar transmittance	Solar reflectance
100µm ETFE foil	0.905	0.094	0.91	0.0893
200µm ETFE foil	0.84	0.16	0.857	0.142
300µm ETFE foil	0.76	0.236	0.794	0.2047
Opti-float glass	0.895	0.105	0.66	0.33
K-glass	0.838	0.16	0.494	0.498

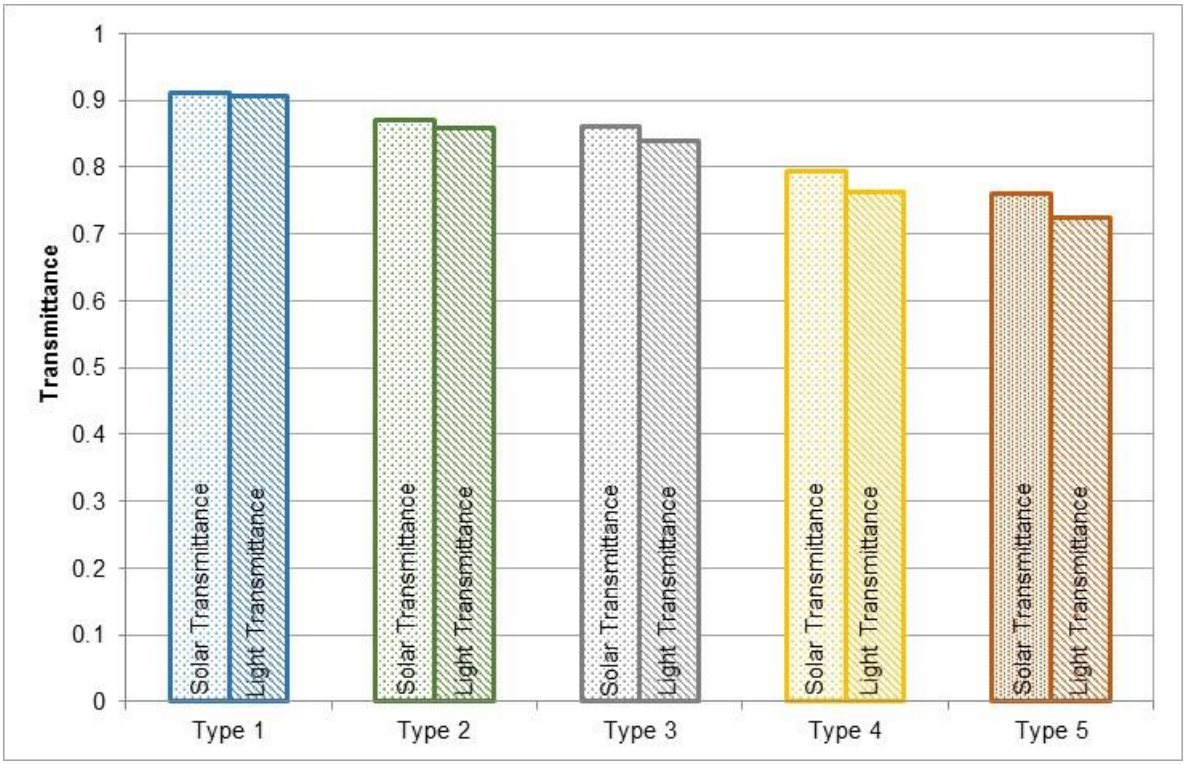


Figure 4-5: Solar Transmittance and Light Transmittance of transparent single layer ETFE foils of different thickness (ETFE-foil types are listed in Table 4-1)

Table 4-5: Total solar energy transmittance (g-value) of single layer ETFE foil

Thickness	Type of ETFE foil	Pigment type	g-value
100µm	transparent		0.91
200µm	transparent		0.86
300µm	transparent		0.79
500µm	transparent		0.76
200µm 25% silver	translucent	Light silver	0.3
200µm 50% silver	translucent	Medium silver	0.07
200µm 100% silver	opaque	Dark silver	0.011

Based on the direct solar transmittance, the total solar energy transmittance (g-value) of transparent, translucent and opaque ETFE-foil samples were determined. The results obtained for total solar energy transmittance of ETFE-foil samples are presented in Table 4-5, which demonstrated that increase of the thickness of foil, the density of pigment in fritted part and fritting coverage reduces total solar energy transmittance considerably. For foil samples, printed with different density of silver pigment, both solar and light transmittance reduces significantly as the density of pigment increased. For example, the solar transmittance of 200µm 25% silver (light silver) foil is 0.3, which reduces to 0.011 for 200µm 100% silver (dark silver) foils.

Figure 4-6 and Figure 4-7 present total solar energy transmittance and light transmittance of single layer fritted foils. Results demonstrated that with an increase of fritting coverage from 25% to 89% of a fritted foil printed with 25% translucent silver (light silver) pigment, overall solar transmittance reduced by 47%. Whereas with the same coverage of 25% fritting, an increase in pigment density from 25% (light silver) to 50% (medium silver) and 100% (dark silver) reduced total solar transmittance by 8.2% and 10.3% respectively. Moreover, it is evident from Figure 4-7 that increase in the percentage of fritted area, as well as the density of pigment in printing, also reduced light transmittance significantly. The maximum light transmittance of 0.708 was calculated for 25% fritted (with 25% translucent light silver pigment) foil, while minimum transmittance was calculated 0.1 for 89% fritted foil printed with opaque silver pigment. Thus, this phenomenon should be taken into consideration while selecting foil type that, it will not only limit solar transmittance but also will allow sufficient daylight required for spaces.

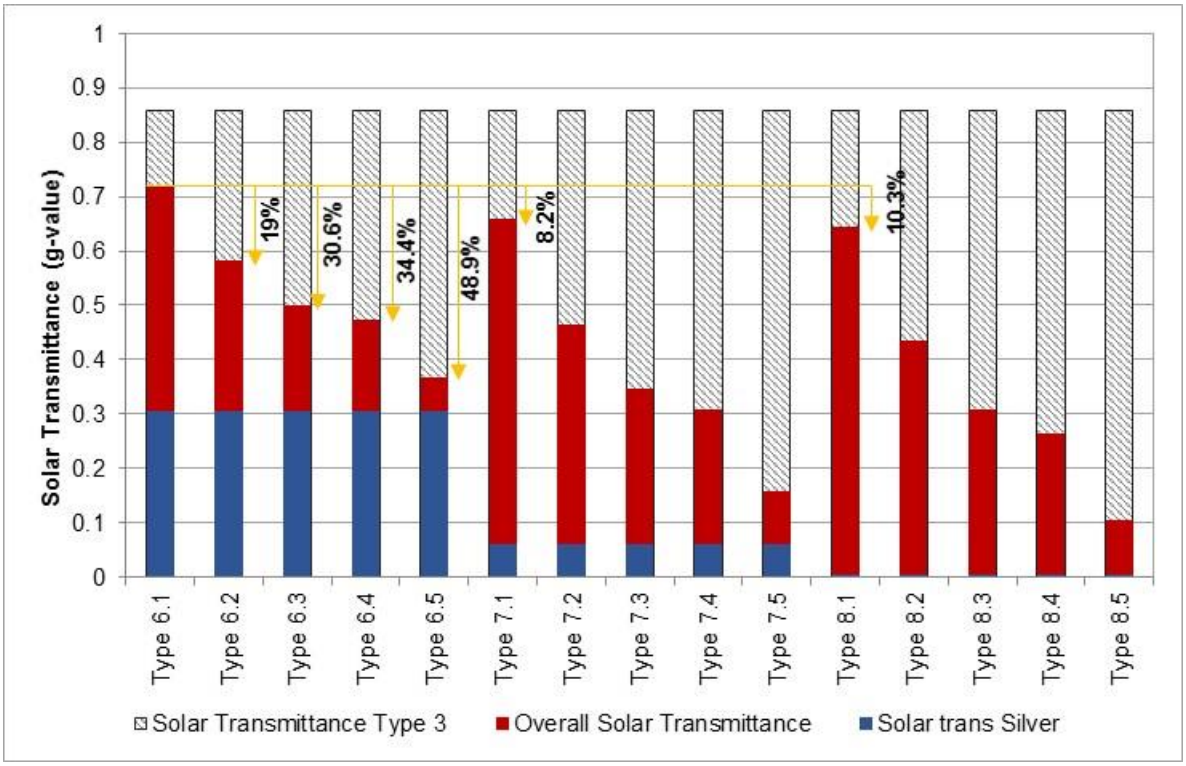


Figure 4-6: Solar Transmittance of single layer fritted ETFE foil panel

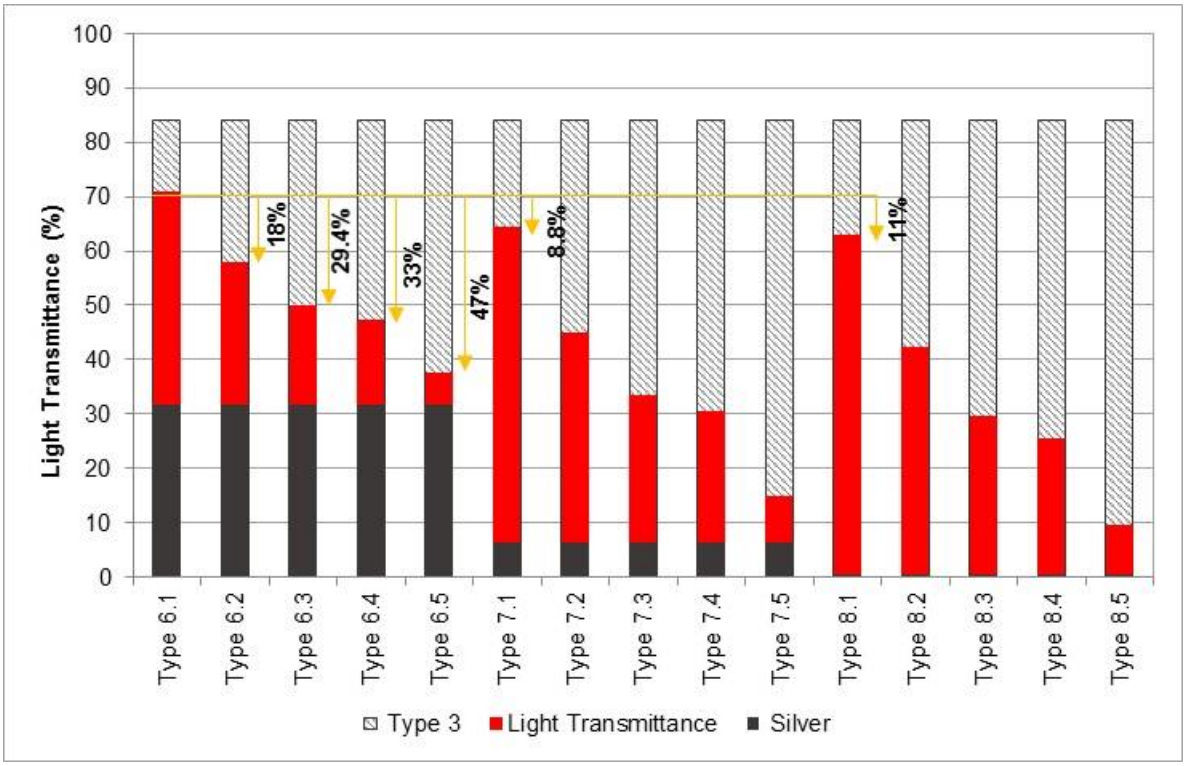


Figure 4-7: Light Transmittance of single layer fritted ETFE foil panel

4.5.4.2 Solar and light transmittance of two-layer and three-layer ETFE foil panel

In the experiment the spectrometers only allowed the spectral transmittance of single layer foil to be measured; hence, the total solar and light transmittance for two-and three-layer ETFE-foil panels was calculated using the method stated in BS EN 410: 2011(BSI, 2011) considering an average air gap of 125mm between foil layers. A list of combinations of two- and three-layer ETFE-foil are presented in Table 4-2 and Table 4-3 respectively.

The results obtained for solar and light transmittance of different combinations of two-layer ETFE-foil panels is illustrated Figure 4-8 and Figure 4-9, while Figure 4-10 and Figure 4-11 present the same properties but for three-layer ETFE-foil panels.

The results demonstrated that in ETFE panels, increase (or decrease) in fritted coverage, increase (or decrease) of the density of pigment, and increase (or decrease) in air gap and ETFE-foil layers, reduce (or increase) overall solar and light transmittance of ETFE-foil panels.

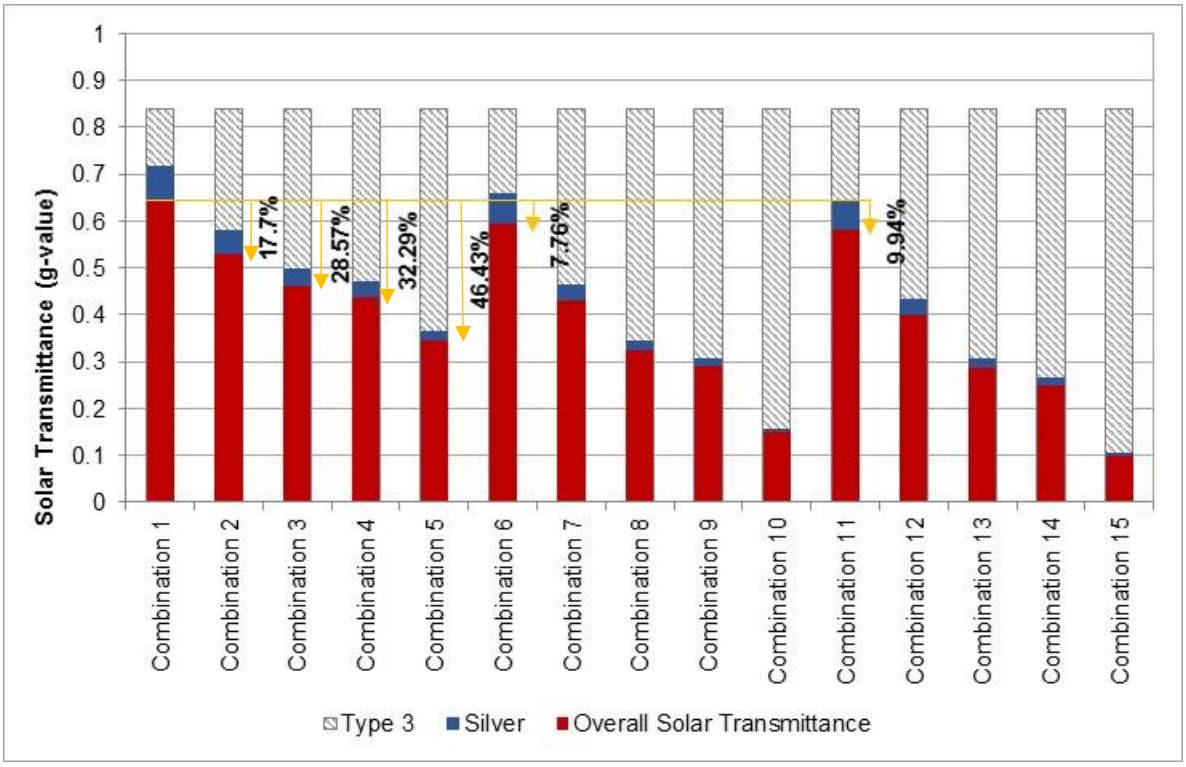


Figure 4-8: Solar Transmittance of two-layer ETFE foil panel

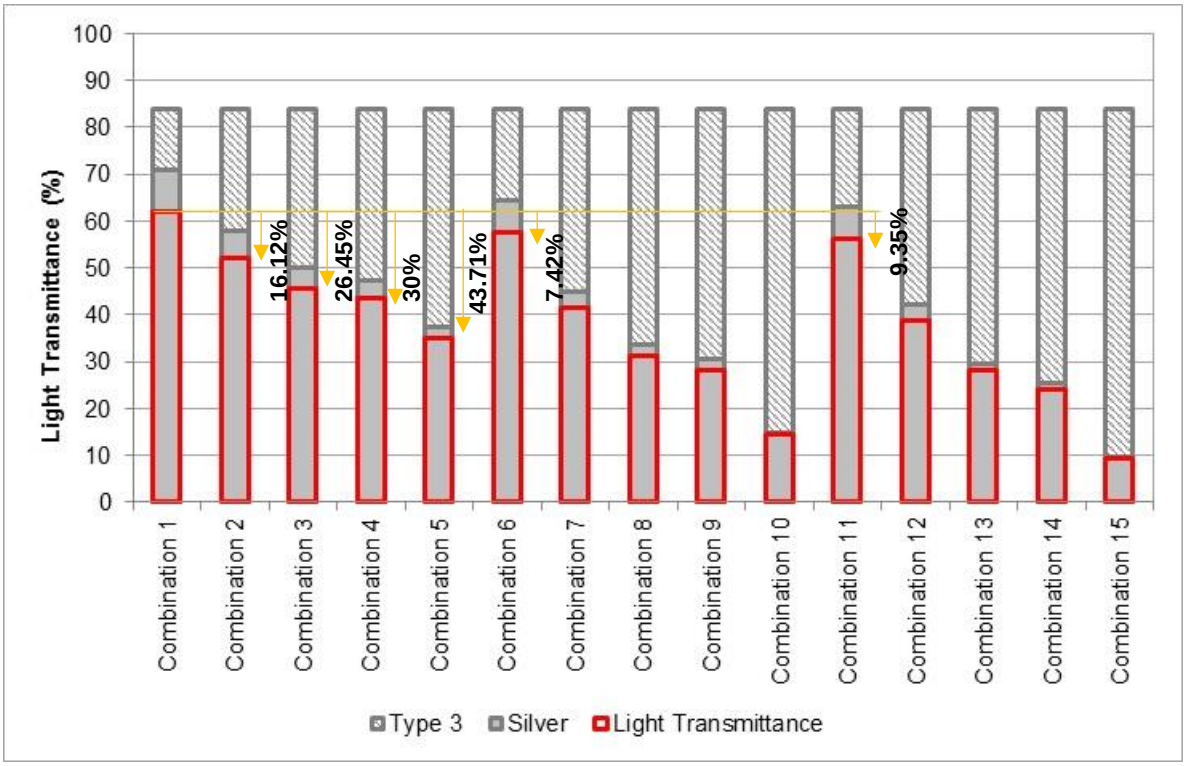


Figure 4-9: Light Transmittance of two-layer ETFE foil panel

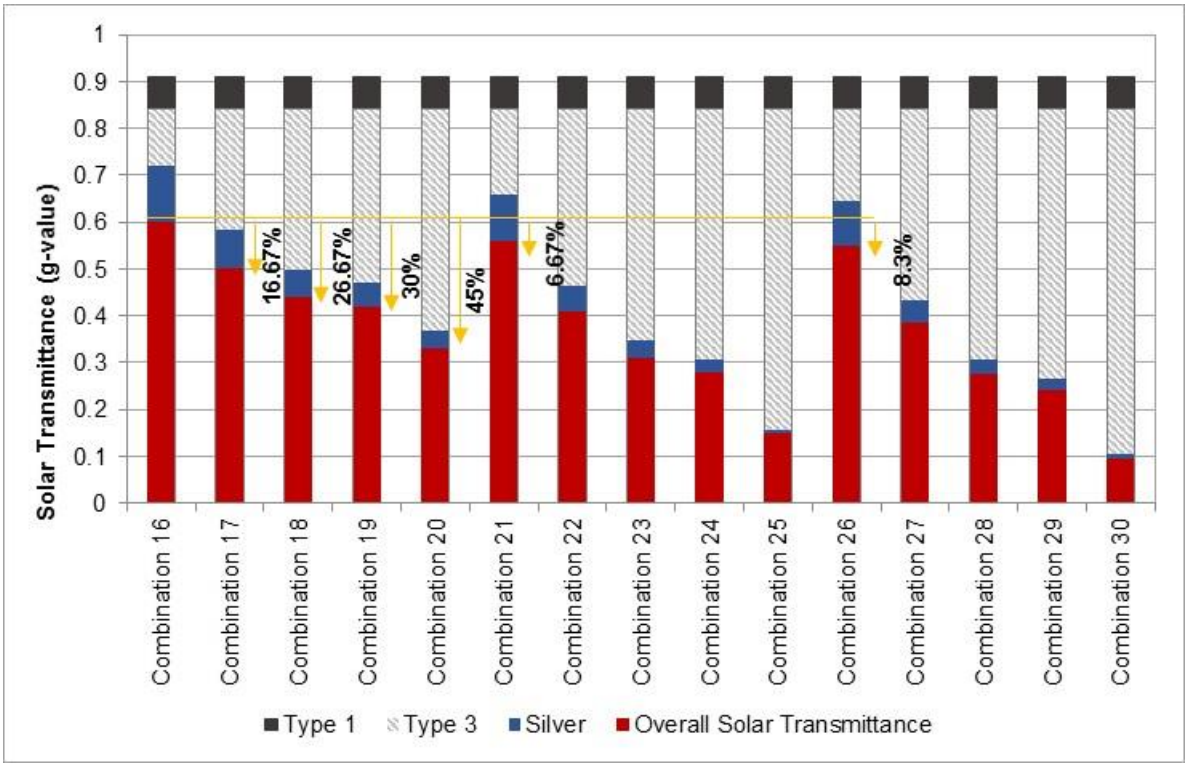


Figure 4-10: Solar Transmittance of three-layer ETFE foil panel

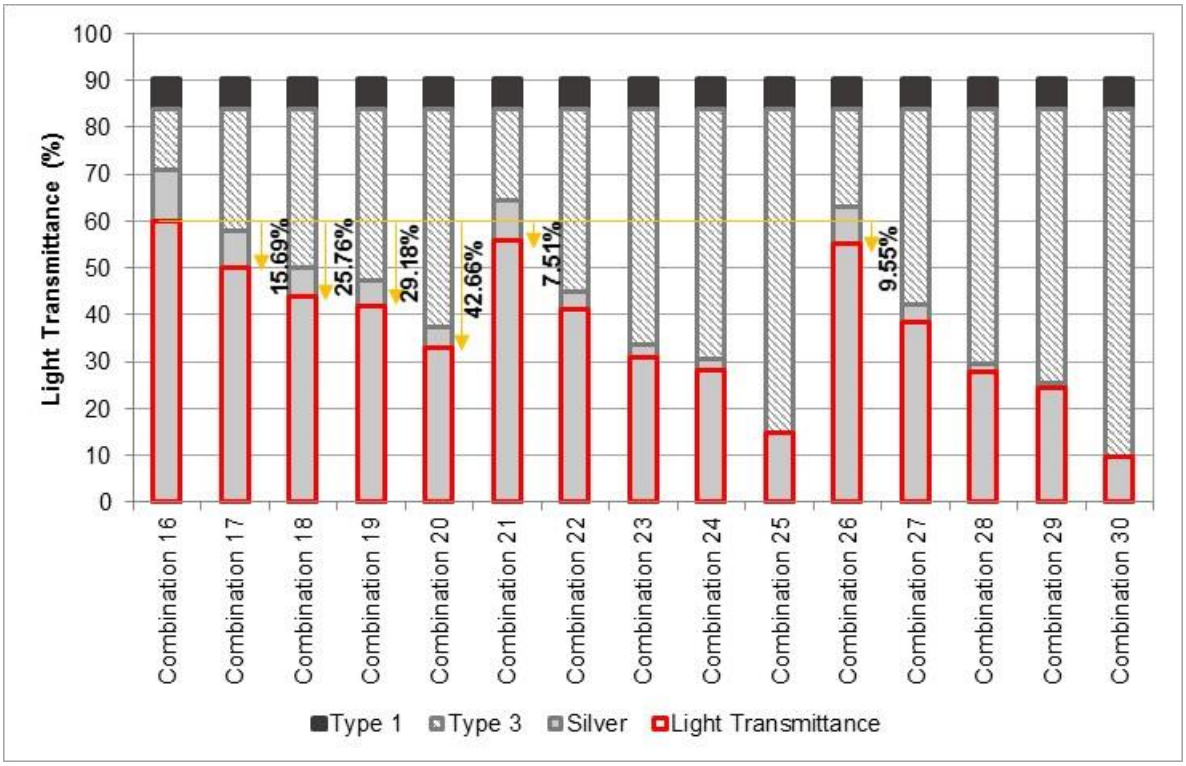


Figure 4-11: Light Transmittance of three-layer ETFE foil panel

The results obtained for direct solar and light transmittance of single-layer ETFE-foil samples were compared with those stated in Robinson-Gayle (2003), DETR (2003) and illustrated in Figure 4-12. The results were in close agreement, with a maximum deviation of 2% being found for both measured light and solar transmittance. The

possible discrepancy was due to the surface condition of samples, techniques employed by the manufacturer during the manufacturing process of polymer foil, spectrometer type used in the experiment etc.

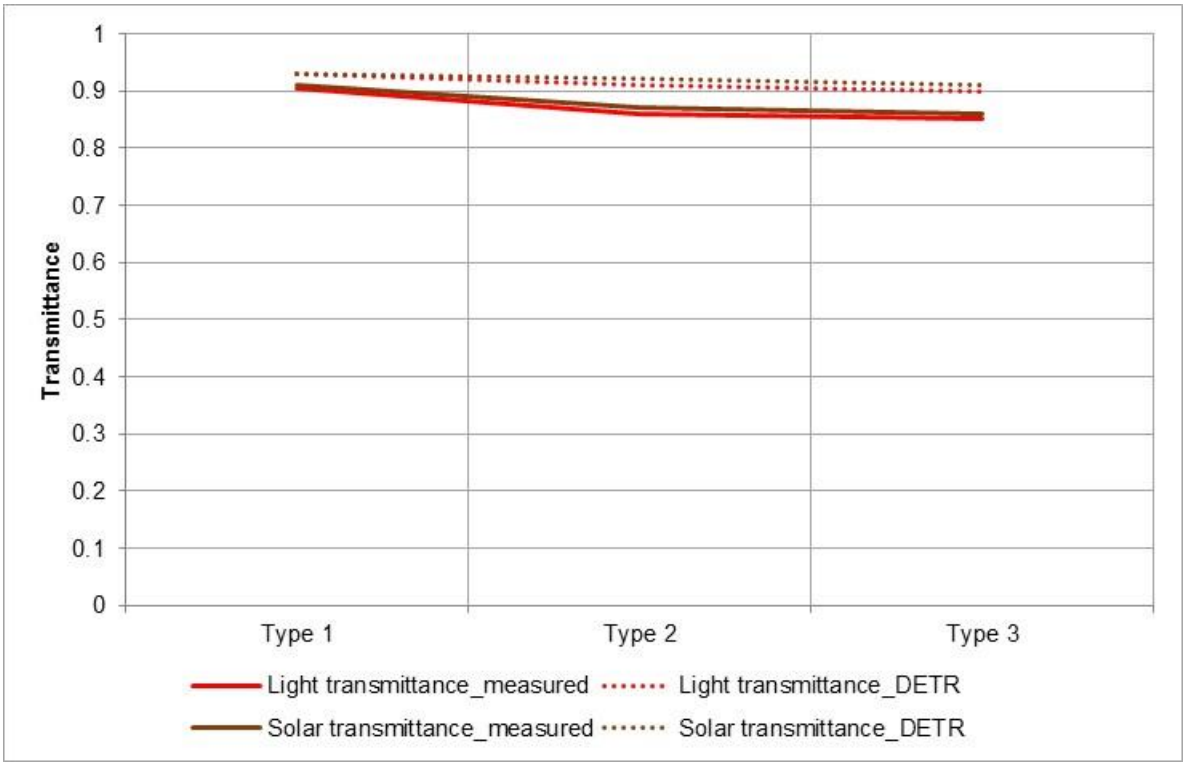


Figure 4-12: Comparison of measured thermal optical properties and the same values obtained from DETR (2003) for the Type 1 (100μm), Type 2 (150μm) and Type 3 (200μm) ETFE foil

It was difficult to validate results obtained for two- and three-layer foil combinations. Although Robinson-Gayle (2003) and DETR (2003) used a similar procedure to calculate solar and light transmittance for the whole cushion. However, the results obtained was not directly comparable, because the combination of foil layers was different from those considered in this study.

4.6 Thermal transmittance

According to BS 6993: Part 1: (BSI, 1989), the thermal transmittance is the heat flux density through a given structure divided by the difference in the environmental temperatures on either side of the structure in a steady-state condition.

The ETFE-foil cushions themselves have thermal insulation due to the large volume of air contained within the cushion. Convective movement of air is limited in a cushion because the air is trapped between foil layers. Thus, this air acts as an insulator and reduces thermal transmittance (DETR, 2003). Thermal transmittance of glazing material can be determined by calculation, physical testing of “as built” configurations etc.

DETR (2003), modelled a three-layer cushion using the finite element analysis program ANSYS and validated the results by comparing with the thermal transmittance (U-value) obtained using the guarded hot box method. The guidelines specified by BS6993 were followed in the Finite Element Analysis program ANSYS, to generate U-value of ETFE-foil cushion. The results produced by ANSYS showed that the heat flux is high around the corner of the cushion compared with those at the central area.

Mainini et al. (2014), measured thermal transmittance of a two-layer ETFE-foil panel in a vertical position using the in-situ procedure. U-value of the vertical panel was calculated based on the thermal flux through the panel, the surface temperatures, indoor temperature and temperature of the climatic chamber.

The results obtained on the thermal transmittance of multi-layer ETFE-foil cushion obtained by previous studies are presented in Table 4-6.

Table 4-6: U-value of ETFE foil cushion

Stated in	Number of layer in ETFE	Method	Horizontal (W/m^2K)	Vertical (W/m^2K)
DETR (2003), Robinson-Gayle (2003)	Three-layer	The guarded hot box and ANSYS	2.73	2.59
Mainini et al. (2014)	Two-layer	In-situ		2.748
Poirazis et al. (2009)	Two-layer	-	2.9	-
	Three-layer	-	1.9	-
	Four-layer	-	1.4	-

4.7 The thermal transmittance of ETFE foil/ cushion

BS 6993: Part 1 (BSI, 1989), specified a method for calculation of U-value (thermal transmittance) of single, double and multiple glazing panels with uncoated and (or) coated low-emissivity surfaces. BS 6993: Part 1 (BSI, 1989), also stated standard values for all parameters required for the calculation.

This study calculated U-value of two layer ETFE-foil cushion on the basis of the steady-state method described in BS 6993: Part 1. The purpose was to investigate if there is any variation in thermal transmittance in the ETFE-foil cushion imposed by double curved surface and air enclosed with it.

4.7.1 Method

Thermal transmittance of ETFE-foil cushion was calculated using Equation 4.3,

$$U = \frac{1}{\frac{1}{h_e} + \frac{1}{h_t} + \frac{1}{h_i}} \qquad \text{.....4.3}$$

Where, h_e = exterior heat transfer co-efficient,

h_i = interior heat transfer co-efficient,

h_t = conductance of ETFE-foil cushion,

$$h_t = [\frac{1}{h_g} + dr]^{-1} \qquad \text{.....4.4}$$

Where, dr = thickness of ETFE-foil layer in cushion,

h_g = Total conductance of gas space,

$$h_g = h_f + h_r \qquad \text{.....4.5}$$

Where, h_f = gas conductance,

$$h_f = \frac{N_u}{S}\,\lambda \qquad \text{.....4.6}$$

$$N_u = C(GrPr)^{\mathrm{n}} \qquad \text{.....4.7}$$

Where, N_u is the Nusselt number,

C (constant) = *0.16* [horizontal position and direction of heat flow upward]

n (constant) = 0.28 [horizontal position and direction of heat flow upward]

$$G_r = \frac{gs^3\Delta T\rho^2\beta}{\mu^2} \qquad \text{.....4.8}$$

Where, *Gr* is the Grashof number,

ΔT=15K, *s* = thickness of air gap,

$$Pr = \frac{\mu C_p}{\lambda} \qquad \text{.....4.9}$$

Where, Pr is the Prandtl number,

μ = Viscosity [kg/ (m s)],

C_p = specific heat [J/(kg K)]

λ = conductivity [(w/m K)]

$$h_r = 4\sigma \left[\frac{1}{\epsilon_1} + \frac{1}{\epsilon_2} - 1\right]^{-1} T_m^3 \qquad \text{.....4.10}$$

Where, h_r is the Radiation conductance,

σ is the Stefan's constant = 5.67 x 10^{-8} [W/m^2K^4]

T_m mean temperature of glazing 283K

ϵ_1 is the effective emissivity of surface 1

ϵ_2 effective emissivity of surface 2.

$$\varphi = \sigma \left[\frac{1}{\epsilon_1} + \frac{1}{\epsilon_2} - 1\right]^{-1} \qquad \text{.....4.11}$$

Where, φ is the inter-surface emittance for infinite plane,

$$h_t = \left[\frac{1}{h_g} + dr\right]^{-1} \qquad \text{.....4.12}$$

Where h_t is the conductance of ETFE-foil layers,

d_r is the total thickness of ETFE-foil

In the calculation, it was considered that cushion consisted of 200μm thick ETFE-foil layers, and emissivity of the external layer and, the internal layer was 0.82 and 0.6 respectively. Exterior and interior heat transfer co-efficient was considered 25 w/(m^2K) and 10 w/(m^2K) respectively as standardised by BS6993: Part 1(BSI, 1989). It was considered that cushion air gap varied between 100mm and 500mm.

Another calculation was made by keeping all the values as above, however, emissivity of internal surface varied between 0.89 and 0.1, considering an air gap of 125mm

(DETR, 2003). This calculation was repeated by considering an air gap of 250mm, 500mm and 1000mm.

4.7.2 The Results

The results obtained from the calculations are presented in Figure 4-14 and Figure 4-15. The results presented in Figure 4-14 and Figure 4-13, demonstrated that the U-value of the same cushion varied at different cross-sections. This was due to the reduced air conductance with the increase of air gap (see Table 4-7). As a result, with an increase in air gap from 10mm to 500mm, the U-value reduced by 12% in the same cushion. Thus, U-value reduces with the increase of air gap.

Table 4-7: Gas conductance in variable air gap

Thickness of air layer (mm)	Gas Conductance (h_f)	Total conductance of gas (h_g)
125	2.178	6.005
250	1.949	5.77
500	1.745	5.57
1000	1.56	5.38

Generally, in a cushion the air gap will vary due to its doubly curved surfaces. Therefore, according to the above result the U-value will also vary at different cross-sections (see Figure 4-13). This might have an impact on the temperatures of the air trapped in between the foil layers and the surface temperatures of the ETFE-foil. This might have resulted in the higher heat flux around the corner compared with the central area of the cushion presented in DETR (2003). This also, might be one of the reasons which caused high surface temperature near the edge of the cushion compared to the middle, observed in an actual enclosure and presented in Chapter 6.

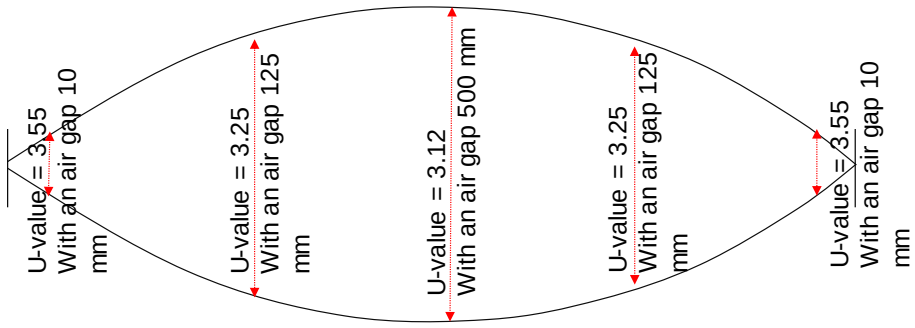


Figure 4-13: Variation in U-value in a single cushion

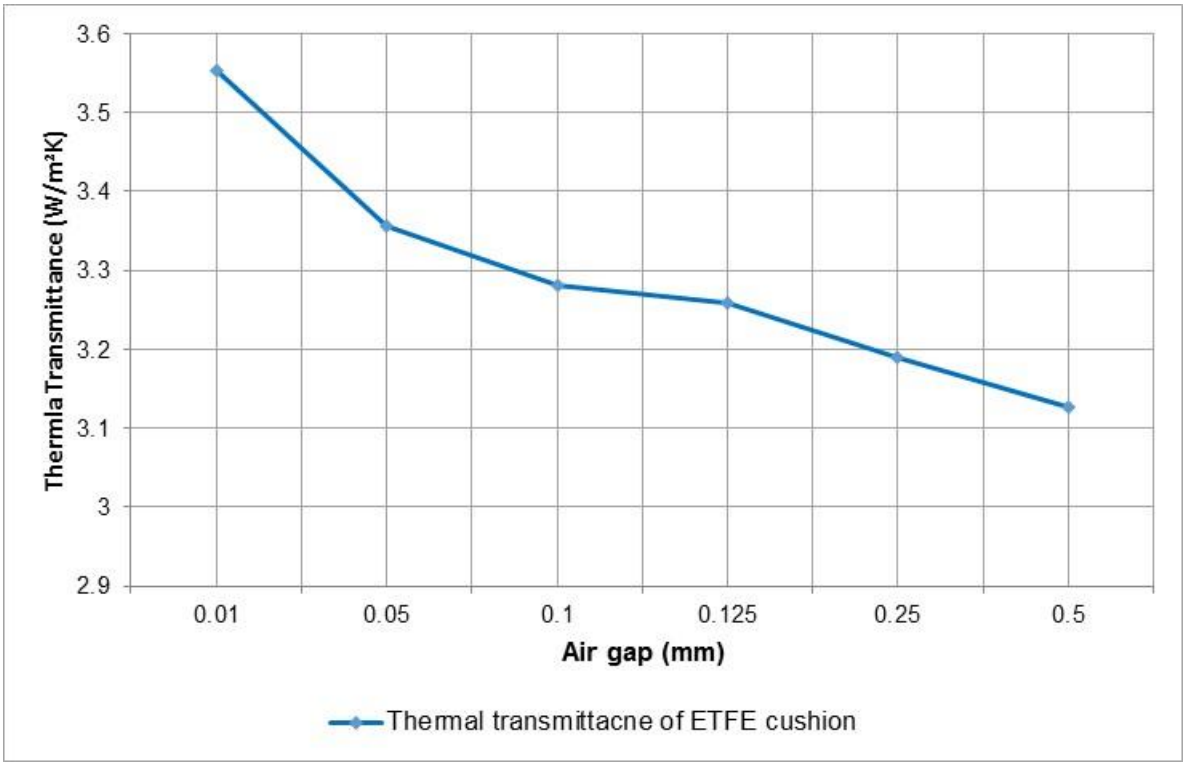


Figure 4-14: Variation of thermal transmittance (U-value) in a single cushion with variation of air gap

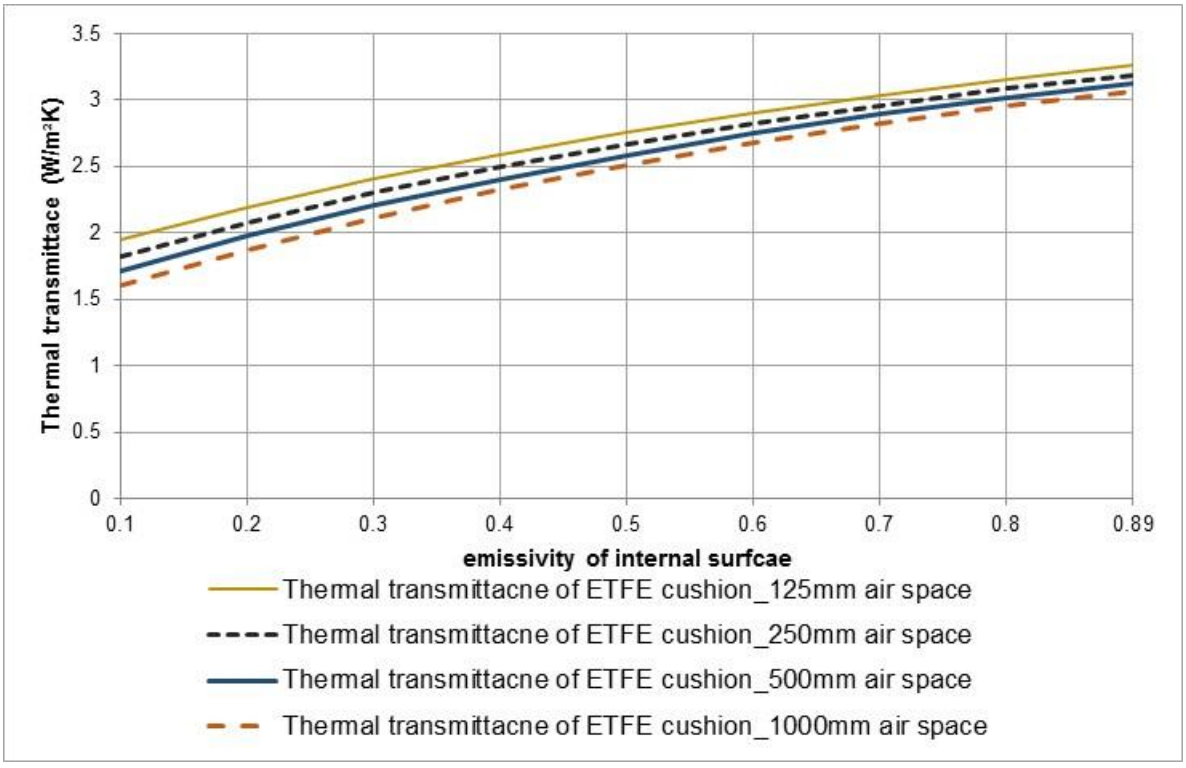


Figure 4-15: Variation of U-value of Two layer ETFE foil cushion with variation in air gap and emissivity of internal surface

The results presented in Figure 4-15 showed that change of emissivity from 0.89 to 0.1, reduced the thermal transmittance of ETFE-foil cushion. Thus, a decrease in emissivity of foil layer reduced the thermal transmittance of ETFE-foil cushion.

Moreover, short-wave and long-wave radiation exchange depend on the surface emissivity (Incropera et al., 2013, Poirazis et al., 2009). Thus, a decrease in emissivity of ETFE-foil surfaces improves thermal performance, by limiting heat gain and loss through the cushion surface, by reducing the impact of short-wave and long-wave heat transfer.

The steady-state method was employed here to calculate the thermal transmittance of a two-layer ETFE-foil cushion. The derived value was 93% (3.12 W/m^{2}K, at the middle of the cushion) to 82% (3.55 W/m2K, at the edge of the cushion) when compared to the value (see Table 4-6) presented in Poirazis et al. (2009). Therefore, using the method stated in BSI (1989), it is possible to generate a U-value. However, these values need to be verified using other established methods such as Hot-Box testing. On the basis of the results obtained for thermal transmittance, a number of assumptions can be made, which might impact the thermal performance of ETFE-foil cushions and spaces enclosed with ETFE-foil cushion envelopes by allowing or limiting exchange of heat with the external thermal environment.

Moreover, the variation in U-value in the different cross-sections of a single cushion may raise difficulties, if a single value is assumed for a two-layer, or three-layer cushion. Particularly in the thermal performance assessment using dynamic simulation tools, a single value of thermal transmittance of cushion envelope might impact the accuracy of predicted results.

4.8 Summary

In the previous chapter, the results of the pilot study revealed that thermal optical properties of ETFE foil cushion affect the thermal performance of the enclosed space . However, the study found limited information on the thermal optical properties of ETFE-foils. Therefore, measurements were carried out in the laboratory using spectrometers (Biochrom Libra S22 and IFS 66v/s) to quantify the thermal optical properties of ETFE-foils. This chapter outlined the methods to obtain thermal optical properties of ETFE-foil samples. This study also measured thermal optical properties of glass samples following the similar method in order to compare properties of ETFE-foils and glass.

Solar optical properties of ETFE-foil and glass samples can be characterised as high transmittance in the visible and near infra-red spectrum. However, the transmittance of both materials decreases at higher wavelengths. The spectral transmittance of glass dropped to nearly 0% at the mid-infrared range, while ETFE-foil samples still

transmitted spectral light to a higher percentage. Therefore, at higher wavelengths, transparent ETFE-foils will exchange a higher percentage of radiation than glass which is effectively opaque.

On the basis of measured light and solar transmittance of single-layer ETFE-foil samples and glass, the procedure described in BS EN 410: 2011(BSI, 2011) was followed to calculate overall light and solar transmittance. Results were in close agreement with previous research. It was revealed that overall light and solar transmittance of ETFE-foils were higher than Opti-float and K-glass. Besides total light and solar transmittance of ETFE-foils reduced from 0.905 to 0.72 and from 0.91 to 0.76 as the thickness of ETFE-foil respectively increased from 100μm to 500μm.

The results obtained on the thermal optical properties of fritted ETFE foils showed that

- With the similar fritting percentage, solar and light transmittance reduced significantly as the density of pigment increased in the fritted part.
- Increase in the percentage of fritted part, as well as the density of pigment, reduced light transmittance significantly.
- This impact of fritting coverage and pigment density on the solar and light transmittance of two-layer and three-layer ETFE panel system was also apparent.
- Above phenomenon should be taken into consideration while selecting fritted foil for the cushion system, therefore it should not only reduce solar gain but also would allow sufficient daylight required for spaces.

U-value of 2-layer ETFE-foil cushion was calculated on the basis of the steady-state method stated in BS 6993: Part 1(BSI, 1989). The purpose was to see if there was any variation in thermal transmittance in the ETFE-foil cushion imposed by double curved surface and air enclosed with it. The results showed that increase of air gap from 10mm to 500mm reduces U-value by 12%. This was because the air conductance reduced with the increase of air gap. Generally, in a same cushion air gap varied due to doubly curved surfaces. Therefore, due to the variation in air conductance in a single cushion, U-value varied at the different cross section. The calculated U-value of the cushion near the edge was 3.55 W/m^2K, while in the middle of the cushion U-value reduced to 3.12 W/m^2K.

This variation in thermal transmittance might have an impact on the temperatures of the air trapped in between the foil layers, and the surface temperatures of ETFE-foils. This might have resulted in high heat flux around the corner than that at the central

area of the cushion presented in DETR (2003). Also, might be one of the reasons which caused high surface temperatures near the edge of the cushion than middle, observed in the actual enclosure and presented in Chapter 6.

The results also demonstrated that decrease in emissivity of foil layers reduced the thermal transmittance of ETFE-foil cushion. Moreover, the short-wave and the long-wave radiation exchange depends on the surface emissivity (Incropera et al., 2013, Poirazis et al., 2009). Thus, the reduction in emissivity of ETFE-foil surfaces improves thermal performance, by limiting heat gain and loss through cushion surface, by reducing the impact of short-wave and long-wave heat transfer.

The steady-state method was employed in this study to calculate the thermal transmittance of a two-layer ETFE-foil cushion. On the basis of the results obtained on the thermal transmittance, a number of assumptions can be made which might impact the thermal performance of ETFE-foil cushion and space enclosed with ETFE-foil cushion envelope.

Moreover, the variation in U-value in the different cross section of a single cushion will raise difficulties, if a single value is assumed for two-layer, three-layer cushion. Particularly in the thermal performance assessment using dynamic simulation tools, a single value of thermal transmittance of ETFE-foil cushion envelope might impact the accuracy of predicted results.

The results obtained on the solar and light transmittance of single, two- and three-layer ETFE-foil was compared with that obtained from the in-situ procedure presented in Chapter 5. Chapter 7 demonstrates the development of a simulation model using EDLS TAS 9.3.3.b, to predict the thermal performance of spaces enclosed with ETFE-foil cushion roof under current and future climatic scenarios, also compared this performance with spaces when enclosed with a glass roof. The properties information presented in this chapter were used to generate simulation models and results obtained from simulation was validated with the actual performance data discussed in Chapter 6.

4.9 Limitation

- The study only measured normal optical properties of ETFE-foil samples because a spectrometer with integrating sphere was not available in the Engineering lab. Thus it was not possible to measure angular solar optical properties of ETFE-foil samples

- ETFE samples used in this experiment was obtained from off-cut samples. Thus, samples were not necessarily very clean and potentially scratched. However, these samples perhaps better represent the material in use.
- The method stated in BS EN 410: 2011 (BSI, 2011) is specifically for glazing with parallel panels. Thus, the results obtained represent thermal and optical properties of ETFE-foil panels rather than a cushion.
- The steady-state method was used to determine the thermal-transmittance of a single cushion.

Chapter 5

5 Thermal performance analysis of ETFE-foil panels

5.1 Introduction and Background

From Chapter 2, it was evident that the thermal performance of actual ETFE-foil enclosures was not investigated in previous studies. Therefore, to understand the thermal performance of ETFE-foil and the space enclosed with it, a pilot study was carried out in the Nottingham High School, where ETFE-foil cushions were incorporated in the roof of the atrium. This pilot study was planned to cover a short period of time, particularly when the school was closed during summer 2013. The results of this pilot study were presented in Chapter 3, which suggested that because of the complexity, the thermal performance of ETFE-foil and the space enclosed with it need to be examined separately. To verify the thermal environment assumed from the pilot study it was decided to start long-term monitoring when the buildings were occupied. Therefore, thermal monitoring of the Nottingham High School and, the Engineering and Science Learning Centre started during summer 2014 and finished during summer 2015. The results of this monitoring is presented in Chapter 6 which showed that ETFE-foil remained very sensitive to the variation of external weather conditions. The significant impact of solar radiation on the surface temperatures of the ETFE-foil cushion was identified. This was also identified by Harvie (1996) in his study, which investigated membrane enclosure, and the author suggested that architectural fabric affects thermal performance of the spaces they enclose through the amount of solar radiation they absorb, reflect and transmits.

The ETFE-foil cushion usually consists of multiple layers of ETFE-foils with air-filled chambers between them. The air between foil layers in an ETFE-foil cushion system has an impact on the thermal environment it encloses which was also identified by Antretter et al. (2008). This air between ETFE-foil layers possibly caused large temperature differences between internal and external layers of the ETFE-foil cushion, where internal layers were always hotter than external layers.

The results obtained from the pilot study (presented in Chapter 3), demonstrated that in hot summer days' strong temperature stratification exist in the spaces enclosed by ETFE-foil cushion envelope. However, the environmental conditions of actual enclosures were uncontrolled during the monitoring. The impact of internal gains, occupancy and HVAC system on the indoor thermal environment are obvious in an

enclosed space. Thus, it was not possible to clearly identify the effect of ETFE-foil cushion separately, on the overall performance of the spaces it enclosed. Therefore, during summer 2014 it was decided to carry out a test rig experiment under a controlled and known environment. From this experiment, it was expected to identify the actual response of ETFE-foil under different weather conditions, and the relationship between monitored thermal environmental of test rigs and the thermal response of ETFE-foils.

The ETFE-foil cushion roof of Nottingham High School is also covered with a rain suppression mesh to reduce rain noise. A thermal imaging of the rain mesh (Figure 5-1) shows that the temperature of the mesh was hotter than the adjacent ETFE-foil cushion surface. However, during the monitoring of Nottingham High School, it was not possible to identify the impact of rain suppression mesh separately, on the internal thermal environment of the atrium.

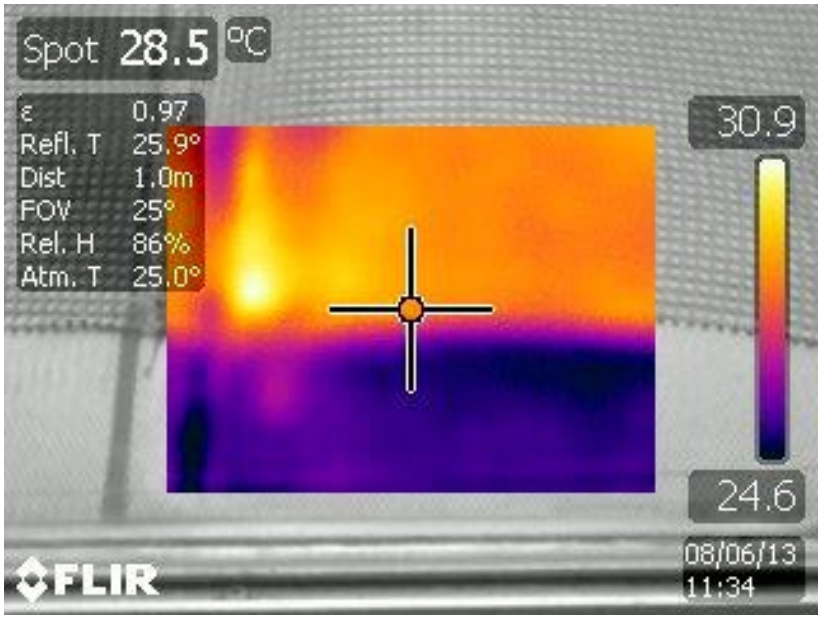


Figure 5-1: Temperature gradient recorded on ETFE-foil cushion roof and rain mesh using thermal image device.

Besides, to predicted the thermal performance of actual enclosures using digital simulation, it was necessary to measure the solar and light transmittance of ETFE-foils as data from the manufacturers were insufficient. Even though this data was generated by lab experiment and presented in Chapter 4, but for fritted foils difficulties arose. Because this type of foils consisted of the transparent part and semi-transparent or printed part. During the lab experiment, it was not possible to identify through which part light was passing. Thus, transmittance of the transparent part and translucent part was measured separately and use to calculate the average transmittance (see 4.5.3).

Hence it was required to validate the approximated solar transmittance of fritted foils. Moreover, the top layers of the ETFE-foil cushion roof of both of the monitored buildings (presented in Chapter 6) were fritted. Therefore, it was necessary to acquire appropriate information on the properties of fritted ETFE-foils, otherwise, it could cause error in the simulation results. Additionally, the laboratory test only measured spectral transmittance through single-layer ETFE-foil samples for particular wavelength ranges, while the actual solar and light transmittance of single, two- and three-layer ETFE-foil panels were calculated according to BS EN410:2011 (BSI, 2011). The method stated in BS EN410:2011 (BSI, 2011) is specified to measure optical properties of glazing material thus it also needs verification.

On the other hand, by comparing the results obtained on solar transmittance of ETFE-foils using different methods, it would be possible to validate the test-rig experiment that was used to measure the solar transmittance of fritted and multiple layer ETFE-foil panels, as presented in this chapter. Additionally, this would provide a basis to generate information for material properties, particularly for fritted foils, which were required for digital simulation (presented in Chapter 7).

The thermal performance of single, two- and three-layer ETFE-foil panels were investigated in two phases:

- The first phase determined solar transmittance of single, two- and three-layer ETFE-foil panels.
- The second phase analysed the thermal performance of single, two- and three -layer ETFE-foil panels, and evaluated the impact of fritting and, rain noise suppression mesh on this performance.

Therefore, the first part of this chapter includes an experimental method, that was used to measure the solar transmittance of single layer and multilayer foil panel under actual outdoor environment. The results obtained from this investigation was compared with the measured solar transmittance obtained in the laboratory, the appropriate British Standard, and information from the supplier (single layer only).

The second part of this chapter describes the analysis of thermal environment of single and multiple layer ETFE-foil panels recorded during summer 2015. This analysis was done by comparing thermal environment of two identical test rigs, roofed with the different configurations of ETFE-foil panels.

5.2 Objectives

The aim of the study was to evaluate the thermal performance of single, two- and three-layer ETFE-foil panels using a test-rig experiment under actual outdoor environmental conditions. The objectives of the study were:

1. to measure the amount of solar radiation transmitted through the different configurations of ETFE-foil panels under actual weather conditions;
2. to evaluate and compare thermal performance of different configurations of ETFE panels based on internal air temperature, air-volume air temperature, surface temperature etc.;
3. to compare and analyse the relationship between surface temperatures of ETFE-foil and air temperatures it encloses;
4. to ascertain the impact of rain suppression mesh on this performance;
5. to compare the impact of different fritting on the thermal environment; and
6. to provide reliable experimental data for the verification of simulation model presented in Chapter 7.

5.3 Methodology

Mainini et al. (2014), conducted an in-situ experiment to obtain thermal transmittance of a vertical ETFE-foil panel. Ward and Doran (2005), also conducted in-situ measurements to examine multi-foil insulation in wall, roof and, floor, as defined by ISO 9896 and, calculated U-value according to BS EN 6946 (BSI, 2007). Results obtained in this in-situ experiment were compared with that obtained by guarded hot box and concluded that the in-situ experiment agreed well with actual data. Max et al. (2012), measured thermal transmittance of a novel glazing system composed of anti-reflection coated glass and, ETFE film used for greenhouses and similar buildings.

Asdrubali and Baldinelli (2011), conducted a hot box experiment taking into account three standards for calibrating hot boxes: The European EN ISO 8990, the American ASTM C1363-05 and the Russian GOST 26602.1-99. The analysis of the result showed that Russian method (Russian GOST 26602.1-99) was the ideal method to define the thermal behaviour of glazing components.

In most of the hot box experiments, the specimen position was vertical while Elmahdy and Haddad (2000), modified this typical position of the specimen and evaluated thermal transmittance of skylights and sloped glazing in various inclination.

Dimitriadou (2015), conducted an in-situ experiment to compare the thermal performance of a two-layer inflated ETFE-foil cushion and double glazed unit. The results of the study were based on night time recorded data. The study concluded that, under cold weather, the ETFE-foil cushion was able to create a comfortable interior environment at a comparatively low energy cost, thus ETFE-foil cushions can be successfully applied to replace glass in buildings. This study was based on night-time and, cold weather conditions only, when the building's thermal environment is mostly controlled by a HVAC system. However, the results provided basic knowledge on energy consumption through the HVAC system, which might have resulted from the use of the ETFE-foil cushion and glass roof.

Poirazis et al. (2009), studied heat transfer through ETFE-foil using mathematical models. The results of the study estimated that, due to night time long-wave radiation exchange, heat loss increased by 12% in ETFE-foil cushions in comparison to glazing.

At the Fraunhofer Institut für Bauphysik, Germany, Antretter et al. (2011) examined a full-scale model of a structure covered by an ETFE-foil cushion. The purpose was to validate results obtained using CFD, to predict heat distribution in an ETFE-foil cushion under different inclinations. Findings of the study showed that heat flux on the ETFE-foil cushion surface resulted from convective and radiative heat flux components. In horizontal positions when the temperature difference between ETFE-foil cushion surface and the outdoor air was 30°K, approximately 30% of the total heat flux was caused by convection and 70% was caused by radiation. As the temperature difference increased, the proportion of convective heat flux increased too. Moreover, at the time when the temperature of top foil of the cushion increased over bottom foil, caused a stable temperature layering, convective heat flux reduced, and almost all energy was transferred by surface to surface radiation.

Hu et al. (2016) developed an experimental setup that was composed of an open structure, covered with three-layer ETFE-foil cushion roof integrated with amorphous silicon photovoltaic cells, consisting of a solar energy control system and a pressure control system. The study aimed to investigate the thermal performance of three-layer a ETFE-foil cushion roof integrated with amorphous silicon photovoltaics on the basis of surface temperature distribution and heat transfer coefficient. The experiment was done in sunny summer conditions and the results were compared with those obtained using computer simulation (using FLUENT). The maximum difference between the air temperature of the experimental setup and the numerical model was 3.4°K. The experimental results showed that in the three-layer cushion, the temperature of the

middle layer was the highest and bottom layer was the lowest. However, the experimental setup was not ideal, because the ETFE-foil cushion roof was used to cover an open structure, thus allowed outdoor air to circulate around and within it. This might have resulted in reduced surface temperature in the bottom layer of the ETFE-foil cushion, whereas the exposed top layer was gaining heat from the sun, resulting in higher temperature than the bottom layer. On the other hand, the middle layer was surrounded by hot static air, which resulted in it having the highest temperature among the three layers. Hence the findings may give a basic impression of the thermal state of ETFE-foil layers in a three-layer cushion system.

Devulder (2004), monitored the thermal behaviour of a typical double layer membrane construction, under real weather condition, using a simple test rig. The analysis of the monitored data showed that the external layer of the membrane construction experienced frequent temperature swing, which was similar to the inner layer, but to a lesser extent.

Harvie (1996), carried out a test-cell investigation for monitoring the internal surface temperature of a range of membrane samples, and the quantity of solar radiation directed into space enclosed by them. This was done by test-cell, built according to ASTM E 1084-86, 'Standard Test Method for Solar Transmittance of Sheet Material Using Sunlight' (ASTM, 1991), with slight alterations. The study was unable to properly measure the surface temperature, because of the slightly rough and, non-stick nature of the membrane surface. The study also faced difficulties due to the overheating of sensors, because the experiment did not take any initiative to isolate sensors from direct solar radiation. The result of the investigation showed that under bright solar radiation, exposed external surface temperature sensors recorded higher temperature than internal surface temperature sensors, while at night it was likely to cool down faster. This investigation underestimated surface convection which is generally caused by the exchange of heat between a surface and air close to it, as a result of temperature difference. According to Harvie (1996), this heat exchange by convection is caused by roughness of the surface. So, with a smooth surface coating, for a millimetre thick fabric membranes, it is usually acceptable to consider that they have a roughness of zero. Therefore Harvie (1996) did not consider surface convection in the test-cell investigation. The study concluded that the selected method, to measure solar transmittance was unreliable and suggested that the test-cell could only be used to investigate the internal surface temperatures of membrane samples.

From the earlier discussion, it was found that the hot-box and in-situ methods were frequently used by previous studies, to measure the thermal transmittance of glazing materials, membranes, and ETFE-foil panels.

The guarded hot-box method is a well-established method, to measure the steady-state thermal performance (thermal transmittance, thermal conductivity, etc.) of a building material and composite assemblies of building materials, using homogenous or non-homogenous specimens, at standardised test conditions. The operation of a hot-box is complex and apparatus requires a significant number of fundamental measurement of temperatures, areas, and power (ASTM, 2014). This test method is applicable for steady-state testing and does not establish criteria for conducting dynamic tests or analysis of dynamic test data.

On the other hand, in-situ thermal testing allows determination of the performance of a real building or a part of a building structure by monitoring over an extended period. In the experiment, the exterior of the structure is exposed to outdoor conditions, thus tests results are dynamic in nature. Data acquisition and, analysis is more complicated. The results obtained using this method reflect the performance of the whole structure. Therefore, it is difficult to obtain robust, accurate values of the thermal characteristics of any individual component (Eames, 2009).

Among the two methods: the guarded hot-box and the in-situ method, the hot-box method is more complex and would require expensive equipment for experimental setup. In the environmental laboratory, the University of Nottingham has a climate chamber which can be used to test material thermal performance using vertical specimens. This study only considered horizontal roof elements. Therefore, the available experimental setup was not considered suitable for this study. Moreover the hot-box experiment requires standard test conditions and uses the steady-state method to determine thermal performance of a material. But this study requires long-time exposure of an ETFE-foil panel to the external environment, to see impacts of it on the structure it encloses. Thus, in this study to evaluate the thermal performance of single and multiple layer ETFE-foil, the in-situ method was used. This procedure allowed determination of the thermal performance of ETFE-foil panels under realistic weather conditions on the basis of data recorded for a longer period and completed the second phase of the experiment.

The first phase of this experiment measured the solar transmittance of single-, two- and three-layer ETFE-foil panels using the similar method stated in ASTM (1986a). This method is applicable for measurement of solar transmittance using a pyranometer

in an enclosure, and considering the sun as the energy source. The spectral sensitivity of the pyranometer extends from the ultraviolet to near infrared wavelengths (0.3μm to 2.8μm), thus encompassing all the solar spectrum. Using this method, the solar transmittance of the test specimens is measured from the ratio of the solar radiation measured when the test specimen is placed between the sun and, the pyranometer, and the solar radiation measured by the pyranometer with no test specimen.

5.3.1 Description of the test rig

For the purpose of this study, two identical test rigs of 1000mm (length) x 800mm (width) x 1000mm (height) were constructed with exterior ply and, lined internally with rigid insulation. To reduce air losses through the corners of the test rigs, silicon sealant was used along the perimeter and, in between the edges of the rigid insulation; which made the test rigs fully sealed. The test rigs were coated with weatherproof paint. The test rigs were located on the roof of the Coates Building at the University of Nottingham. Exposed area of foil was 1000 x 800mm and test rigs were tilted towards the south at an angle of 14° from horizontal. While selecting this configuration, it was considered that foil exposed to the direct beam solar radiation would also have a large view of the sky dome. This would emphasize the effect of short-wave and long-wave radiation exchanges on the thermal balance of foils.

Each test rigs consisted of a frame of 1000mm (length) x 800mm (width) x 250mm (height) to attach the ETFE-foils. This frame was used as a cap to fit above the test rigs. This approach allowed to attach various types of ETFE-foils (e.g. single-layer, double layered, etc.). In a single-layer system, one foil was tensioned on top of the frame; to develop a double layer foil panel, two foils were tensioned on top and bottom of this frame parallel to one another, with an air gap of approximately 250mm. This panel was then used to cap these insulated and instrumented test rigs. For the three-layer panel systems, a single layer foil was tensioned in a different frame and clamped on top of the two-layer system to provide an air gap of 250mm. These panels were also constructed with exterior ply and, rigid insulation and, to reduce air loss, the edge of the panel was filled with silicon sealant.

In the first phase of this test-rig experiment, the solar transmittance of single, two and three-layer ETFE-foil panels were measured. ASTM (1986b), describes the method to measure solar transmittance, by the ratio of average radiation with and without a test specimen, using a box and a pyranometer located inside it. However, in this study, two test-rigs (Test-rig 1, Test-rig 2) were used, and both of the test-rigs were equipped with a pyranometer, located in the same relative position. One test-rig (Test-rig 1) was

covered with ETFE-foil panels while the immediately adjacent test-rig (Test-rig 2) was uncovered. The pyranometer located in Test-rig 1 and covered with the ETFE-foil panel measured transmitted solar radiation. Whereas, the pyranometer located in Test-rig 2 measured incident solar radiation. Thus, solar transmittance was measured from the ratio of transmitted and incident solar radiation.

In the second phase of the experiment, both of the test-rigs were covered with ETFE-foil panels of different combinations. A part of this test rig experiment also included rain suppression mesh, which was placed on top of the ETFE-foil panel of one of the test-rigs while the adjacent test rig was capped with a similar ETFE-foil panel without mesh. The thermal performance was evaluated by comparing the air temperature within the test-rigs and, surface temperatures of the ETFE-foil panels, used to cover test-rigs.

5.3.1.1 Irradiance

Kipp & Zonen CMP3 Pyranometers (sensitive wave band: 0.3-2.8µm) were employed to measure the incident and transmitted solar radiation.

At the first phase of the experiment, a pyranometer was placed in Test-rig 1. At the same relative position as the first pyranometer of the Test-rig 1, a second pyranometer was placed in Test-rig 2. This was because the pyranometer measuring solar radiation was slightly recessed inside the test-rigs, so hemispherical solid angle viewed by this sensor was slightly obstructed. Therefore, the view factor of both pyranometers was same. Figure 5-2 presents schematic drawing and position of the pyranometer in test-rigs during phase 1 experiment.

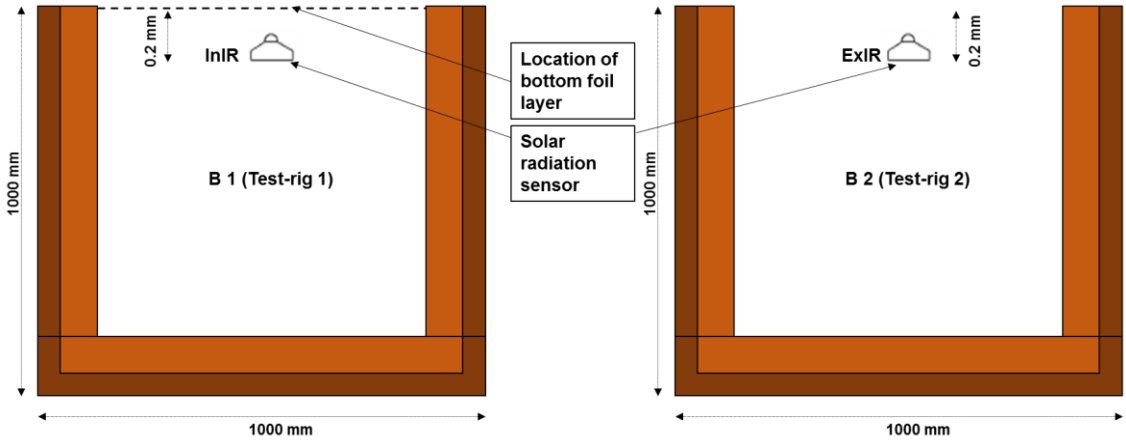


Figure 5-2: Diagrammatic sectional drawings and position of pyranometer in test-rigs during phase 1

At the second phase of the experiment, pyranometers placed inside the Test-rig 1 and Test-rig 2 were aligned to be parallel to the ETFE-foil panels and located immediately below the internal layer of foil to record transmitted solar radiation. A third pyranometer

was placed externally at 4 metres above the floor level of the roof adjacent to test-rigs, to record incident total solar radiation. Figure 5-3 presents diagrammatic sectional drawings and position of pyranometers in test-rigs during phase 2 experiment.

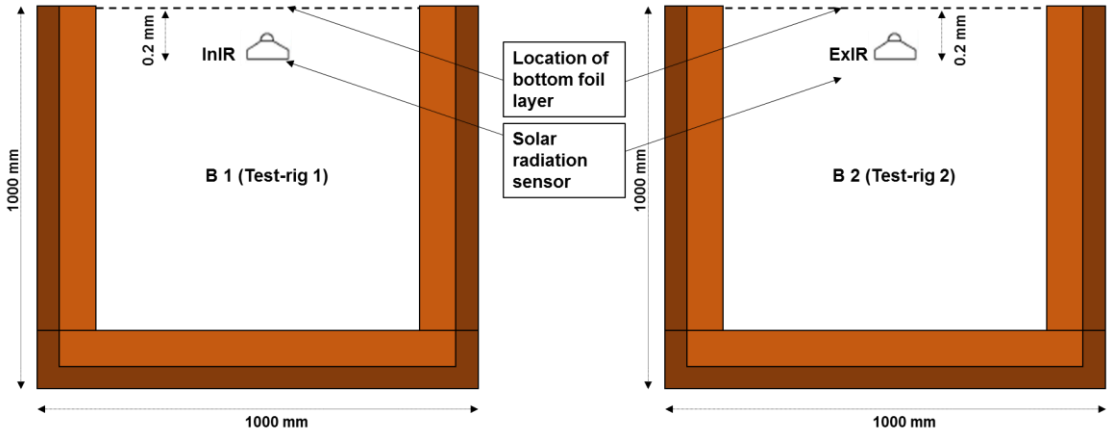


Figure 5-3: Diagrammatic sectional drawings and position of pyranometer in test-rigs during phase 2

5.3.1.2 Temperature sensors

In the second phase of the experiment, internal air temperatures of the test-rigs, air temperatures between foil layers (in the two-layer and three-layer ETFE-foil panels), and the surface temperatures of each ETFE-foil layers were recorded using screened thermocouple (ϕ0.1 mm, K-type) temperature sensors, similar to those installed in the actual enclosure monitoring (presented in Chapter 6). Location of this sensors are shown in diagrammatic section of test rig in Figure 5-7.

The tip of thermocouple sensors measuring air temperatures was shielded in a lightweight aluminum tube to minimise solar radiation effects from the measurements. To measure surface temperatures, thermocouple tips were directly attached to the ETFE- foil surface as well as test-rig surface by using silver tape. Besides small pieces of ETFE-foils were placed in between silver tape and thermocouple tip so that temperature sensors would not heat by reflective aluminum foil tape surface.

5.3.1.3 Data logger

The thermocouples and pyranometers were connected to a Data Taker 85 data logger. The thermocouples were wired in a shared input configuration and their electromagnetic shields connected to the appropriate input of the data logger. The sampling rate was set to one minute. This sampling period of one minute was selected to record the frequent change of thermal state of ETFE-foils as an impact of the change in external environment. Description of the sensors attached with this logger can be found from Table 5-2 (First phase) and Table 5-3 (Second phase).

Table 5-1: Description of measurement sensors

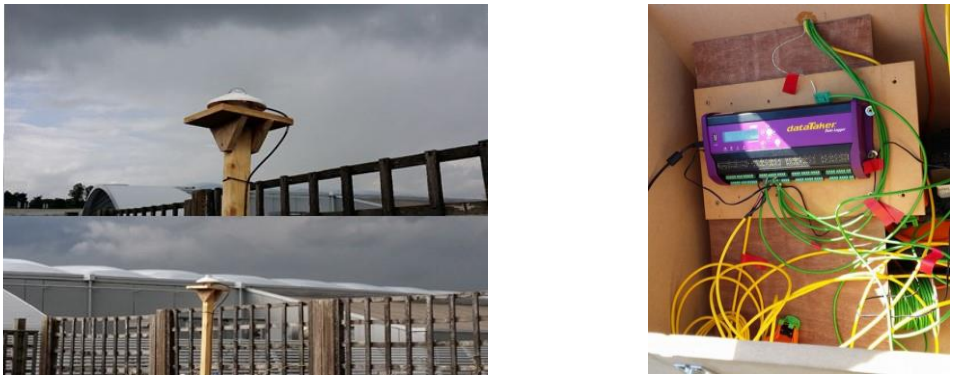
Measurement type	Sensor type
Data logger	DataTaker DT 85
Air Temperature and foil surface temperature	ϕ0.1 mm K-type thermocouple connected to dataTaker DT 85
Solar radiation (internal & external)	Kipp & Zonen CMP3 Pyranometer (spectral range: 0.3-2.8µm)

Table 5-2: List of parameters measured on the test-rigs (First phase)

Monitored data	Sensor ID for test-rig 1	Sensor ID for test-rig 2
Test-rig	B1 (Test-rig 1)	B2 (Test-rig 2)
solar radiation	InIR_B1 (Transmitted solar radiation)	ExIR_ B2 (Incident solar radiation)

Table 5-3: List of parameters measured on the test-rigs (Second phase)

Monitored data	**Sensor ID for test-rig 1**	**Sensor ID for test-rig 2**
Test-rig	**B1 (Test-rig 1)**	**B2 (Test-rig 2)**
solar radiation	InIR _B1 (Transmitted solar radiation)	InIR _B2 (Transmitted solar radiation)
Top layer surface temperature	Ts1_B1	Ts1_B2
Middle layer surface temperature	Ts2_B1	Ts2_B2
Bottom layer surface temperature	Ts3_B1	Ts3_B2
Test box internal surface temperature	Ts_B1	Ts_B1
Internal air temperature of test rig	TaH1_B1	TaH1_B2
Mean radiant temperature of test rig	Tmrt_B1	Tmrt_B2
Air temperature of air-volume 1	TaV1_B1	TaV1_B2
Air temperature of air-volume 2	TaV2_B1	TaV2_B2
Air temperature of air-volume 3	TaV3_B1	TaV3_B2



(a) (b)

Figure 5-4: (a) Pyranometer measuring incident total solar radiation, (b) DT85 Datalogger attached with temperature and radiation sensors and located inside equipment box



(a) (b)

Figure 5-5: (a) Temperature sensors measuring mean radiant temperature and, air temperature, and solar radiation sensor measuring transmitted solar radiation, located just below ETFE-foil panel (b) Temperature sensors measuring internal surface temperature

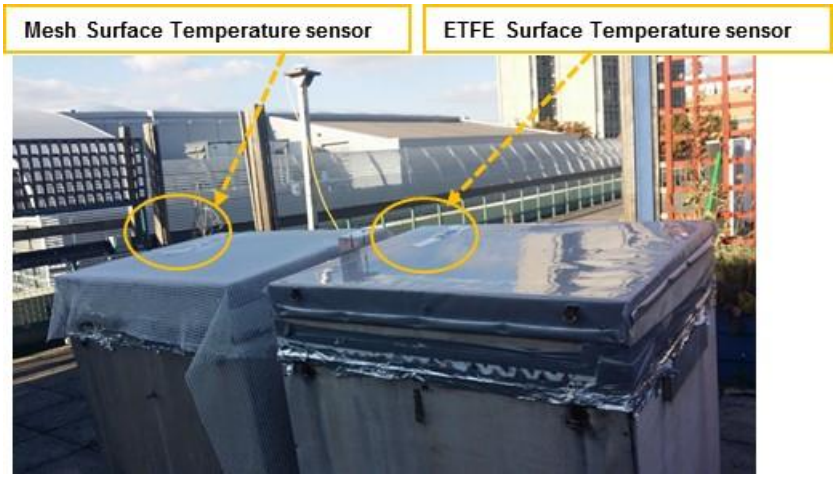
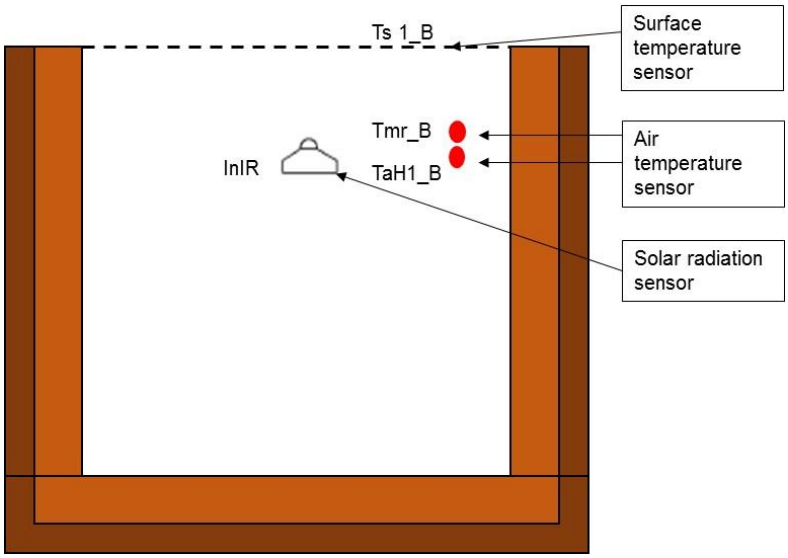
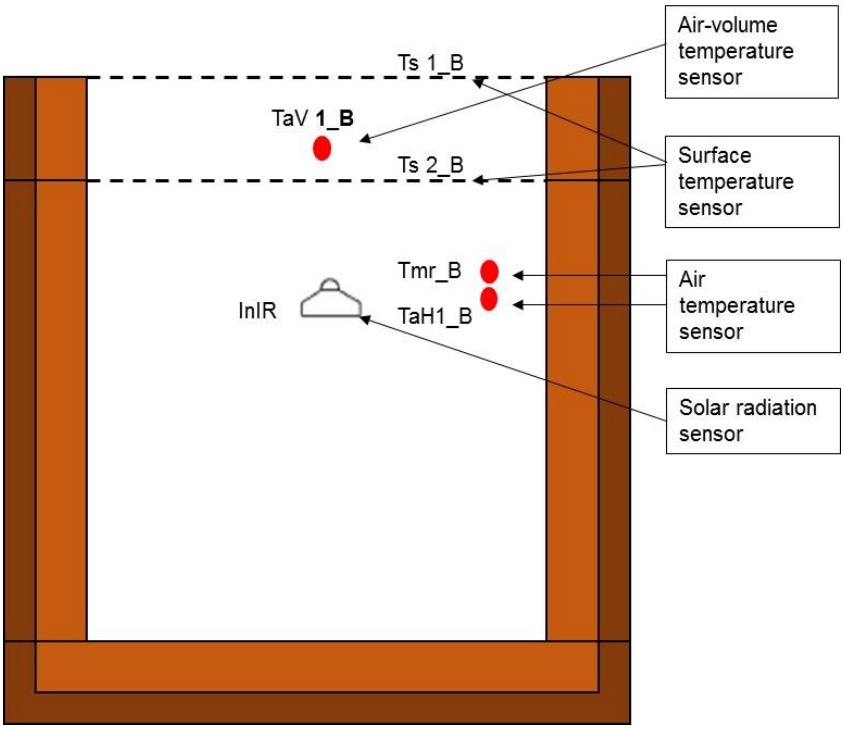


Figure 5-6: Temperature sensors measuring external surface temperature and mesh surface temperature

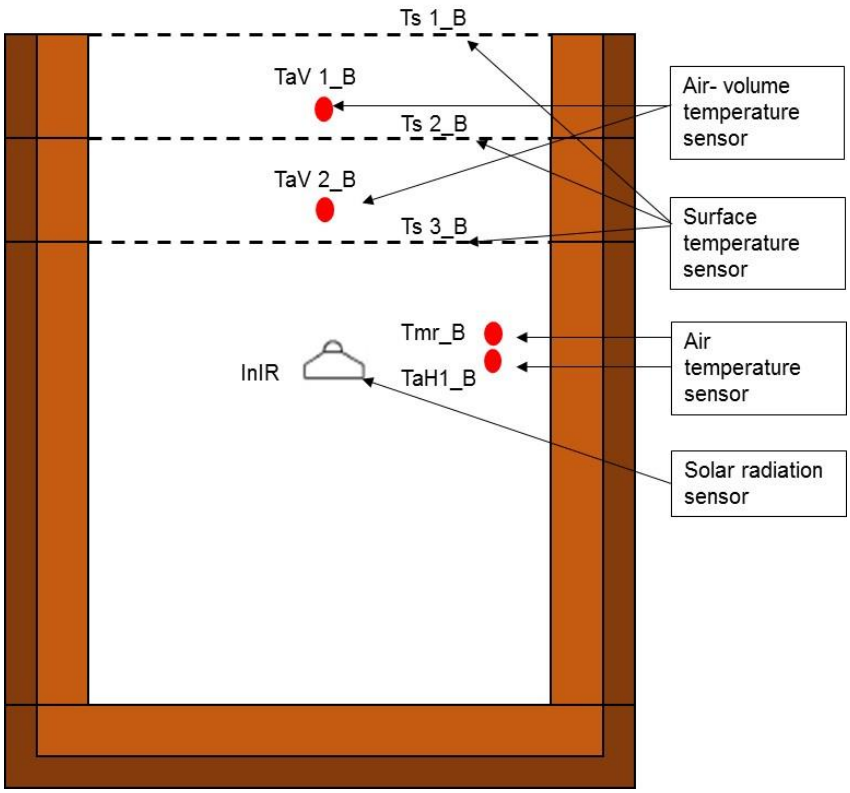


(a)



(b)

(Figure 5-7 continued to the next page)



(c)

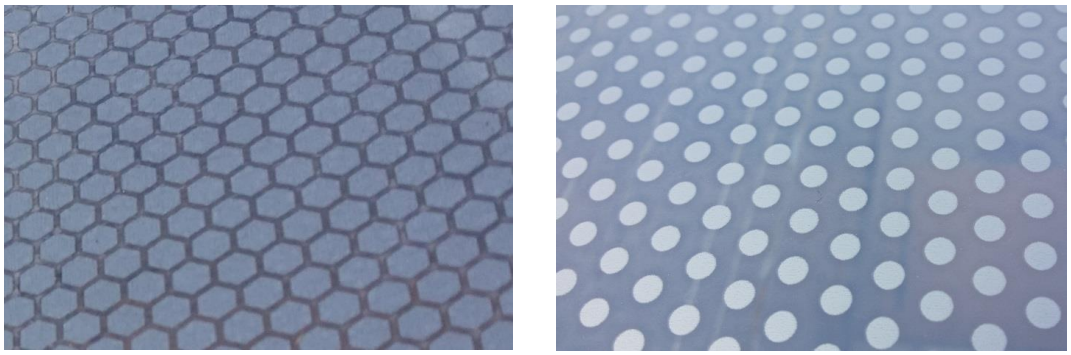
Figure 5-7: Diagrammatic section of test-rigs (a) with single layer ETFE-foil panel, (b) with two-layer ETFE-foil panel and, (c) with three- layer ETFE panel during the Second phase experiment

5.3.2 ETFE foil selection

ETFE-foils that are typically used in the construction of single, two- and, three-layer ETFE-foil cushions, were selected. In two-layer and three-layer foil panel construction, the top and bottom layer were 200 μm thick foils, while the middle layer was 100 μm thick. This was because, in an ETFE-foil cushion construction, top and bottom layers are usually composed of thick layers, to carry wind load and the pre-stress developed in the top and bottom layer in an inflated cushion. Alternatively, top layers usually consist of fritted foils with different percentage of fritting, such as foil with 75% fritting comprised of 75% fritted area and, 25% transparent area.

Foil samples were provided by Architen Landrell Associates Ltd. Selected ETFE-foil foil samples for test-rig experiment were:

- 100 μm transparent
- 200 μm transparent
- 200 μm transparent with 75% fritting (75% fritted and 25% transparent foil)
- 200 μm transparent with 25% fritting (25% fritted and 75% transparent foil)



(a) (b)

Figure 5-8: (a) 200 μm transparent with 75% fritting, (b) 200 μm transparent with 25% fritting

Figure 5-8 presents 200 μm transparent foil with 75% fritting and 200 μm transparent foil with 25% fritting. Among the selected types, foils similar to the 200 μm transparent with 75% fritting [see Figure 5-8 (a)] and, 200 μm transparent foils were used to construct the cushion roof of one of the case study buildings (Nottingham High School), presented in Chapter 6.

5.3.3 Weather data

Weather data e.g. outdoor air temperature and humidity was monitored by a Tiny tag Plus 2 - TGP-4017 data logger. This data logger was attached to the exterior of Test-rig 1. Although this sensor was water proof, extra care was taken to avoid contact with rain water and direct solar radiation by placing a steel frame around the datalogger. A sampling period of one minute was applied. External incident solar radiation was measured by a Kipp & Zonen CMP 3 pyranometer, located adjacent to the test-rigs which was already mentioned in section 5.3.1.1. Figure 5-9 presents sensors used to measure environmental parameters and Table 5-4 presents sensor types used to measure environmental parameters. Table 5-5 presents identifications of environmental data used in the analysis.



(a)



(b)



(c)

Figure 5-9: (a) Temperature sensor measuring external ambient temperature and humidity, (b) steel frame around the sensor, (c) pyranometer measuring total horizontal solar radiation

Table 5-4: Description of measurement sensors

Measurement type	Sensor type
Data logger	DataTaker DT 85
External total horizontal solar radiation (external)	Kipp & Zonen CMP3 Pyranometer (spectral range: 0.3-2.8µm)
Outdoor air temperature	Tinytag Plus 2 (-40°C to 0+85°C)

Table 5-5: Measured environmental parameters and identifications

Environmental data	Identification
Outdoor ambient temperature	OAT
Relative humidity	RH
External total horizontal solar radiation	ExIR

5.3.4 Timescale of the monitoring

Continuous monitoring commenced on 15 April 2014. A number of observations were made and the test-rig position was changed depending on the sun's position so that the ETFE-foil panels had the largest view of the sky dome. The position of the pyranometer measuring incident solar radiation was changed so that the view factor of the pyranometer would not be obstructed by adjacent structures. After completion of all necessary steps, it was possible to start the experiment from 1st July 2014. The priority of this study is to observe and analyse the optical and thermal performance of single and multi-layer ETFE-foil under different weather conditions. The orientation of both test-rigs was the same throughout the monitoring period to obtain sufficient data to represent the thermal performance of ETFE-foil panels.

This test-rig experiment was conducted in two different phases. The first phase was conducted between July 2014 and October 2014. In this phase solar transmittance of different types of single, two- and three-layer flat ETFE-foil panels was measured. During this experiment Test-rig 1 was capped with ETFE-foil panels of different single and multiple layer configuration while Test-rig 2 was kept open. Each box contained one Kipp & Zonen CMP3 pyranometer which was placed internally and at the same height. So pyranometer in one of the test-rig with ETFE-foil panel measured transmitted radiation while another pyranometer in another test-rig without any cap measured incident solar radiation. The results were obtained from the ratio of transmitted and incident solar radiation. Using this procedure the solar transmittance of single, two- and three-layer ETFE-foil panels were determined. Table 5-6 presents the schedule of monitoring for the first phase experiment.

Table 5-6: Different combinations of ETFE-foil in Test-rig 1 (First phase)

Test rig 1				Test rig 2	
ETFE-foil layer number in panels	**Combination**	**Foil type**	**Thickness**	**ETFE-foil layer number in panels**	**Study Period**
Two-layer	Layer 1 (Top layer)	Fritted (75% fritted and 25% transparent)	200μm	None	1st July to 20th July 14
	Layer 2 (Bottom layer)	Transparent	200μm		
Single-layer	Layer 1 (Top layer)	Fritted (75% fritted and 25% transparent)	200μm	As above	25th July to 31st July 14
Three-layer	Layer 1 (Top layer)	Fritted (75% fritted and 25% transparent)	200μm	As above	5th August to 25th August 14
	Layer 2 (Middle layer)	Transparent	150μm		
	Layer 3 (Bottom layer)	Transparent	200μm		
Three-layer	Layer 1 (Top layer)	Fritted (25% fritted and 75% transparent)	200μm	As above	1 September to 25th September 14
	Layer 2 (Middle layer)	Transparent	150μm		
	Layer 3 (Bottom layer	Transparent	200μm		
Single-layer	Layer 1	Fritted (25% fritted and 75% transparent)	200μm	As above	25th October 14 to 10th November 14
Two-layer	Layer 1 (Top layer)	Fritted (25% fritted and 75% transparent)		As above	30th April to 10th May 15
	Layer 2 (Bottom layer)	Transparent	200μm		

The second phase test-rig experiment was conducted between May 2015 and October 2015 to examine the thermal performance of a variety of single, two-layer and three-

layer flat ethylene-tetra-fluoro-ethylene (ETFE) foil panels under different weather conditions. A number of multi-layer combinations incorporating different thicknesses of transparent and/or fritted ETFE-foils were examined. A part of this test-rig experiment also included rain suppression mesh which was placed on top of the ETFE-foil panel of one of the test-rigs while the adjacent test-rig was capped with an ETFE-foil panel without mesh. The purpose was to determine the effect of rain noise suppression mesh on the thermal performance of ETFE-foil panels. Table 5-7 presents the schedule of monitoring of second phase experiment.

Table 5-7: Different combination of ETFE-foil in Test-rig 1 and Test-rig 2 (Phase 2)

Test-rig 1			**Test-rig 2**			
Position of ETFE layers in panel	**Foil type**	**Thick -ness**	**Position of ETFE-foil layers in panel**	**Foil Type**	**Thick -ness**	**Study Period**
Layer 1 (Top layer)	Fritted (75% fritted and 25% transparent)	200μm	Layer 1 (Top layer)	Fritted (25% fritted and 75% transparent)	200 μm	1st September 15 to 10th September 15
Layer 2 (Bottom layer)	Transparent	200μm	Layer 2 (Middle layer)	Transparent	150 μm	
			Layer 3 (Bottom layer)	Transparent	200 μm	
Layer 1 (Top layer)	Fritted (75% fritted and 25% transparent)	200 μm	Layer 1 (Top layer)	Fritted (25% fritted and 75% transparent)	200 μm	18th September to 24th September
Layer 2 (Middle layer)	Transparent	150 μm	Layer 2 (Middle layer)	Transparent	150 μm	
Layer 3 (Bottom layer)	Transparent	200 μm	Layer 3 (Bottom layer)	Transparent	200 μm	
Layer 1 (Top layer)	Fritted (75% fritted and 25% transparent)	200 μm	Layer 1 (Top layer)	Fritted (25% fritted and 75% transparent)	200 μm	25th September to 2nd October

5.4 Measurement of solar transmittance of ETFE-foil panels

In the first phase, field measurements of actual solar transmittance are compared with the solar transmittance measured in the laboratory and calculated according to BS

EN410:2011(BSI, 2011) and presented in Table 5-8. Here, the spectral transmittance of different types of transparent and silver single layer ETFE-foil was measured in the laboratory which is described in Chapter 5. For fritted ETFE-foil overall transmittance was approximated based on the percentage of fritted area and transparent part. The overall solar transmittance of single, two- and three-layer ETFE-foil panel was calculated based on the measured transmittance of single layer ETFE-foil and according to BS EN410:2011.

Solar transmittance measured in the test-rig experiment was estimated from the incident solar radiation (unobstructed) recorded in Test-rig 2 and, the transmitted (through ETFE) solar radiation recorded in Test-rig 1. This procedure to estimate solar transmittance is stated in ASTM (1986b). Figure 5-10 shows Test-rig 1 and Test-rig 2, with and without ETFE-foil. The results recorded on a clear day were considered. Data recorded between 9.00 am and 3.00 pm was averaged as stated in ASTM (1986b). According to ASTM (1986b), during this period the solar radiation is at least 80% of the value obtained at solar noon for that day. This procedure was followed to measure solar transmittance of single, two- and three-layer ETFE-foil panels of different combination stated Table 5-6. Measured solar transmittance of ETFE-foil panels was within 88.2% to 97% of the results obtained from lab and calculated using BS EN410:2011(BSI, 2011) and also information obtained from Architen Landrell (single layer only). The results of the experiment are presented in Table 5-8. Figure 5-11, Figure 5-12, Figure 5-13, Figure 5-14, Figure 5-15, Figure 5-16 illustrated solar radiation transmission through single, two- and three-layers 25% and 75% fritted ETFE-foil panels.

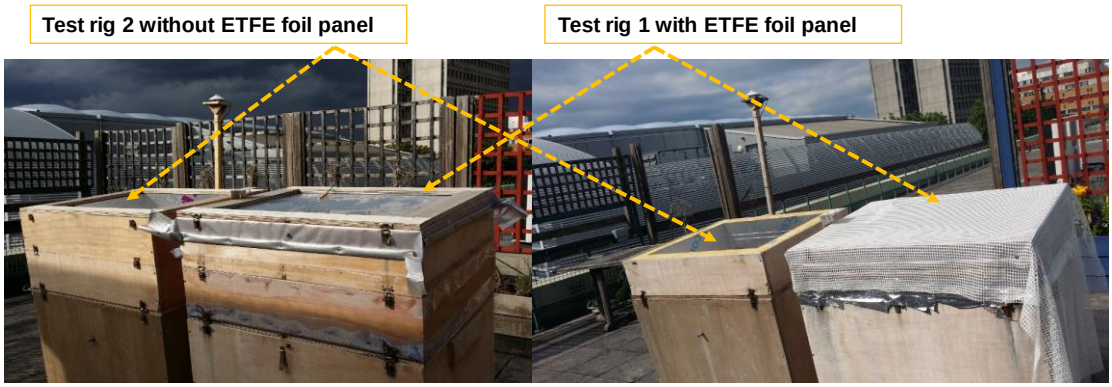


Figure 5-10: Phase 1 test-rig experiment

Table 5-8: Comparison of measured and calculated transmittance of ETFE-foil panel with that of test-rig experiment

Layer number in the ETFE-foil panel		Type of ETFE-foil in panels	Solar transmittance (measured in lab, calculated according to BS EN410:2011)	Solar transmittance (measured in test rig)	Information provided by Architen Landrell	Ratio laboratory/test rig
Single layer	Layer 1	25% fritted and 75% transparent	0.76	0.78		97%
Single layer	Layer 1	75% fritted and 25% transparent	0.47	0.53	0.43	88.6%
Two-layer	Layer 1	25% fritted and 75% transparent	0.67	0.75		89.3%
	Layer 2	100% transparent				
Two-layer	Layer 1	75% fritted	0.44 -	0.48 -		91.6%
	Layer 2	200 µm				
Three-layer	Layer 1	25% fritted	0.6 - -	0.68 -		88.2%
	Layer 2	150 µm				
	Layer 3	200 µm				
Three-layer	Layer 1	75% fritted	0.42 - -	0.4 - -		105%
	Layer 2	150 µm				
	Layer 3	200 µm				

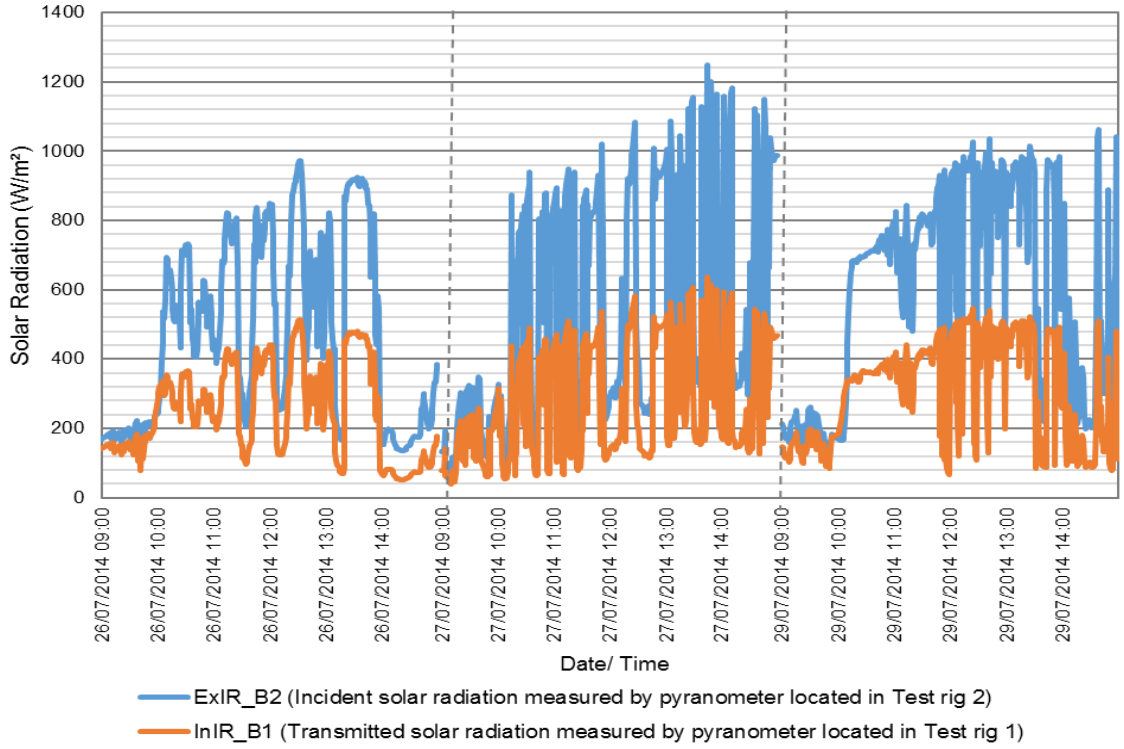


Figure 5-11: Incident and Transmitted Solar Radiation comparison (Single layer panel with 75% fritted ETFE-foil)

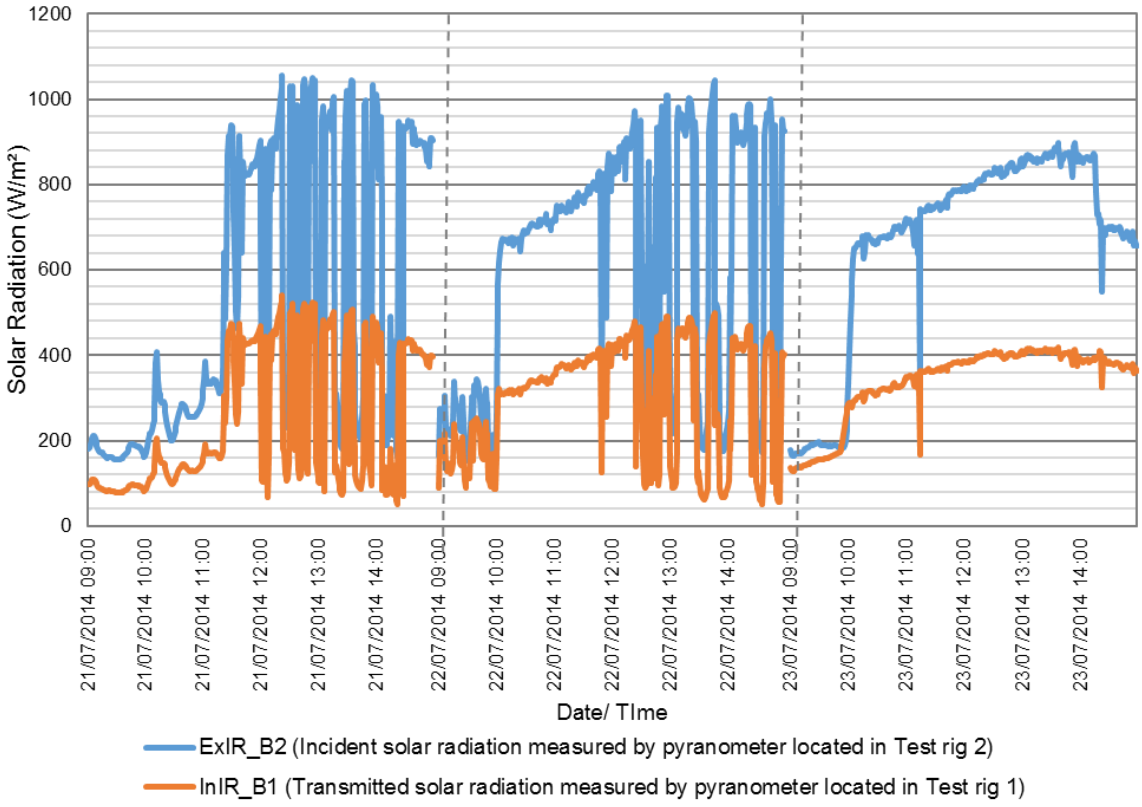


Figure 5-12: Incident and Transmitted Solar Radiation comparison (Two-layer panel with 75% fritted top ETFE-foil)



Figure 5-13: Incident and Transmitted Solar Radiation comparison (Thee-layer panel with 75% fritted top ETFE-foil)

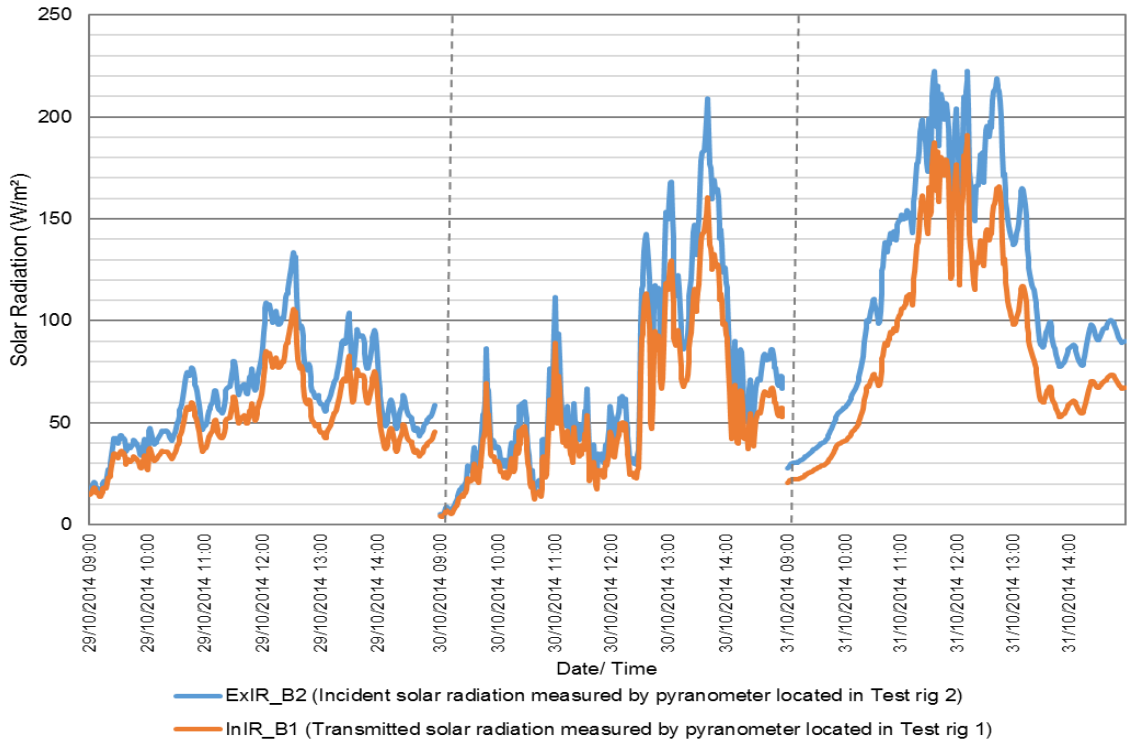


Figure 5-14: Incident and Transmitted Solar Radiation comparison (Single layer panel with 25% fritted top ETFE-foil)

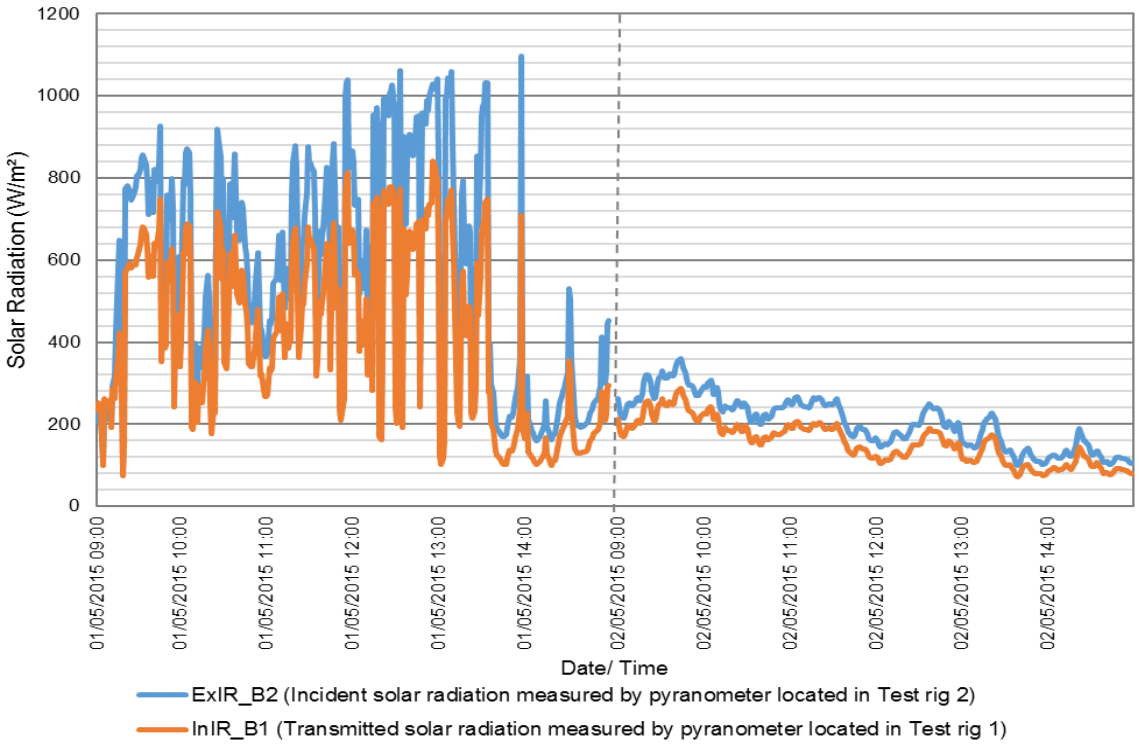


Figure 5-15: Incident and Transmitted Solar Radiation comparison (Two-layer panel with 25% fritted top ETFE-foil)

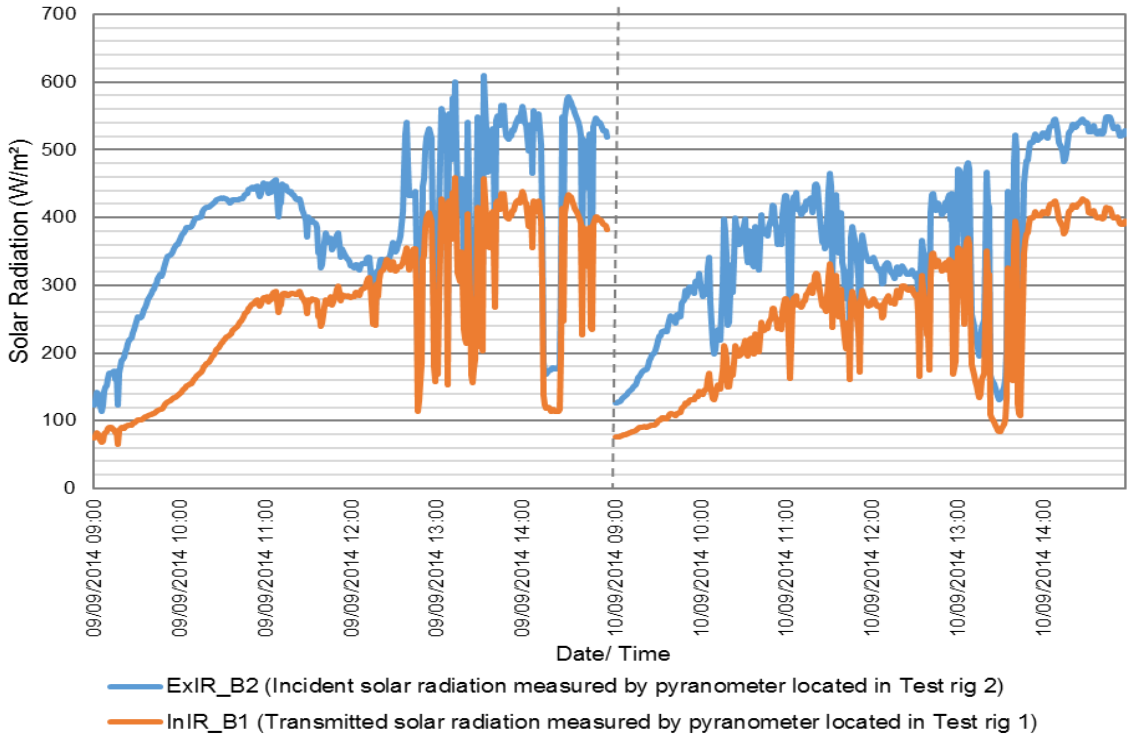


Figure 5-16: Incident and Transmitted Solar Radiation comparison (Three-layer panel with 25% fritted top ETFE-foil)

5.5 Thermal performance analysis of ETFE-foil panels

Combination, specification and study periods of ETFE-foil panels used in two different test-rigs are presented in Table 5-7. To measure the thermal behaviour of the ETFE-foils the following parameters were measured from Test-rig 1 and Test-rig 2:

- internal air temperature,
- air-volume air temperature,
- mean radiant temperature,
- surface temperature (both external and internal),
- incident and transmitted solar radiation.

In between 6th and 11th September 2015, Test-rig 1 and Test-rig 2 were equipped with two-layer ETFE-foil panels with 75% fritted top layer and a three-layer ETFE panel with a 25% fritted top layer, respectively. Between 19th and 24th September 2015, Test-rig 1 and Test-rig 2 were roofed with a three layer ETFE-foil panel with 75% fritted top layer and a three layer ETFE-foil panel with 25% fritted top layer, correspondingly. For the study period between 26th September and 2nd October 2015, Test-rig 1 and Test-rig 2, respectively, were capped with 75% and 25% fritted single layer ETFE-foil panels.



Figure 5-17: Second phase test-rig investigation (without mesh)



Figure 5-18: Second phase test-rig investigation (with and without mesh)

On 9th September 2015 the range of the outdoor temperature was 10.7°C to 19.85°C and the maximum incident solar radiation was 658.28 W/m^2, which was on average 208.83 W/m^2 during daylight hours. During 19th September, the outdoor ambient temperature varied between 9°C and 20.4°C, average solar radiation during daylight hours recorded was 316.7 W/m^2. On 26th September 2015 the range of outdoor ambient temperature was recorded as 13.95°C to 22.73°C , whereas the maximum and average incident solar radiation was correspondingly 584.77 W/m^2 and 342.1 W/m^2 during daylight hours.

The extent of variation of internal air temperatures of test-rigs recorded on 9th September, 19th September and 26th September 2015 are presented in Figure 5-19, Figure 5-20 and, Figure 5-21. Figure 5-19, Figure 5-20 and Figure 5-21 represents the distribution of data recorded (e.g. air temperatures, surface temperatures, etc.), in Test-rig 1 and Test-rig 2 during the monitoring. The maximum and minimum recorded values showed by the 'whiskers', the central rectangle spans from the first quartile (25th percentile) to the third quartile (75th percentile), whereas the segment inside the rectangle shows the median (50th percentile). In addition, horizontal axis shows the identification of the measured parameter (see Table 5-3). It can be seen that maximum spread of data from median towards the third quartile was 13°C for Test-rig 1 and 18.6°C for Test-rig 2, which was relatively high in each test-rig. Therefore, the relative thermal environment of test-rigs with respect to one another, and outdoor air temperatures were mainly analysed here, to evaluate the thermal performance of single, two- and three-layer ETFE-foil panels. The reason for this variation in median

air temperature might be that both test-rigs were air tight and no air circulation was allowed while the physical conditions of the both test-rigs were identical.

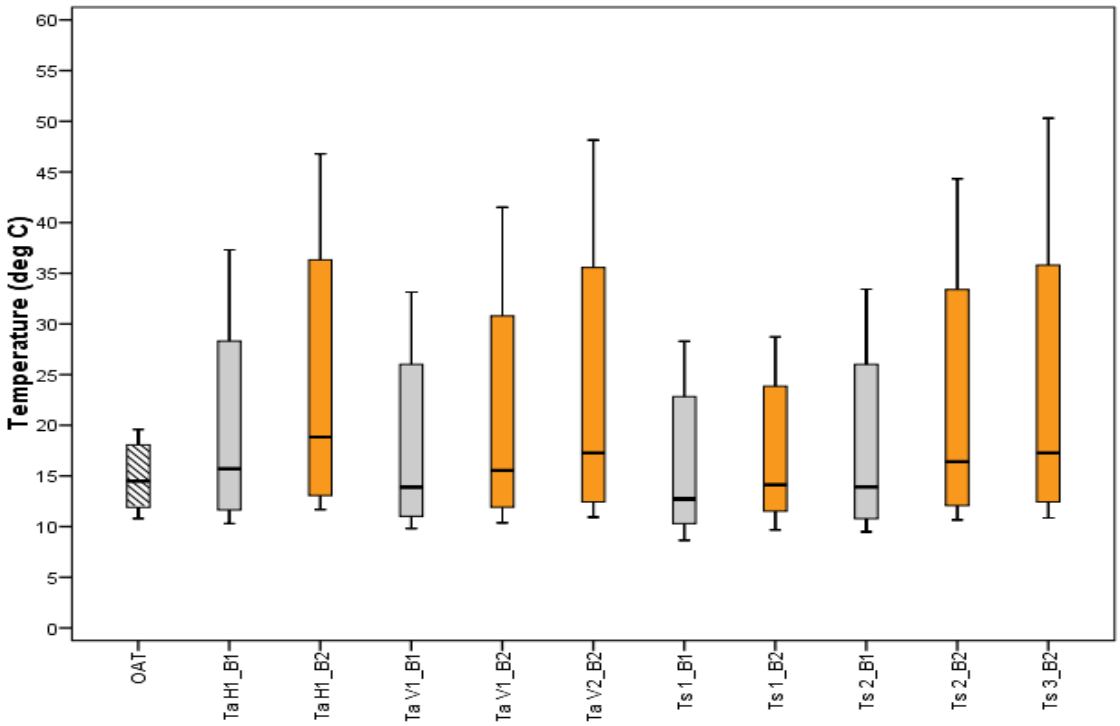


Figure 5-19: Comparison of Test-rig 1 and Test-rig 2 air temperature, air volume air temperature and surface temperature recorded during 9th Sep 15

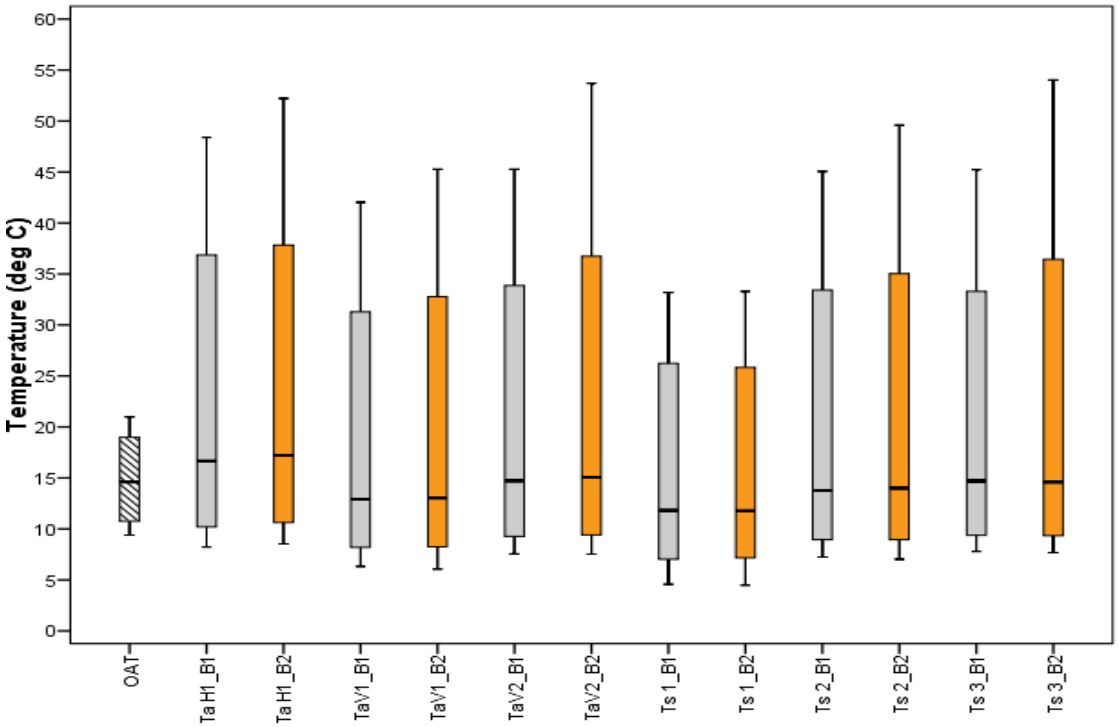


Figure 5-20: Comparison of Test-rig 1 and Test-rig 2 air temperature, air volume air temperature and surface temperature recorded during 19th Sep 15

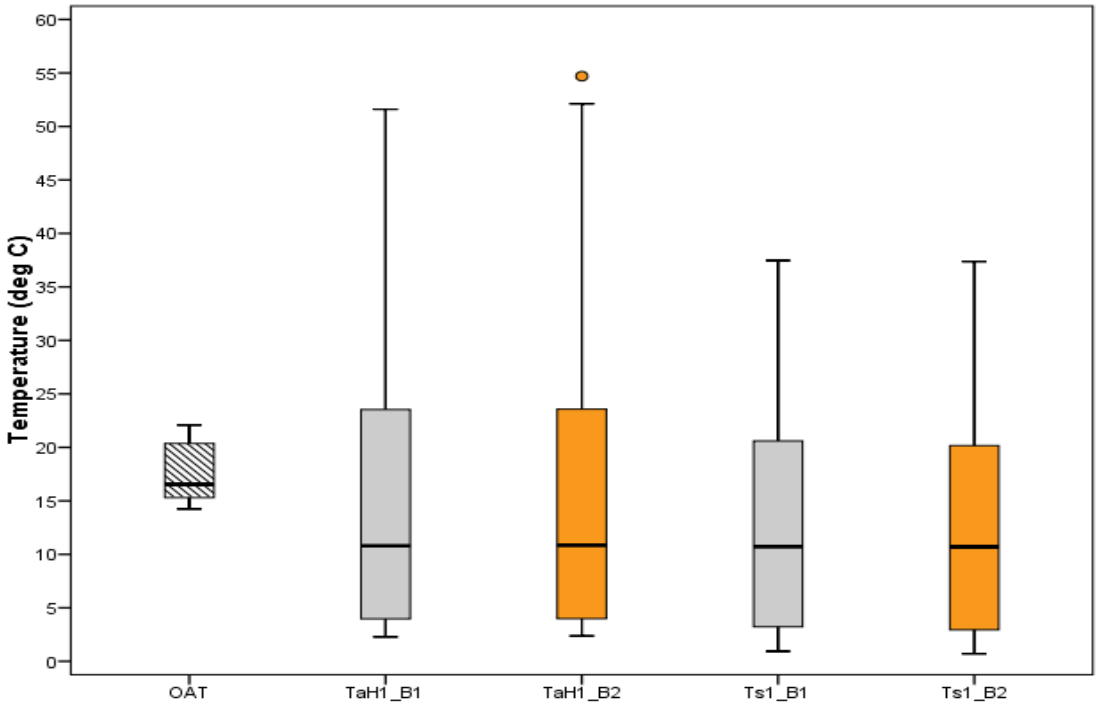


Figure 5-21: Comparison of Test-rig 1 and Test-rig 2 air temperature, air volume air temperature and surface temperature recorded during 26th Sep 15

Here it should be mentioned that Test-rig 1 ETFE-foil panel configuration on 9th September was approximately similar to the ETFE-foil cushion roof of Nottingham High School (presented in Chapter 6). Nevertheless, it was evident from the onsite monitoring presented in Chapter 6 that the thermal environment of Nottingham High School was uncontrolled and influenced by the HVAC system, internal gains etc. On the other hand, the test-rigs were more controlled and air tight. Because of this variation in the thermal environment, the results (e.g. air temperature, the surface temperature of ETFE-foils, etc.) cannot be compared directly with that of Nottingham High School. Only a number of assumptions can be made on the basis of heat transfers between the ETFE-foil layers and internal air temperatures of the test-rigs.

Variations of air temperatures, air-volume air temperatures, and surface temperatures of the ETFE-foil of Test-rig 1 and Test-rig 2 obtained during 6th to 11th September 2015, 19th to 24th September 2015 and 26th September to 2nd October 2015, are presented in Figure 5-22, Figure 5-23 and Figure 5-24 respectively. These parameters represent the thermal environment of the test-rigs and ETFE-foil panels, with and without rain suppression mesh, which were also investigated during this period (Figure 5-18). This is also indicated in Figure 5-22, Figure 5-23 and Figure 5-24 as appropriate.

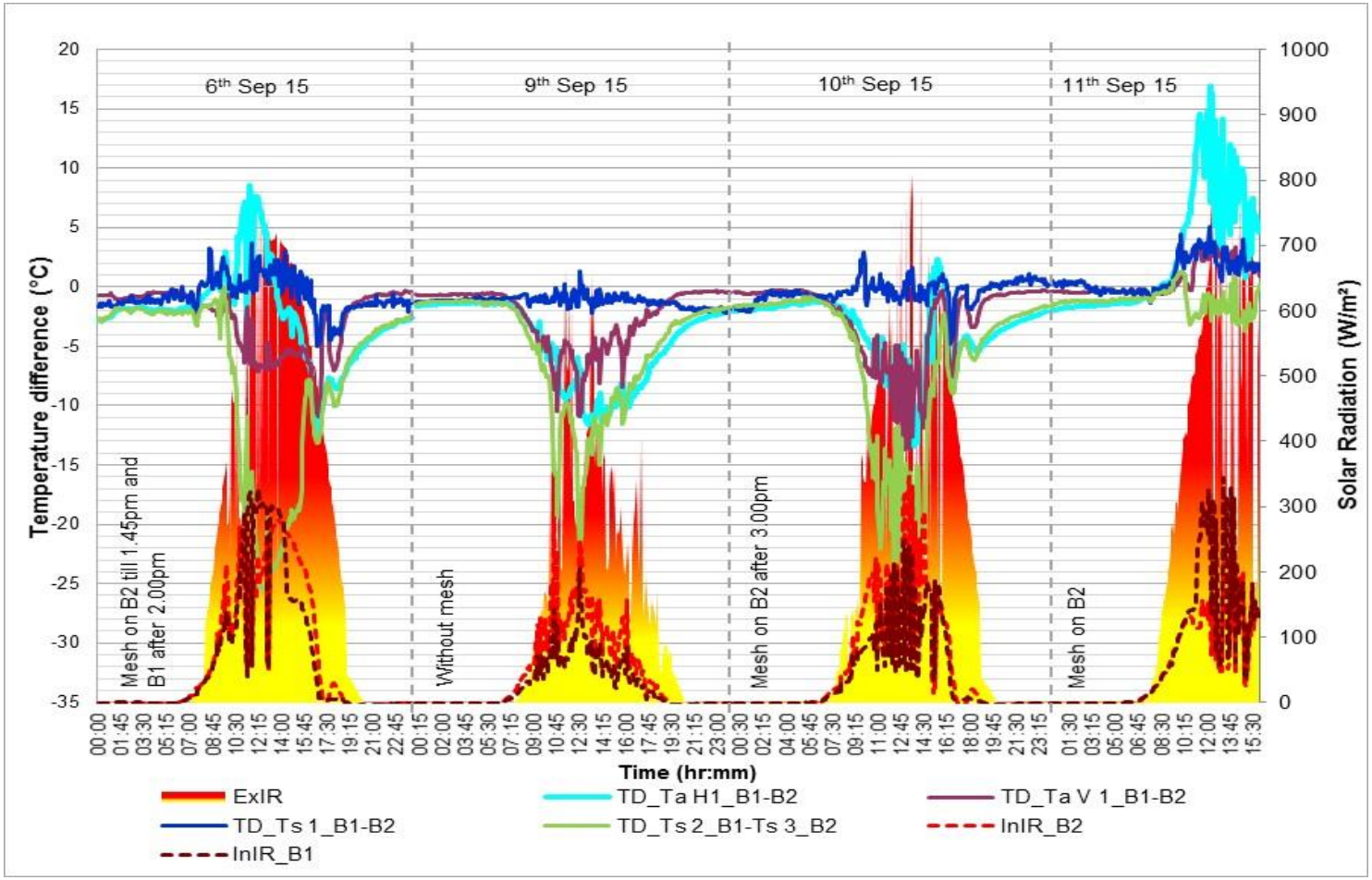


Figure 5-22: Relative condition of experimental Test-rig 1 and Test-rig 2

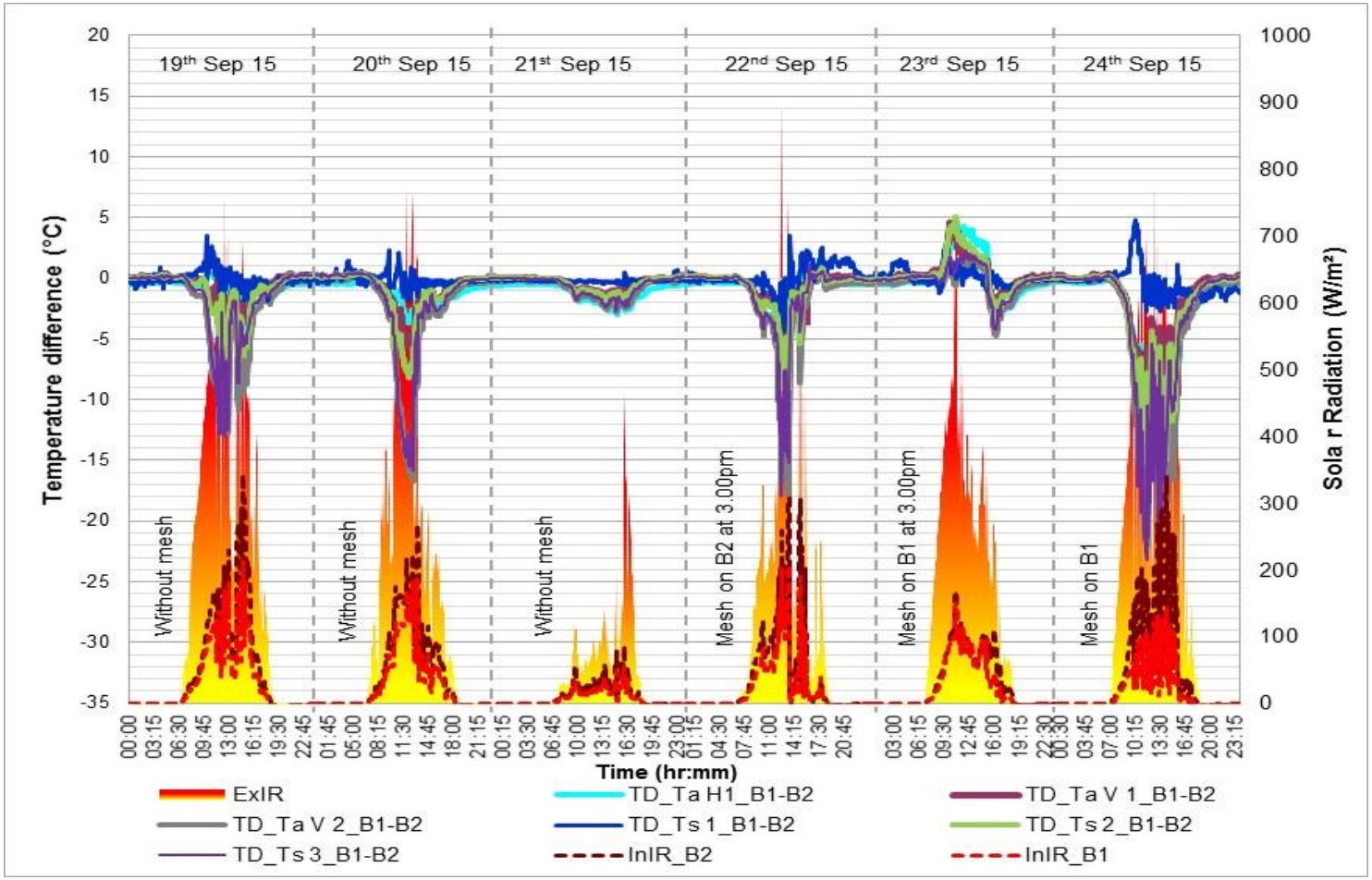


Figure 5-23: Relative internal condition of Test-rig 1 and Test-rig 2

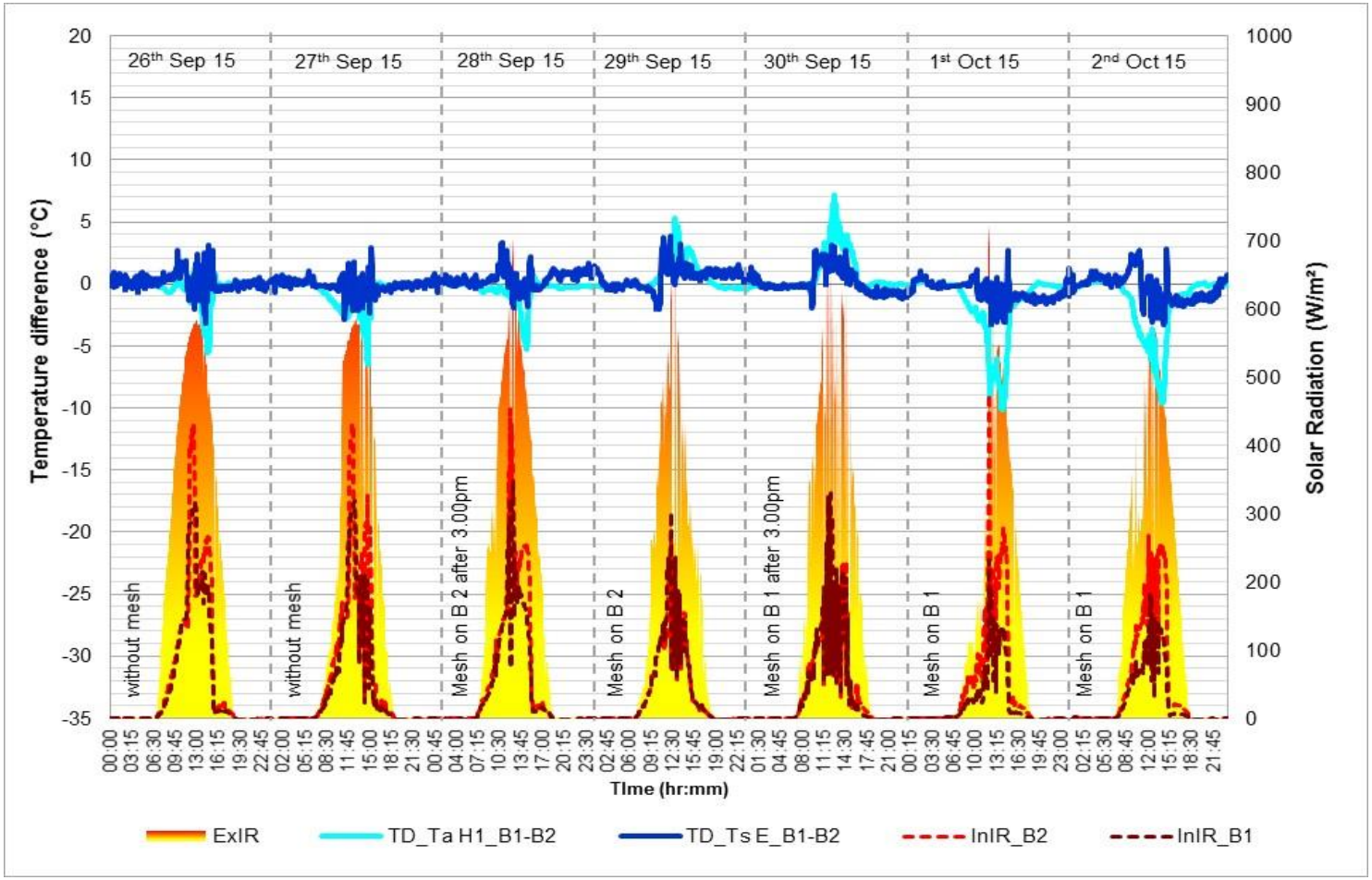


Figure 5-24: Relative condition of Test-rig 1 and Test-rig 2

The results of the study obtained during 9th September showed that the solar radiation recorded in Test-rig 1 (enclosed with two-layer ETFE panel with 75% fritted top layer) was on average 41.9% less than the solar radiation recorded in Test-rig 2 (enclosed with three -layer ETFE panel with 25% fritted top layer). This had an impact on the air temperatures of the test-rigs and resulted in an average 5°C less air temperature in Test-rig 1 than the Test-rig 2. The maximum air temperature of Test-rig 2 was 9°C hotter than the same of Test-rig 1 and occurred at noon. This maximum difference of internal air temperature of the test-rigs was 4°C on 19th September when both of the test-rigs were enclosed with three layer panels. On that day, Test-rig 2 internal air temperature was also hotter than Test-rig 1.

Table 5-9 presents average solar radiation transmitted through the ETFE-foil panels recorded during daylight hours of 9th September, 19th September and 26th September 2015. The results presented in Table 5-9 showed that Test-rig 1 three-layer ETFE-foil panel (75% fritted top layer) transmitted 30.7% less solar radiation than Test-rig 2 three-layer ETFE-foil panel (25% fritted top layer). This is the result of the density of fritting of top ETFE-foil layer in three-layer ETFE-foil panel of Test-rig 1 while compared to Test-rig 2. While comparing the thermal environment of the test-rigs on 9th September, Test-rig 2 internal air temperature was also influenced by an extra layer of ETFE-foil and air volume enclosed by it. This increased the insulation properties of Test-rig 2 and caused rise in air temperature over Test-rig 1. On the other hand, Test rig 1 internal thermal environment was shaded by fritting, which reduced solar gain, this in turn resulted in lower air temperature in Test-rig 1 than Test-rig 2.

Table 5-9:Average transmitted solar radiation recorded during daylight hours

ETFE-foil panel description	Average transmitted solar radiation during the day time in 9th September 2015	Average transmitted solar radiation during the day time in 19th September 2015	Average transmitted solar radiation during the day time in 26th September 2015
	W/m^2	W/m^2	W/m^2
Single-layer ETFE-foil with 25% fritted top layer	-	-	113.65
Single-layer ETFE-foil with 75% fritted top layer	-	-	97.6
Two-layer ETFE-foil with 75% fritted top layer and transparent bottom layer	51.6	-	-
Three-layer ETFE-foil with 25% fritted top layer, transparent middle and bottom layer	88.8	95.81	-
Three-layer ETFE-foil with 75% fritted top layer, transparent middle and bottom layer	-	66.37	-

The results of temperature variation between Test-rig 1 and Test-rig 2 air temperatures and air-volume air temperatures of ETFE-foil panels are presented in Table 5-10. From Table 5-10, it can be demonstrated that average test-rig air temperatures and air-volume air temperatures were high in test-rigs when enclosed with 25% fritted ETFE-foil panels of different combination, while this average air temperatures were relatively lower when they were enclosed with 75% fritted ETFE-foil panels of different combination presented in Table 5-7 (single, two- and three-layer panels). However, this temperature differences varies depending on weather conditions.

The results presented in Figure 5-19,Figure 5-20,Figure 5-21 demonstrated that, the first quartile, third quartile, median air temperature of Test rig 2 was respectively 1.5°C, 8.7°C and 3.2°C higher than the same of Test-rig 1. This also indicated that the test-rig's thermal environment enclosed with 25% fritted ETFE-foil panels was hotter than when enclosed 75% fritted ETFE-foil panels.

Table 5-10:Temperature differences between Test-rig 1 and Test-rig 2 air temperatures and air-volume air temperatures

Description	Identification	Night and early morning	Day time
Temperature difference between air temperature of test rigs enclosed with single-layer panel with 75% ETEF layer and 25% fritted ETFE-foil layer	TD_TaH1_B1-B2	similar	0.6°C (TaH1_B1< TaH1_B2)
Temperature difference between air temperature of test rigs enclosed with two-layer panel with 75% top layer and three- layer 25% fritted ETFE-foil	TD_TaH1_B1-B2	1.4°C (TaH1_B1< TaH1_B2)	5°C (TaH1_B1< TaH1_B2)
Temperature difference between air temperature of air-volume enclosed with two-layer panel with 75% top layer and three-layer 25% fritted ETFE-foil	TD_TaV1_B1-B2	0.65°C (TaV1_B1< TaV1_B2)	3°C (TaV1_B1< TaV1_B2)
Temperature difference between air temperature of test rigs enclosed with three-layer panel with 75% top layer and 25% fritted ETFE-foil	TD_TaH1_B1-B2	0.4°C (TaH1_B1< TaH1_B2)	1.4°C (TaH1_B1< TaH1_B2)
Temperature difference between air temperature of air-volumes enclosed with three-layer panel with 75% top layer and 25% fritted ETFE-foil	TD_TaV1_B1-B2	No difference in air temperature	1.5°C (TaV1_B1< TaV1_B2)
	TD_TaV2_B1-B2	As above	4.4°C (TaV2_B1< TaV2_B2)

On a sunny day hourly temperature swing recorded in Test-rig 1 (with double layer ETFE panel) was (+/-) 1.5°C to 13°C, while in Test-rig 2 (with three-layer ETFE panel) air temperature fluctuated by (+/-) 1°C to 14°C. However, within five minutes, air temperature increased by 5°C (with double-layer ETFE panel) and 3°C (with three-layer ETFE panel). Again, this can be explained as an impact of the additional air layer in Test-rig 2, which better controlled frequent fluctuation of air temperature. In addition, within five minutes, in the presence of moving cloud in front of the sun, air temperature swung by 2°C to 4°C in the morning and in the afternoon in both test-rigs enclosed with single, two- and three-layer ETFE-foil panels. In both test-rigs, this fluctuation of internal air temperatures observed particularly during the day time and in the presence of solar radiation. Additionally, a maximum hourly increase of air temperature by 14°C was observed in Test-rig 2 during 19th September 15. This was the results of 40% increase of solar radiation within an hour.

Figure 5-25, Figure 5-27 and Figure 5-29 presents Test-rig 1 and Test-rig 2 internal air temperatures and, air-volume air temperatures relative to outdoor air temperatures obtained between 6th and 11th September, 19th and 24th September, and 26th September and 2nd October 2015.

The results demonstrated that during the day time, on average the air temperature of test-rigs enclosed with single-layer, two-layer and three-layer ETFE-foil panel went above outdoor temperature. Test-rigs air temperature covered with a two-layer 75% fritted ETFE-foil panel and three-layer 25% fritted ETFE-foil panel went maximum 45.7°C and 47.8°C above outdoor air temperature during the afternoon of 6th September 2015. Whereas between night and early morning, internal air temperatures of test-rigs enclosed with double layer and three-layer ETFE-foil panels stayed close to outdoor air temperatures under cloudy sky but went below outdoor temperature under clear sky. The test-rig's internal air temperature, when enclosed with a single layer ETFE-foil panel went on average 11.6°C below outdoor air temperature between night and morning of 26th September when average outdoor temperature was 14.5°C. Here because of the additional layers of ETFE-foil and volume of air layers in multilayer ETFE-foil panels, the test-rig's internal thermal condition was warmer than the same when enclosed with single layer ETFE-foil panels. Thus, single layer panels release more heat to the external environment and causes significant decrease in internal air temperatures of the

test-rigs below outdoor air temperatures particularly at night. While during the day time, in a single layer fritted system interaction with the external environment was more rapid than that of multilayer panel systems, where heat is transmitted, absorbed and reflected through more layers.

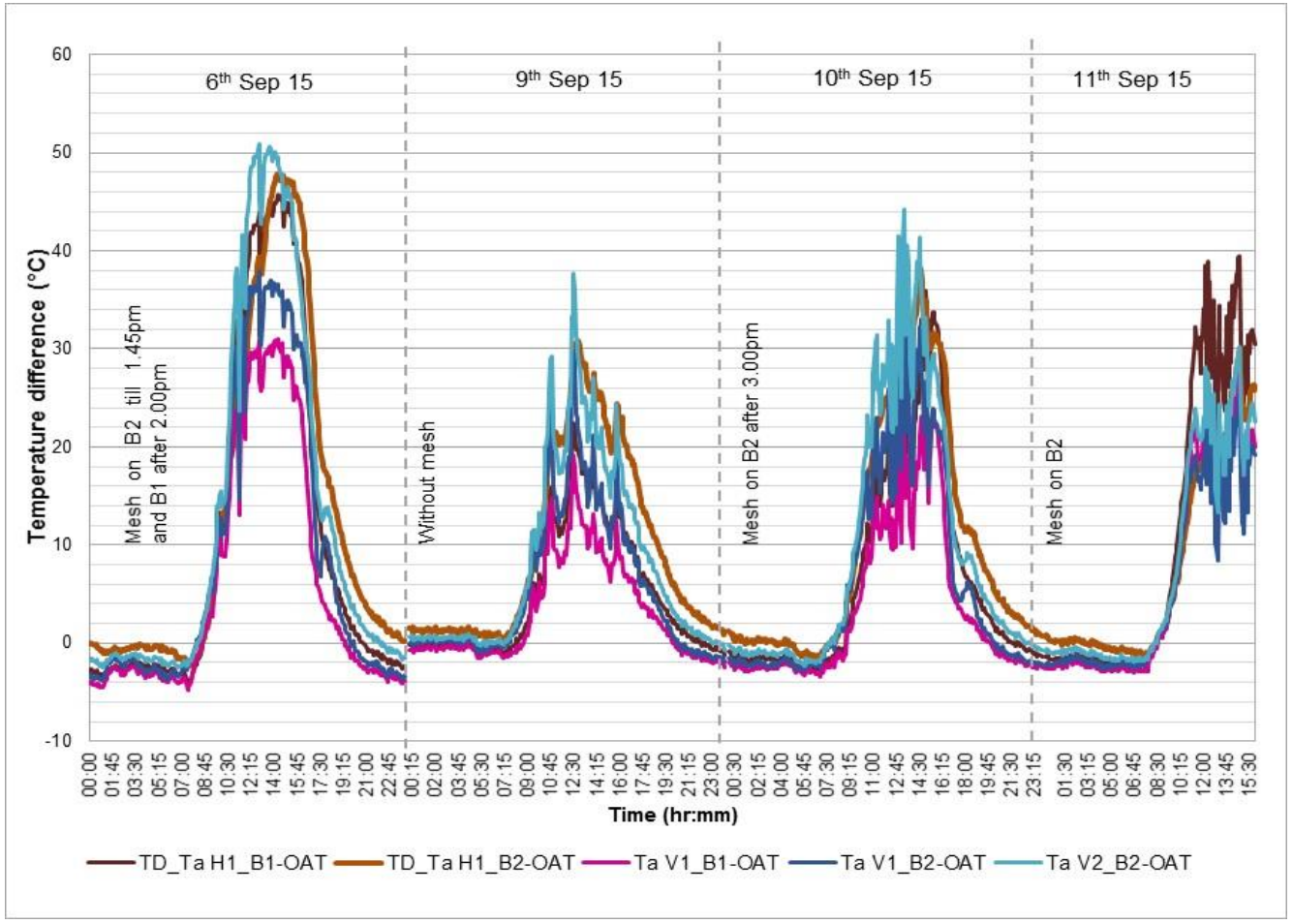


Figure 5-25: Test-rig 1 (two-layer 75% fritted top layer) and Test-rig 2 (three-layer 25% fritted top layer) internal air temperatures, air-volume air temperatures, relative to outdoor ambient temperatures

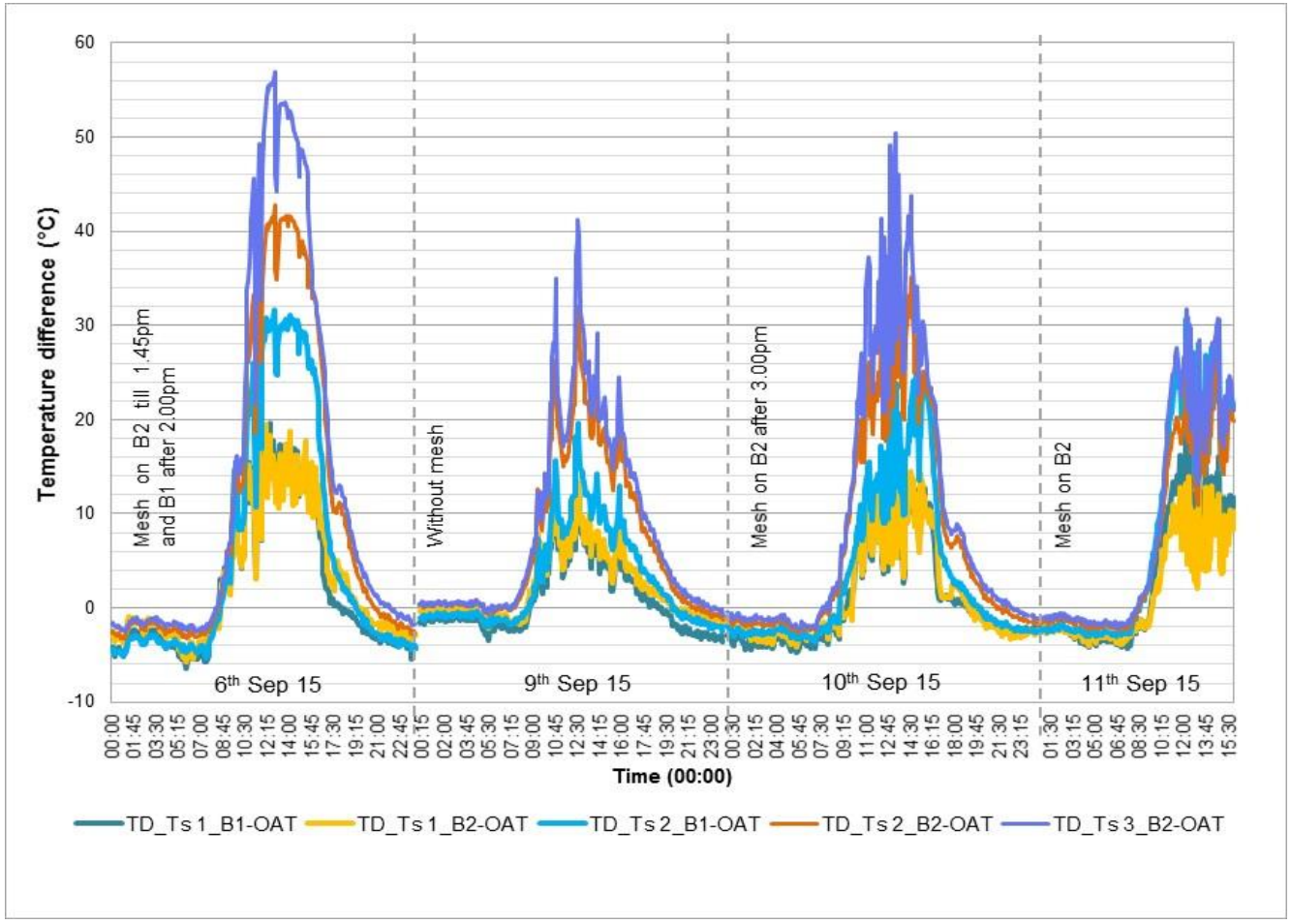


Figure 5-26: Test-rig 1 (two-layer 75% fritted top layer) and Test-rig 2 (three-layer 25% fritted top layer) ETFE-foil panel surface temperatures relative to outdoor ambient temperature

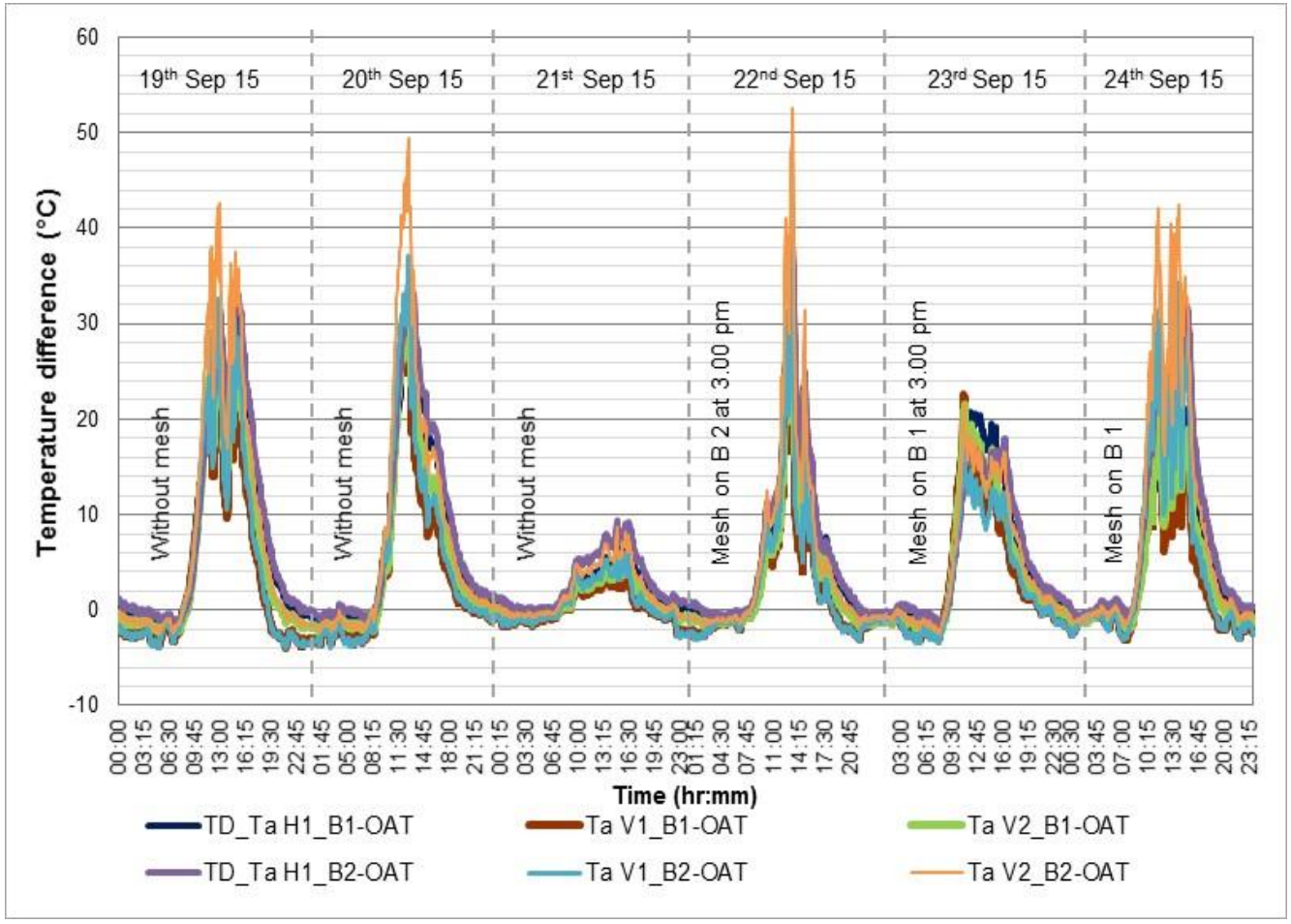


Figure 5-27: Test-rig 1 (three-layer 75% fritted top layer) and Test-rig 2 (three-layer 25% fritted top layer) internal air temperatures, air-volume air temperatures, relative to outdoor ambient temperatures

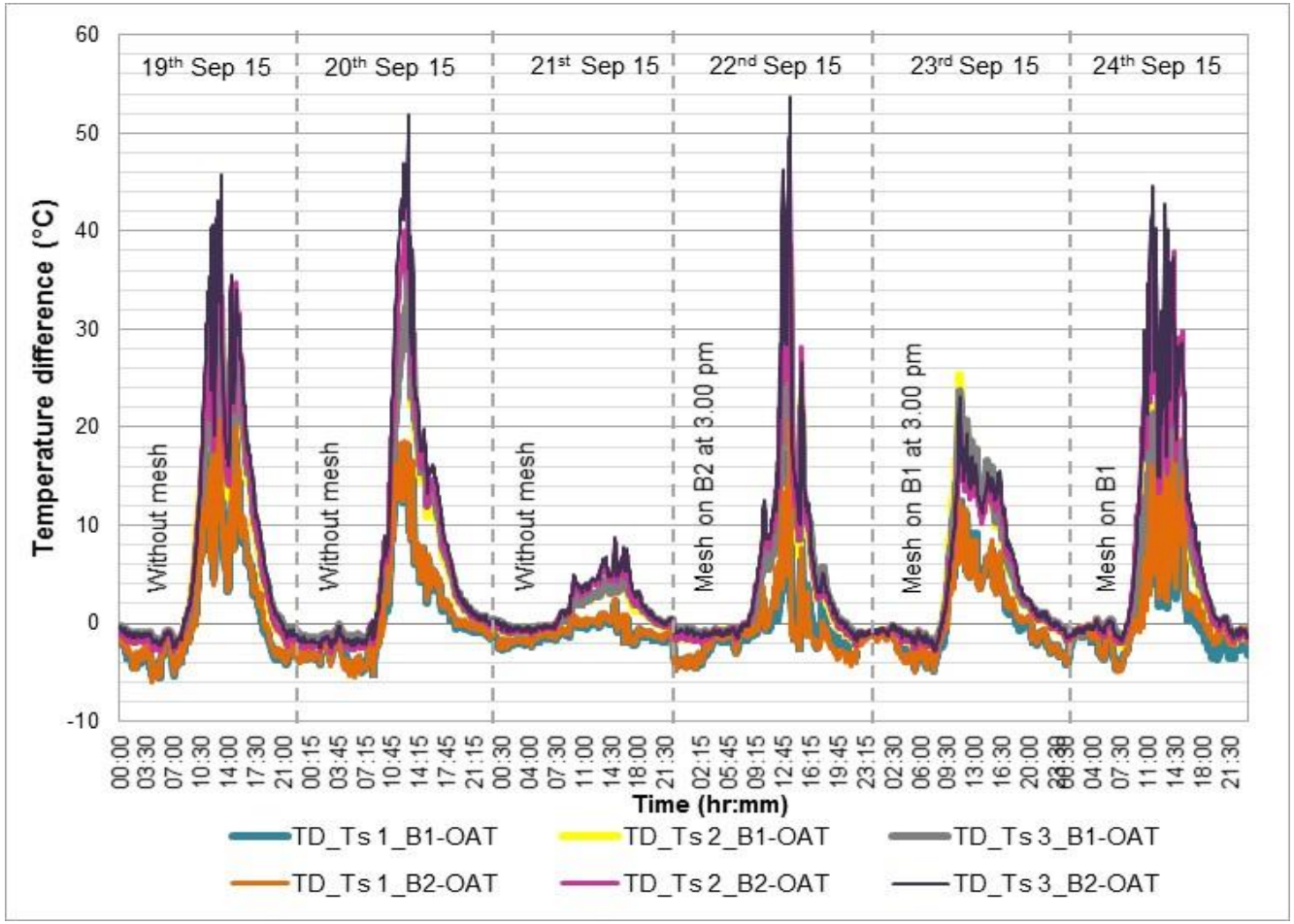


Figure 5-28: Test-rig 1 (three-layer 75% fritted top layer) and Test-rig 2 (three-layer 25% fritted top layer) ETFE-foil surface temperatures relative to outdoor ambient temperatures

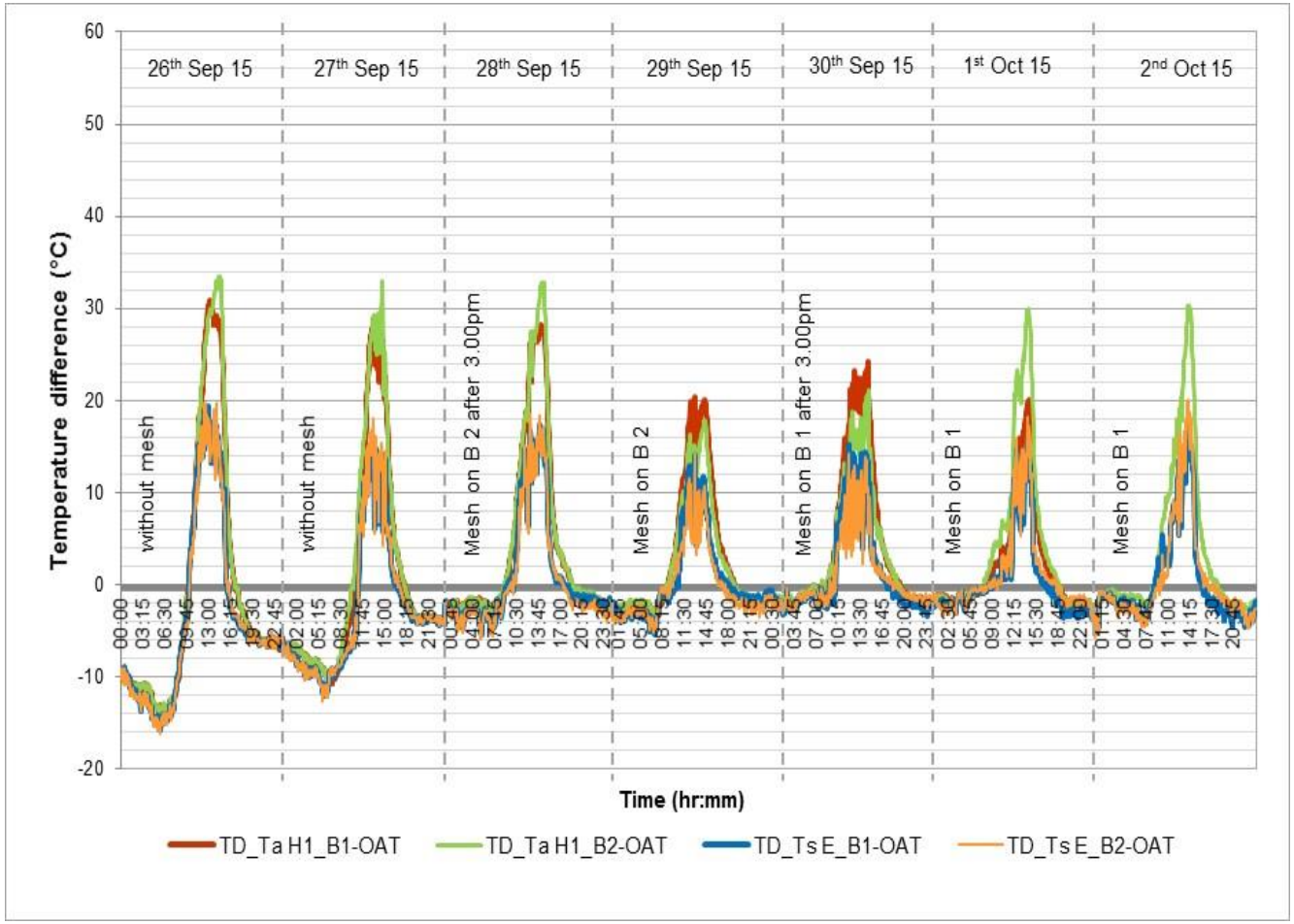


Figure 5-29: Test-rig 1 (single layer 75% fritted) and Test-rig 2 (single layer 25% fritted) internal air temperatures, air-volume air temperatures, and ETFE-foil surface temperatures relative to outdoor ambient temperatures

Relative conditions of ETFE-foil surfaces to outdoor air temperatures obtained between 6th and 11th September 2015, 19th and 24th September 2015, 26th September and 2nd October 2015 are presented in Figure 5-26, Figure 5-28 and Figure 5-29 respectively. From the results, it is apparent that external surface temperatures of ETFE foil in both test-rigs (enclosed with single, two- and three-layer ETFE-foil panels) dropped to below outdoor air temperature during the night and early morning. This is due to the longwave radiation losses from the ETFE-foil surfaces to the cold sky.

It was observed that the fluctuations of solar radiation directly impact surface temperatures of ETFE-foil. This scenario was apparent during 10th September in the afternoon, when in five minutes solar radiation increased from 292.4 W/m^2 to 722.9 W/m^2 and outdoor air temperature increased by 1.5°C. This change of external conditions, in turn, caused an increase of external surface temperatures of the ETFE-foil by 5°C in Test-rig 1 and 6°C in Test-rig 2. Whereas the internal surface temperatures of the ETFE panel of Test-rig 1 and Test-rig 2 also increased by 10°C and 15°C respectively. Again, just after this time in the next five minutes' solar radiation dropped to 362.89 W/m^2. This caused decrement of external and internal surface temperatures of Test-rig 1 ETFE-foil panel by 6°C and 8°C respectively. Whereas the Test-rig 2 ETFE-foil panel external surface temperature also dropped by 6°C and internal surface dropped by 12°C. Fluctuation of air-volume air temperatures and test-rig air temperatures were also evident within this 10 minutes. During this time air-volume and Test-rig 1 internal air temperature fluctuated by (+/-) 4°C ~ 6°C whereas in Test-rig 2, air-volume and rig air temperature fluctuated by (+/-) 8°C ~10°C.

The extent of increase in surface temperatures was more in internal surfaces than external surfaces. This can also be the result of the extremely hot thermal condition of the test-rigs which impacts surface temperatures as a result of convective heat transfer. Here it was also noticed that the fluctuations of the test-rig's surface temperature were less than that of ETFE-foil surfaces. Therefore, even if the ETFE-foil surface temperature fluctuated by 5°C~15°C within 5 minutes, the test-rig's internal insulation surface temperature increased by 1°C~ 2°C during this time.

Additionally, it was also noticed that during the day time the air-volume 2 (lower chamber) air temperature in a three-layer ETFE-foil panel system was on average 4°C and 8°C higher than air-volume 1 (upper chamber) air temperatures and the test-rig's internal air temperature, respectively. The reason behind this was that air-volume 2 air is mainly influenced by insulation of upper air chamber and hot ETFE-foil surface

temperatures adjacent to it (Ts3, Ts2) whereas test-rig's internal air temperatures was particularly influenced by ETFE-foil surface (Ts3) next to it and the internal surfaces of the test-rig. Whereas air-volume 1 air temperatures were influenced by surrounding ETFE-foil surfaces (Ts1, Ts2) which had relatively low temperatures compared to the bottom surface of ETFE-foil (Ts3). But at night and in absence of adequate solar radiation, surface temperatures, air-volume air temperatures, and the test-rig's internal air temperatures stayed close to outdoor air temperatures in the test-rigs enclosed with two-layer and three-layer ETFE-foil panels.

A gradual increase of air temperature and surface temperature was observed from the external surface towards the internal volume of Test-rig 1 and 2 which was more significant in Test-rig 2 because it was enclosed with three layer ETFE-foil panel.

Test-cell investigation carried out by Harvie (1996), on fabric membranes found it difficult to measure the surface temperature of the membrane, research also mentioned that sensors attached to the external surface recorded higher temperature than those attached to the internal surface of the membrane. But this on-site experiment on ETFE- foil panels of the different type found a different scenario where internal surface temperatures of the ETFE-foil were hotter than the external surface, which should be the actual scenario. This is because the internal surface of the ETFE-foil panel during the day time was in contact with extremely hot air temperatures within the test-rigs, whereas the external surface was exposed to outdoor air, which was relatively cooler. This variation of surface and air temperatures was influenced by heat transfer mechanisms - convective and radiative heat transfer in particular. Harvie (1996), specified in his study that because of smoothness of membrane surface, there would be no convective heat transfer. This phenomenon proved incorrect while analysing the thermal performance of ETFE-foil in this study as the impact of convective heat transfer between the ETFE-foil surface and it's adjacent air was apparent.

In this analysis the effect of the radiative process is presented by the measured incident irradiance. This parameter during the day time presents the effect of short-wave solar irradiance while at night pyranometer measurement with negative readings represent the magnitude of net long-wave radiation losses (Kipp & Zonen, 2016).

Long wave radiation losses to the clear sky affect more strongly the surface temperature of the outer ETFE-foil of both test-rigs than the air temperature within the test-rig and air-volume between ETFE-foil layers in panels. As a result, the external

surface dropped below outdoor air temperature during clear night by 1°C~4°C whereas internal surfaces dropped by 1°C ~2°C below outdoor air temperature, while panel air-volume air and test-rigs internal air temperature stayed within +/-0.5°C ~1.5°C of outdoor air temperature until incident solar radiation was significant over longwave radiation during the day. These phenomena were evident in each test-rigs mostly during the night and early morning, was significant in test-rig when enclosed with single layer foil panel where on a clear sky morning surface temperature and test-rig internal air temperature dropped 15.5°C and 13°C below outdoor air temperature respectively.

Therefore, it can be explained that the combined effect of convective and radiative heat transfer was pronounced on surface temperatures of the ETFE-foil panel both external and internal. Heat captured and stored in the air tight test-rigs also influenced internal surface temperatures as a process of convective heat transfer. As a result, although the external surface shielded internal layers in the panel, the internal surface temperature exceeded the external surface temperature during day time. Besides, at night long-wave radiation loss to the external environment resulted in drop of external surface temperature below outdoor ambient temperature.

In order to see the extent of convective and radiative heat transfer on the surface of the ETFE-foil an attempt was made to calculate the heat transfer based on the equation of heat transfer which is presented in section 5.5.1.

5.5.1 Relationship between the surface temperature of ETFE-foil layers and test-rig internal condition

It was observed that ETFE-foil surfaces and the test rig's air temperatures were strongly influenced by outdoor environment e.g. incident solar radiation, outdoor ambient temperature, longwave radiation. Harvie (1996), stated that with no thermal mass architectural fabrics affect the spaces by the amount of solar radiation they transmit and heat they introduce into space as a result of the temperature of their surface. In this study transmittance of solar radiation through different type of ETFE-foils was measured which is presented in section 5.4. Besides it was already discussed earlier that convective and radiative heat transfer particularly affects the thermal environment of test-rigs enclosed with ETFE-foil panels. Therefore, it was important to evaluate the impact of these two heat transfer mechanisms on the thermal environment of the test-rigs. This was done by calculating convective and radiative heat transfer through the surface of the ETFE-foil, on the basis of measured surface temperatures of ETFE-foil, adjacent air temperatures of foil panel and emissivity of the ETFE-foil

surface. Convective heat transfer that occurred between the surface of the ETFE and adjacent air (air-volume of the ETFE-foil panels) of Test-rig 1 and Test-rig 2 during 6th and 11th September 2015 is presented in Figure 5-30, whereas Figure 5-31 presents the radiative heat transfer that occurred through the surface of ETFE-foil during the same period.

It can be assumed that the convective heat transfer occurred in between the ETFE-foil surface and the internal air of test-rigs through natural convection, where the flow was induced by buoyancy forces which arise from density differences, caused by the temperature difference in the test-rig air. The rate of this convective heat transfer was calculated on the basis of Equation 5.1, stated in Incropera et al. (2013). This expression is also known as Newton's law of cooling.

$$q = h(T_s - T_a) \qquad \text{.....(5.1)}$$

Here, q is convective heatflux (W/m^2),

Ts is surface temperature (K) of ETFE-foil,

Ta is air temperature adjacent to ETFE-foil,

h (W/m^2 K) is the convective heat transfer co-efficient.

The convective heat transfer co-efficient was calculated according to (BSI, 1989).

As stated by Incropera et al. (2013), radiation transfer efficiently occurs in the volume of air which is similar to the test-rig's internal environment. Radiative heat transfer depends on the emissivity of the ETFE-foil surface. The radiative heat flux emitted by the ETFE-foil surface was calculated using Equation 5.2.

$$E = \varepsilon \sigma T_s^4 \qquad \text{.....(5.2)}$$

Here, E represents radiative heat flux (W/m^2),

ε is the emissivity,

Ts is the surface temperature (K) of ETFE-foil.

Boundary conditions obtained during the experiment were directly applied in these equations to calculate convective and radiative heat flux. From Figure 5-30 and Figure 5-31 it can be stated that convective heat flux governs in the heat transfer process in both of the test-rigs. Because this type of heat flux depends on temperature difference, therefore heat was transferred between each layer of the ETFE-foils and air adjacent

to it. This heat transfer was particularly significant between the external ETFE-foil surface of the multilayer panel and adjacent air-volume, which was the result of higher temperature difference.

It is known that ETFE-foil is relatively transparent to longwave radiation. Radiative heat transfer occurring in the ETFE-foil surfaces was calculated using Equation 5.2 and presented in Figure 5-31. The radiative heat transfer here represents the combined effect of shortwave and long-wave radiation. Because it was not possible to isolate the effect of long-wave radiation. It can be assumed that during the day, heat transfer occurred on the surfaces was dominated by short-wave radiation. Whereas at night due to longwave radiation losses surface temperature dropped, this, in turn, reduced heat transfers in air and ETFE-foil layers. For optically thin surfaces, the radiative heat transfer decreases with the decrease of surface emissivity (Libby et al., 1967). Therefore, among the different layers of ETFE foils in multi-layer panels, radiative heat transfer was more pronounced on internal transparent ETFE-foil surfaces. Whereas little less in external fritted surfaces which were the result of low emissivity and the relatively lower temperature of external surfaces (Ts1) while compared with internal surfaces (Ts2 and Ts3) in each test-rig. Besides particularly at night and early morning, stable conditions occurred, however as soon as the external surface temperatures increased above the internal surface, radiative and convective heat transfer was constant for all the surfaces and increased as the temperature difference increased between the surface of ETFE-foil and adjacent air layers during the day.

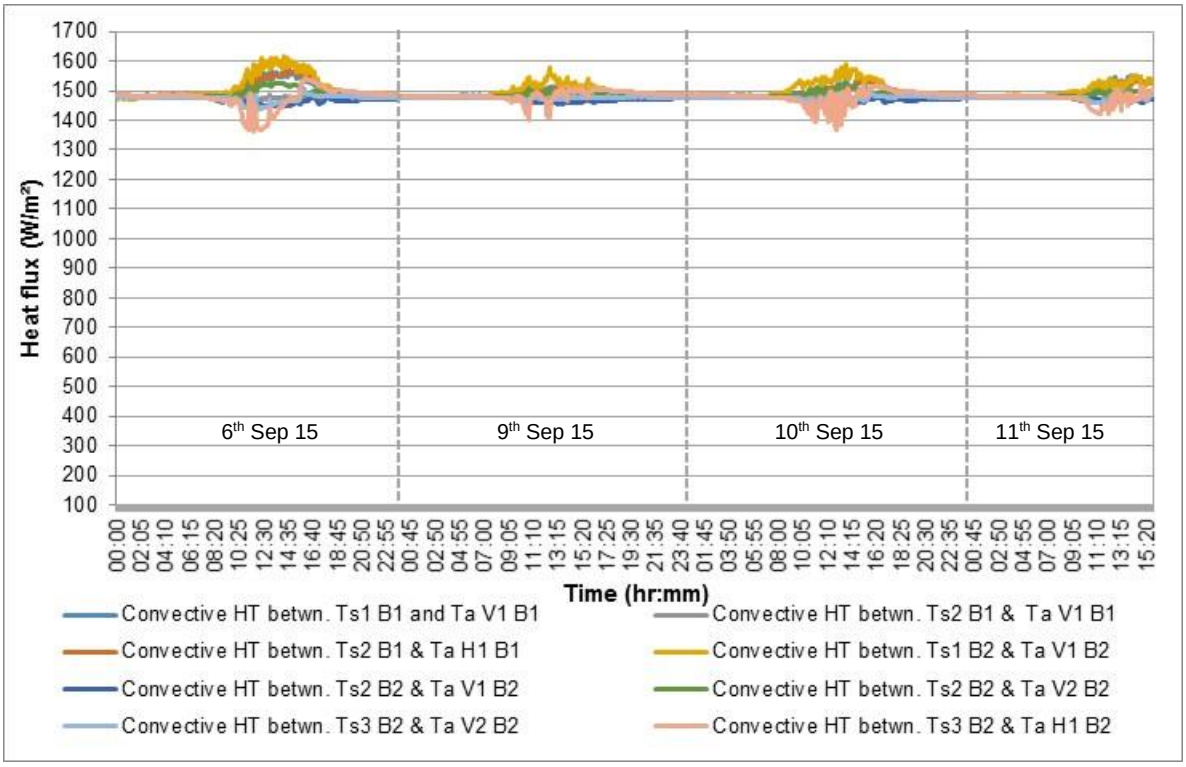


Figure 5-30: Convective heat transfer between ETFE surface and air temperature adjacent to it in Test-rig 1 and Test-rig 2

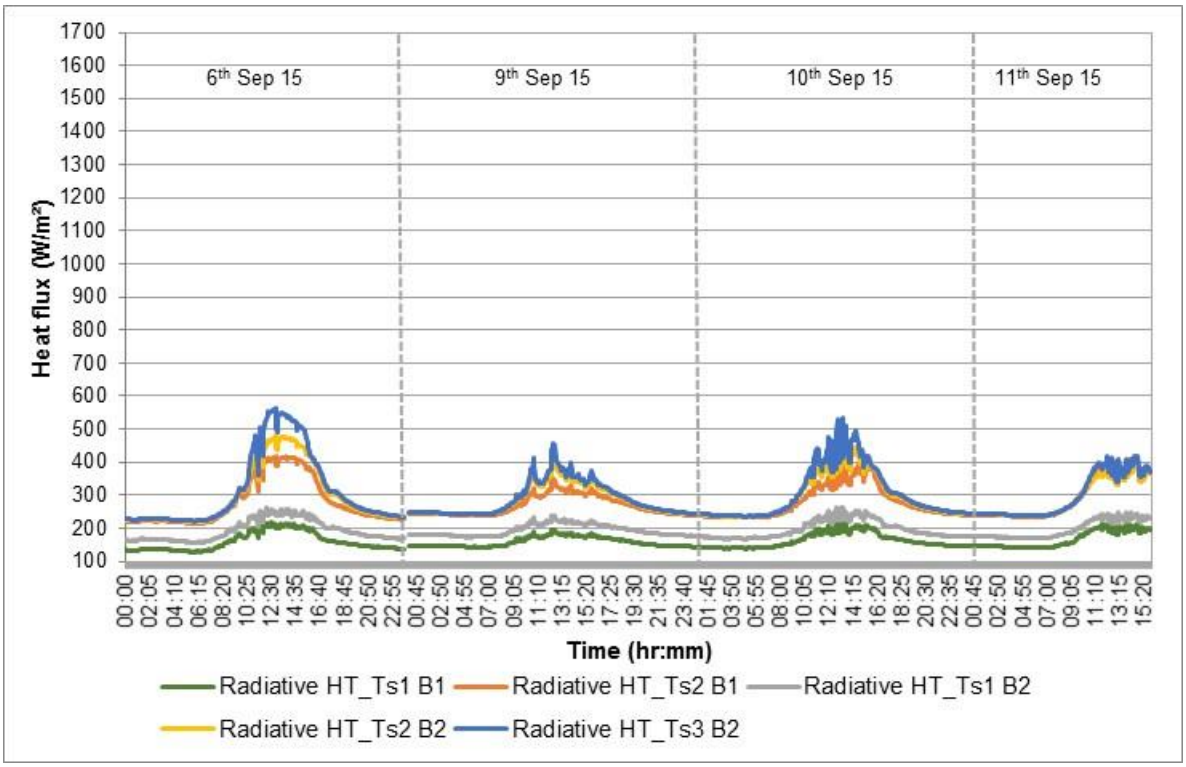


Figure 5-31: Radiative heat transfer through ETFE-foil surface in Test-rig 1 and Test-rig 2

Impact of mesh on convective heat transfer was also evident particularly on 6th September, when a sudden increase in heat transfer was apparent at 3.00pm, one hour after the rain mesh was removed from Test-rig 2. Heat transfer accelerated

between internal surface (Ts3_B2) of the ETFE-foil and internal air temperatures (Ta_H1 B2) of Test-rig 2.

5.5.2 Impact of rain mesh on internal thermal condition of the experimental boxes

In order to see the impact of rain mesh on the internal air temperature of test-rigs, rain mesh was placed on top of two-layer and three-layers ETFE-foil panels. Figure 5-22, Figure 5-23 and Figure 5-24 illustrated relative internal air temperature, air-volume air temperature, mean radiant temperature of Test-rig 1 and Test-rig 2, surface temperature (both external and internal), incident and transmitted solar radiation recorded during 6th to 11th September, 19th to 24th September, 26th September to 2nd October 2015 respectively. Figure 5-22, Figure 5-23 and Figure 5-24 also showed the impact of mesh on test-rigs internal thermal environment as indicated. The configuration of ETFE-foil panel of Test-rig 1 and Test-rig 2 can be found from Table 5-7.

On 6th September rain mesh was placed on top of Test-rig 2 till 1.45pm, after that time it was removed and placed on top of Test-rig 1 at 2.00pm. It can be noticed from Figure 5-22 that from morning till noon (1.00pm) transmitted solar radiation through Test-rig 1 two-layer ETFE-foil panel (with 75% fritted top layer) and Test-rig 2 three-layer ETFE-foil panel (with 25% fritted top layer) was 36.9% and 32.5% of that of the incident solar radiation respectively. Even though ETFE-foil panel of Test-rig 2 comprised with 25% fritted three-layer system but due to the rain mesh, it transmitted 4.5% less solar radiation than Test-rig 1. It was also noticeable that during that period, on average Test-rig 2 air temperature was 1.5°C lower than Test-rig 1.

It can be noticed that during 6th September 2015, at night and in the morning (till 8.00am), the air temperature of Test-rig 2 was up to 2.7°C above Test-rig 1 air temperature. However, after 8.00am in the morning, solar radiation increased in each hour, causing an increase in internal air temperature of both test-rigs. Test-rig 1 air temperatures were above Test-rig 2 air temperatures until mesh was placed on it, at 1.45pm. During this period (between 8.00am and 1.45pm) the air temperature of Test-rig 1 went a maximum of 7°C above Test-rig 2 air temperature. After the mesh was removed and placed on Test-rig 1, the average transmission of solar radiation (between 2.00pm and 7.00pm) of Test-rig 2 ETFE-foil panel increased by 6% than that of Test-rig 1 ETFE-foil panel. This also had an impact on the recorded internal air

temperatures and Test-rig 2 air temperature on average rose 5°C above Test-rig 1 air temperature in between 2.00 pm and 7.00pm.

Therefore, 75% fritted two-layer panel system with mesh performed better with 5°C less temperature than three-layer 25% fritted ETFE-foil panel system. It can be assumed that mesh reduced air temperature of the test-rigs by creating shading.

Mesh surface temperature was on average 4°C lower than outdoor air temperature during the day time. Whereas at night, its temperatures stayed relatively close to outdoor air temperatures similar to the ETFE-foil and test-rig's internal air temperatures. Mesh surface temperature increased up to 5°C above the external surface temperature of ETFE-foil during the night and early morning. Moreover, between noon and late afternoon, this external surface temperature of ETFE-foil went to a maximum of 18°C above mesh surface temperature. The temperature difference between mesh surface and external ETFE foil surface was also identified in the Nottingham High School (see Figure 5-1) roof. This elevated temperature of ETFE-foil surface may be due to the influence of the outdoor temperature, heated air-volume air temperature of ETFE-foil panel adjacent to it. However, it was necessary to identify the impact of rain mesh individually on thermal environment of test rigs.

An investigation was carried out between 12th September and 14th September 2015 to determine the impact of rain mesh on the test-rig's internal thermal environment. During the experiment, Test-rig 1 was roofed over by two-layer transparent ETFE-foil panel (200μm top layer and bottom layer of 100 μm), also covered with mesh. While Test-rig 2 was roofed over by the similar configuration of ETFE-foil panel as Test-rig 1, but no mesh was placed on it. Relative air temperatures, surface temperatures and air-volume air temperatures of Test-rig 1 and Test-rig 2 are presented in Figure **5-32**. Comparison of thermal environment of two test-rigs showed no variation between measured surface temperatures, air temperatures of Test-rig 1 and Test-rig 2 at night and early morning. But particularly between 5.00am to 8.00pm, ETFE-foil panel of Test-rig 1 with mesh transmitted on average 12% less solar radiation than that of ETFE-foil panel of Test-rig 2. During this time, internal air temperature of Test-rig 2 went 2°C above Test-rig 1 air temperature, while the internal surface temperature of ETFE-foil panel of Test- rig 1 was 4°C less than same of Test-rig 2.

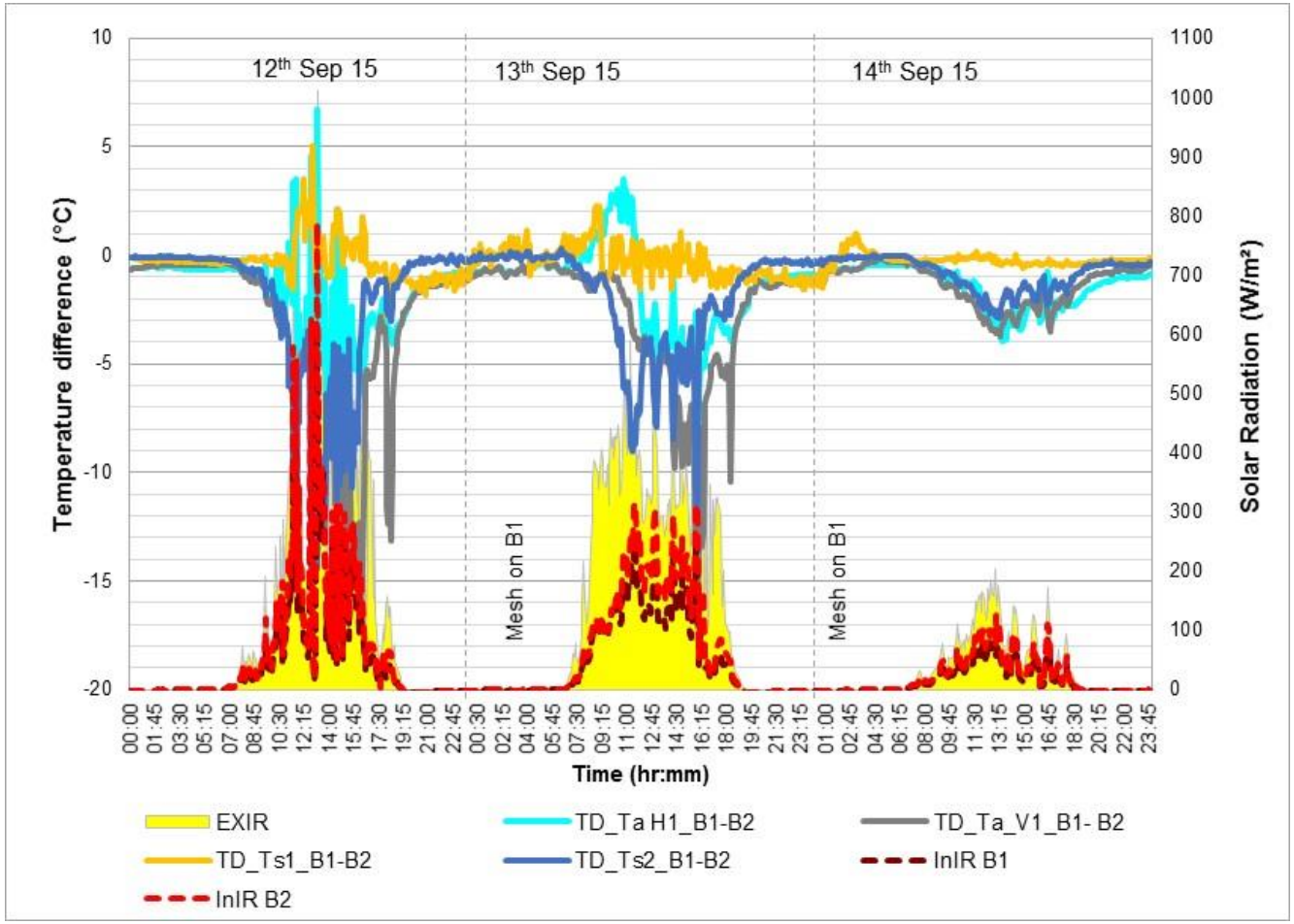


Figure 5-32**: Relative condition of surface temperature, air volume air temperature and air temperature of Test-rig 1 and Test-rig 2**

Data recorded during 13th September 15 is presented in Figure 5-33, here grey and orange coloured boxes indicated the range of air temperature of test-rigs, air-volume air temperatures and surface temperatures recorded in Test-rig 1 and Test-rig 2 respectively. From Figure 5-33 it is also evident that presence of mesh reduced the range of air temperature and surface temperature in Test-rig 1 while comparing with Test-rig 2.

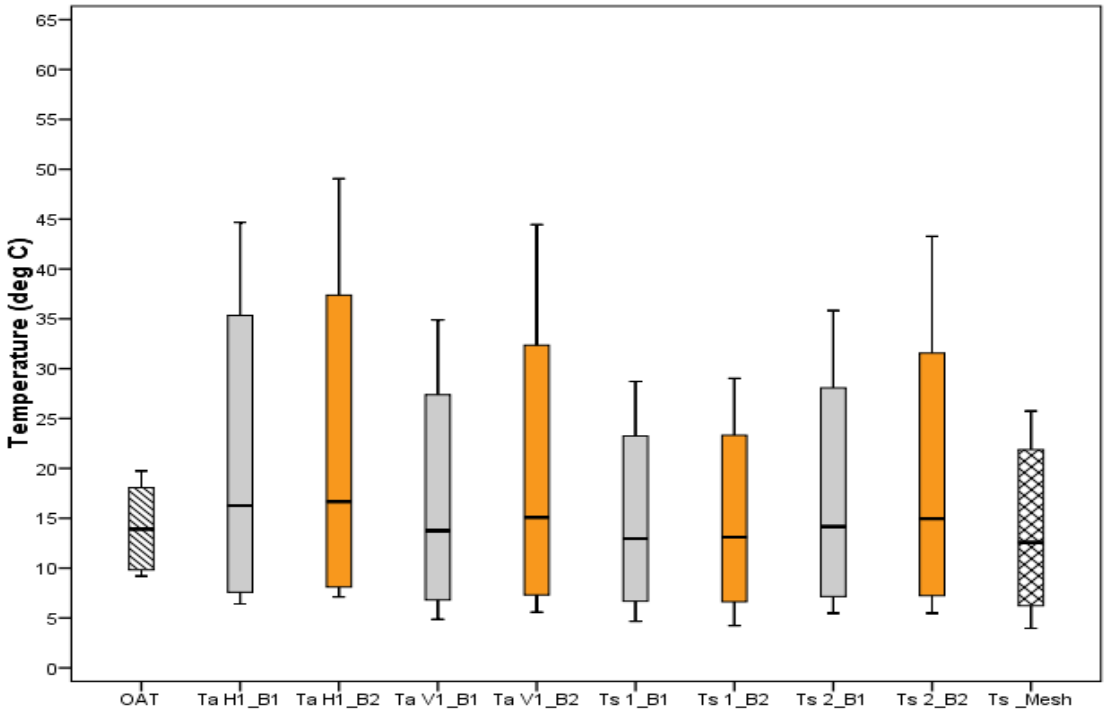


Figure 5-33: Comparison of Test-rig 1 and Test-rig 2 condition 13th Sep 15

From the study, it was apparent that incident solar radiation and surface temperatures of ETFE-foil panels (both external and internal) influenced the thermal environment of the test-rigs. This phenomenon is typical in a membrane enclosure which was also identified by Harvie (2015). Although air temperature ranges in each test-rig was significantly higher because of the air tightness, when comparison was made between air temperatures, air volume temperatures and surface temperatures of the ETFE-foil panels, it was evident that application of rain mesh reduced air-volume air temperatures, internal air temperatures of the test-rig and internal surface temperatures of the ETFE-foil panel. Therefore, it can be stated that rain mesh impacts the thermal environment of the test-rig by reducing solar gain and by creating shading, which also reduces surface temperatures of the ETFE-foil panel and air temperatures of the test-rig.

5.6 Summary

The fundamental purposes of this chapter were to analyse the thermal performance of single, two- and three-layer ETFE-foil panels. This was done in two phases-

- First phase: Measured the solar transmittance of single, two- and three-layer ETFE-foil panels through an in-situ method and compared results with values calculated according to BS EN410:2011.
- Second phase: Analysed thermal performance of single, two- and three-layer ETFE-foil panels and also evaluated the impact of fritting and rain-mesh on this performance.

In the first phase of the test-rig experiment solar transmittance of single, two- and three -layer ETFE-foil panels were determined following the similar method stated in ASTM (1986b) with slight alterations. Measured solar transmittance was validated with the results obtained in the laboratory experiment (Chapter 4) and calculated according to BS EN410:2011 (BSI, 2011). The results were in close agreement with 88% to 100% accuracy.

The second phase of the experiment analysed the thermal environment of the test-rigs, and the thermal state of the ETFE-foil panels that were used to enclose the test-rigs. The results showed that the thermal environment of the test-rigs and thermal state of ETFE-foils changed rapidly as a result of the variations in the outdoor environment. Comparison of the thermal environment enclosed with two-layer (75% fritted top layer) and three -layer (25% fritted top layer) ETFE-foil panels showed that air temperature of the test-rig enclosed with three-layer ETFE-foil panel was on average 5°C hotter than the test-rig when enclosed with two-layer ETFE-foil panel. This was because the extra layer of air and ETFE-foil increased the insulation properties of the test-rig enclosure, thus reducing heat transmission from the test rig's internal environment towards the exterior. Hence in three-layer ETFE-foil panel systems heat was better preserved than in the two-layer ETFE-foil panel system. Therefore, increase in layer number of ETFE-foils in the panel increased insulation properties of the space it enclosed. Besides, under the same outdoor condition the air temperature of enclosed test-rig with three-layer ETFE-foil panel with 25% fritted top layer, was on average 1.4°C warmer than the test-rig, when enclosed with a three-layer panel with 75% fritted top layer. Thus, the density of fritting also influenced thermal environment enclosed with ETFE foil panel by reducing solar gain.

In ETFE-foil panels, air temperatures of the air-volume enclosed with ETFE-foil also varied depending on fritting and number of foil layers in the panel. Moreover, air-volume air temperatures were influenced by adjacent ETFE-foil surface temperatures. In turn, both ETFE foil surface temperatures and air-volume air temperatures of the ETFE-foil panels affected air temperatures of the test-rigs they enclosed.

This variation of temperature in ETFE-foil surfaces and air temperatures of air-volume and test-rigs occurred by convective and radiative heat transfer mechanisms. Convective heat flux depends on temperature difference, therefore heat was transferred between each layer of ETFE-foil panel and air adjacent to it by natural convection. Besides radiative heat transfer occurred on the ETFE-foil surfaces, and was dominated by short-wave radiation during the day and longwave radiation during the night. However, radiative heat transfer depends on the emissivity of materials. Therefore, in two and three-layer ETFE-foil panels with fritted top layer and transparent middle and bottom layers, radiative heat transfer was more pronounced on transparent layers than fritted foil surfaces. Besides particularly at night and early morning, stable conditions occurred as external surface temperature increased over the internal surface, radiative and convective heat transfer was constant for all the surfaces, and increased as the temperature difference increased between the surface of ETFE-foil and adjacent air layers during the day.

In this experiment impact of rain-mesh on test-rigs thermal environment was evident. The shading created by rain suppression mesh reduced surface temperatures as well as air temperatures inside the test-rigs. The experimental investigation also found that presence of mesh reduced solar radiation transmission by 12%. Air temperature of the test-rig and internal surface temperature of ETFE-foil also reduced by 2°C and 4°C respectively.

In this study the test-rigs' thermal environment were evaluated based on its air temperatures and surface temperatures of ETFE-foils. This focused on the actual thermal performance of ETFE-foil but it is necessary to compare this thermal performance with that of glass, which is typically used in construction for similar purposes. In Chapter 7, a simulation model replicating Test-rig 1 and Test-rig 2 was developed using EDSL TAS version 9.3.3. The results obtained from this in-situ experiment was then used to verify the simulation model. After verification, this simulation model was used to simulate different types of glass panels, particularly used as overhead glazing. Thermal performance of single, two- and three-layer ETFE-foil panels was then compared with that of similar glass panels.

Chapter 6

6 Thermal performance of existing space enclosed with an ETFE- foil cushion envelope

6.1 Introduction

Building integration of ETFE-foil cushions has increased significantly in recent years, which has been addressed in Chapter 1. However, available information about the thermal performance analysis of ETFE-foil cushion enclosures is limited and no study had investigated the actual thermal performance of ETFE-foil cushion systems as well as spaces enclosed by it. The unknown performance specifications of ETFE-foil cushions may be a barrier to identifying actual building performance.

A number of studies which carried out environmental performance analysis of tensile membrane enclosures were reviewed and presented in Chapter 2, considering that similar challenges exist in the case of ETFE-foil enclosures.

Chapter 3 presented a simple pilot study of the thermal performance of an ETFE-foil cushion enclosure. Depending on the complexity observed in the study it was considered to carry out an investigation of the thermal performance of ETFE-foil cushions and the space enclosed by them, separately.

This study also carried out an experimental investigation on the thermal and optical properties of different types of ETFE-foil which is presented in Chapter 4. Chapter 5 discussed results obtained on the thermal performance of different types of ETFE-foil panel construction using a test-rig investigation.

To investigate the actual thermal performance of ETFE-foil cushions and the spaces enclosed by them, two different atria incorporating ETFE-foil cushions in the roof were selected. The rationale behind the selection of the buildings along with detailed methods of data collection and assessment procedure are discussed in Chapter 3. The first case study atrium is a part of the building complex of the Nottingham High School, located in the central part of Nottingham, United Kingdom; whereas the second case study is the Engineering and Science Learning Centre (ESLC) building, University Of Nottingham.

This chapter addresses Objective 4 of the research which was to:

- Evaluate thermal performance of occupied spaces enclosed with ETFE-foil cushion envelope

To achieve this objective long-term thermal monitoring was conducted at Nottingham High School and Engineering and Science Learning Centre (ESLC) to observe following features:

- thermal responsiveness of the ETFE-foil cushions,
- vertical and horizontal temperature stratification,
- the impact of outdoor weather changes on the internal thermal environment,
- effect of the thermal condition of the atrium on adjacent occupied spaces, and
- impact of the thermal performance of ETFE-foil cushion enclosures on thermal comfort

6.1.1 Outdoor weather

According to CIBSE guide A (CIBSE, 2006, CIBSE, 2015b),1st May to 30th September is considered as the UK summer period. This period was also considered as summer in environmental monitoring.

During summer 2014, the average outdoor air temperature was 2°C hotter than that of summer 2015. However, the maximum outdoor air temperature (1st July 2015) was 3.5°C hotter than the maximum outdoor air temperature (10th July 2014) recorded in summer 2014. Figure 6-1 and Figure 6-2 present outdoor air temperature, solar radiation and daily mean temperature recorded during summer 2014 and 2015 respectively.

The data presented in Figure 6-2 shows that during summer 2015, the maximum outdoor temperature was 33.5°C on 1st July 2015 which was 24°C hotter than the minimum outdoor temperature recorded during 14th September 2015. On this date (1st July 2015) during occupied hours (8.00am to 15.00pm) the difference between maximum and minimum outdoor temperature was 11.1°C (maximum 33.5°C, minimum 22.4°C).

Therefore, the period between 29th June and 3rd July 2015 can be considered as peak period of summer 2015. Variation of air temperature during that period can be seen in Figure 6-2. Thus, to investigate the thermal condition of spaces enclosed with an ETFE-foil cushion envelope under extreme outdoor conditions, such as a day with a maximum temperature of the year (1st July 2015), the period between 29th June and 3rd July 2015 was considered for further analysis. Also, the thermal conditions that occurred in the atrium during 14th September 2015 was considered to examine the impact of lowest outdoor temperature and limited solar radiation on the spaces enclosed with an ETFE-foil cushion envelope.

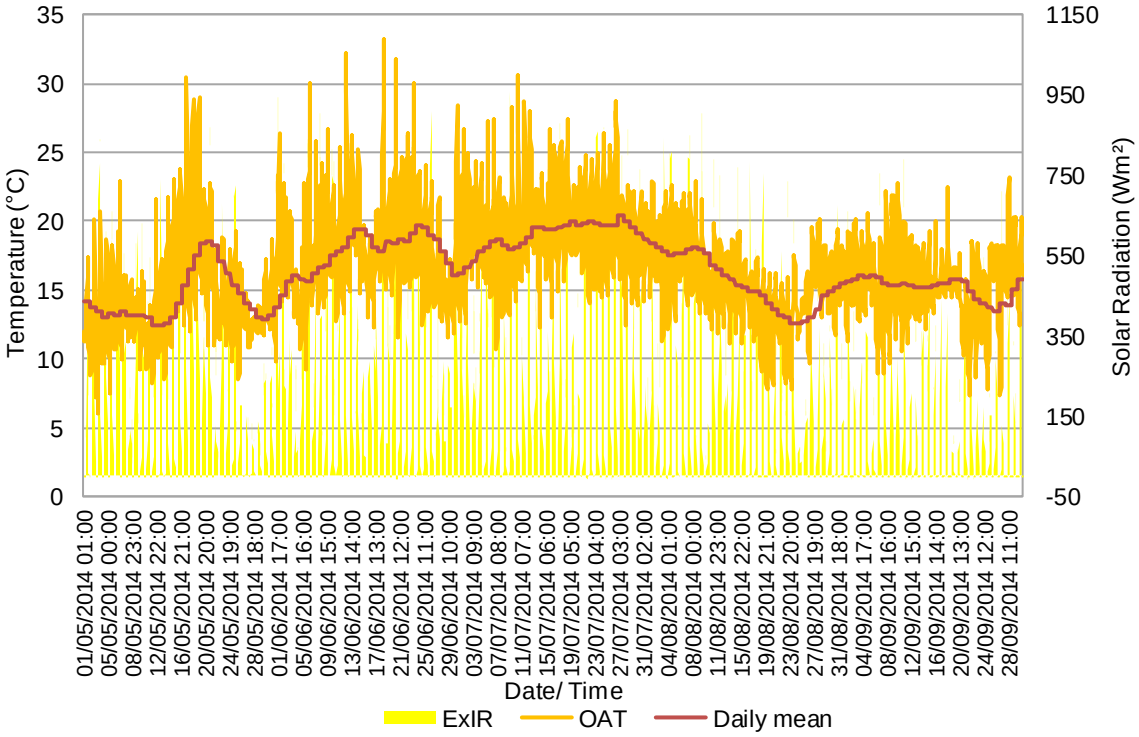


Figure 6-1: OAT, daily mean temperature and ExIR recorded during summer 2014

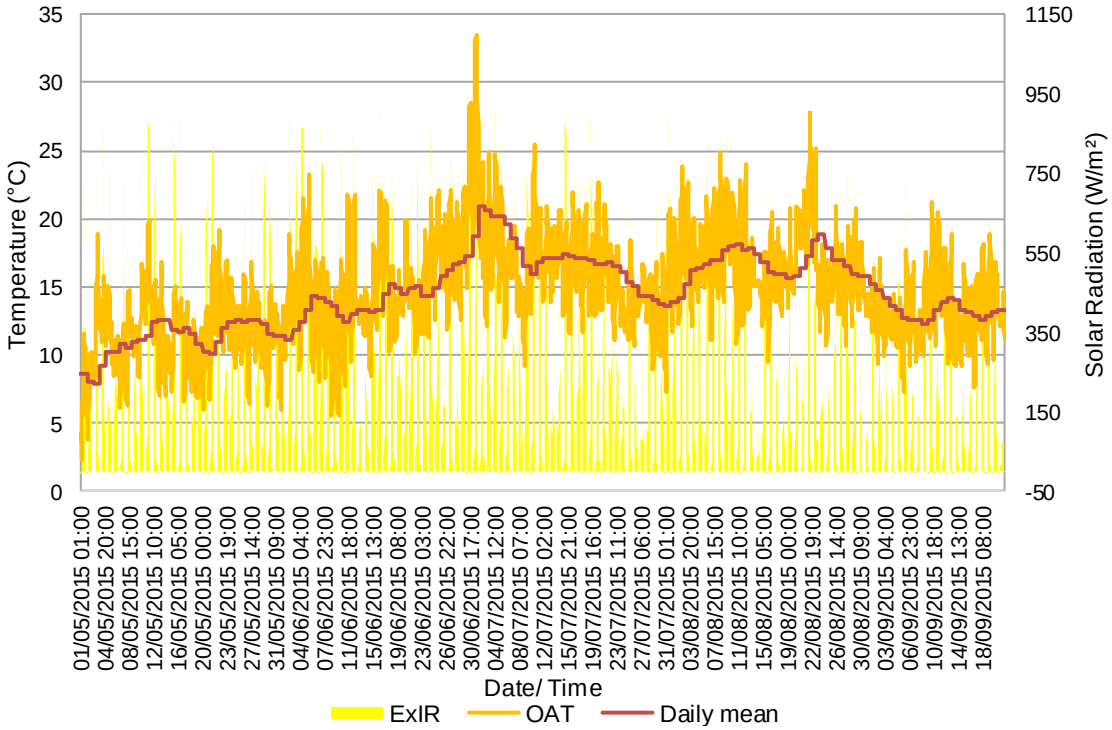


Figure 6-2: OAT, daily mean temperature, and ExIR recorded during summer 2015

Both of the case study buildings – Nottingham High School and the Engineering Science Learning Centre (ESLC) are located in Nottingham. It was already addressed in Chapter 3 that outdoor temperature of Nottingham High School was recorded from a weather station that was located on a different roof, adjacent to the ETFE-foil cushion roof. However, outdoor temperature adjacent to the ESLC building atrium was measured using a Tiny Tag Plus 2- TGP-4017 data logger. External incident solar radiation on these two locations were measured using Kipp & Zonen CMP3 pyranometers. Variation was observed in recorded incident solar radiation and outdoor air temperature. Figure 6-3 shows the outdoor air temperature recorded at Nottingham High School and ESLC.

Average outdoor air temperature measured adjacent to ESLC building (during 2015) was 1.4°C hotter than that at the Nottingham High School. A possible reason for this difference was the location of the temperature sensors, shading from adjacent structures etc.

However, according to CIBSE guide A (CIBSE, 2015b, CIBSE, 2006), for a realistic assessment of the thermal environment, the outdoor condition such as outdoor air temperature, solar radiation etc. should be measured in the vicinity of the building to be assessed. Thus, to analyse the impact of the outdoor condition on the thermal environment of the Nottingham High School atrium and ESLC atrium, environmental data recorded from the vicinity of both of the buildings were considered.

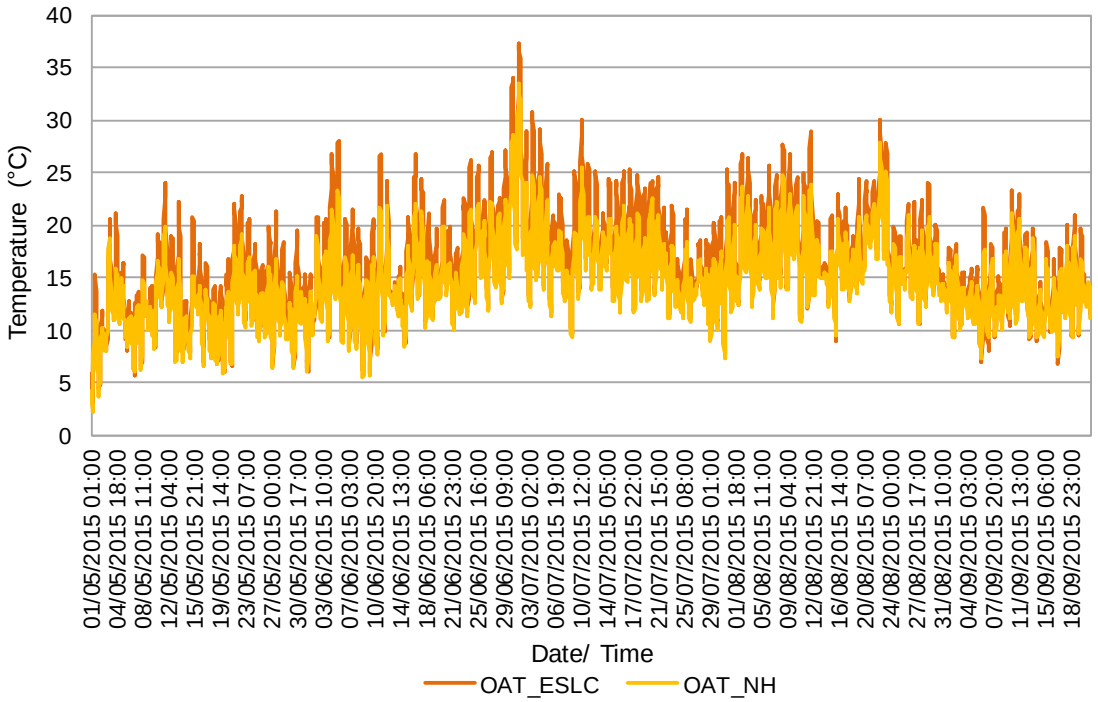


Figure 6-3: Outdoor air temperature recorded adjacent to Nottingham High School and ESLC

6.2 Case Study A: Nottingham High School

This section discusses the thermal behaviour of the Nottingham High School atrium. The atrium roof consists of two–layer ETFE-foil cushions with fritted top layer and clear bottom layer both of 200µm, covered with a rain noise suppression mesh. Detailed description of the building and monitoring setup is presented in Chapter 3 (section 3.8).

The thermal behaviour was analysed on the basis of data recorded during summer 2014 and 2015.

A summary of the salient features of the monitored atrium of Nottingham High School, its roof and time period of environmental monitoring is presented in Table 3-3.

While selecting days for the analysis, it was considered that the school was operating on its normal schedule within the summer period in the UK.

Sensors identifications used to describe outdoor environment are presented in Table 6-1, while Table 3-4, and Table 3-5 (Chapter 3) present sensors identification used to discuss the thermal conditions of the atrium and ETFE-foil cushion roof respectively. Detailed description of the method and installed equipment for monitoring is presented in Chapter 3.

Table 6-1: Identification of environmental parameters

Identification	environmental parameter
OAT	Outdoor air temperature
Tcomf	Comfort temperature (category II building)
Tmax	Maximum acceptable temperature (category II building)
Tmin	Minimum acceptable temperature (category II building)
ExIR	Incident solar radiation
InIR	Transmitted solar radiation
RH	Relative humidity

6.2.1 Analysis of monitored data and discussion

The graphs in this section represent monitored data recorded at five-minute intervals. This allowed to graphically represent dynamic thermal responsiveness of the ETFE-foil cushion envelope. All numerical values specified in a text format are based on instant readings.

6.2.1.1 Overview of typical thermal environment

Two specific patterns in the thermal environment of the spaces enclosed by ETFE-foil cushion envelopes were identified. Based on the sky conditions these can be defined as thermal environment under clear sky conditions and overcast sky conditions. The typical thermal environment observed under clear sky conditions and overcast conditions are illustrated in Figure 6-4 and Figure 6-5 respectively. The results indicated that the thermal environment under clear sky condition (30th June, 1st July and 3rd July 2015) was largely influenced by large swings in cushion surface temperatures (ST Loc 4_NH) relative to its surrounding air temperatures [Tsi 4(a)_NH), Tsi3(a)_NH]. This significant variation in cushion surface temperatures was observed to coincide with the extent of the vertical air temperature stratification. Thus, it resulted in strong positive stratification during the daytime and negative at night (Figure 6-4).

Thermal environment on typical sunny days (30th June, 1st July and 3rd July 2015) was particularly influenced by the surface temperature of the ETFE-foil cushions, radiant temperature, solar gain into the enclosure and outdoor air temperature. Here the effect of the HVAC system on indoor thermal environment [Tsi3(a)_NH] seemed to be very poor in relation to the effect of heat gain from solar radiation and hot outdoor temperature.

In the case of limited cloud cover, moving clouds and fluctuations in intensity of solar radiation, surface temperature as well as indoor air temperature reacted rapidly

affecting the thermal environment of the atrium particularly on hot summer days observed during 29th June, 1st July and 2nd July 2015.

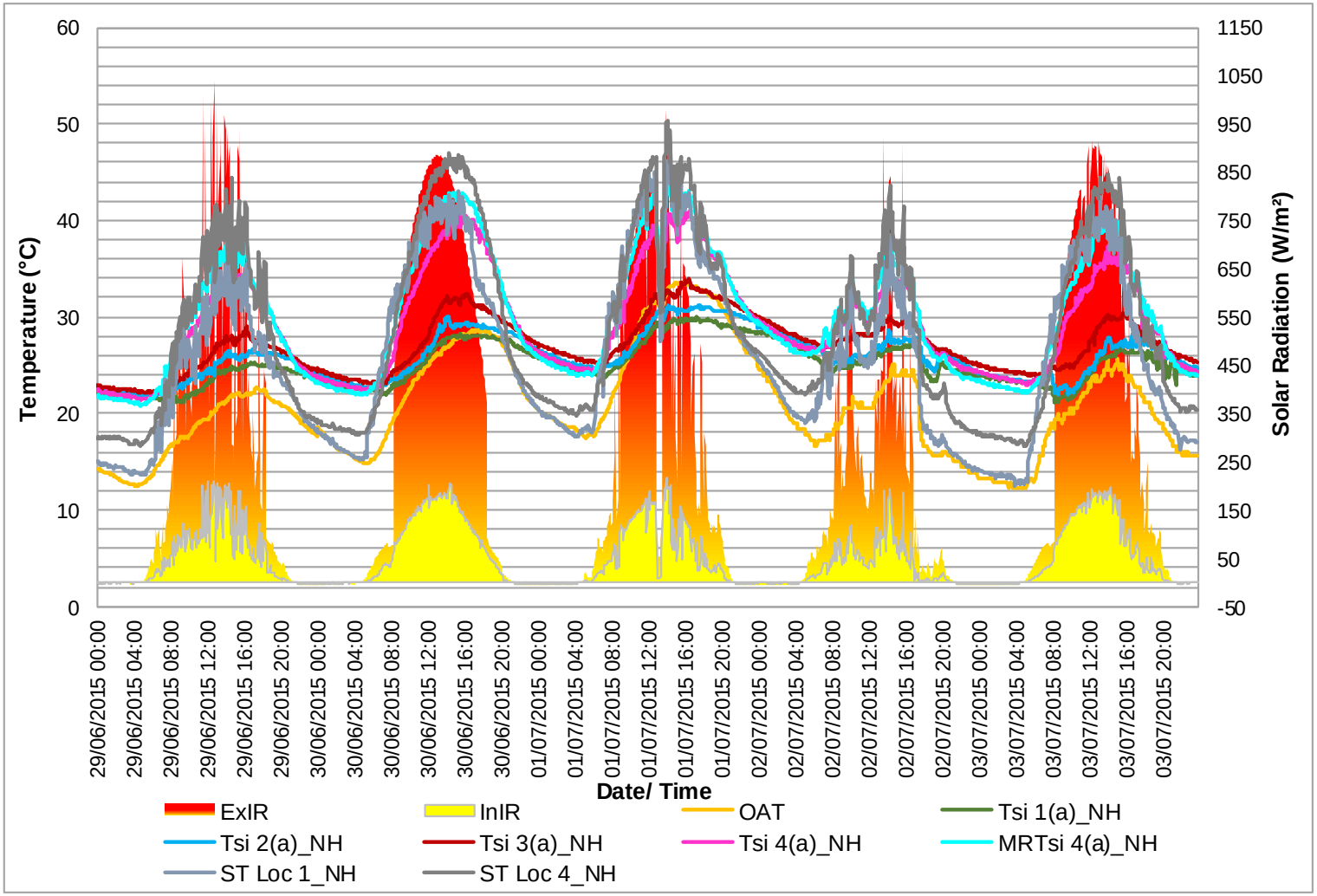


Figure 6-4: Indoor air temperatures and solar radiation recorded in Nottingham High School atrium between 29th June and 3rd July 2015 – clear sky conditions

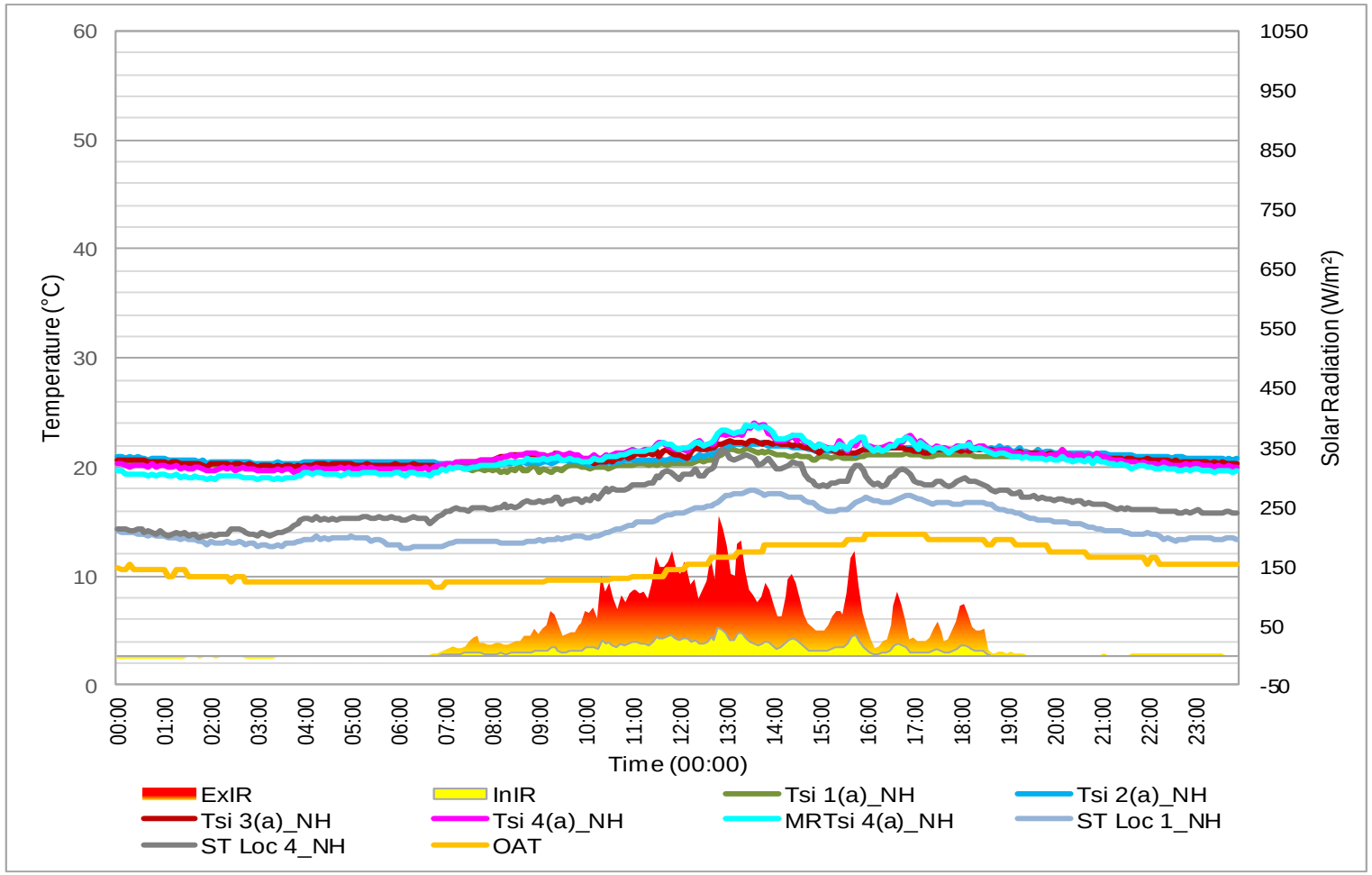


Figure 6-5: Indoor air temperatures and solar radiation recorded in Nottingham High School atrium during 14th September 2015 – overcast sky conditions

However, the thermal environment (Figure 6-5) under overcast sky condition was different. Typically, during an overcast day, the thermal condition of spaces enclosed with ETFE-foil cushions was more stable with relatively uniform temperature distribution. This seemed to be the result of relatively low outdoor air temperature and radiant temperature, limited solar gains, little variation in cushion surface temperature and surrounding air temperature, the impact of HVAC system etc. Therefore, this resulted in limited vertical stratification throughout the day and night.

6.2.2 Indoor air temperature distribution

During the summer period, the variations of outdoor air temperatures and incident solar radiation significantly impact surface temperatures of the ETFE-foil cushions. Thus, the variation of the indoor air temperatures of adjacent occupied levels appeared to be determined by the variations in surface temperatures of the ETFE-foil cushions and the amount of solar radiation transmitted though the ETFE-foil cushion roof. The average temperature difference between the occupied levels and the exterior were oscillating between 4.2°C to 6.3°C where the occupied level temperatures were hotter than the outdoor temperatures. However, as the outdoor temperature increased a sharp decrease in this temperature difference was evident particularly on 1st July 2015 (between 12.00pm and 8.00pm). Figure 6-6 presents temperature differences between occupied levels in the atrium and outdoor air temperature. The results presented in Figure 6-6 shows that during 1st July 2015, the outdoor air temperature was a maximum of 4°C hotter than the air temperature of occupied levels (ground floor and first floor) at noon. This was the result of extreme high outdoor temperature (33.8°C) and stability of occupied level air temperatures due to the HVAC system, shading from the floors above and the thermal inertia of the adjacent atrium floors and masonry walls. However, during the same period the occupied level 3 (second floor) air temperature stayed close to outdoor air temperature while the air temperature of level 4 (adjacent to the ETFE-foil cushion roof) was hotter than the outdoor air temperature. This was due to level 4 air being heated by radiant heat from warmer inner ETFE-foil surface as well as direct solar radiation accessing through translucent ETFE cushion. This accumulated hot air of level 4 in turn affected air temperature of the level (level 3) adjacent to it.

On the other hand, in the absence of solar radiation, during the day with low solar gain (e.g. overcast day) and low outdoor temperature the occupied level air temperatures were stable between 21°C and 22°C and stayed on average 9°C above outdoor temperature (Figure 6-7). This stable condition can be explained as an impact of

thermal inertia, insulation provided by ETFE-foil cushion roof on indoor air temperature. Thus, the thermal conditions of the occupied levels agreed well with indoor design temperature.

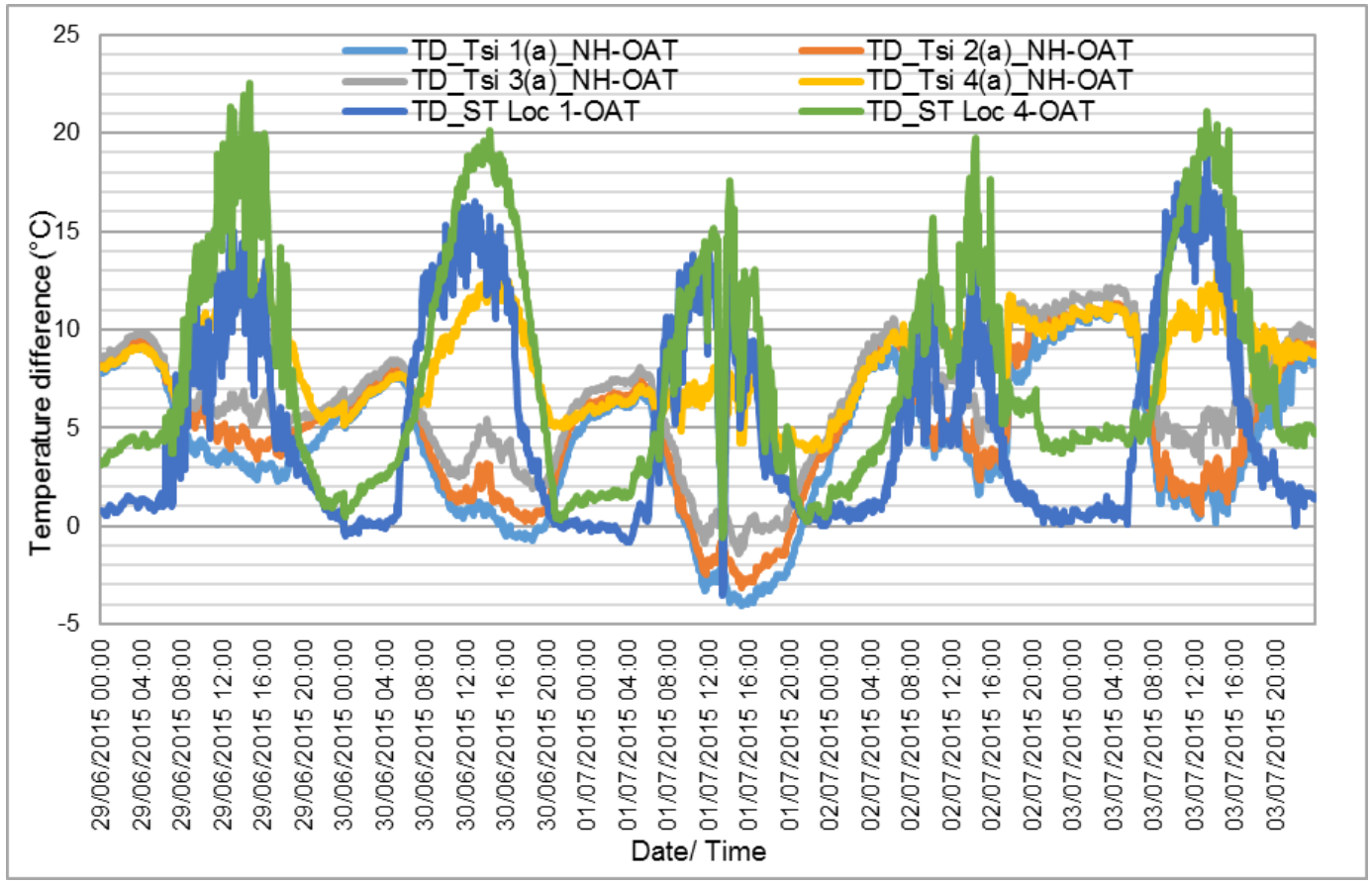


Figure 6-6: Temperature differences between air temperatures of different atrium levels of Nottingham High School and outdoor air temperatures between 29th June and 3rd July 2015

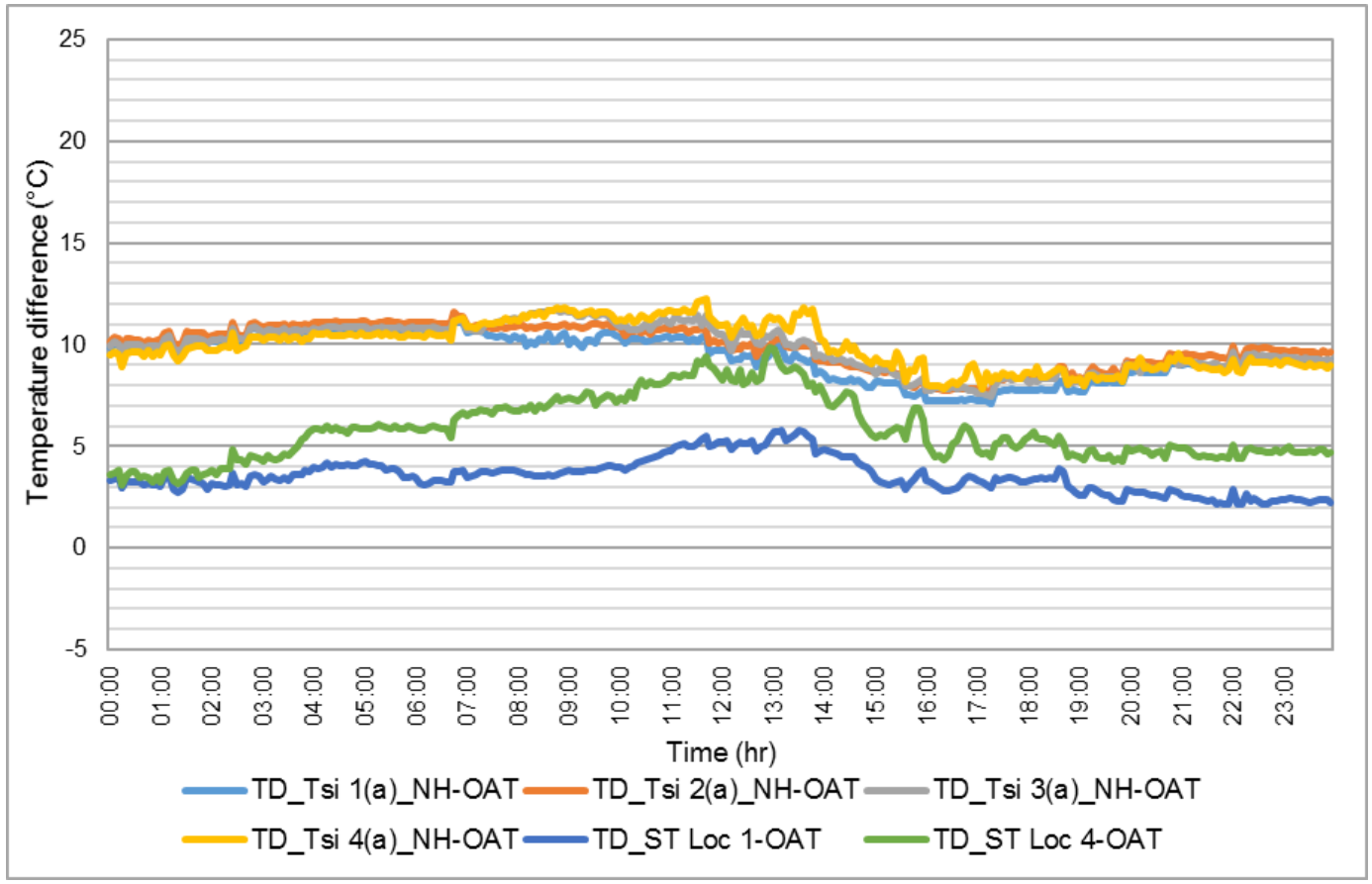


Figure 6-7: Temperature differences between air temperatures of different atrium levels of Nottingham High School and outdoor air temperatures during 14th September 2015

The recorded vertical temperature gradient was on average positive during the day and negative during the night. Diurnal temperature swing was high during peak insolation periods while less on overcast days of summer. Figure 6-8 and Figure 6-9 present air temperature difference between occupied level 1, 2, 3 and level 4 during the peak period (between 29th June and 3rd July 2015) and overcast day (14th September) respectively. During the peak period, maximum vertical temperature stratification observed was 11.5°C (between occupied level 1 and level 4). This was relatively weak (2.62°C) on the overcast day. Moreover, the maximum variation of internal air temperature range of occupied level 3 observed on a peak day (1st July 2015) was 8.9°C, this was also significant while compared to the same on an overcast day (2.5°C).

At night (30th June, 1st July 2015) the air temperature of level 4 dropped while at occupied levels 2 and 3 the air temperature was 1°C warmer than that of level 4 i.e. negative stratification.

During hot summer days (1st July, 30th June 2015), this positive stratification resulted from solar gain, hot outdoor temperature, radiant temperature and surface temperature of ETFE-foil cushion. During occupied periods this was also influenced by occupancy and internal gains etc. The average temperature difference between occupied levels and the level adjacent to the ETFE-foil cushions ranged from 4.5°C (occupied level 3) to 6.8°C (occupied level 1). At night, the decrease in air temperature at the level adjacent to the ETFE-foil cushions (level 4) can be explained by the longwave infrared radiation losses experienced by the ETFE-foil cushion surface.

Under warm sunny conditions direct solar radiation and warmer ETFE cushion surfaces form a reservoir of warm air accumulating near to the ETFE-foil cushion roof. This hot air is also heated by radiant heat thus the air temperature at the level adjacent to the ETFE-foil cushions rose to a maximum of 41°C, which was 11.4°C and 7.7°C hotter than level 1 and level 3 air temperature, respectively.

The effect of high outdoor air temperature was significant even after the solar radiation intensity reduced after 8.00 pm but the air temperature of the occupied levels remained high (Figure 6-4) and varied between 26.5°C and 32.2°C (30th June and 1st July 15).

There are automatic windows on the west façade of the atrium, which operate when the air temperature of the second floor (level 3) rises to 25°C. However, on hot summer days (30th June, 1st July 2015) no significant variation in air temperature or any drop of

air temperature was evident particularly on the upper levels of the atrium (level 4) close to those automatic windows.

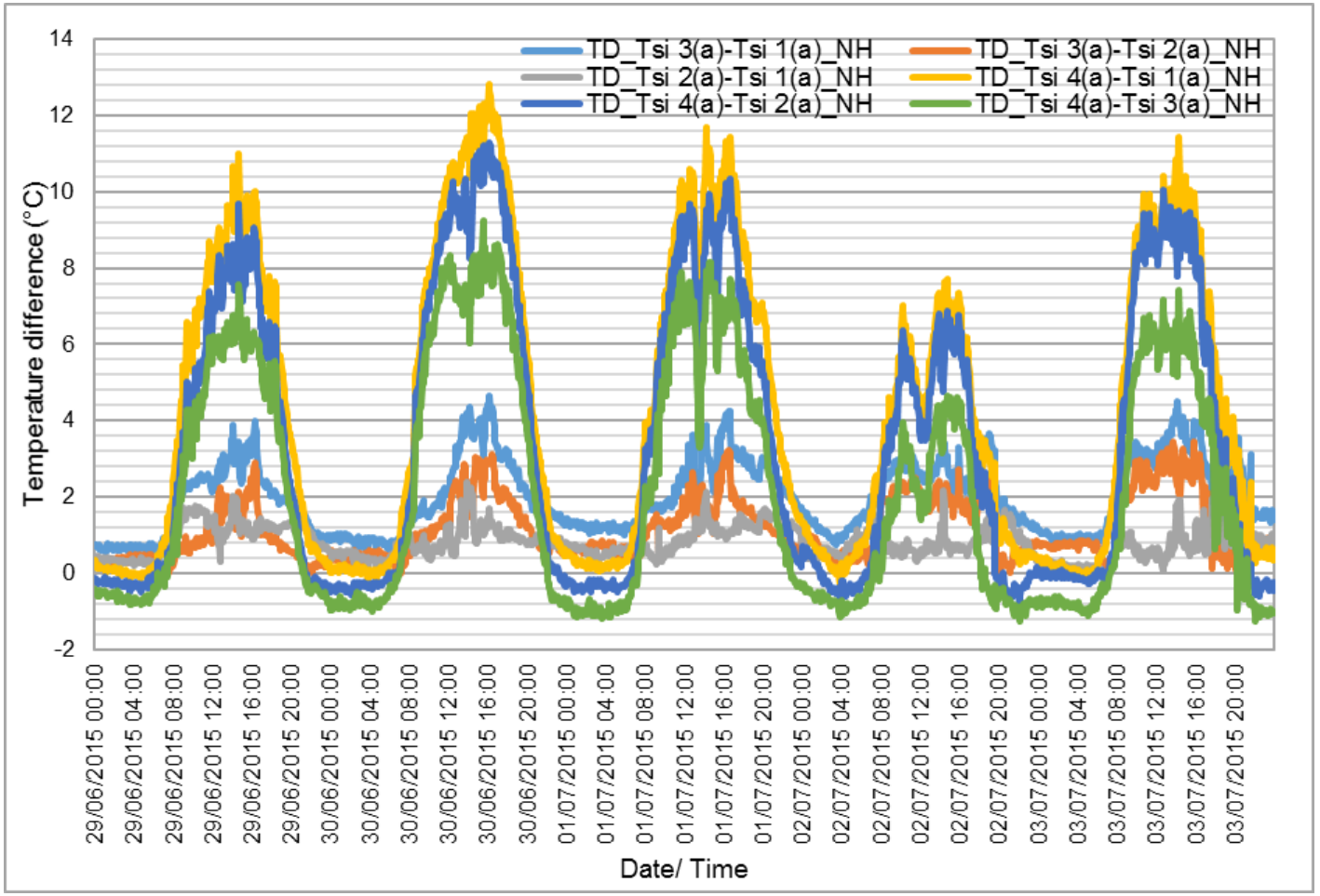


Figure 6-8: Temperature difference between Nottingham High School atrium level 1, 2, 3 and 4, between 29th June and 3rd July 2015

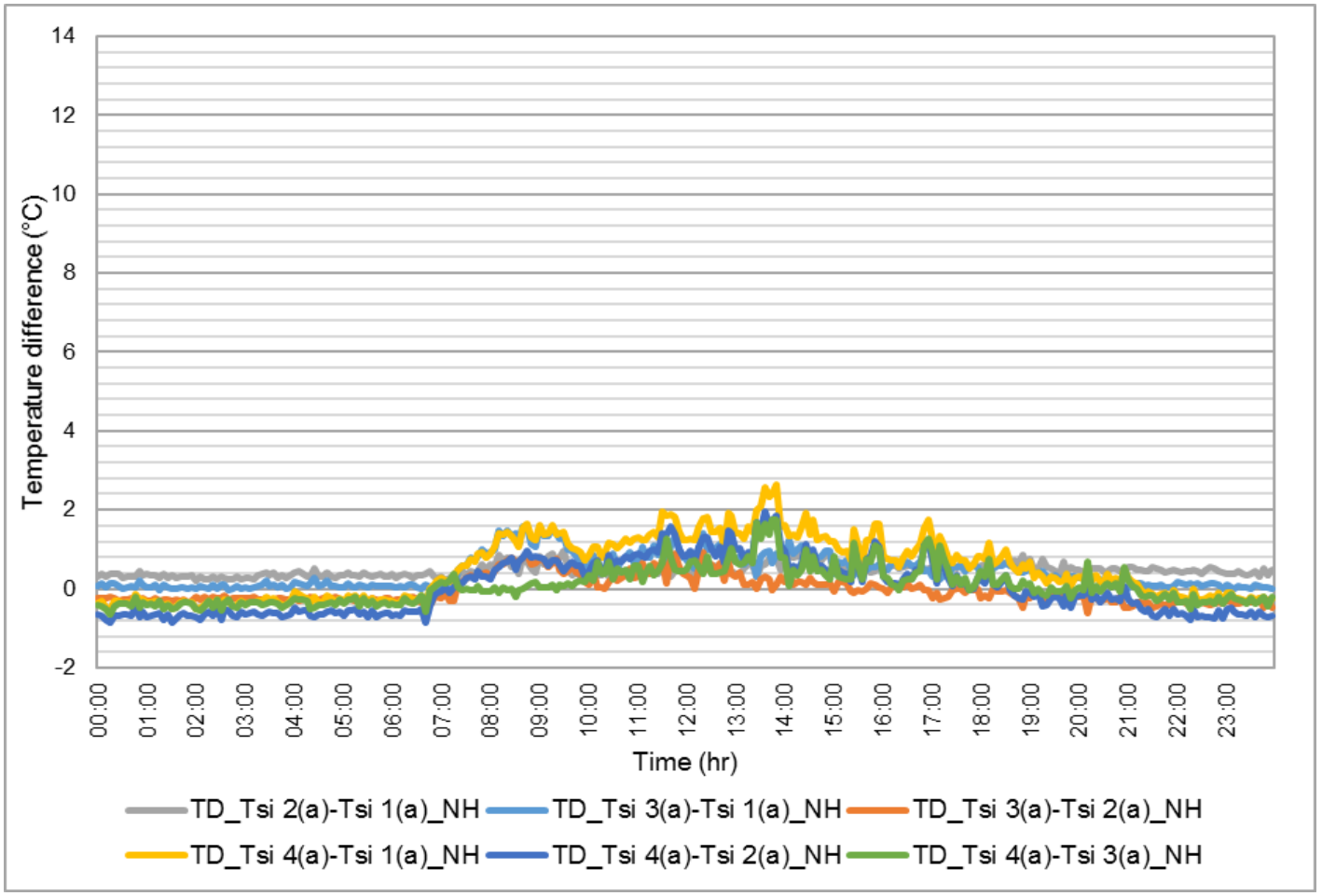


Figure 6-9: Temperature difference between Nottingham High School atrium level 1, 2, 3 and 4 during 14th September 15

6.2.3 Overview of typical thermal behaviour of the ETFE-foil cushion roof

The ETFE-foil cushion roof was very responsive to external weather conditions e.g. solar radiation. The roof demonstrated more extreme thermal behaviour under clear sky conditions where both direct solar and long-wave infrared radiation appeared to govern the fluctuation of the ETFE-foil surface temperatures. However, under overcast sky conditions this variation in ETFE-foil cushion surface temperatures were influenced by the limited amount of diffuse radiation filtering through the cloud and mean radiant temperature of the sky. This variation in the temperature of the ETFE-foil cushion surface affects the thermal environment of the atrium and may result in temperature stratification. Internal and external cushion surface temperatures, occupied level 3 air temperatures, level 4 air and mean-radiant temperatures, incident and transmitted solar radiation, and outdoor air temperature recorded under clear sky conditions and overcast conditions is illustrated in Figure 6-10 and Figure 6-5 respectively.

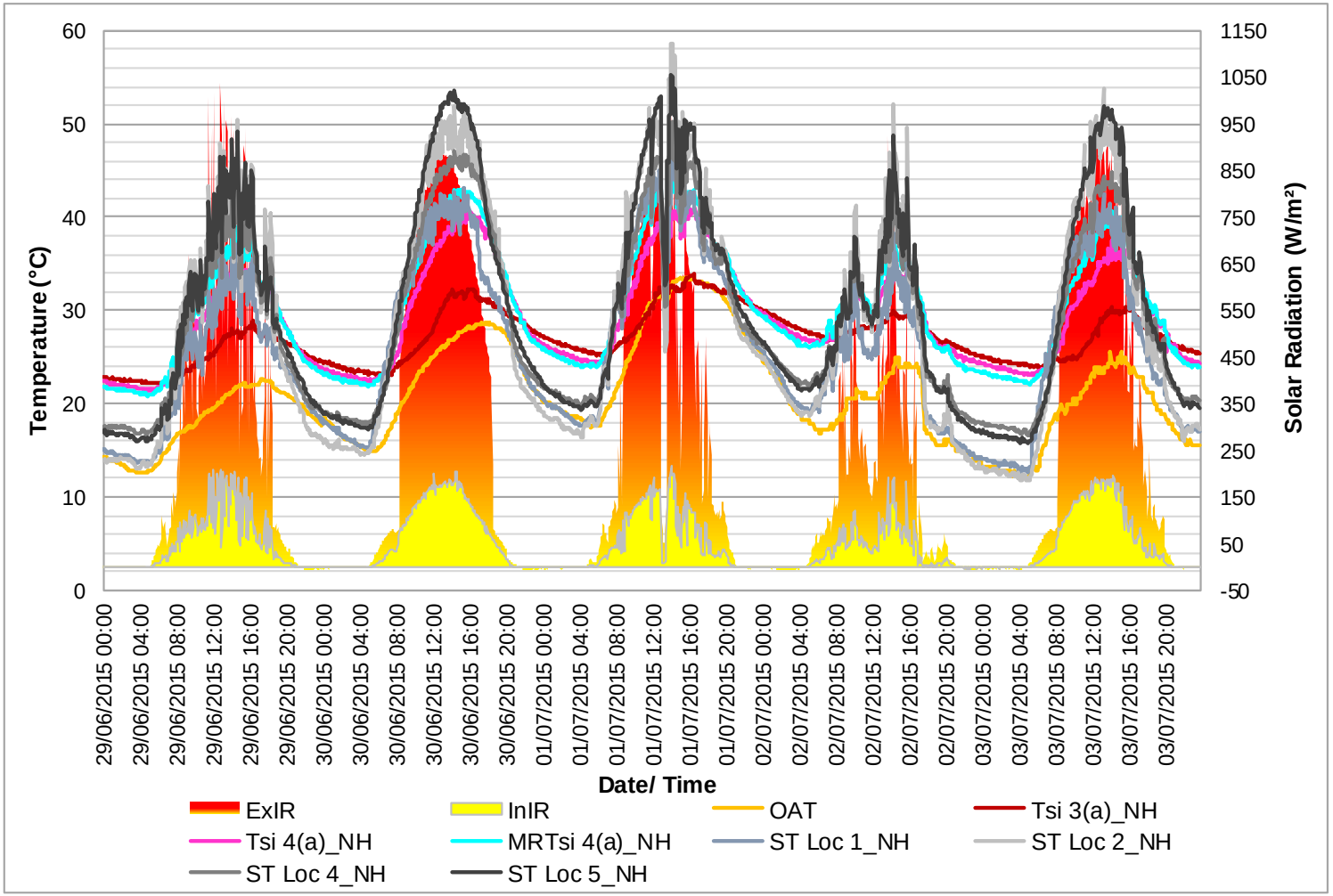


Figure 6-10: Internal and external cushion surface temperatures, occupied level 3 air temperatures, level 4 air and mean-radiant temperatures, incident and transmitted solar radiation, and outdoor air temperature recorded between 29th June and 3rd July 2015

An increase (or decrease) in solar radiation directly impacts on the foil surface temperature, both external and internal. This was observed on both warm sunny and cloudy days. In the presence of cloud internal surface temperatures (ST Loc4_NH) of the ETFE-foil cushion remained close to the average between indoor (Tsi 4(a)_NH) and outdoor air temperature (Figure 6-10, Figure 6-5). This was also apparent when there was no solar radiation.

During the warm cloudy days, the limited amount of diffuse radiation filtering through the cloud and high mean radiant temperature of sky resulted in radiative heat exchange as well as convective heat transfer at the surface of the cushion.

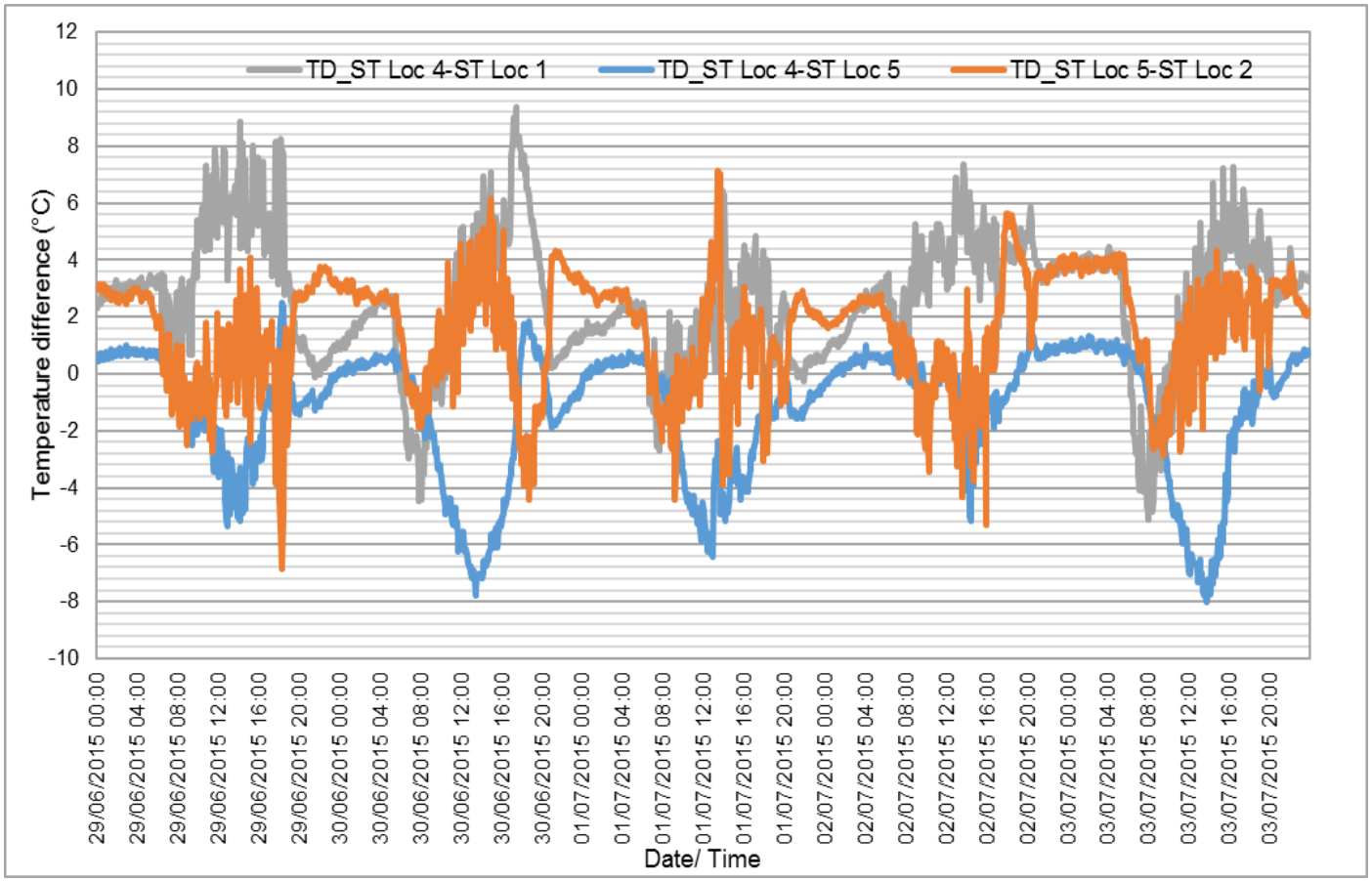


Figure 6-11: Temperature difference between external surface temperature (ST Loc1)– internal surface temperature (ST Loc 4) [middle of the cushion]; internal surface temperature [ST Loc 4 (middle of the cushion)]- internal surface temperature [ST Loc 5 (edge of the cushion)]; external surface temperature (ST Loc 2) – internal surface temperature [ST Loc 5 (edge of the cushion)]

During the warm sunny day, radiative heat exchange effects dominated those of convective heat transfer. As a result, a higher difference (15.6°C on the warm sunny day, 4.2°C on the warm overcast day) was observed between foil surface temperatures (ST Loc 4) and the average of indoor and outdoor temperature. Moreover, the air in between the cushion layers creates a thermal barrier between the two 200µm ETFE-foil layers and the external and internal air. For that reason, although the external surface temperature stays close to the outdoor air temperature in the absence of solar radiation, the internal surface temperature is always higher than that of the external surface temperature. Moreover, it was apparent from Figure 6-11 that during the day the edge of the cushion (STLoc4_NH) was a maximum of 8°C hotter than the middle of the cushion (STLoc1_NH). This might be the result of the variation in the thermal transmittance of the middle and edge of the same cushion (discussed in Chapter 4) resulting from the variation in air conductance between these two location of a single cushion and proximity to the aluminium clamping profile.

At night external surface temperatures stayed close to the external air temperature during both warm sunny and overcast sky conditions. But variation was observed during the day time. A sharp increase (from 17.15°C to 23°C) in exteranl surface temperature was observed in the morning on the warm sunny day (1st July 2015). During that period (around 6.30 am) the external surface temperature reached close to the internal surface temperature and stayed 1°C to 2°C above the internal surface temperature until 8.30am. After this time (8.30am), as the intesity of solar radation increased (from 129 W/m^2 to 559.56 W/m^2), the internal surface temperature increased above that of the external surface. Furthermore between 8.30am and 12.00 pm the temperature differences between internal and external surface varied by 1°C to 2°C. However after this hour (12.00pm) internal surface temperature remained above the external surface temperature until the night. On the warm sunny afternoon, the maximum internal foil surface temperature was 50.3°C (4.1°C hotter than external surface), while the adjacent (internal) air temperature Tsi 4(a)_NH was 40.5°C (1st July 2015). Maximum and minimum temperature difference observed between the internal and external surfaces of the ETFE-foil cushion were 9.36°C and 0.5°C on the clear warm sunny day, whereas during the warm cloudy day this difference was 4.4°C and 0.2°C.

On the warm sunny day at mid-day, the internal surface temperature was influenced by radiative heat transfer at the surfaces of the cushion, also radiation from the sky and internal surfaces. In turn this warm internal ETFE-foil surfaces and direct solar

radiation accessing through transclusent ETFE cushion impacting air temperature of atrium levels (level 3, level 4). As there was no opening for the warm air to escape through the high level it also influences the surface temperature of the cushion as a process of convective heat transfer. Therefore the temperature of internal foil surfaces rose above the air temperature of level 4 (level adjacent to ETFE-foil cushion roof). Warm air rising from the lower levels is also heated by internal incident radiation entering through the translucent ETFE-foil cushion roof impacting the temperature of occupied level 3 and atrium level 4.

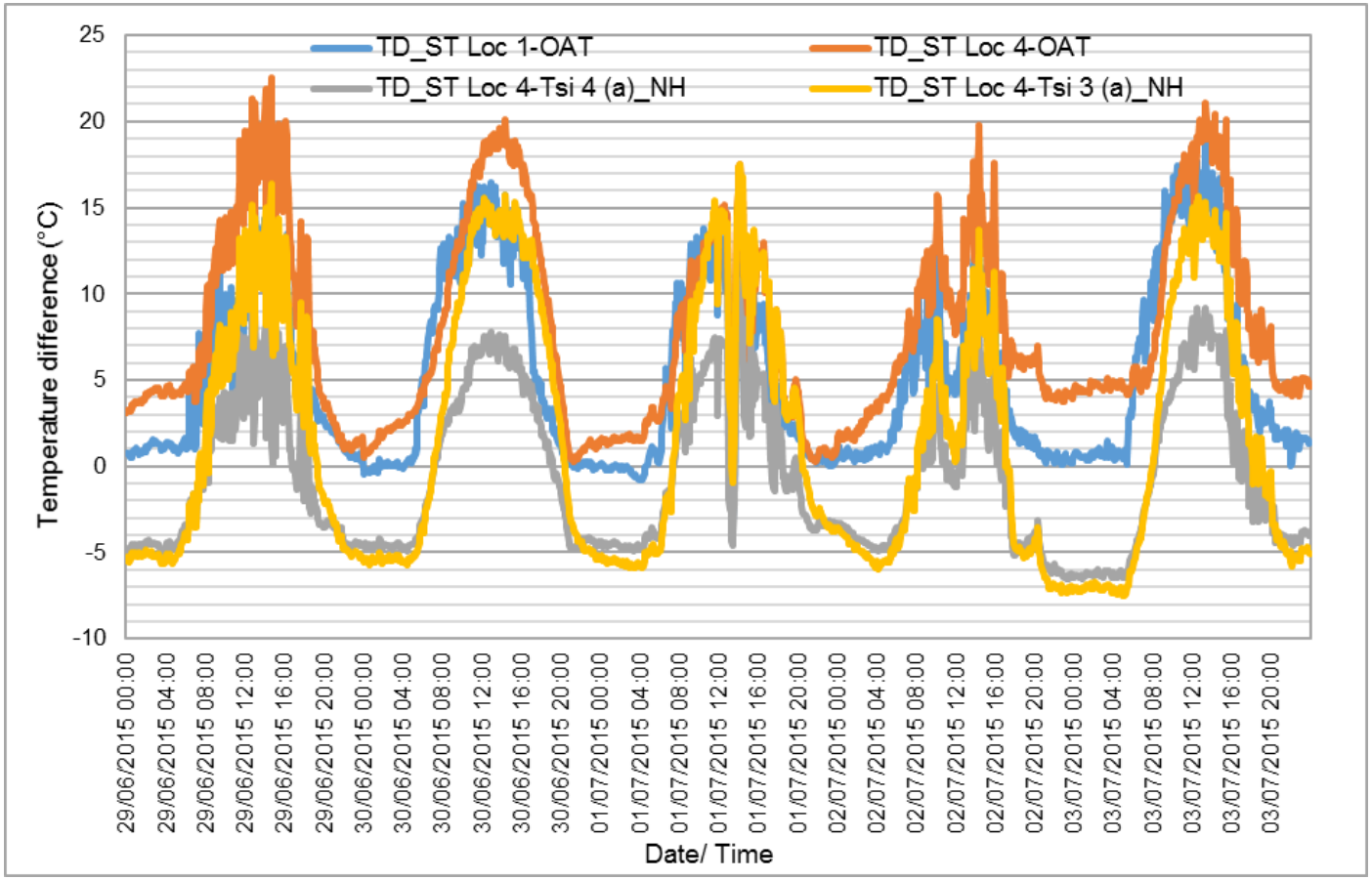


Figure 6-12: Temperature difference between external surface temperature (ST Loc 1) -outdoor air temperature; internal surface (ST Loc 4)- outdoor air temperature, internal surface temperature (ST Loc 4)- level 4 (adjacent to ETFE-foil cushion air temperature); internal surface temperature (ST Loc 4)- level 3 (second floor) between 29th June and 3rd July

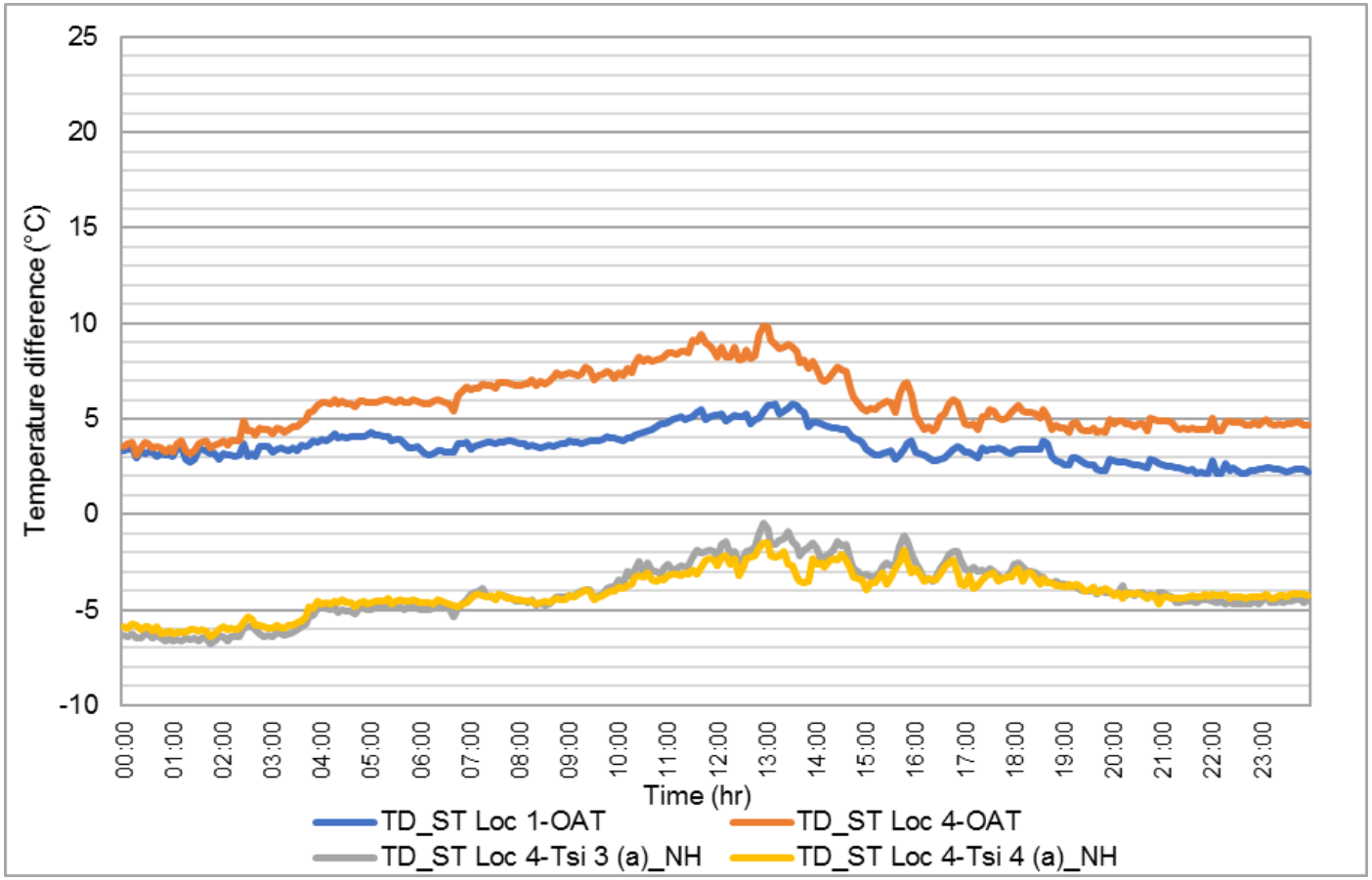


Figure 6-13: Temperature difference between external surface temperature (ST Loc 1)-outdoor air temperature; internal surface (ST Loc 4)- outdoor air temperature, internal surface temperature (ST Loc 4)- level 4 (adjacent to ETFE-foil cushion air temperature); internal surface temperature (ST Loc 4)- level 3 (second floor) during 14th September 2015

Figure 6-12 and Figure 6-13 present the difference between external surface temperature and outdoor air temperature; internal surface and outdoor air temperature; internal surface temperature and atrium level 4 (adjacent to ETFE-foil cushion) air temperature; internal surface temperature and occupied level 3 (second floor) air temperature recorded between 29th June and 3rd July, and 14th September 2015 respectively.

The roof demonstrated more extreme thermal behavior under clear sky conditions where both direct solar and long-wave infrared radiation appeared to govern the fluctuation of the ETFE-foil surface temperatures. It was noticed that before sunset (during 30th June between 7.00pm and 8.00pm) external and internal surface temperature respectively drop by 8°C and 6°C within 1 hour due to the long wave radiation losses to the exposed sky dome. Here solar radiation reaching the surface was insufficient to counterbalance this long wave radiation loss. During this hour, the minimum difference between internal surface and outdoor air temperature observed at this time was 1.2°C. After this hour a gradual decrease of internal and external surface temperature was observed until just before sunrise (see Figure 6-12). This also had an impact on the air temperature and mean radiant temperature of level 4 (level adjacent to ETFE-foil cushion roof).

Because of ETFE-foil's higher transparency to long wave radiation, when compared to glass, radiation losses from the foil surfaces caused a decrease in surface temperature. This, in turn, had an impact on the air temperature and mean radiant temperature at level 4 (level adjacent to ETFE-foil cushion roof). It also resulted in negative stratification at night. The internal surface temperature was lower than the occupied level 1 (ground floor) temperature, the opposite scenario to that observed at mid-day with bright sunshine. After sunset, the external foil surface temperature stays close to the external air temperature but the internal foil surface temperature is approximately equal to the average of indoor and outdoor air temperature, due to long-wave radiation exchange to the clear night sky and convective heat transfer effects. A gradual decrease in foil surface temperature was observed until about 1 hour before sunrise. During bright sunny days both foil surface temperatures are greater than the air temperature immediately below the cushion (level 4), from morning till late afternoon.

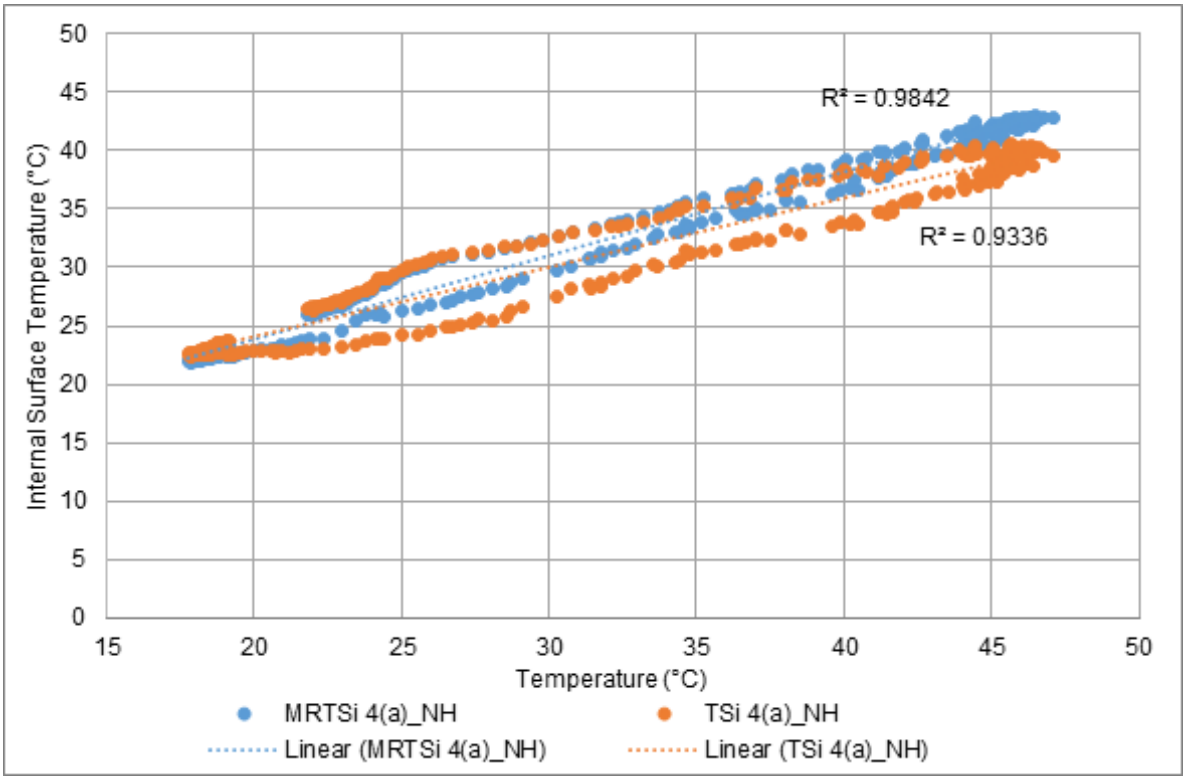


Figure 6-14: Relationship between internal surface temperature (STLoc4_NH), air temperature [Tsi 4(a)_NH] and mean radiant temperature [MRTsi 4(a)_NH]

The internal surface temperature of the ETFE-foil cushion is plotted against the air temperature [Tsi 4(a)_NH] and mean radiant temperature [MRTsi 4(a)_NH] of level 4 (adjacent to ETFE cushion) in a scatter plot and presented in Figure 6-14. The purpose was to identify the impact of surface temperature on adjacent air and mean radiant temperature. The result presented in Figure 6-14 shows that both air temperature and mean radiant temperature increased linearly with internal surface temperature of ETFE-foil cushion. A higher value of regression coefficient R^2 (0.984,0.933) also indicated that internal surface temperature was correlated with adjacent air and mean radiant temperature and contributed in increase and decrease of air temperature and mean radiant temperature of the level 4 of the atrium.

6.2.4 Effect of ETFE-foil surface temperature on thermal comfort

It was apparent from the above discussion that during the day thermal behaviour of the ETFE-foil cushion was dominated by short-wave solar radiation however at night this was particularly influenced by longwave radiation exchanges with the surrounding surfaces e.g. clear sky vault.

This shortwave and longwave thermal radiation does not rely on an intermediate fluid for its transmission. However, the effect of temperature difference will be experienced by the occupant as a deviation of mean radiant temperature from air temperature.

It was already identified in section 6.2.2 (Figure 6-4) that mean radiant temperatures were higher than air temperatures of the level 4 (adjacent to ETFE-foil cushion) particularly during the day and went below air temperatures during the night. This had impact on mean radiant temperatures of the levels below affecting the thermal comfort of the occupants on those levels.

The thermal environment under clear sky condition was largely influenced by large swings in cushion surface temperatures, relative to its surrounding air temperatures. This significant variation in cushion surface temperatures observed to coincide with the extent of the vertical air temperature stratification which was positive during the day and negative at night. This temperature stratification effects thermal comfort by creating difference in temperature in different locations at the same time and, is influenced by heat transfer to the air from the heated surfaces in the upper levels of a large space such as an atrium (IEATask12, 1996).

Research on the effect of asymmetric radiant fields stated that occupants would be more sensate to warm ceiling than to a cool ceiling.

Thus, surface temperatures of ETFE-foil roof (effectively ceiling) particularly influence occupants' thermal comfort by increasing mean radiant temperature during the day and reducing it at night, as well as inducing temperature stratification during day and night.

Air temperatures of level 3 and level 4 of the atrium fluctuated relatively quickly as an impact of frequent change in surface temperature, also because of the curved surface the view factor of the ETFE-foil cushion roof was generally large. Therefore, even small variations in the internal surface temperatures of ETFE-foil resulted in noticeable variation in air temperatures as well as mean radiant temperatures of level 3 and level 4.

6.2.5 Impact of environmental variable on indoor thermal environment

The results of the onsite monitoring presented and discussed in the section 6.2.3 showed that the thermal condition of the atrium on a typical sunny day was particularly influenced by the surface temperature of the ETFE-foil cushion, radiant temperature, solar radiation and outdoor air temperature. However, the relationship between

individual environmental parameters and the resulting thermal condition of the atrium are unknown because the recorded condition was the combined effect of all the monitored parameters. Therefore, the correlation coefficient R^2 formula was used to determine this interrelationship between air temperature of atrium occupied levels and environmental parameters such as incident and transmitted solar radiation, outdoor air temperature and presented in Table 6-2. This found a strong correlation between outdoor air temperatures and occupied levels air temperatures (R^2 value ranged from 0.884 to 0.966). However, outdoor temperature, as well as transmitted solar radiation, had a strong positive relationship with indoor air temperatures of occupied levels and level adjacent to ETFE-foil cushion roof (R^2 value ranged from 0.952 to 0.984). This relationship between outdoor and indoor environment (level 3 and level 4 of the atrium) was found to be established by the ETFE-foil cushion roof, through its responsiveness to outdoor conditions as well as continuous interaction with indoor environment.

Table 6-2: correlation between air temperature at different occupied level and incident, transmitted solar radiation and outdoor ambient temperature 1st July 15

Environmental parameters	level 1 Tsi 1(a)_NH	level 2 Tsi 2(a)_NH	level 3 Tsi 3(a)_NH	level 4 Tsi 4(a)_NH
R^2 (Incident Solar radiation)	0.101	0.082	0.156	0.44
R^2 (Transmitted Solar radiation)	0.096	0.081	0.153	0.436
R^2 (OAT)	0.884	0.865	0.923	0.966
R2 (Incident Solar radiation and OAT)	0.949	0.947	0.954	0.984
R^2 (Transmitted Solar radiation and OAT)	0.951	0.946	0.954	0.984
R^2 (Transmitted and Incident Solar radiation)	0.1 (only impact of transmitted radiation to 0.093)	0.082	0.156	0.442
R^2 (OAT, Transmitted and Incident Solar radiation)	0.952 (Transmitted Solar radiation and OAT)	0.946 (only impact of transmitted radiation and ODT)	0.954 (only impact of transmitted radiation and ODT)	0.984

6.2.6 Impact of atrium thermal environment to the adjacent spaces

To examine the impact of the atrium's thermal condition on other internal spaces, temperature sensors were installed in the spaces (e.g. classroom, corridor etc.)

adjacent to the atrium. These recorded data between 21st August and 1st September 2015. Figure 6-15 presents location of the sensors.

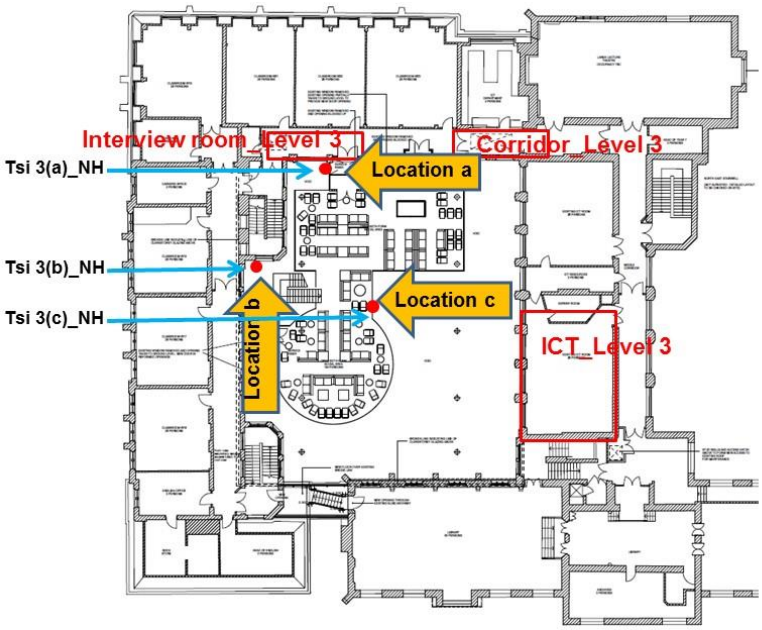


Figure 6-15: Location of temperature sensors in level 3 (second floor) [Plan (nts): drawing courtesy Maber architect]

Thermal conditions in the atrium influence air temperatures of the adjacent spaces (classroom, corridor). Figure 6-16 presents air temperatures of occupied level 3 (Tsi 3(a)_NH), corridor, interview room and outdoor measured during 29th and 30th August 15. The results presented in Figure 6-16 showed that air temperatures of the interview room and corridor varied within 1.5°C of the air temperature of Tsi 3(a)_NH during the day while little variation was observed at night.

To see the extent of this impact of the atrium's thermal condition on indoor spaces, air temperatures of the interview room and corridor were plotted against air temperatures of Tsi 3(a)_NH and presented in Figure 6-17. These indicated that the interview room and corridor air temperatures had a linear relationship with Tsi 3(a)_NH air temperatures. Whereas higher correlation coefficient R^2 value (0.89, 0.86) confirmed the impact of atrium's thermal condition on indoor air temperatures of the school building such as spaces adjacent to the atrium. This was the result of air circulation between the spaces (interview room, corridor etc) and the atrium through window openings.

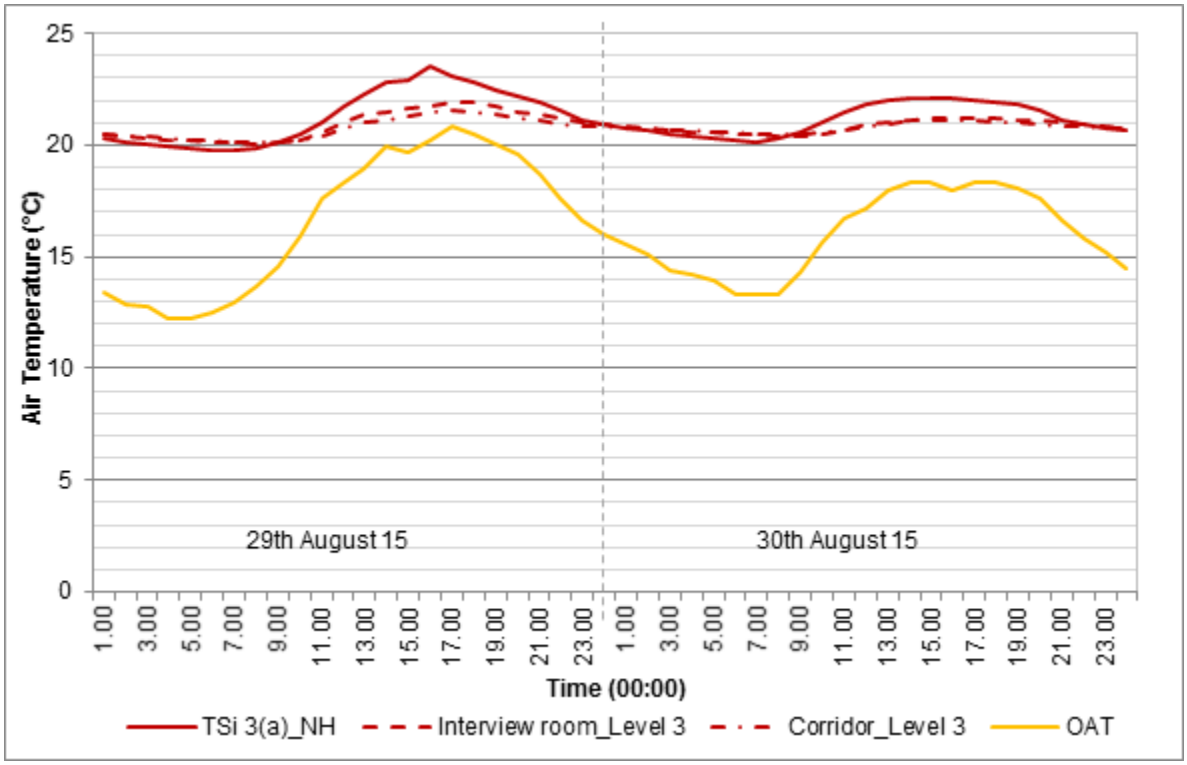


Figure 6-16: Air temperatures of different vertical and horizontal positions in the atrium and space adjacent to atrium during 29th August and 30th August

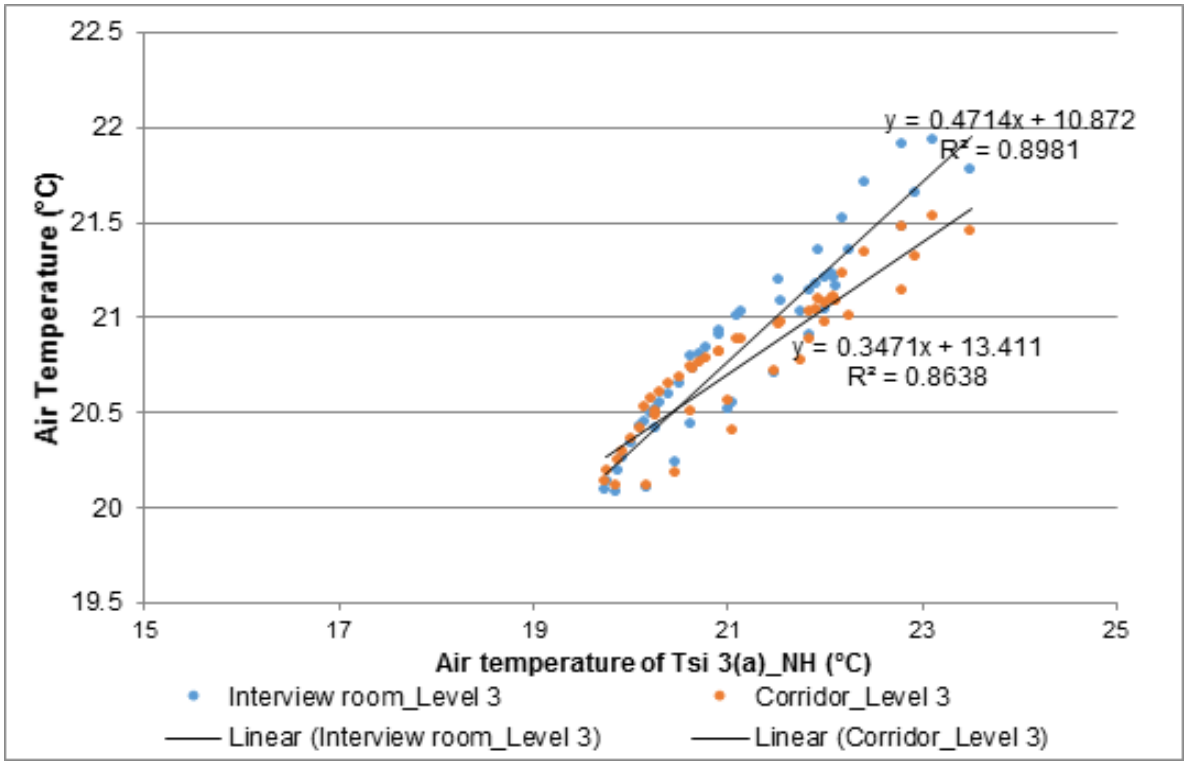


Figure 6-17: Impact of atrium level 3 (Tsi (a)_NH) air temperature on internal space adjacent to it

6.3 Case Study B: Engineering and Science Learning Centre (ESLC)

This section discusses the thermal behaviour of the ESLC atrium. The atrium roof consists of three-layer ETFE-foil cushions with fritted top layer (200μm) transparent middle (150μm) and bottom layer (150μ m). Detailed description of the building and monitoring setup is presented in Chapter 3 (section 3.9).

Summary of the salient features of the monitored atrium of ESLC, its roof and time period of environmental monitoring is presented in Table 3-3 (Chapter 3).

When selecting days for analysis, it was considered that the building was operating on its normal schedule within the summer period in the UK.

Sensor identification used to describe the outdoor environment are presented in Table 6-1, while Table 3-7 (Chapter 3) presents sensors identification used to discuss the thermal conditions of the atrium. Detailed description of the method and installed equipment for monitoring is presented in Chapter 3 (section 3.9).

6.3.1 Analysis of monitored data and discussion

The graphs in this section represent monitored data recorded at fifteen minute intervals. This allowed to graphically represent dynamic thermal responsiveness of the ETFE-foil cushion envelope. All numerical value specified in a text format are based on instant readings. Indoor air temperature here represents air temperature at a particular time of the day at shielded measuring points along the same vertical line and horizontal plan position on each floor.

6.3.1.1 Overview of typical thermal environment

The typical thermal behaviour of the Engineering and Science Learning centre and the Nottingham High School were found to be similar. Two specific patterns in the thermal environment were also identified in the ESLC building. Figure 6-18 and Figure 6-19 presents the typical thermal conditions observed under clear sky conditions and overcast conditions respectively.

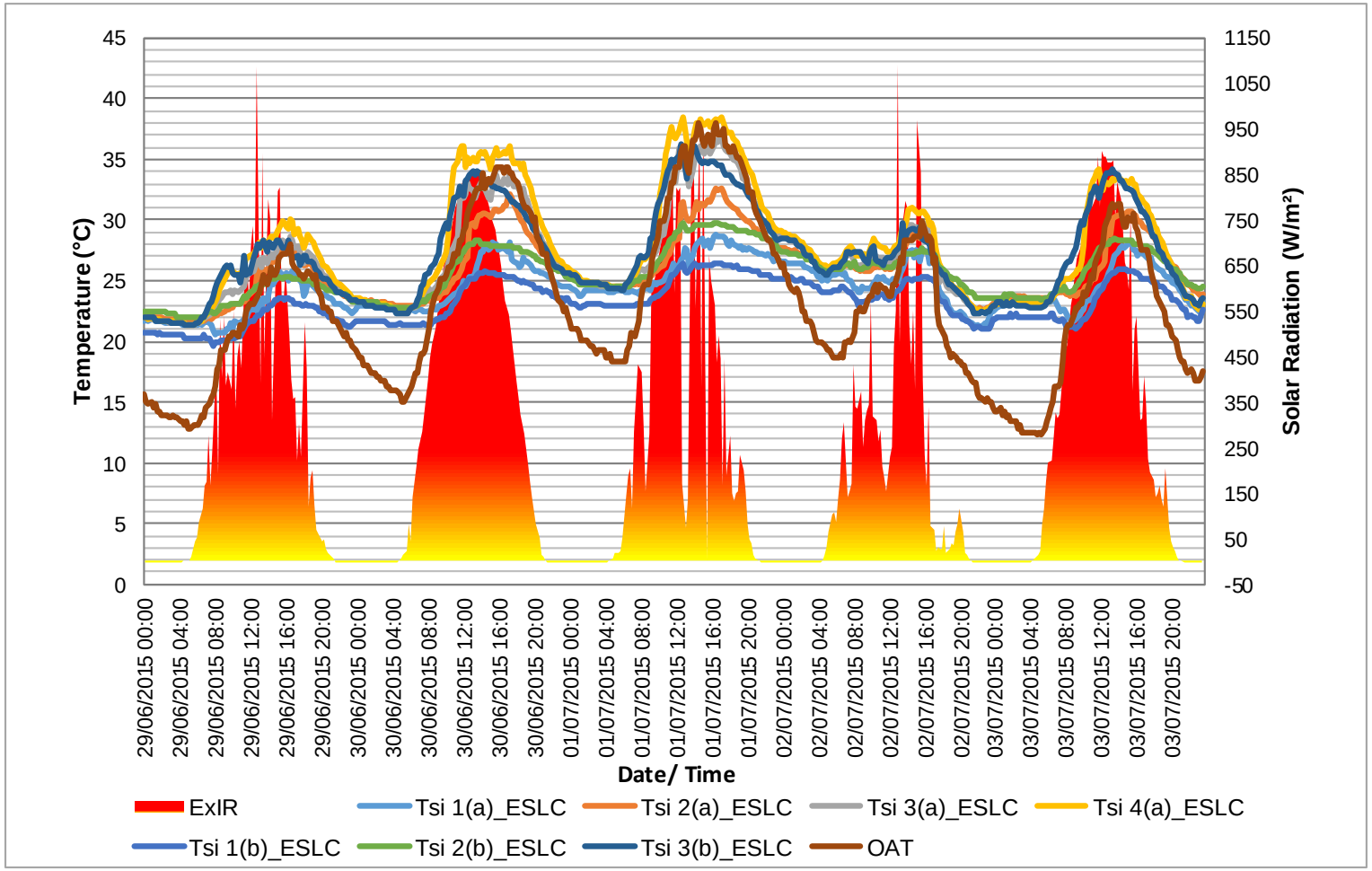


Figure 6-18: Indoor air temperatures and solar radiation recorded in the ESLC atrium between 29th June and 3rd July 2015 – clear sky conditions

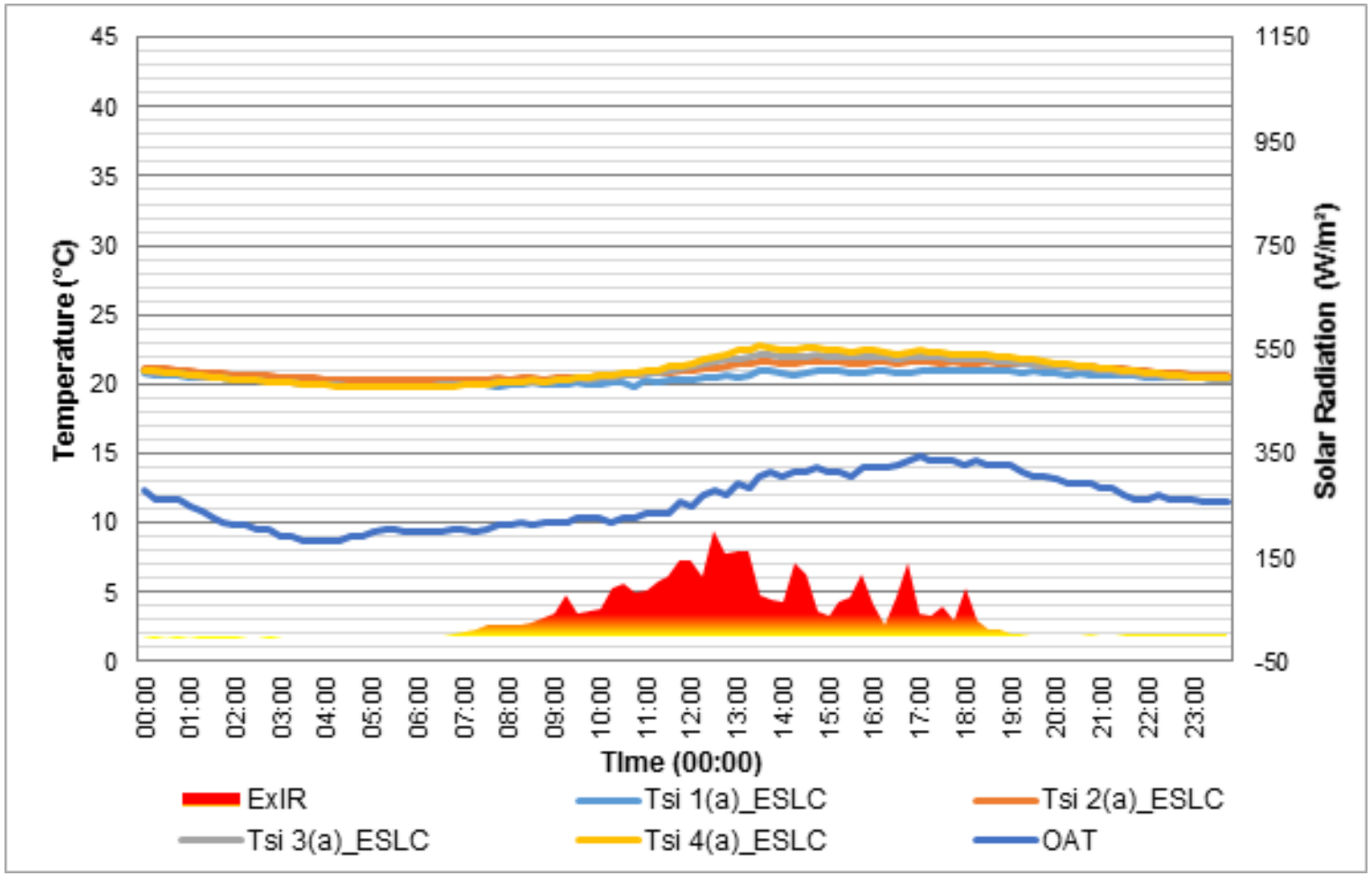


Figure 6-19: Indoor air temperatures and solar radiation recorded in the ESLC atrium between 14th September 15 – overcast sky

6.3.2 Indoor air temperature distribution

The ground floor (level 1) air temperature was generally the lowest among the three levels of the atrium. Figure 6-22 presents temperature differences between the occupied levels (1, 2, 3 and 4) of the atrium and outdoor air temperature. The result presented in Figure 6-22 shows that on an extremely hot day (1st July 15) air temperature of the ground floor was a maximum of 11°C lower than outdoor air temperature. During warm sunny conditions the range of temperature of the ground floor (6.5°C) was found to be similar in both ESLC and Nottingham High School atria.

Correspondingly, air temperature at the first floor [shown by Tsi 2(a)_ESLC] was slightly higher than that on the ground floor and slightly more affected by outdoor weather conditions. Figure 6-20 presents temperature differences between atrium level 1, 2, 3 and 4 during warm sunny days. From Figure 6-20 it can be noticed that during the warm sunny days the maximum temperature difference between ground floor and first floor was 4.5°C. However, this temperature difference between ground floor and first floor air temperature was comparatively less (2°C) in Nottingham High School atrium. In both of the buildings, this difference occurred during the afternoon. The highest temperature recorded at first floor over the two days (30th June and 1st July 15) was 32°C (32°C in Nottingham High School). During the warm sunny days, the direct and diffuse radiation could penetrate more deeply to lower atrium levels resulting in raised air and mean radiant temperatures. Extremely hot outdoor air temperature also had an influence on this significant rise in air temperature.

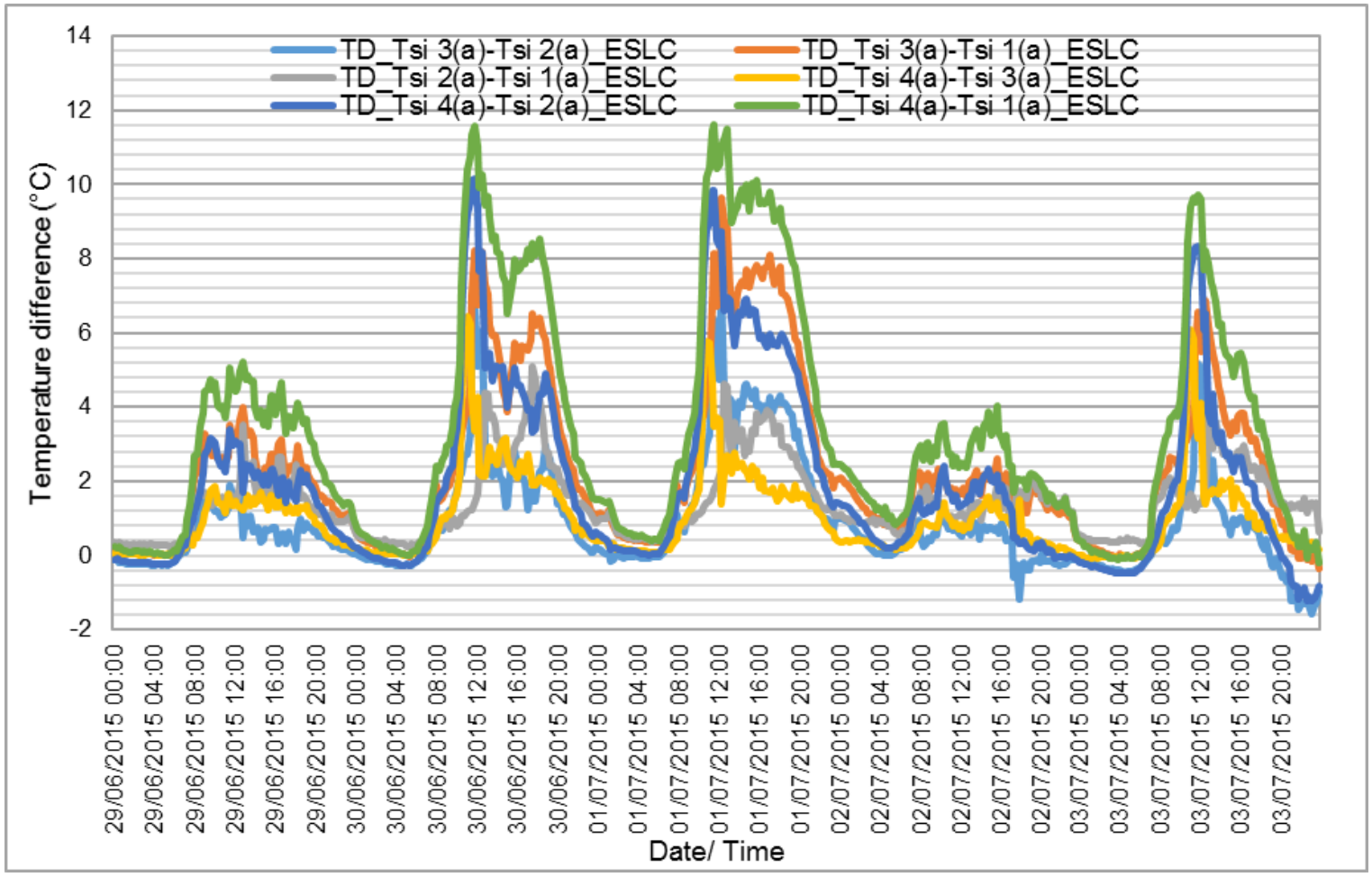


Figure 6-20: Temperature difference between ESLC atrium level 1, 2, 3 and 4, between 29th June and 3rd July 2015

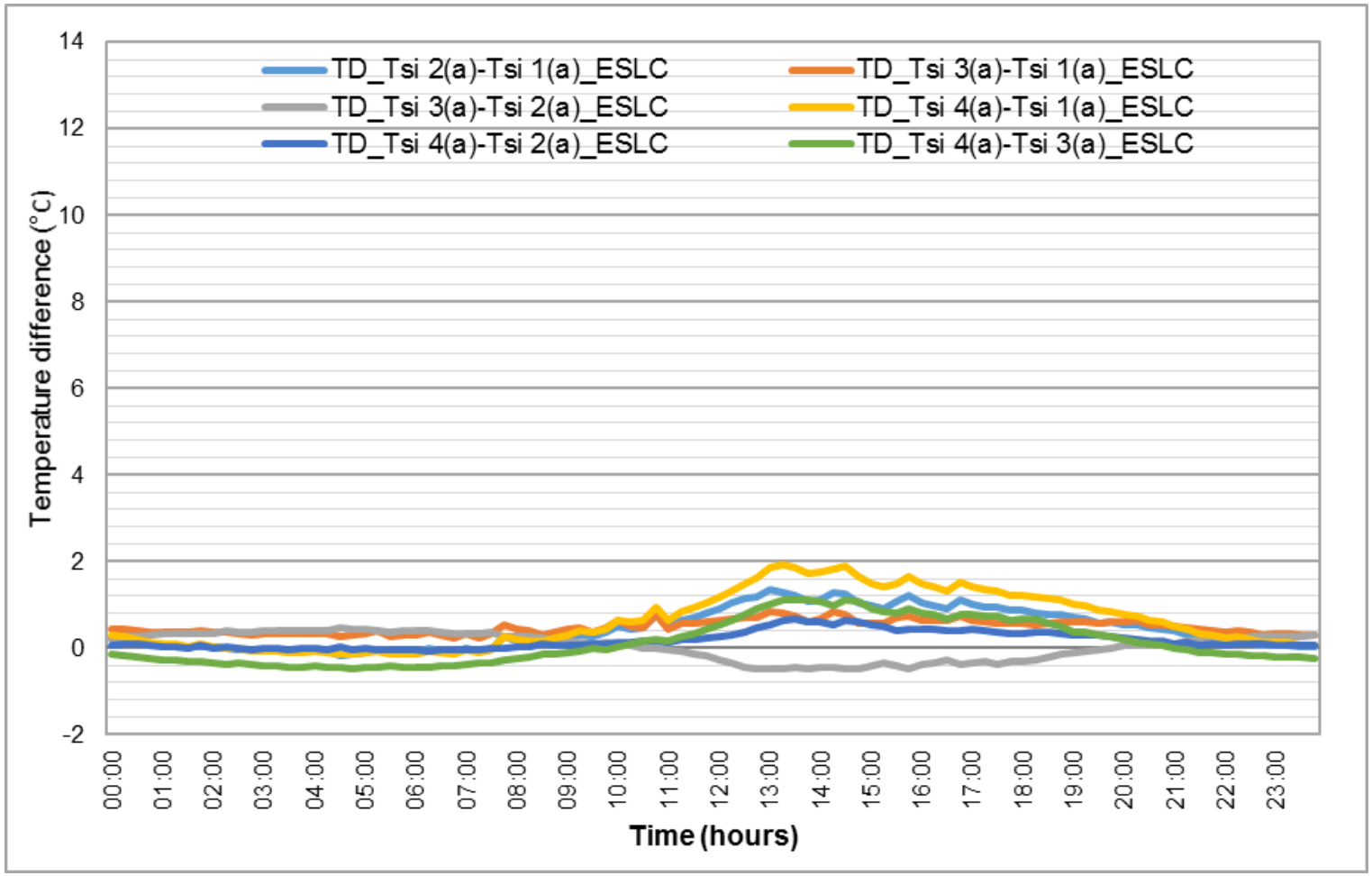


Figure 6-21: Temperature difference between ESLC atrium level 1, 2, 3 and 4, during 14th September 2015

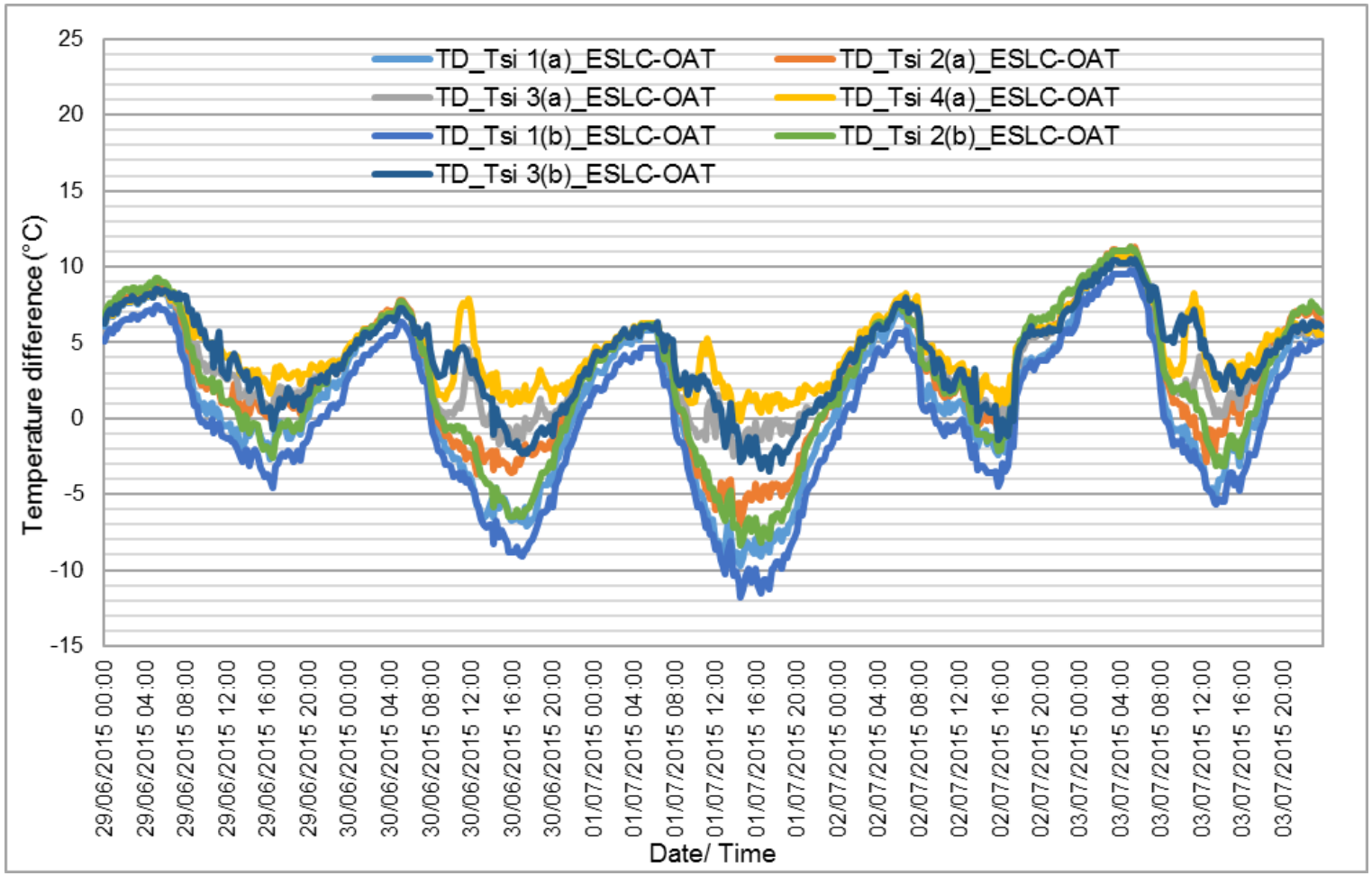


Figure 6-22: Temperature differences between air temperatures of atrium levels of ESLC and outdoor air temperatures between 29th June and 3rd July 2015

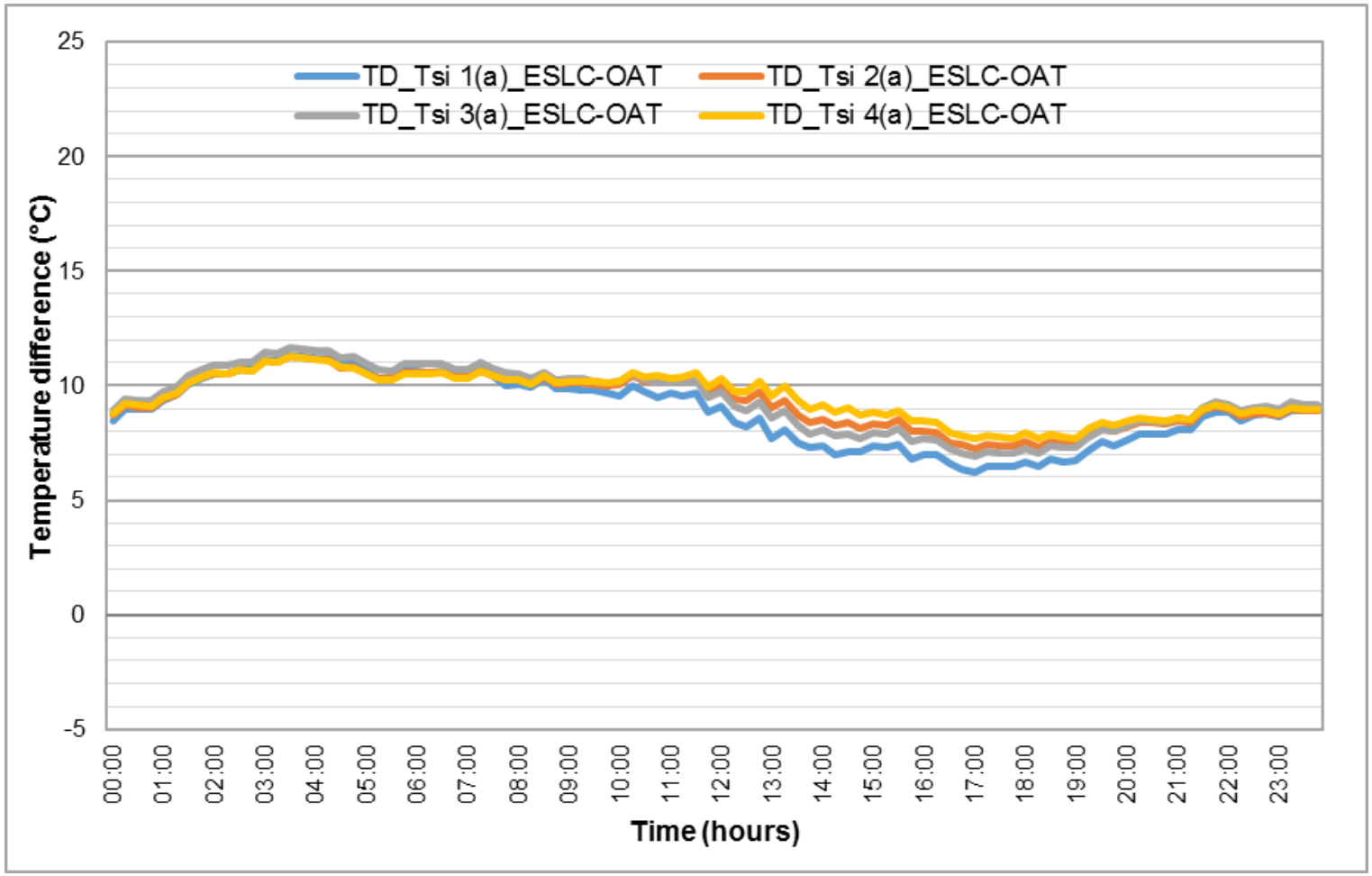


Figure 6-23: Temperature differences between air temperatures of atrium levels of ESLC and outdoor air temperatures during 14th September 2015

On the second floor, air temperatures [shown by Tsi 3(a)_ESLC] were higher than ground and first floor. Around noon on the sunny day (1st July 2015), second floor air temperatures rose to 33°C (30°C in Nottingham High School) then increased to a maximum of 36.8°C in the afternoon (33.5°C in Nottingham High School). It is considered that the main reason for this is the proximity of the translucent ETFE-foil cushion roof to this atrium level which increases the sky view factor, radiant heat effects from the ETFE-foil cushion roof surfaces as well as radiant heat from the direct sunlight.

Besides, at noon a significant temperature rise was observed in air temperature of level 4 (approx. 4m above the second floor), which was 6.5°C higher than the second floor air temperature. The amount of incident solar radiation affects the thermal environment of the second and third floors significantly, creating strong vertical positive stratification during the daytime. Whereas in the absence of solar radiation, longwave radiation exchange to the clear cold sky may cause negative stratification at night. This positive and negative stratification was also observed during the overcast day but to a lesser degree. During the warm sunny and overcast days, the maximum temperature difference between level 4 [Tsi 4(a)_ESLC] and ground floor [Tsi 1(a)_ESLC] was 11.6°C (during 30th June and 1st July 15) and 1.9°C respectively, whereas between the second floor [Tsi 3(a)_ESLC] and ground floor [Tsi 1(a)_ESLC], it was 9.6°C and 0.8°C correspondingly. However, in Nottingham High School maximum temperature difference between level 4 [Tsi 4(a)_NH] and ground floor [Tsi 1(a)_NH] was 11.6°C, whereas between second floor [Tsi 3(a)_NH] and ground floor [Tsi 1(a)_NH], it was 4.3°C.

It was mentioned in Chapter 3 (section 3.9), that the ETFE-foil cushion roof was not reachable from inside of the ESLC atrium. Therefore, it was not possible to install sensors closer to ETFE-foil cushion roof. Hence level 4 (approx. 4m below the ETFE-foil cushion roof) air temperatures were not directly comparable with those of Nottingham High School level 4 (directly adjacent to the ETFE-foil cushion roof) air temperatures.

However, temperature stratification (the difference between second floor and ground floor air temperature) was high (5.3°C) in the ESLC atrium than that of Nottingham High School atrium.

In both of the buildings during hot days (30th June and 1st July 2015) air temperatures of the second floor of the atria were similar to outdoor temperatures, particularly during the day (Figure 6-6 and Figure 6-22).

It was not possible to monitor the thermal condition of the ETFE-foil cushion in the ESLC atrium due to limited accessibility. However, on 7th August 2014 the internal surface temperature of the cushion was assessed using a thermal imaging camera (FLIR T900) and compared with that of ETFE-foil cushion roof of Nottingham High School, as presented in Figure 6-24. The results showed that internal surface temperatures of the cushion roof in Nottingham High School atrium varies more rapidly than the ETFE-foil cushion roof of ESLC atrium. It was apparent that at 1.00pm the cushion surface temperature of Nottingham High School was 9°C higher than that of ESLC ETFE-foil cushion roof, although just over an hour later the situation was reversed with ETFE-foil cushion roof of ESLC was hotter than that of Nottingham High School by 2.5 °C. This observed variation may be due to the impact of the number of foil layers and/or different insolation levels at the two sites. Detail of the analysis can be found in Afrin et al. (2015), also attached in the Appendix.

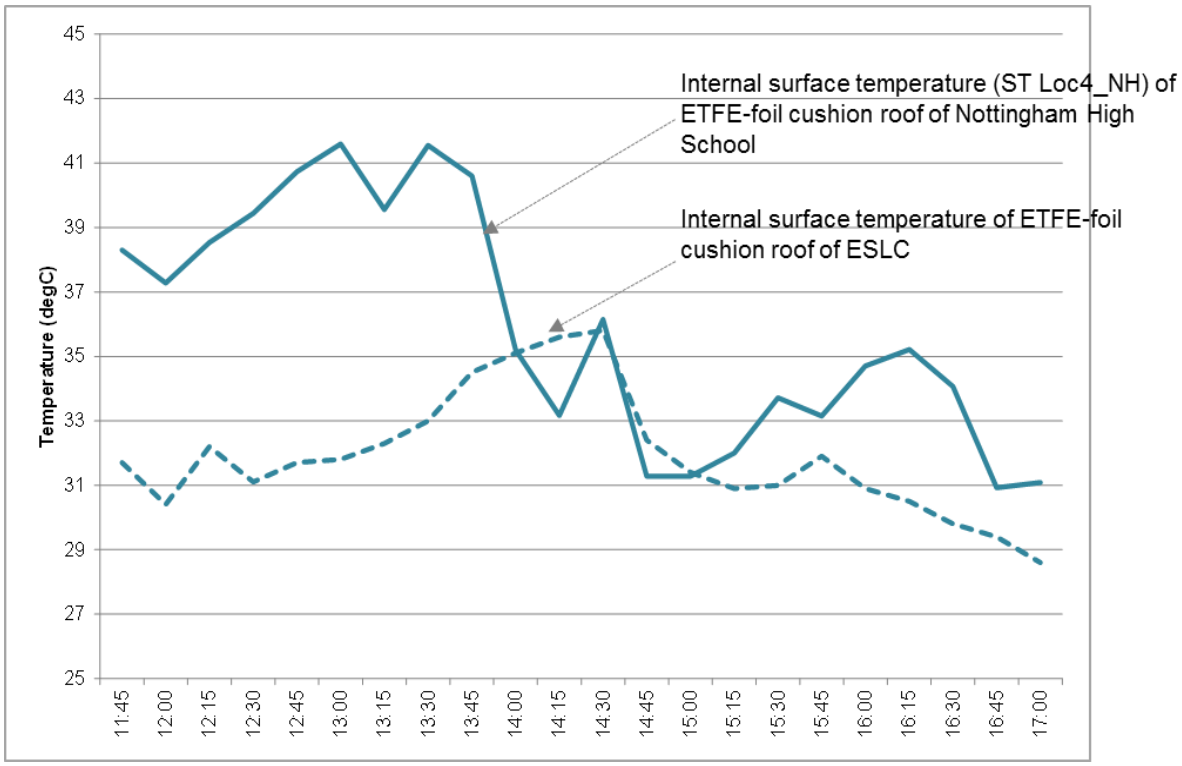


Figure 6-24: Internal surface temperatures variations of ETFE-foil cushion roof of Nottingham High School (fixed sensor) and ESLC (thermal imaging) atria (7th August 2014)

The air temperatures of the adjacent functional spaces of the atrium were not largely influenced by the air temperatures of the ESLC atrium, because, there was no opening except doors that link the internal functional spaces (e.g. graduate centre, seminar rooms, class rooms etc.) with the atrium. Therefore, although the influence of atrium air on internal spaces (e.g. interview room, corridor etc.) was apparent in the Nottingham High School, here in the ESLC this impact was not very significant.

6.3.3 Comparison of the thermal environment of the Nottingham High School and the Engineering and Science Learning Centre (ESLC) atrium

It was evident from the earlier discussion that in the ESLC atrium, air temperatures of occupied levels (first floor and second floor) were higher than that of same occupied levels in the Nottingham High School atrium. Figure 6-25 presents temperature differences between air temperatures of occupied levels (1,2 and 3) of the ESLC and the Nottingham High School atrium. The result presented in Figure 6-25, indicated that during warm summer days (between 8.00am and 8.00pm during 30th June, 1st and 3rd July 2015) the air temperature of occupied level 3 [Tsi 3(a)_ESLC (second floor)] of ESLC atrium was continuously hotter than that of Nottingham High School atrium [Tsi 3(a)_NH (second floor)]. During this period, average air temperature difference between these two atria was 2.6°C (occupied level 3) while during the afternoon (30th June 2015) occupied level 3 of ESLC atrium was maximum 5.4°C hotter than occupied level 3 of Nottingham High School atrium. But reverse conditions occurred on summer nights and early in the mornings when air temperature of each occupied level of the Nottingham high school was on average 1°C to 2°C hotter than that of the same occupied levels of the ESLC atrium because of thermal inertia of surrounding masonry wall and floor.

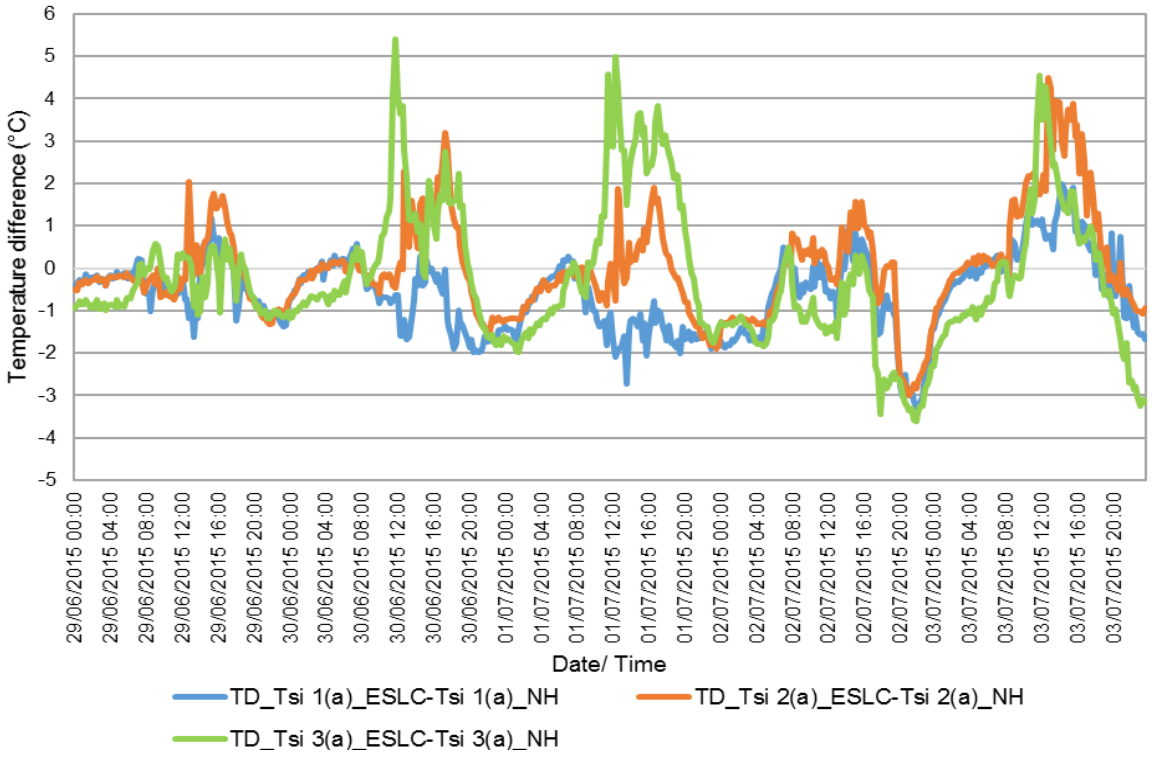


Figure 6-25: Temperature difference between occupied level 1, 2 and 3 of ESLC and Nottingham High School atrium between 29th June and 3rd July 2015

The significant difference in air temperatures of the two different atria may be the result of the higher surface temperature of inner layers of ETFE-foil cushion and radiant heat from the hot foil surface of the three-layer cushion. With similar levels of insolation the air temperature adjacent to the inner foil layer (level 3) was significantly higher in the ESLC atrium, reflecting the higher level of thermal insulation provided by the 3-layer cushion (compared to insulation provided by 2-layer ETFE-foil cushion roof of Nottingham High School). On the other hand, high-density fritting coverage (75% fritting) and rain mesh reduced solar gain as well as surface temperature. That in turn resulted in a lower air temperature in Nottingham high school atrium. It was discussed in section 6.1.1 that the average outdoor temperature was 1.4°C lower in the surrounding environment of Nottingham High School. This may have contributed to the lower air temperature, particularly in the occupied levels 2 and 3 (first floor and second floor), of the atrium compared to the ESLC atrium.

Alternatively, during overcast days in summer, no significant difference between outdoor air temperature of the two different locations (adjacent to the both atria) was evident. It was also apparent that thermal conditions of both atria were similar on overcast days and air temperature of occupied levels varied between 19.5°C and 22°C.

6.4 Thermal performance of atria enclosed with ETFE-foil cushion roof

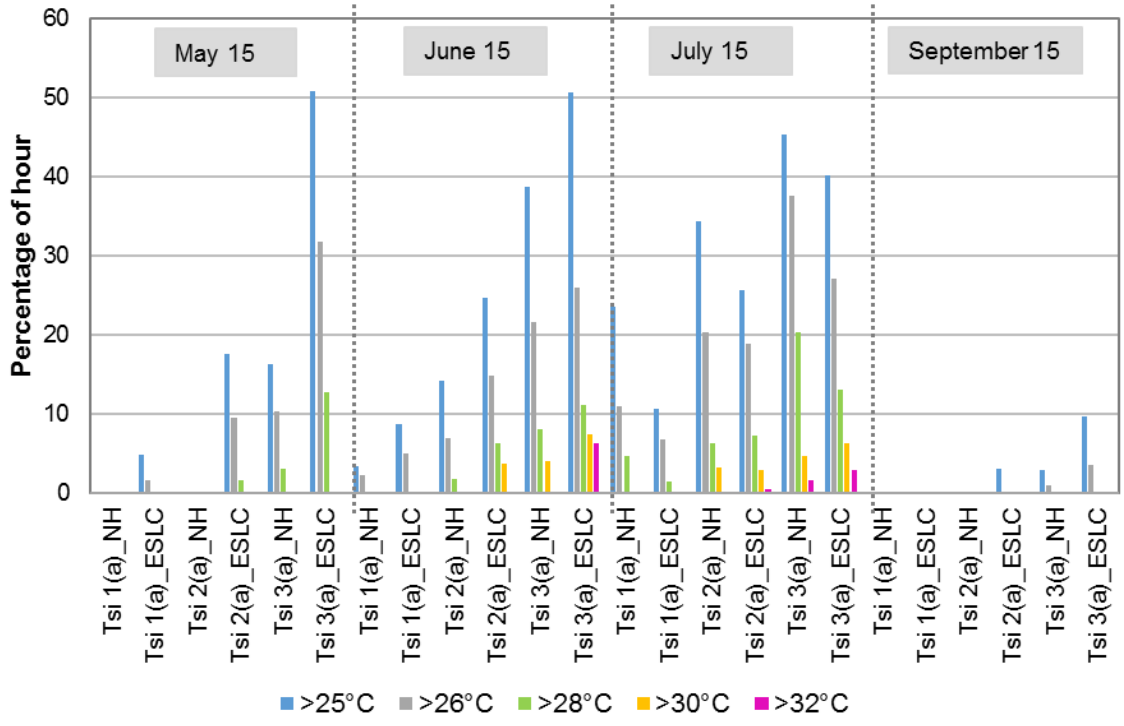


Figure 6-26: Percentage of occupied hours when Nottingham High School and ESLC atrium level 1, 2 and 3 were above 25°C, 26°C, 28°C, 30°C and 32°C

During hot summer days, the excessive solar gain, hot outdoor temperature and high surface temperature over the large roof area may adversely affect user thermal comfort. In order to investigate the extent of variation of air temperature that might impact thermal comfort of the users, the percentage of occupied hours that exceeded 25°C, 26°C, 28°C, 30°C and 32°C in each occupied level of both Nottingham High School and ESLC atria was calculated and plotted in Figure 6-26.

Results presented in Figure 6-26 demonstrated that in both atria during July 2015, 1.5% to 4.5%, 6% to 7% and 13% to 30% of occupied hours, respectively ground floor, first floor and second floor air temperature was above 28°C. However, in both atria, a significant rise of air temperature of occupied level 3 was also evident, as for 1.6% to 2.9% of occupied hours the air temperature exceeded 32°C. This significant rise in air temperature of occupied levels, as well as the duration, affects the thermal comfort of the occupants.

Thermal comfort of the Nottingham High School and ESLC atria enclosed with an ETFE-foil cushion roof was evaluated based on overheating analysis methods. TM52 adaptive comfort criteria, CIBSE temperature benchmark and Building Bulletin 101 (performance standard for the avoidance of overheating) were used in the analysis procedure, as detailed in Table 6-4. Discussion on these methods adopted in this study was provided in Chapter 3.

Table 6-3: Summary of occupied periods in summer 2014, 2015

	Monitoring period	Year	Occupied hours	Number of days monitored during summer	Number of occupied hours	Annual occupied hours/ year	Space type
Nottingham High School	1st May- 30th September	2014	8.00-15.00	77	536	1236	Atrium
	1st May- 21st September	2015	8.00-15.00	60	480	1236	Atrium
ESLC	1st August - 30th Septembe	2014	9.00-17.00	43	387	1578	Atrium
	1st May- 30th September	2015	9.00-17.00	82	738	1578	Atrium

Table 6-4: Criteria for assessing internal temperature in naturally ventilated atrium space

Assessment metrics	Source	Criterion	Applicability	Comments
CIBSE guide A	CIBSE guide A	peak temperature exceeds more than 1% of annual occupied hours above 28°C.	Engineering and Science Learning Centre and Nottingham High School	Irrespective of location, time of the year
Adaptive comfort category II building envelope: threshold of maximum indoor operative temperature	CIBSE TM52	Threshold of acceptable range	As above	Used to calculate maximum acceptable temperature
Criteria 1: Hours of exceedance		∆T>/= 1K shall be not more than 3% of occupied hours from May to September		An enclosed space that fails to meet any two of the criteria is classed as overheated.
Criteria 2: Daily weighted exceedance		In any one day weighted exceedance shall be less than or equal to 6	As above	
Criteria 3: Upper limit temperature		Value of ∆T shall not exceed 4K	As above	
Criteria 1: Total hours dry bulb temperature above 28°C	BB101	No more than 120 hours above 28°C	Nottingham High School only	In order to show that the proposed school will not suffer overheating two of these three criteria must be met
Criteria 2: Total hours internal above 5°C of external air		Internal air shall not rise above 5°C of external air temperature	As above	
Criteria 3: Total hours dry bulb temperature above 32°C		Internal temperature shall not exceed 32°C	As above	

6.4.1 CIBSE Temperature benchmark

Table 6-5 presents the results of overheating performance according to CIBSE criteria. According to CIBSE Guide A, overheating occurs when 1% of annual occupied hours are above the temperature benchmark (28°C), which is equivalent to 12.36 hours per annum for Nottingham High School atrium and 15.78 hours per annum for ESLC atrium. The number of occupied hours (both atria) presented in Table 6-5 is based on

summer occupied period only. Considering this level 3 of Nottingham High School atrium and, level 2 and 3 of ESLC atrium experienced overheating problems even with data for a limited period (summer only). These results suggest that level 3 (second floor) of these atria suffer significant overheating problem according to CIBSE criteria.

Table 6-5: Total occupied hours above 28°C for summer 2014 and 2015

Description		2014			2015		
		level 1	level 2	level 3	level 1	level 2	level 3
Nottingham High School atrium (annual occupied hours 1236)	Number of occupied hours above 28°C	0	0	8	3	7	31
	Percentage of annual occupied hours	0.00%	0.00%	0.647%	0.243%	0.566%	2.5%
Engineering and Science atrium (annual occupied hours 1578)	Number of occupied hours above 28°C (location a)	0	0	10	3	24	50
	Percentage of annual occupied hours	0.00%	0.00%	0.6337%	0.2%	1.52%	3.17%
	Number of occupied hours above 28°C (location b)	0	0	36	3	10	116
	Percentage of annual occupied hours	0.00%	0.00%	2.28%	0.2%	0.633%	7.35%

6.4.2 Adaptive comfort

The CIBSE TM52 overheating criteria have been applied to all 3 levels of both of the atria. The results presented in Table 6-6 shows that level 2 and 3 of both atria fail to comply with the requirement particularly in summer 2015.

Figure 6-27 and Figure 6-28 respectively present the indoor temperatures of the level 3 of the Nottingham High School and ESLC atrium and the thermal comfort band according to BS EN 15251 Category II building (blue lines in dotted and dashed pattern shows upper and lower acceptable temperature respectively). The results show that level 3 of both atria experienced higher than comfort temperatures in summer 2014 and 2015. In 2014 at this level the temperature went closer to the maximum acceptable temperature and exceeded it on a number of occasions, while in 2015 temperature at this level frequently exceeded the maximum acceptable temperature.

Figure 6-29 and Figure 6-30 correspondingly presents the indoor temperatures of the level 2 of the Nottingham High School and ESLC atrium and the thermal comfort band according to BS EN 15251 Category II band (blue lines in dot and dashed pattern shows upper and lower acceptable temperature respectively). The results show that at this level air temperature was mostly in between comfort bands in summer 2014 but exceeded the maximum acceptable temperature band in summer 2015, particularly during June and July.

Thus, among different levels of the atrium, level 3 experienced substantially higher temperatures compared to other levels. The severity of overheating was observed to be extreme in Location b of ESLC atrium which is widely exposed to ETFE-foil cushion roof.

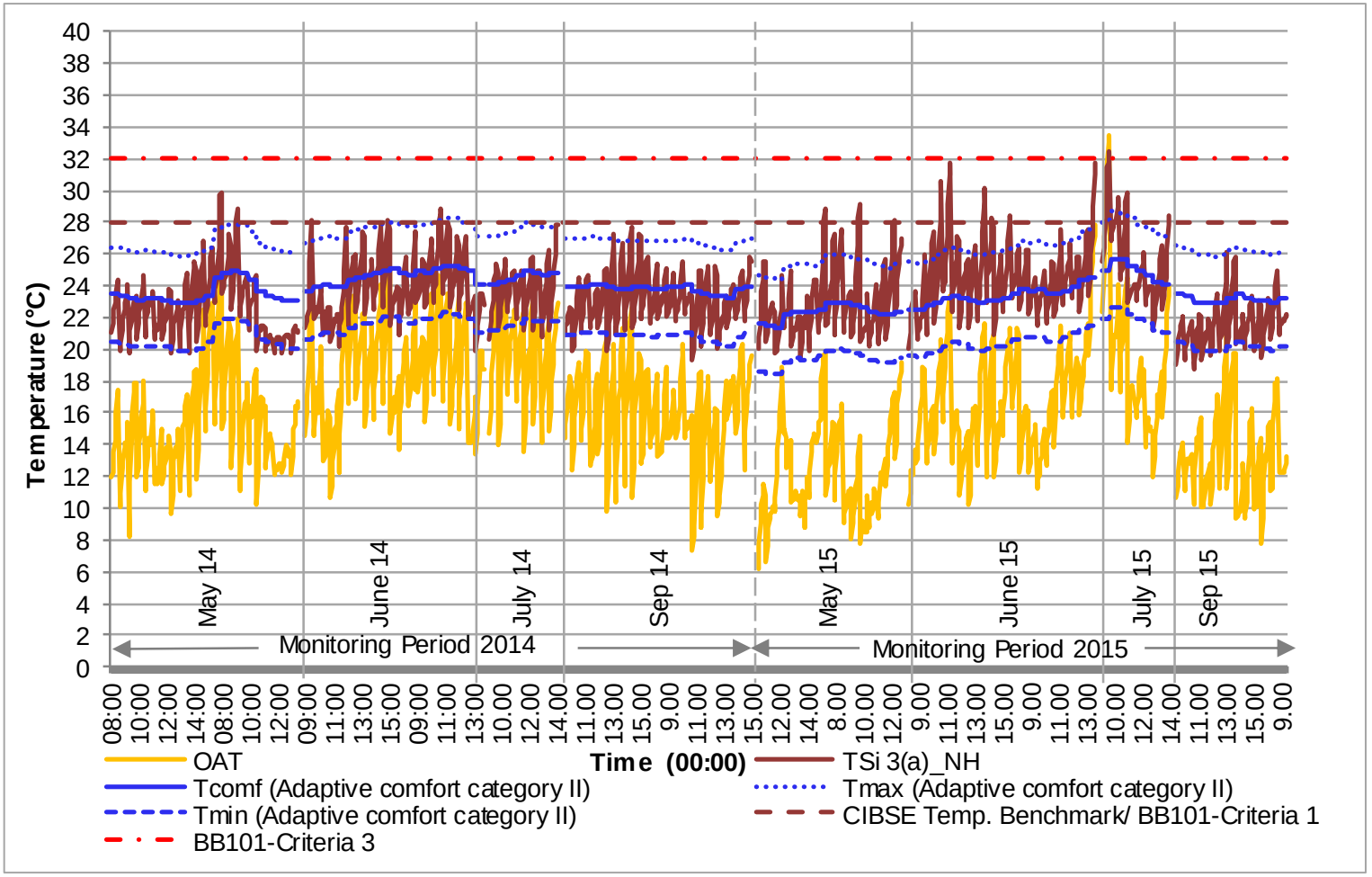


Figure 6-27: Air temperature of level 3 (second floor) of Nottingham High School atrium, CIBSE temperature benchmark, maximum and minimum acceptable temperature range for category II building, BB101 Criteria 1 & 3 temperature benchmark

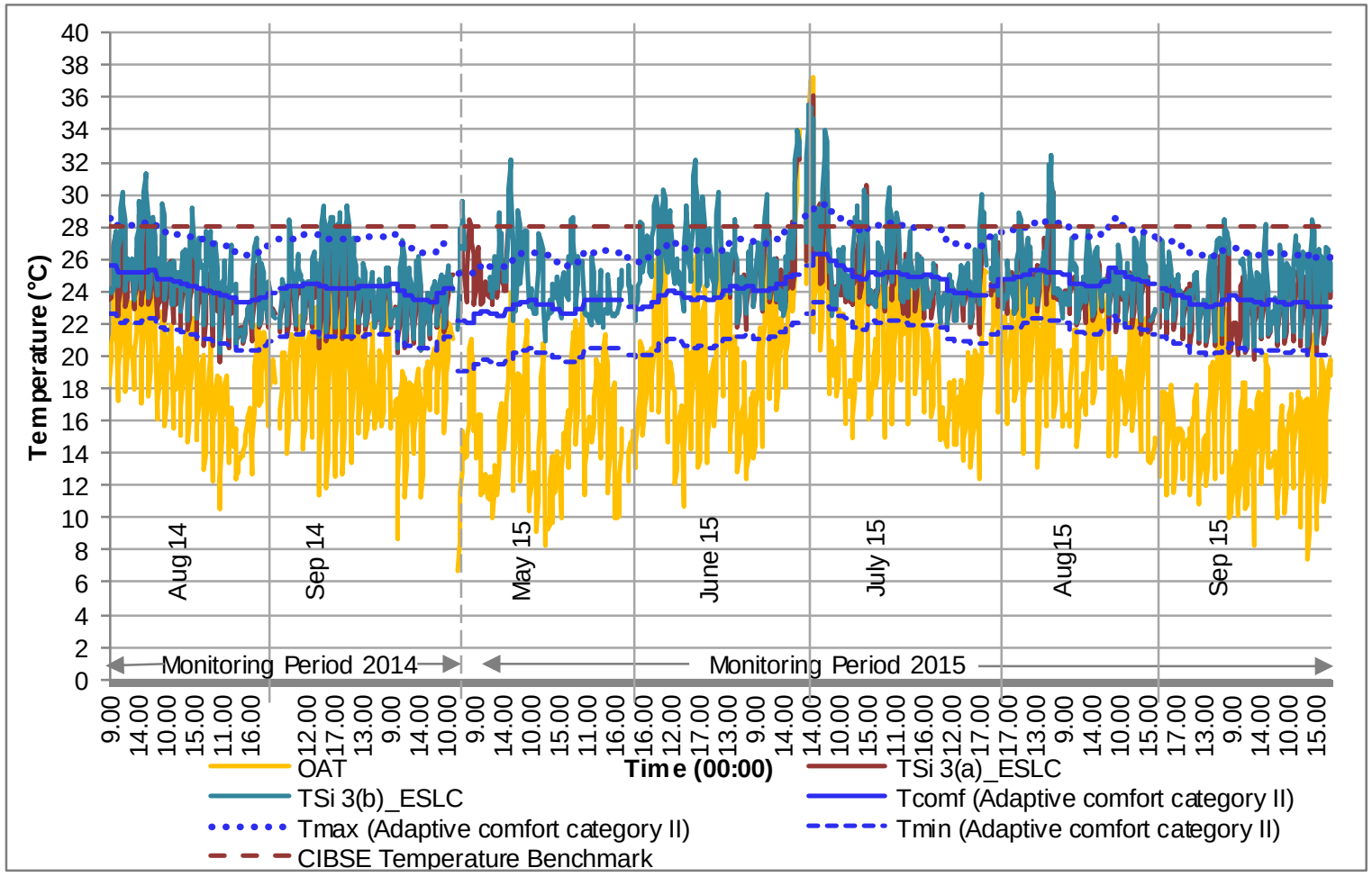


Figure 6-28: Air temperature of level 3 (second floor) of ESLC atrium, CIBSE temperature benchmark, maximum and minimum acceptable temperature range for category II building

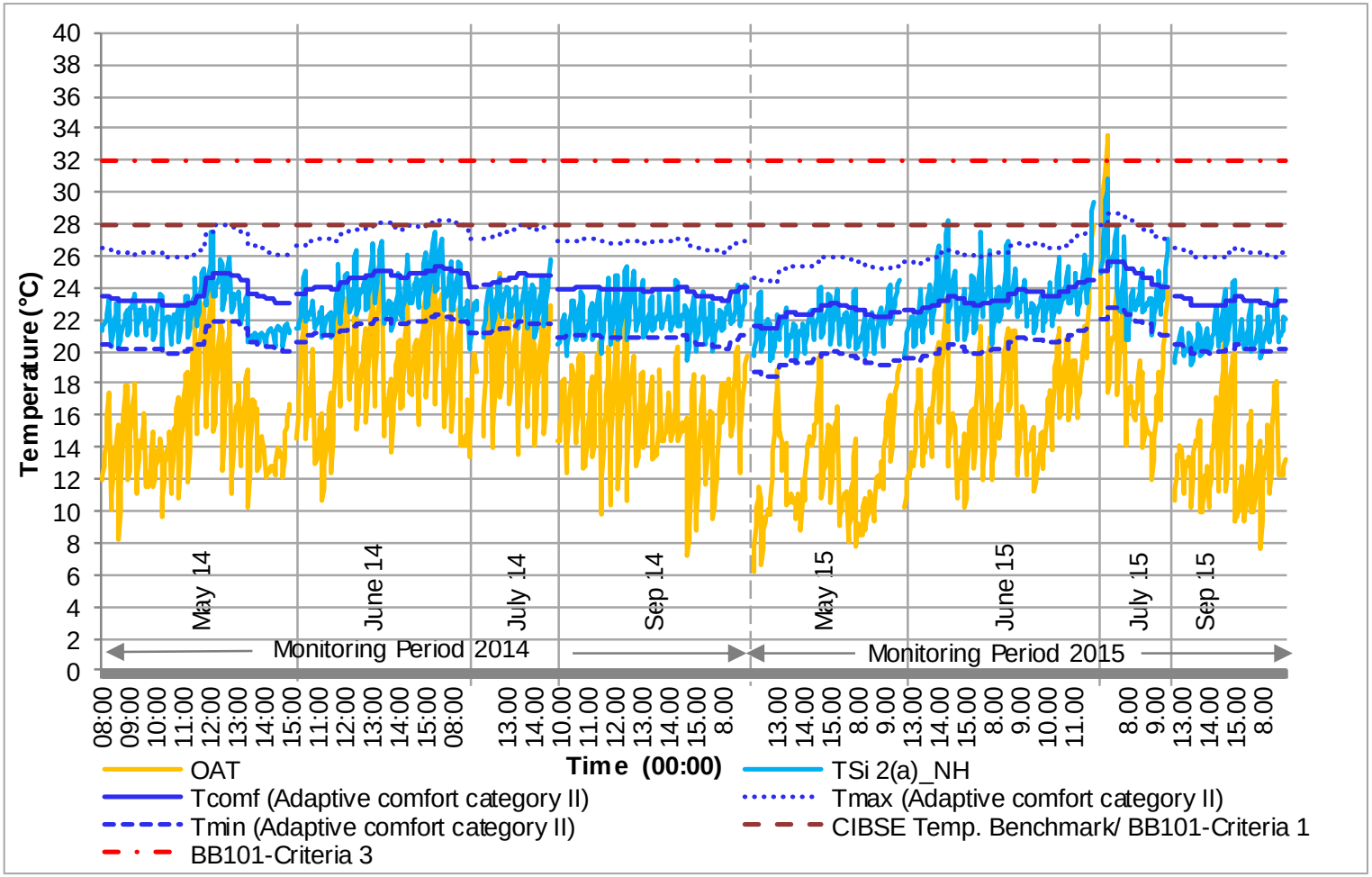


Figure 6-29: Air temperature of level 2 (first floor) of Nottingham High School atrium, CIBSE temperature benchmark, maximum and minimum acceptable temperature range for category II building

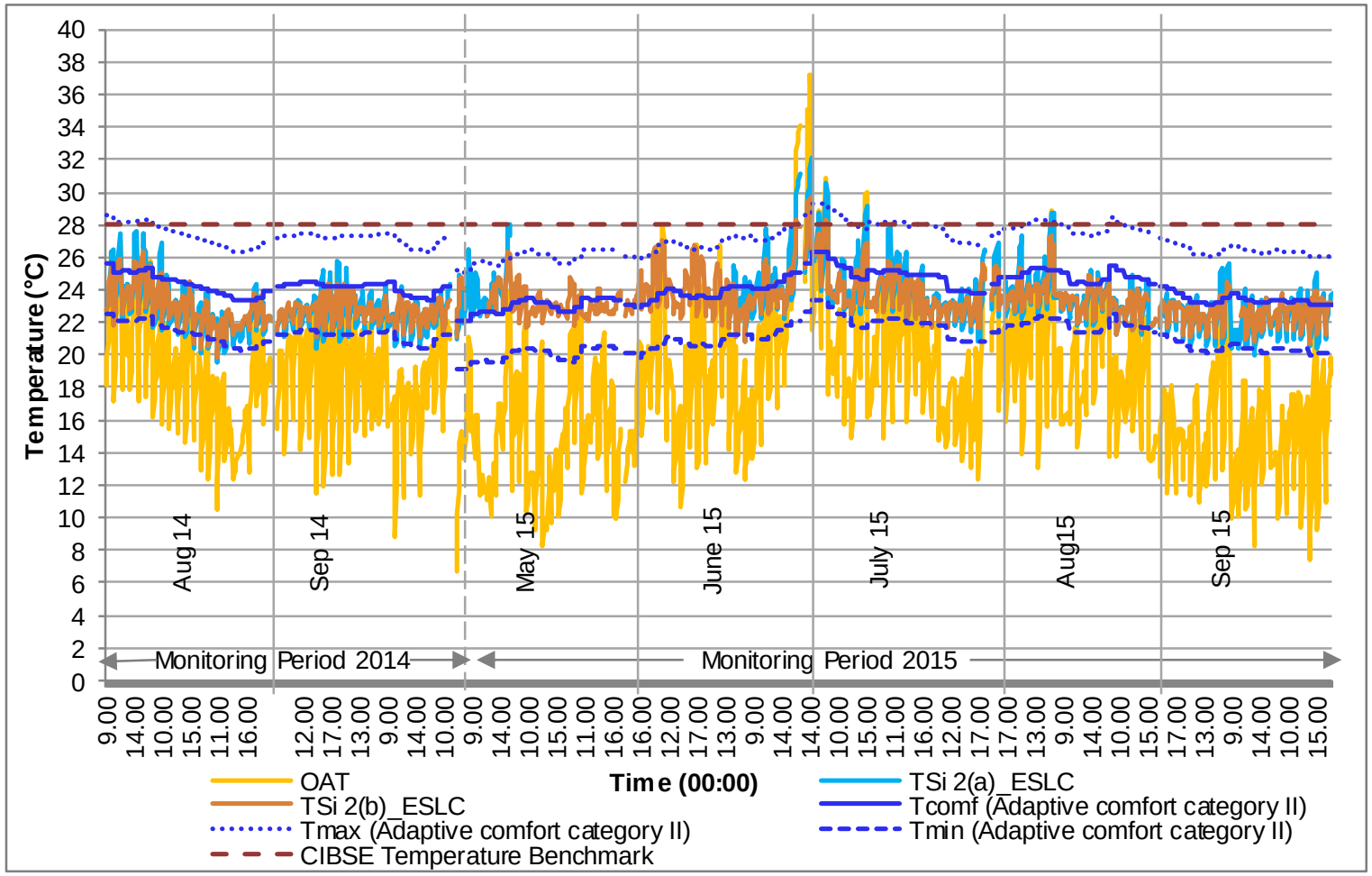


Figure 6-30: Air temperature of occupied level 2 (first floor) of ESLC atrium, CIBSE temperature benchmark, maximum and minimum acceptable temperature range for category II building

Table 6-6: TM52 Overheating assessment of the Nottingham High School and the ESLC atria

Summer	**Nottingham High School**	**level 1**	**level 2**	**level 3**
2014	Criteria 1: Hours of exceedance	0	0	1.83% (10hr)
	Criteria 2: Daily weighted exceedance	√	√	√
	Criteria 3: Upper limit temperature	√	√	√
Status in summer 2014		Pass	Pass	Pass
2015	Criteria 1: Hours of exceedance	0.625% (3hr)	2.29% (11hr)	10.63% (51hr)
	Criteria 2: Daily weighted exceedance	√	We = 7 (max)	We = 13 (max)
	Criteria 3: Upper limit temperature	√	√	1.67%(8hr)
Status in summer 2015		Pass	Fail	Fail
Summer	**Engineering and Science Learning Centre**	**level 1 Location a**	**level 2 Location a**	**level 3 Location a**
2014	Criteria 1: Hours of exceedance	0	0	1.29% (5hr)
	Criteria 2: Daily weighted exceedance	√	√	√
	Criteria 3: Upper limit temperature	√	√	√
Status in summer 2014		Pass	Pass	Pass
2015	Criteria 1: Hours of exceedance	0	3.38% (25hr)	7.59% (56hr)
	Criteria 2: Daily weighted exceedance	√	We = 12 (max)	We = 36 (max)
	Criteria 3: Upper limit temperature	√	√	0.94% (7hr)
Status in summer 2015		Pass	Fail	Fail
Summer	Engineering and Science Learning Centre	**Location b**	**Location b**	**Location b**
2014	Criteria 1: Hours of exceedance	√	√	4.9% (19hr)
	Criteria 2: Daily weighted exceedance	√	√	7
	Criteria 3: Upper limit temperature	√	√	√
Status in summer 2014		Pass	Pass	Fail
2015	Criteria 1: Hours of exceedance	√	2.03% (15hr)	9.75% (72hr)
	Criteria 2: Daily weighted exceedance	√	√	We = 42 (max)
	Criteria 3: Upper limit temperature	√	√	1.49% (11hr)
Status in summer 2015		Pass	Pass	Fail

6.4.3 Building Bulletin 101

Thermal performance of Nottingham High School atrium was also assessed using the overheating assessment criteria of Building Bulletin 101. The results presented in Table 6-7 indicated that level 3 of the atrium also failed to comply with the requirement in summer 2015.

Table 6-7: BB101 Overheating assessment of the Nottingham High School atrium

Criteria	2014			2015		
	level 1	level 2	level 3	level 1	level 2	level 3
Number of hours > 28°C	0	0	8	3 hr	7 hr	31 hr
TD_OAT greater than 5°C	281hr	354hr	427hr	338 hr	391 hr	445 hr
Number of hours > 32°C	0	0	0	0	0	1
Status	Pass	Pass	Pass	Pass	Pass	fail

The results presented in Figure 6-27 (also Figure 6-28, Figure 6-29 and Figure 6-30) also included CIBSE temperature benchmark (28°C) and maximum temperature limit (32°C) according to BB101 and CIBSE TM52. It can be observed from Figure 6-27 that in summer 2014 maximum acceptable temperature was closer to the CIBSE temperature benchmark. However particularly in July 2015, this maximum limit of acceptable temperature even exceeded temperature benchmark (28°C). This was the result of extreme hot outdoor temperature, that even exceeded the maximum temperature limit (32°C) pushing the acceptable temperature higher than the CIBSE temperature benchmark. Thus, it is important to identify the occurrence of this type of extreme outdoor condition in future that will impact thermal performance by creating overheating problem in the spaces such as atria enclosed with ETFE-foil cushion roofs. In this study, this was done by applying the United Climate Impacts Program (UKCIP) projected scenario on the predictive models of both of the case study buildings. This is discussed in Chapter 7.

6.5 Comparison of the thermal behaviour of space enclosed with ETFE-foil cushion roof and fabric membrane roof

Table 6-8 presents a comparison of the the results of research on the thermal behaviour of spaces enclosed with different single and double layer membrane roofs and observed thermal behaviour of spaces enclosed with ETFE-foil cushion roofs. From the results presented in Table 6-8, it can be identified that thermal behaviour of spaces enclosed with two and three layer ETFE-foil cushion roofs doesn't vary

significantly from that of spaces enclosed with different types of double layer fabric membrane roof. However, temperature stratification was found to be higher in the spaces enclosed with a single layer membrane roof compared to the spaces enclosed with double- and three-layer ETFE-foil cushion and, fabric membrane roofs.

Table 6-8: Summary of results obtained for research on thermal behaviour of space enclosed with membrane envelope

Study	Space type, Location, Weather	HVAC system	Method	Envelope type	Surface temperature	Temperature difference between air closed to membrane and outdoor air	Temperature difference between air closed to membrane and near to the floor
Wu et al. (1984)	Stadium moderately cold climate	Air conditioned (seating area of a stadium only)	On-site monitoring	air-supported roof, composed of single and double layer membrane		3°C above outdoor temperature	warm summer day 9°C (without AC) 11°C (with AC operating in the seating area)
Croome and Moseley (1984a)	Air house, The University of Bath	Inflation fans	Same as above	air-supported structure with PVC-coated polyamide skin	40°C	8°C above outdoor temperature during day, 1°C below outdoor air temperature at night	4°C
Harvie (1996)	Factory, Chepstow, UK	Air conditioning system, destratification fans, natural ventilation through the apex of the roof	Same as above	Double membrane composed of PVC coated polyester membrane and permeable proban treated cotton calico	31°C		8°C (free running period)
Harvie (1996)	Arena, Llangollen, Clwyd.	Apex extract fans, low level natural ventilation is provided by small openings	Same as above	Single layer, PVC coated polyester	33°C (maximum 40°C)	12.5°C (maximum) above outdoor temperature during day	10°C (positive stratification during the day) 1.1°C (negative stratification during the night)

(Table 6-8 continued)

Harvie (1996)	Lawn Tennis and Croquet Club Wimbledon, London.	Louvres provide natural ventilation, ventilators to extract air from occupied space, infra-red heaters	Same as above	PVC coated polyester membrane	45°C (maximum 50°C)		5.6°C (positive stratification during the day)
Devulder (2004)	New Inland Revenue Amenity Building (IRAB), Nottingham, UK	Electric radiant heaters	Same as above	Single skin PTFE/glass		15°C (maximum) above outdoor temperature during day	6°C to 12°C (positive stratification during the day) 3°C (negative stratification during the day)
This research - Case study	Nottingham High School atrium, Nottingham	Heating system consisted of ran coil units, fan convectors, under floor heating system, mechanical ventilation, natural ventilation operates automatically through windows at high level.	Same as above	Two–layer ETFE-foil cushions with fritted top layer and clear bottom layer both of 200µm and covered with a rain noise suppression mesh	External layer – 30.5 (average), 46.4°C (maximum) Internal layer –32.8°C (average), 50.3°C (maximum)	5.88°C (average) and 8.1°C (maximum) above outdoor temperature during day [Measured adjacent to ETFE-foil cushion roof]	4.89°C (average) and 11.7°C (maximum), [positive stratification during the day] [Measured adjacent to ETFE-foil cushion roof]
This research - Case study	Engineering and Science Learning Centre Atrium, Nottingham	Primary heating system in the atrium consists of ground source heat pump, district heating, under floor heating system, glazed motorised louvres and windows at high level	Same as above	Fritted top layer (200µm), transparent middle (150µm) and bottom layer (150µ m)		3°C (average), 6.27°C (maximum) [Measured at 4.75 meter (approx.) below ETFE-foil cushion roof]	5.19 (average) 11.63 (maximum) [Measured at 4.75 meter (approx.) below ETFE-foil cushion roof]

6.6 Summary

6.6.1 Summary of thermal behaviour of space enclosed with ETFE-foil cushion roof

- The thermal environment under clear sky condition is particularly influenced by –
    - large swings in cushion surface temperatures
    - radiant heat from the sun and hot ETFE-foil cushion surface that increases mean radiant temperature
    - high outdoor temperature
    - longwave radiation losses (at night)
- These above phenomena result in strong positive stratification during the day and weak at night.
- During overcast sky conditions and in the absence of solar radiation (at night) steady conditions exist in the ETFE cushion surface. Consequently, the indoor thermal environment was stable with relatively uniform temperature distribution. This also confirmed the operation of the HVAC system and its impact on indoor air temperature.
- The surface temperature of the ETFE-foil cushion affects thermal comfort of the atria by increasing (or decreasing) mean radiant temperature and creating temperature stratification during the day and night
- During day time the extent of stratification was more significant in the ESLC atrium (enclosed with three-layer cushion) than in the Nottingham High School atrium (enclosed with two-layer cushion). However, at night air temperature of ESLC atrium was on average 2°C lower than in the Nottingham High School atrium. Possible reasons for this variation could be:
    - the rain noise suppression mesh and fritting (75% fritting) of the top ETFE-foil layer, reducing surface temperature and solar gain by creating higher shading in the Nottingham High School atrium,
    - higher level of thermal insulation provided by the 3-layer cushion roof of ESLC atrium.
- On an extremely hot day (1st July 2015) atrium level 3 air temperature coincided with outdoor air temperature, indicating that a similar thermal environment exists indoors and outdoors, particularly between 12.00pm and 8.00pm. This was apparent at level 3 of both atria.

- On hot days in summer the effect of the HVAC system, window operation etc. on indoor air temperature was found to be poor in relation to the effect of heat gain from solar radiation and high outdoor temperature.
- Outdoor temperature, as well as transmitted solar radiation, had a strong positive relationship with indoor air temperature of occupied levels and level adjacent to ETFE-foil cushion roof while the surface temperature of the ETFE-foil cushion was strongly related with adjacent mean radiant temperature (Correlation coefficient R^2 value ranged from 0.952 to 0.984).
- Air temperature of the atrium had an impact on the air temperature of adjacent spaces (main school building). This was the result of air circulation between those spaces (e.g. interview room, corridor etc.) and the atrium through window openings.
- Operable window area (2.3% of floor area) in the atrium was found to be inconsistent with the area recommended in Building Bulletin 101 (UKGOV, 2014) (recommended operable window area is 5% of floor area).
- In both of the atria poor ventilation system, insufficient window area might have result in longer delay to eliminate heat from indoor spaces.

6.6.2 Summary of thermal performance of space enclosed with ETFE-foil cushion roof

Thermal performance of the Nottingham High School and ESLC atria during summer 2014 and 2015 was assessed based on overheating performance. The result of this assessment showed that in summer 2015, level 3 of both of the atria failed to fully comply with the requirements stated in CIBSE temperature benchmark, CIBSE TM52, and BB101.

Thus, both of the atria (level 3 and 2) overheated during summer 2015. Particularly this was reflected when additional air conditioning systems were installed to avoid heat stress in level 3 of the Nottingham High School atrium (Figure 6-31). However according to school management, these air-conditioning systems were not operating until the end of September 2015, thus its impact on the thermal condition of the atrium was not reflected in the results presented in this study.



(a) In summer 2014 (b) In summer 2015 (August)

Figure 6-31: Atrium level 3 without (before) and wih (after) air conditioning system

Findings from this chapter imply the necessity of further investigation of the atrium spaces covered with ETFE-foil cushion roofs to evaluate overheating mitigation scenarios. Considering this agenda, the purpose of the next chapter is to conduct detailed thermal modelling and simulation. The purpose is to predict the thermal performance of both of the atria enclosed with ETFE-foil cushion roof. Based on the validity of the result, these models will be used to improve the existing thermal environment that was recorded and analysed in this section. Also predicted models of both of the buildings were used to analyse overheating performance using UKCIP projected scenarios to investigate the impact of frequency of overheating in the existing buildings in future climate.

6.6.3 Challenges

- Direct access to the case study buildings to collect data for long period.
- School environment is relatively sensitive, thus safety procedures were followed to install monitoring equipment and also during data collection.
- Within budget constraints, equipment to monitor these buildings were carefully selected.
- To find location to install sensors/ data loggers so that recorded parameters would represent the thermal environment of the atrium.
- Work at height to install equipment close to the ETFE-foil cushion roof.
- Careful measures were followed while sensors were attached to the ETFE-foil cushion surface to avoid damage.

6.6.4 Limitations

- Study considered spaces enclosed with multi-layer ETFE-foil cushion systems.
- Selection of space to install equipment was restricted due to safety issues.
- Access to building occupancy schedule was not available, in this study this was based on personal observation and communication with Estate (both Nottingham High School and ESLC).
- Data logger unauthorised removal from site was a common issue.

Chapter 7

7 Modelling thermal performance of ETFE foils and spaces enclosed with ETFE foil cushion roofs

7.1 Introduction

This chapter presents a simulation-based analysis to evaluate and compare the thermal performance of spaces enclosed with ETFE-foil cushion and glass roofs with a view to identifying the specific influence of these materials may induce. TAS version 3.2.2 was used to simulate the building which includes the atrium roofed with ETFE-foil cushion. A simulation approach was used to improve existing thermal conditions of the spaces by altering thermal optical properties of the ETFE-foil cushion roof. The thermal performance was assessed using the criteria mentioned in CIBSE guides (Guide A and TM52). The thermal performance of the spaces enclosed with ETFE-foil cushion roof was also assessed in current and future climatic scenarios.

This chapter depicts the simulation procedure and necessary modifications and considerations to validate simulated results with measured data. Because most of the dynamic simulation tools (e.g. TAS, IES) do not have any template that includes properties of ETFE foil, material templates of different types of ETFE foils were created based on measured properties. The methods used to measure and calculate the properties of ETFE-foil were already discussed in Chapter 4. At this stage, the simulation results were validated against measured data collected from a test-rig experiment. Environmental data were collected from the test-rig for a selected period. Details of data collection process and results were discussed in Chapter 5. A simulation model was created to replicate the test-rig, and results were compared with the measured data to calibrate and validate the simulation models.

The simulation study further considered different types of roof configuration to represent an original curvilinear form of ETFE-foil roof. While modelling the curvilinear roof consisted of ETFE-foil cushions, a traditional approach using flat surface was found not appropriate, hence a customised approach was identified and applied in this study.

Finally, simulation models of two different buildings were created, they were: Nottingham High School, and Engineering and Science Learning Centre. Results from the simulation were compared with monitored data from these two buildings as well to

calibrate and validate the models. Details of on-site data collection and results were discussed in Chapter 6. The simulation process considered climatic scenarios using current and future weather data and performed overheating analysis.

Findings of this chapter address the Objective 5, which is to evaluate and compare the thermal performance of space enclosed with ETFE foil cushion and glass roof and build up the knowledge to achieve Objective 6 of the original aim.

7.2 Calibration of the simulation model

Simulation is useful for designers to determine the performance of buildings on the basis of various information (e.g. building operation, material properties etc). The results obtained from simulation create the basis for evaluation of building design. However, simulation result accuracy depends on knowledge of real scenarios. A performance gap was evident between measured and simulation output (Kim and Park, 2016, Reddy, 2007, Clarke et al., 1993). Nevertheless, to have accurate results and match this closely with real data, calibration has become an essential procedure to be carried out for building simulation. The calibration procedure is influenced by the details of initial models (Kim and Park, 2016). Therefore, without accurate data from a real building, there may be high levels of uncertainty (Tamburrini et al., 2003, Clarke et al., 1993). Therefore, it is necessary to carry out sensitivity analysis of input parameters. Lomas and Eppel. (1992), described the importance of sensitivity analysis and compared different approaches. They emphasised that sensitivity analysis may require a set of parametric simulations to identify the influence of various parameter changes as well as error analysis to estimate the biased result of various parameters. But these methods require high technical knowledge and extensive computing power. In a different study, a sensitivity analysis was done by Westphal and Lamberts (2005), where they calibrated simulated output by modifying different parameters of a base model. In the simulation, they modified one parameter at a time. Although this method of sensitivity analysis did not consider the influence of multiple parameters, it requires less computing knowledge and does not require a large number of parametric simulations. However, clear knowledge of input parameters can eliminate this error. A similar approach was adopted by Paliouras. P. et al. (2015), in their study. This method was used for calibration of simulation in this study also.

Pellegrino et al. (2016), Macdonald and Strachan (2001), Hopfe and Hensen (2011), compared measured and simulated air temperatures to validate their study. They calibrated the simulation models by adjusting materials' thermal transmittance (U-value), occupancy profile and ventilation. An earlier study by Lomas et al. (1997)

adopted a similar approach. In their study, they described Phase 1 as a blind phase whereas Phase 2 was described as an open phase where the model was modified and tested against measured data.

7.3 Weather file

At the beginning of the simulation, Design Summer Year (DSY) weather data for Nottingham was selected. But the measured and simulated results were not in good agreement. This might be because the DSY weather data was made of hourly collected data during the year 2005. However, it was necessary to select accurate weather data from different available sources, which would represent the actual outdoor condition of the simulated buildings. Because weather data selected for simulation has a large influence on simulation results (CIBSE, 2006, CIBSE, 2015b), it was decided to measure various external weather parameter with available equipment and the remaining values were either collected from recognised local weather stations or calculated based on established methods.

Table 7-1: Weather file parameters used in simulation

Parameters	**For simulation model of Nottingham High School**	**For simulation model of Engineering and Science Learning Centre (ESLC)**	**For simulation model of Test rig**
Outdoor temperature	Obtained from weather station, located at Nottingham High School	Measured using Tiny Tag Plus 2- TGP-4017 data logger	Same as ESLC
Humidity	Obtained from weather station, located at Nottingham High School	Same as above	
Global Solar radiation	Measured using Kipp & Zonen CMP3 pyranometer	Measured using Kipp & Zonen CMP3 pyranometer	
Diffuse radiation	Calculated following Szokolay (2008)	Calculated following Szokolay (2008)	
Cloud cover	Same as above	Same as above	
Wind velocity	Obtained from weather station, located at Nottingham High School	Obtained from EoN house weather station, university of Nottingham	
Wind direction	Obtained from weather station, located at Nottingham High School	Obtained from EoN house weather station, university of Nottingham	

TAS weather file format (*.epw) is a simple text-based generalised format. Values of this format can be changed easily to create or customise a weather file. Data collected from different sources to create the weather file are listed in Table 7-1.

7.4 Properties of ETFE foil panels and glazing panels used in simulation

The study developed material templates of transparent and fritted ETFE-foils in the TAS material library. The solar and light transmittance of ETFE-foils measured in the laboratory and calculated using appropriate British Standards was used. The detailed procedure of determination of thermal optical properties of ETFE-foils was presented in Chapter 4.

To predict thermal performance, glazing panels typically used as overhead glazing were used and listed in Table 7-2. Properties of glass panels were obtained from NCM material library (EDLS TAS Version 9.3.3.b) and used in the simulation models. Properties of ETFE-foils and glazing panels used in the simulation models are presented in Table 7-8,

Table **7-9** and Table 7-10.

Table 7-2: Glazing types used in the Predicted model (EDLS TAS Version 9.3.3.b)

Identification	Number of panes	Description
Glazing type 1	double	Roof-light- notional building Coated polycarbonate Air gap 20mm Coated polycarbonate
Glazing type 2	double	Roof-light- notional building Coated polycarbonate Air gap 6mm Coated polycarbonate
Glazing type 3	double	6mm glass (low-e) Air gap 20mm 6mm float clear (inner)
Glazing type 4	single	6mm clear float glass
Glazing type 5	single	6mm glass (Low-E coated)
Glazing type 6	single	8mm glass (Low-E coated)
Glazing type 7	single	Roof light panel glazing (coated polycarbonate -55)

7.5 Simulation of test rig

The objectives of the simulation approach were the following:

- To predict thermal performance of single, two- and three-layer ETFE-foil panels

- To assess and compare this thermal performance with that of polycarbonate and glass panels

7.5.1 Calibration

The dynamic simulation requires a range of input parameters to assign to model actual scenarios. These parameters include detailed construction properties of materials, environmental control features (e.g. doors, windows), occupancy profile, building services, etc. Gathering all this information in detail from actual buildings may be difficult or in some cases not possible. Therefore, it is important to make approximations and assumptions.

At first, simulation models were created in EDLS TAS (Version 9.3.3.b) to replicate test-rigs used in the ETFE-foil panel testing. This gave the opportunity to compare simulation results with the data collected. As these test-rigs were less complex compared to actual buildings, assumptions also included a lower number of parameters as described below. Construction materials for the simulation model of test-rig are listed in Table 7-3. Table 7-4 and Table 7-5 respectively present thermal properties of the ETFE panels and input parameters used in the simulation models.

Table 7-3: Construction of simulation model

Construction	Simulation model	U-value
Wall/ floor	75mm thick Polyurethane (foil faced) insulation 18mm thick plywood	0.4 ($W/m^2°C$)
ETFE foil panel	Single layer 75% fritted ETFE-foil panel	5.85 ($W/m^2°C$)

Table 7-4: Thermal Properties of ETFE foil used in simulation model

Properties	Simulation model ETFE properties (75% fritting layer)
Emissivity (ex)	0.82
Emissivity (int)	0.6
Solar Transmittance (G-value)	0.474
Shading Coefficient	0.557

Table 7-5: Input parameters in simulation

Weather data	According to Table 7-1
Calendar	1st May to 30th September was considered as summer 1st October till 30th April considered as winter
Internal gain	
Infiltration (ach)	Variable (0.05 to 8)

Ventilation	No ventilation
Heating/ cooling	Not considered

A series of repeated simulations were performed by changing infiltration between 0.05ach and 8ach. Values were modified in each model until a reasonable agreement was achieved between predicted and measured results. All simulation results are not presented in this section; only selected simulation results closer to the measured results are presented in Figure 7-1.

Figure 7-1 shows air temperatures (TaH1_B1) recorded in the test-rig roofed with a single layer 75% fritted ETFE foil panel in tested during 26th and 27th September 2015, and air temperatures obtained from simulation using replicate models (e.g. model 1, model 2, model 3, model 4 and model 5) of a test-rig roofed with a single layer 75% fritted ETFE foil panel. The simulation results that have been selected and presented in Figure 7-1 present the thermal condition of simulation models which were closest to the measured data (TaH1_B1).

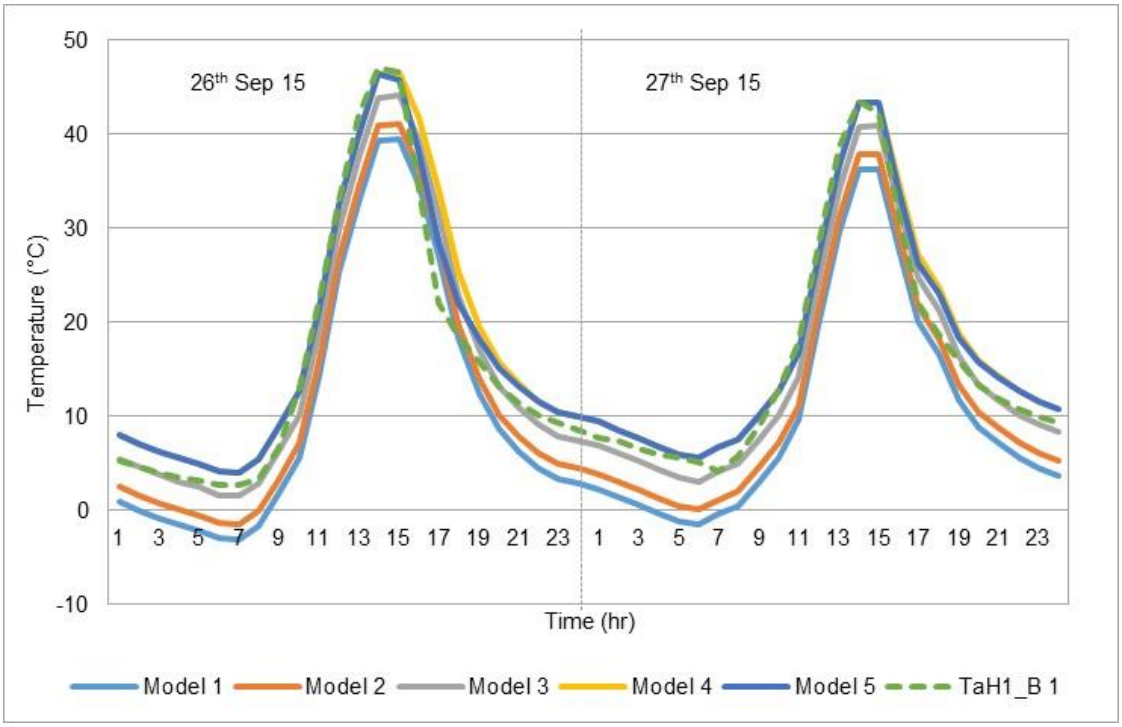


Figure 7-1: Results obtained from model calibration of single layer ETFE panel roof with 75% fritted ETFE foil panel

Table 7-6: Pearson Correlation of measured and predicted result with variable infiltration rate

Model	Infiltration (ach)	Pearson Correlation coefficient
Model 1	5.5	0.969
Model 2	5	0.97

Model 3	3.5	0.976
Model 4	3	0.979
Model 5	2.5	0.984

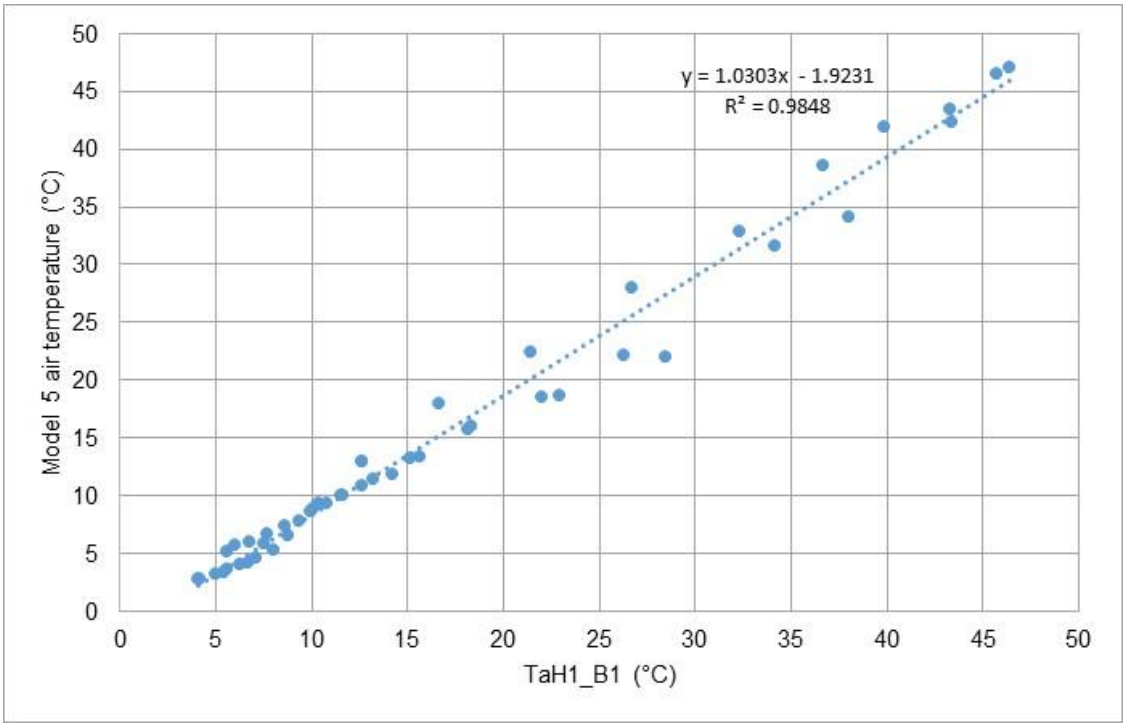


Figure 7-2: Linear relationship between predicted (model 5) and measured data

Infiltration rates used in simulation models are presented in Table 7-6. It is evident from Figure 7-1 that air temperatures of the test rig vary with variable infiltration rate. Among different simulated models, model 5 agreed well with measured results particularly around mid-day. Maximum deviation between measured and simulated air temperature recorded was 2.5°C, where the measured air temperature was less than that of the simulated temperature. However, the R^2 coefficient of determination presented in Figure 7-2 as well as Pearson correlation coefficient listed in Table 7-6 indicated that the air temperature of model 5 was closely correlated (0.984) with measured air temperature. Thus, this model 5 was used as a base case model to simulate and compare ETFE foil panels, polycarbonate and glass panels where infiltration rate was set to 2.5ach.

The following sections describe the method, assumptions and results obtained from the simulated test-rig roofed with single-, two- and three-layer ETFE foil panels, polycarbonate and glass panels.

I. Scope and Method

A series of simulations were performed to predict the thermal performance of models enclosed with ETFE-foil panels, polycarbonate and glass panels. The results obtained

from these simulations were validated by comparison with measured data. In the simulation, no internal gain was considered except the infiltration rate. Space conditioning using heating and cooling was not included. Thus, the simulation results demonstrated the influence of outdoor weather conditions on thermal condition of the simulation model.

II. Input parameters in simulation

In the dynamic simulation, it is required to input parameters for analysis model. Input parameters used in the simulation models are presented in Table 7-7.

Table 7-7: Input parameters in simulation

Weather data	According to Table 7-1
Calendar	1st May to 30th September was considered as summer 1st October till 30th April considered as winter
Internal gain	
Infiltration (ach)	Variable (2.5)
Ventilation	No ventilation
Heating/ cooling	Not considered
Construction	
Wall/ floor	75mm thick Polyurethane (foil faced) insulation 18mm thick plywood U-value- 0.4 ($W/m^2°C$)
ETFE foil, polycarbonate and glass	Table 7-8, Table 7-9, Table 7-10

Table 7-8: Properties of ETFE-foil panels (single layer) and glazed panels

Description	**ETFE properties (75% fritting)**	**ETFE properties (25% fritted)**	**Glazing type 4**	**Glazing type 5**	**Glazing type 6**	**Glazing type 7**
Emissivity (ex)	0.82	0.82	0.84	0.84	0.84	0.05
Emissivity (int)	0.60	0.75	0.84	0.10	0.10	0.72
Solar Transmittance (G-value)	0.474	0.72	0.816	0.651	0.62	0.344
Thermal Transmittance (U-value W/m2° C)	5.857	5.857	5.682	5.682	5.556	5.759
Shading Coefficient	0.557	0.827	0.938	0.748	0.713	0.396

Table 7-9: Properties of ETFE-foil (two-layer) panels and glazed panels

Description	ETFE		Glazing type 1	Glazing type 2	Glazing type 3	Glazing type 5	Glazing type 6	Glazing type 7
	Layer 1	Layer 2						
Solar Transmittance (G-value)	0.474	0.863	0.203	0.202	0.566	0.651	0.62	0.344
	0.436							
Thermal Transmittance (U-value W/m2°C)	5.857	5.857	1.42	2.469	1.555	5.682	5.556	5.759
Shading Co-efficient	0.827	0.991	0.233	0.232	0.651	0.748	0.713	0.396

Table 7-10: Properties of ETFE foil panels (three-layer)

Description	ETFE (75% fritted top layer)			ETFE (25% fritted top layer)		
	Layer 1	Layer 2	Layer 3	Layer 1	Layer 2	Layer 3
Solar Transmittance (G-value)	0.474	0.91	0.863	0.72	0.91	0.863
	0.42			0.6		
Thermal Transmittance (U-value W/m2°C)	5.857	5.87	5.857	5.857	5.87	5.857
Shading co-efficient	0.827	1.037	0.991	0.827	1.037	0.991
Description	**Glass type 1**	**Glass type 2**	**Glass type 3**	**Glass type 5**	**Glass type 6**	**Glass type 7**
Solar Transmittance (G-value)	0.203	0.202	0.566	0.651	0.62	0.344
Thermal Transmittance (U-value W/m2°C)	1.42	2.469	1.555	5.682	5.556	5.759
Shading co-efficient	0.233	0.232	0.651	0.748	0.713	0.396

7.5.2 Simulation results

Internal air temperature of the simulation model covered with 25% fritted and 75% fritted single layer ETFE-foil panels, respectively, was less than the average air temperature of the same model when enclosed with single glazing (**Glazing** type 4, **Glazing** type 5, **Glazing** type 6, **Glazing** type 7). However, relative internal air temperatures of the model with double glazing panels and two-layer and three-layer ETFE-foil panels varied depending on glazing type. Figure 7-3 and Figure 7-4 present

relative air temperatures of the model enclosed with various glazed roofs and two-layer (75% fritted top layer) and three-layer (75% fritted and 25% fritted top layer) ETFE-foil panels.

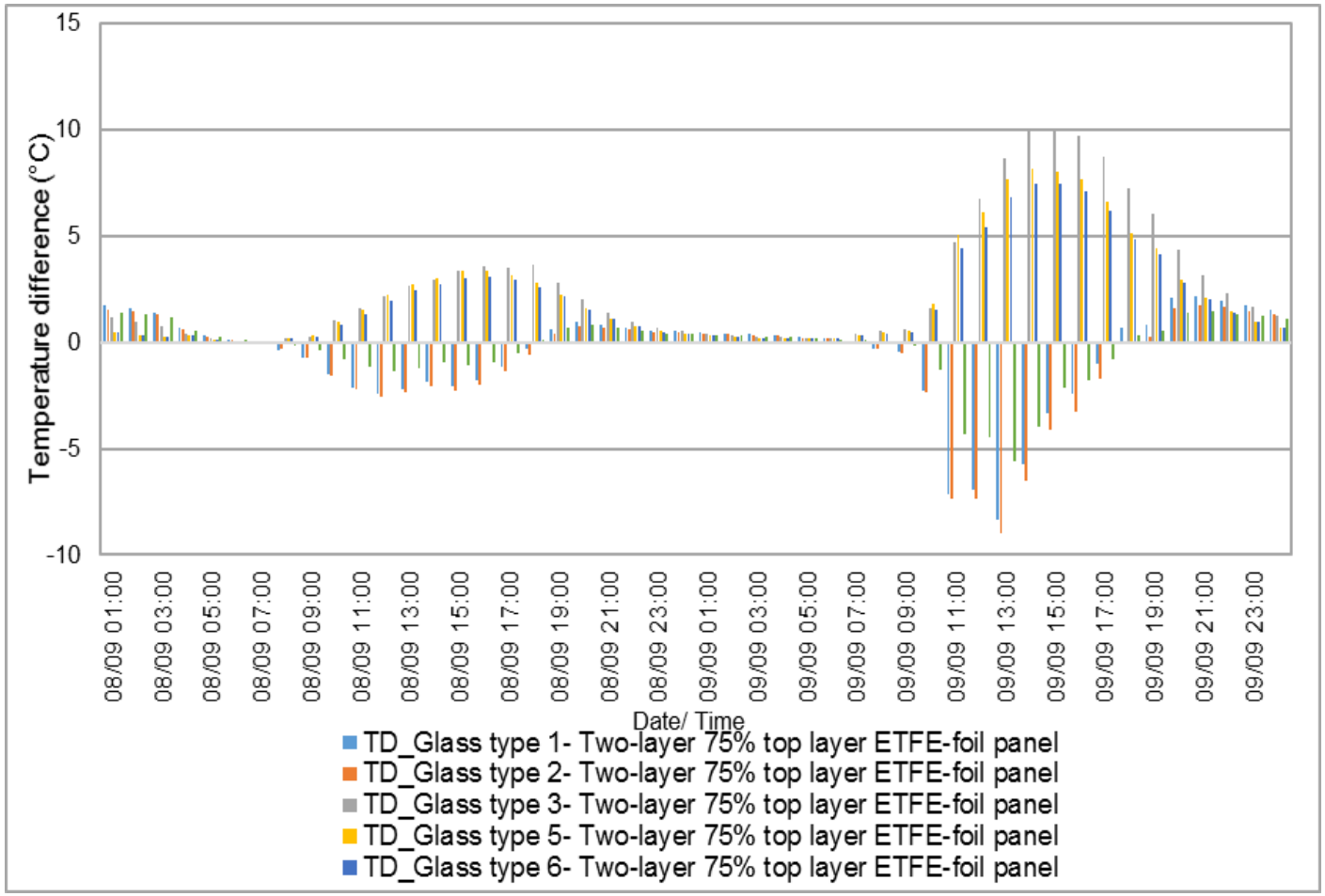


Figure 7-3: Temperature differences between simulation model enclosed with glass roof and two-layer ETFE foil panel with 75% fritted top layer

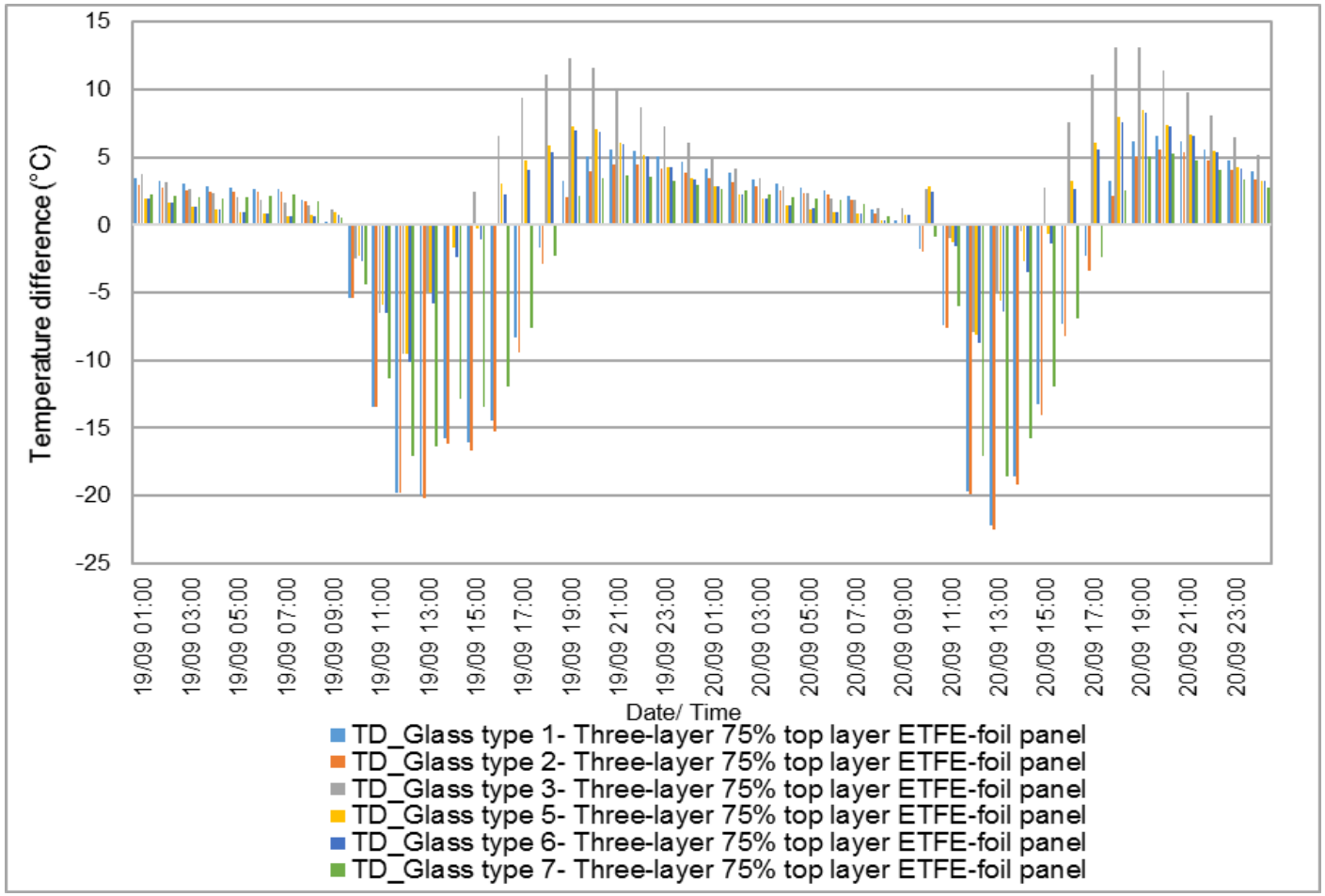


Figure 7-4: Temperature differences between simulation model enclosed with glass roof and three-layer ETFE foil panel with 75% fritted top layer

The results demonstrated that at particular times of the day (between 11.00 am and 3.00pm), internal air temperatures of the model enclosed with two-layer and three-layer ETFE-foil panels were hotter than the models when enclosed with polycarbonate glazing roofs, this variation was significant between models enclosed with ETFE-foil panels and Glazing type 1, 2 and 7. The maximum difference found between average internal air temperature of Glazing type 2 and three-layer ETFE-foil panel (with 25% fritted top layer) was 3.78°C. It was also apparent that average air temperatures of models enclosed with Glazing type 3, 5 and 6 were hotter than models when enclosed with two-layer, also three-layer ETFE-foil panels. The maximum difference found between average internal air temperature of two layer ETFE-foil and Glazing type 3 was 3.71°C. The reason behind these variations in air temperature was the high solar transmittance of double glazing unit (0.566) compared to ETFE-foil panels (75% fritted two-layer panel solar transmittance was 0.42), while low thermal transmittance (1.55 W/m^2K) of glazing panels and low-E coating reduced heat exchange between the interior and exterior, thus the increased air temperature of the simulation model. Between the ETFE-foil panels and glazing panel constructed with polycarbonate, solar transmittance of polycarbonate (0.203) was lower than the two-layer (75% fritted top layer) and three-layer (75% and 25% fritted top layer) ETFE-foil panels. However, presence of air-volume in the ETFE-foil panels might also have an impact on this temperature difference when compared with different glazing types (Glazing type 1, 2 and 7).

7.6 Simulation model of ETFE-foil cushion roofs in TAS

A number of simplifications and assumptions were made to create the models of ETFE-foil cushion roofs using the simulation tool.

One of the limitations of dynamic simulation tools is that there is no option to draw curved shapes in the simulation model. Curved shapes are usually divided into many smaller surfaces and drawn as series of flat plane surfaces. For this reason, the curvature of the ETFE-foil cushions could not be accurately represented here in TAS model.

It can be seen from Figure 7-5 that height of the steel truss as well as the ETFE-foil cushion increase towards the middle of the roof in both of the case study buildings - Nottingham High School and Engineering Science Learning Centre. This variation was taken into account while modelling ETFE-foil cushion roof using TAS modeller.



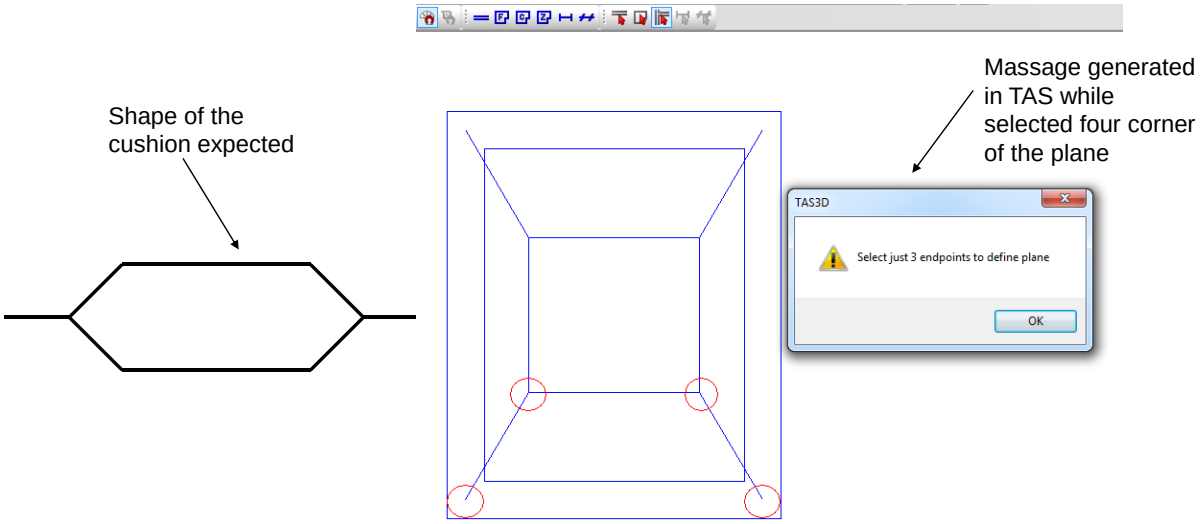
Figure 7-5: ETFE cushion roof structure (two-way curve) of Nottingham High School (top), Engineering and Science Learning Centre (Bottom)

Most of the simulation tools convert the curved shape into planes, therefore it was decided to use planar surfaces to draw the three-dimensional roof in TAS modeller. Employing planar surfaces, a number of alternative shapes were examined before the final shape was adopted for the predictive model. The following section discusses the approach adopted to model the ETFE-foil cushion roof.

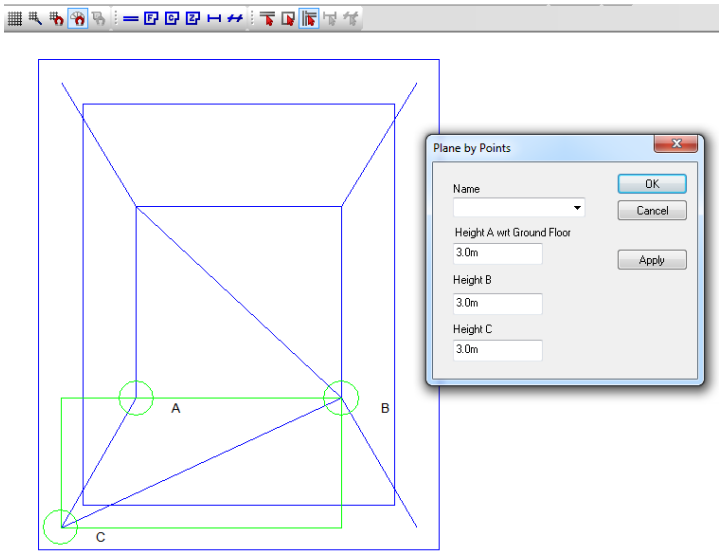
On the other hand, in simulation models incorporating ETFE-foil layers in the roof construction similar to other building fabric (e.g. construction layers of wall, floor) would generate an error. This is because an ETFE-foil cushion is a compound construction which consists of separate ETFE-foil layers and the air gap between them. And the occurrence of convective heat transfers between ETFE-foil layers and air inside the cushion was evident in onsite monitoring presented in Chapter 5 and Chapter 6, also stated in (Antretter et al., 2008). Therefore, each layer of ETFE-foil in the cushion roof was considered as an individual construction layer.

7.6.1 Approach adopted to model the ETFE cushion roof

Construction of the ETFE-foil cushion roof in TAS modeller was a difficult task. This difficulty arose particularly from the double curved surface of the ETFE-foil cushion. Therefore, it was decided to model a single cushion at the initial stage. Using planar surfaces four different shapes were examined. Figure 7-6 presents alternative models of ETFE-foil cushion roof. The difficulties that arose from each of the approaches adopted to model the ETFE-foil cushion roof, are listed in Table 7-11.

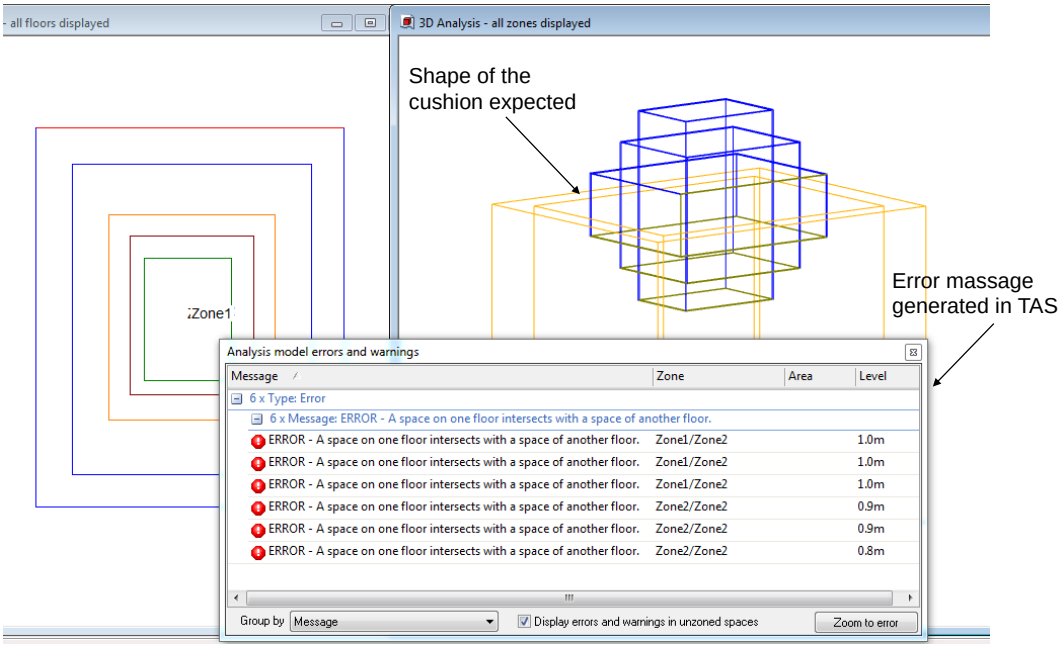


(i) Roof model 1

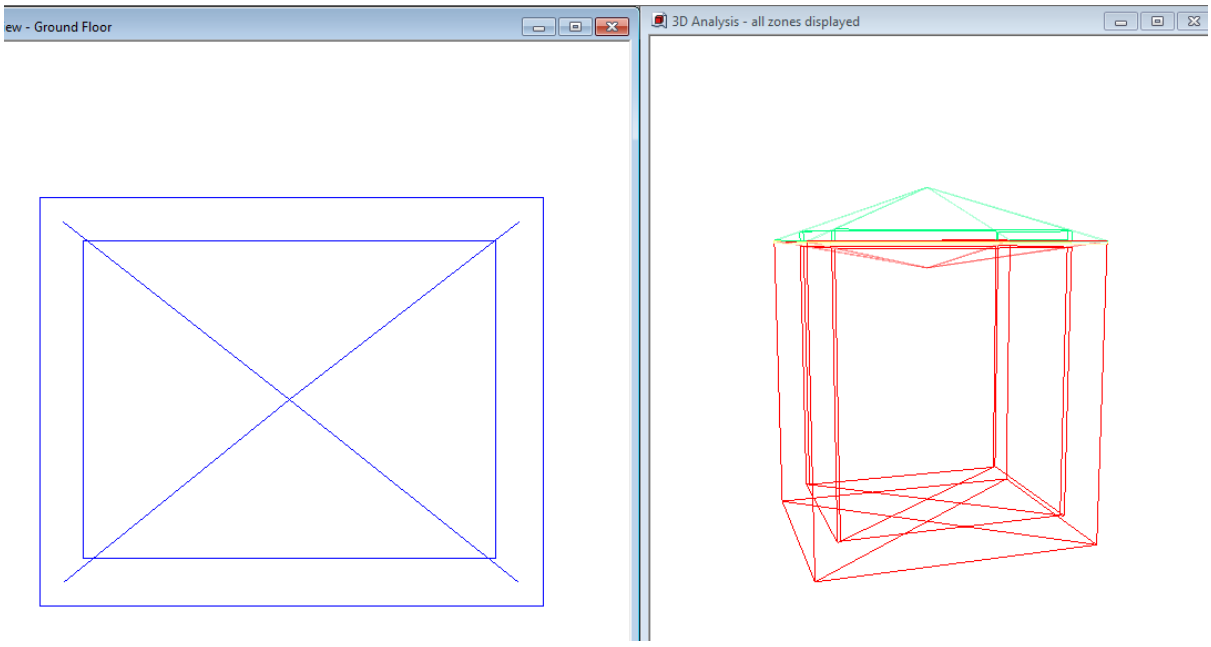


(ii) Roof model 2

Figure 7-6: (i), (ii) studied models [Figure 7-6 continued to the next page]



(iii) Roof model 3



(iv) Roof model 4

Figure 7-6: Representation of ETFE cushion roof in studied models (i) Roof model 1, (ii) Roof model 2, (iii) Roof model 3, (iv) Roof model 4

Table 7-11: Selection of model

Alternative roof model	Approach to draw planar surface	Difficulties	Further consideration
Roof model 1	Model plane required four points to create a planar surface	Three points were required to generate plane in TAS	Therefore, it was decided to divide each of the planes into two triangles
Roof model 2	Each of the planes divided into two triangular plane	This model required 20 triangular planes to generate doubly curved surface, to represent one single cushion	This procedure of modelling of ETFE roof would increase complexity in simulation as the number of planes will be significant
Roof model 3	In this model small boxes representing double curved roof created at different floor height	Box spaces intersect one another at different height caused error while generating analysis model	Too complex to model large ETFE-foil cushion roof, Simplification was necessary to build complex atrium model
Roof model 4	A rectangular surface divided into four triangular plane	No difficulties raised while generating analysis model	Using this procedure eight triangular planes were required to build two sided curved cushion

Using the configuration of Roof model 4 it was possible to approximate a double curved surface of the ETFE-foil cushion. It required 8 planar surfaces, each plane can be created using three points as required by TAS modeller.

It can be identified from Figure 7-5 that the height of the ETFE-foil cushion supporting frame varied in both of the case study buildings. Camber of the cushion near the edge and middle of the roof was also different. Using Roof model 4 it was possible to include both of these by changing the height of the planar surfaces.

7.6.2 Simulation model of Nottingham High School building and atrium ETFE-foil cushion roof

The ETFE-foil cushion roof of Nottingham High School consisted of 25 cushions. In TAS modeller each of the cushions was modelled using 8 triangular planes, therefore 200 triangular planes were used to build the double curved ETFE-foil cushion roof of Nottingham High School atrium. Figure 7-7 presents plan and section (not to scale) of the roof model of ETFE-foil cushion roof.

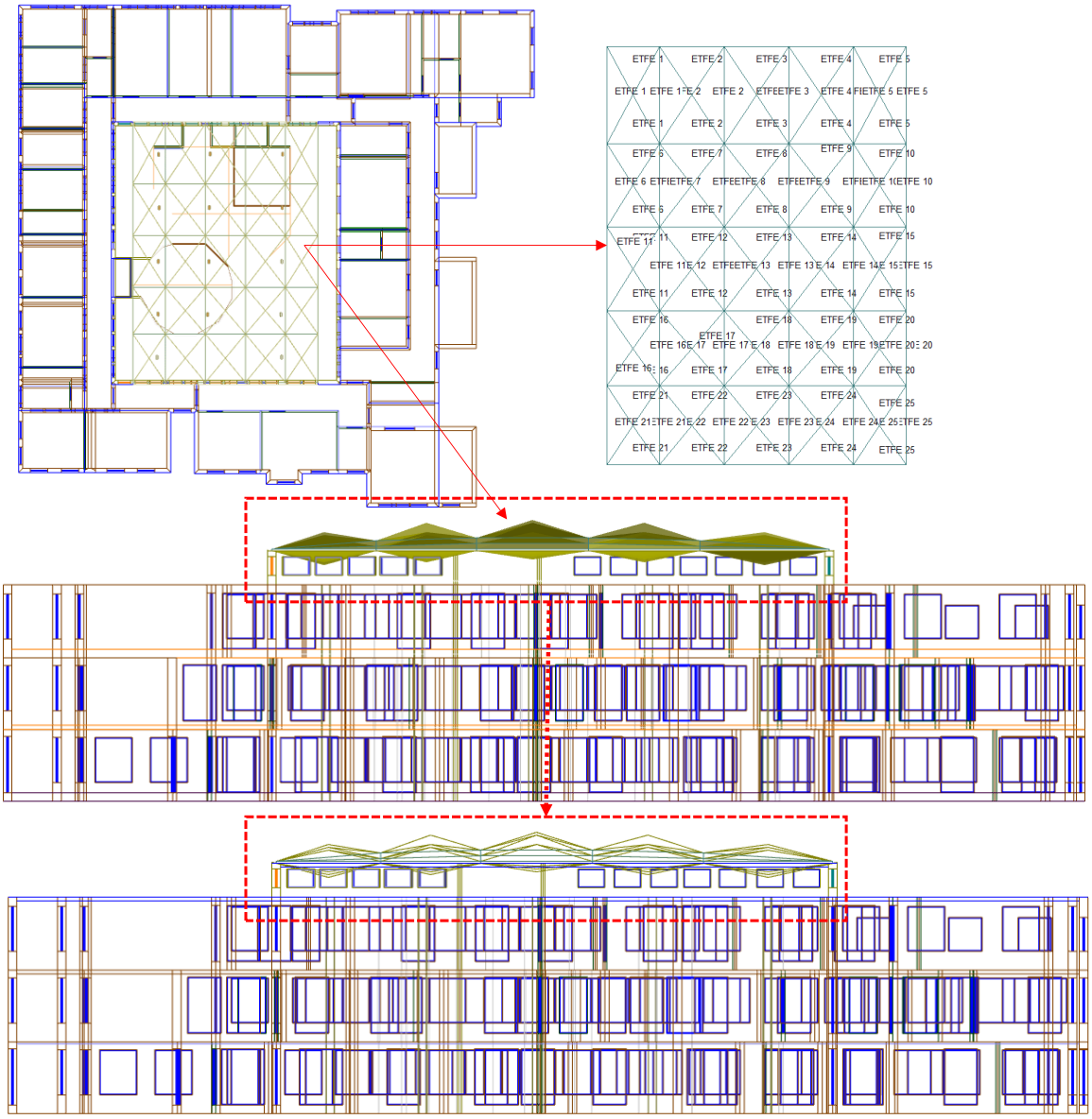


Figure 7-7: Simulation model of ETFE-foil cushion roof of Nottingham High School atrium

7.6.3 Simulation model of Engineering and Science Learning Centre and atrium ETFE-foil cushion roof

The configuration of the ETFE-foil cushion roof of the Engineering and Science Learning Centre (ESLC) is different from the ETFE-foil cushion roof of Nottingham High School. The ETFE-foil cushion roof of ESLC was built using 150 planar surfaces in total. Figure 7-8 presents plan and section (not to scale) of the ETFE-foil cushion roof of the ESLC.

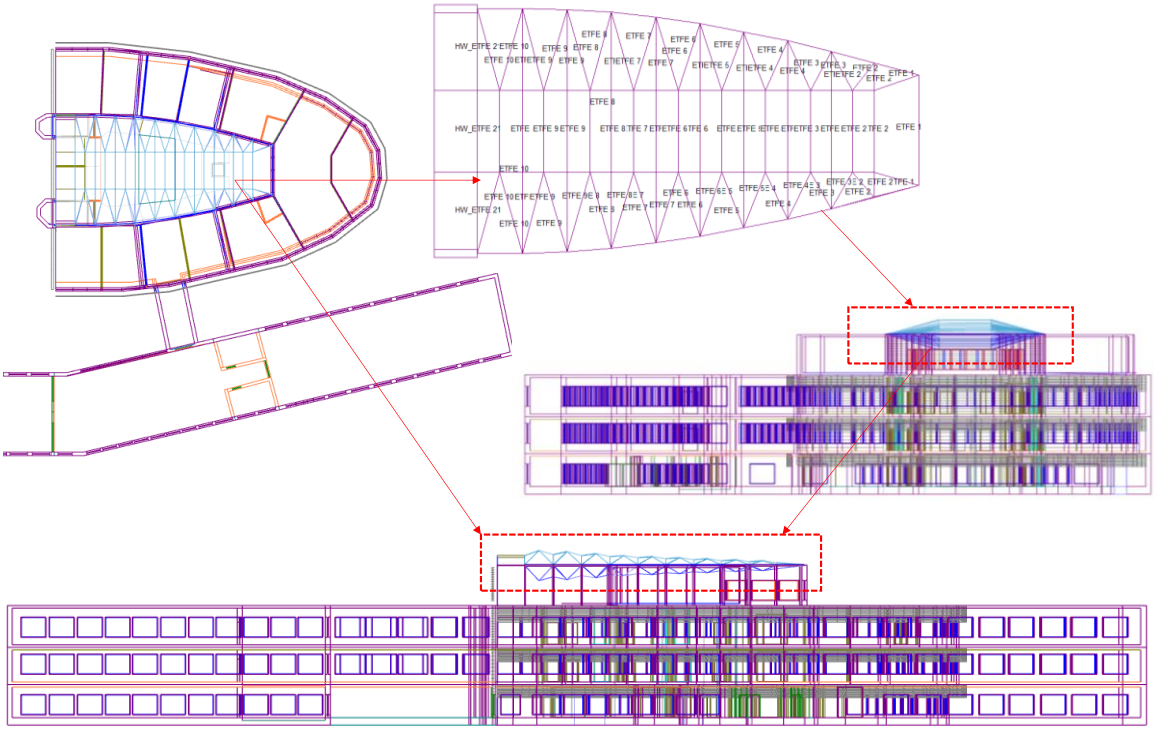


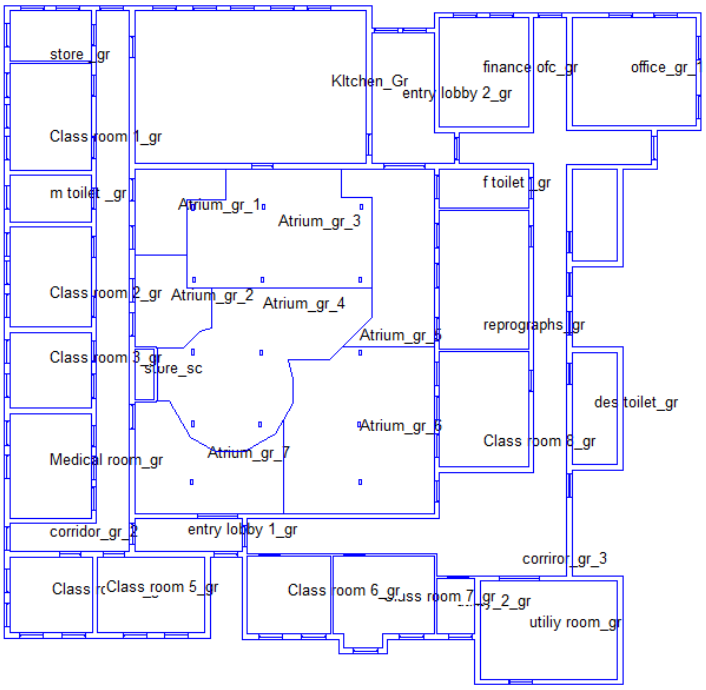
Figure 7-8: Simulation model of ETFE foil cushion roof of Engineering and Science Learning Centre atrium

7.7 Zoning

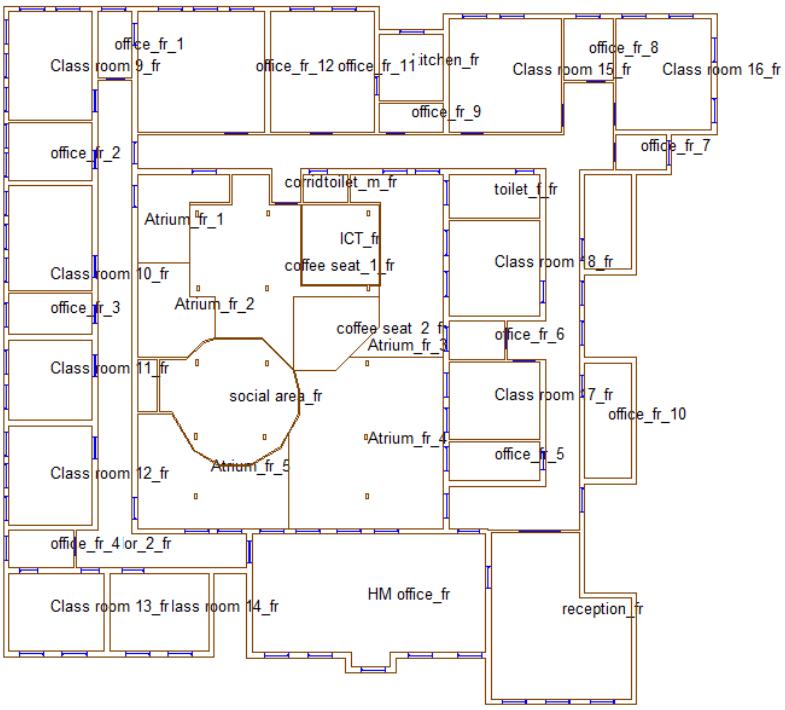
In the simulation model of Nottingham High School and the ESLC each space was zoned according to its functional use. Complexity rose while zoning the atria. According to IEATask12 (1996) horizontal and vertical zoning of the atrium model is the most important parameter for the correct temperature calculation in the simulation. Without appropriate portioning, the whole atrium will give a single average temperature. In an atrium temperature stratification is very important. Thus the simulation result should consider this while evaluating thermal performance. IEATask12 (1996), also presented different studies that conducted the simulation of the atrium by dividing its big volume into small vertical and horizontal zones. Therefore, in the simulation model, a similar approach was adopted in this study. This process also allowed the specification of the internal gains and occupancy pattern of each part of the atrium separately.

7.7.1 Zone specification of Nottingham High School

Figure 7-9 illustrates the simulation model plan showing functional zones located on the ground floor, first floor and second floor of the Nottingham High School.

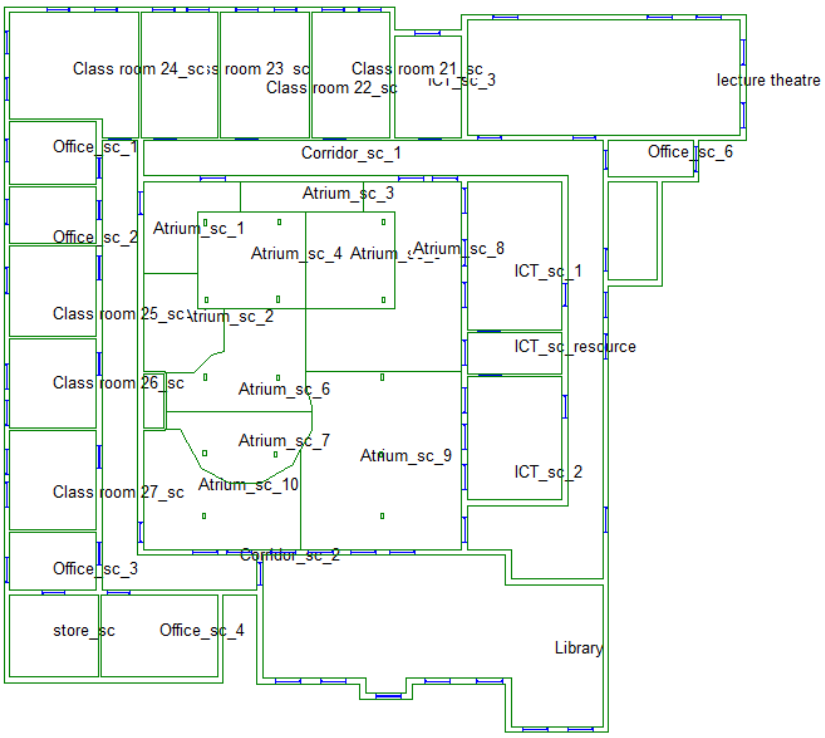


(a) Ground floor



(b) First floor

(Figure 7-9continued to the next page)

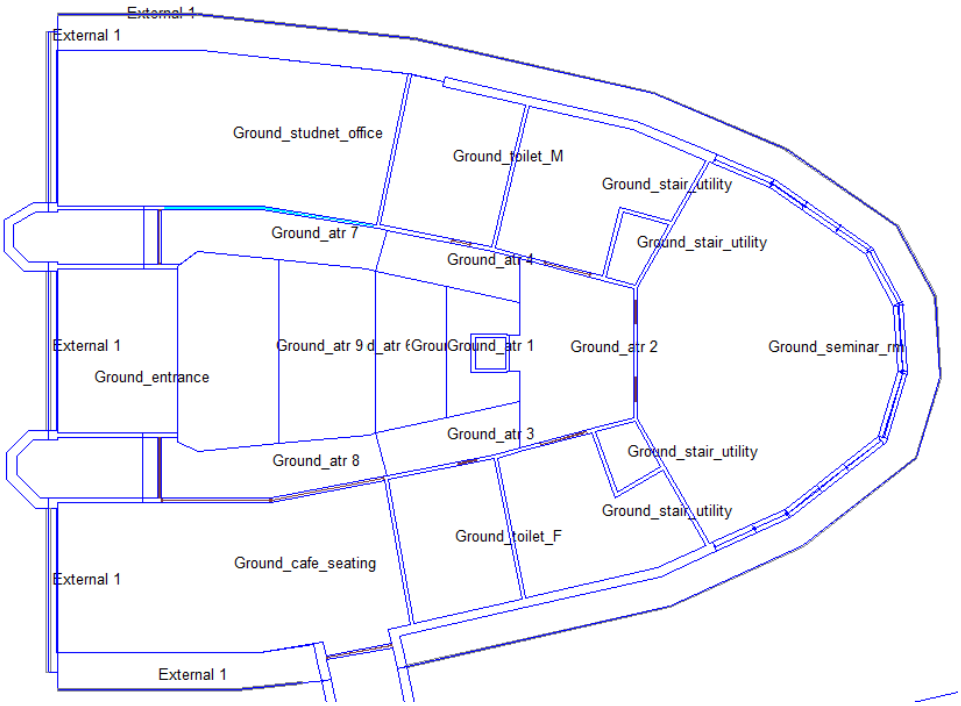


(c)Second floor

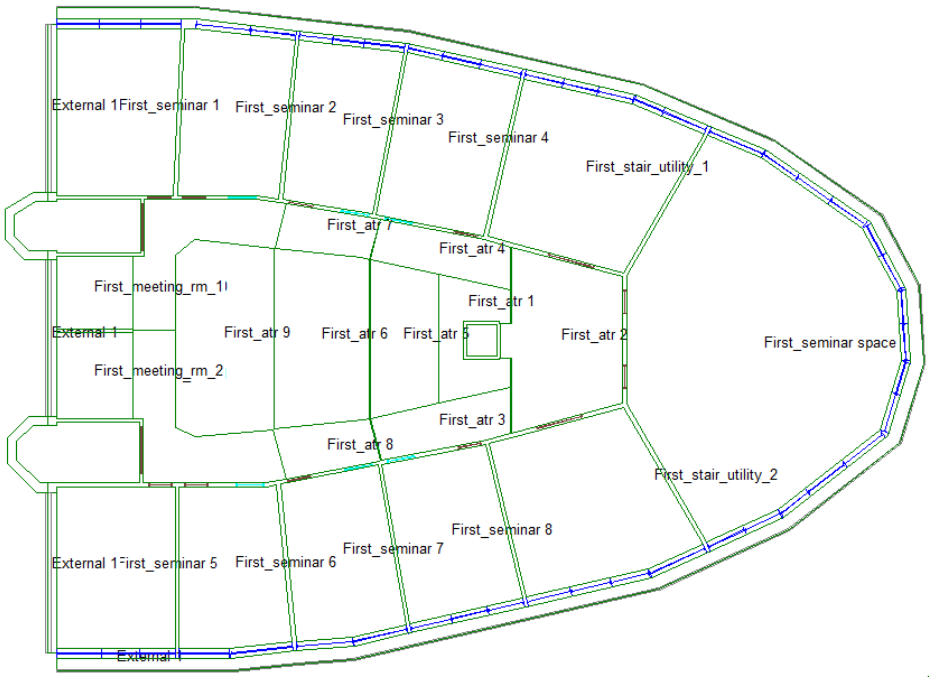
Figure 7-9: Zoning of (a) Ground floor, (b) First floor, (c) Second floor of simulation model (Nottingham High School)

7.7.2 Zone specification of Engineering and Science Learning Centre

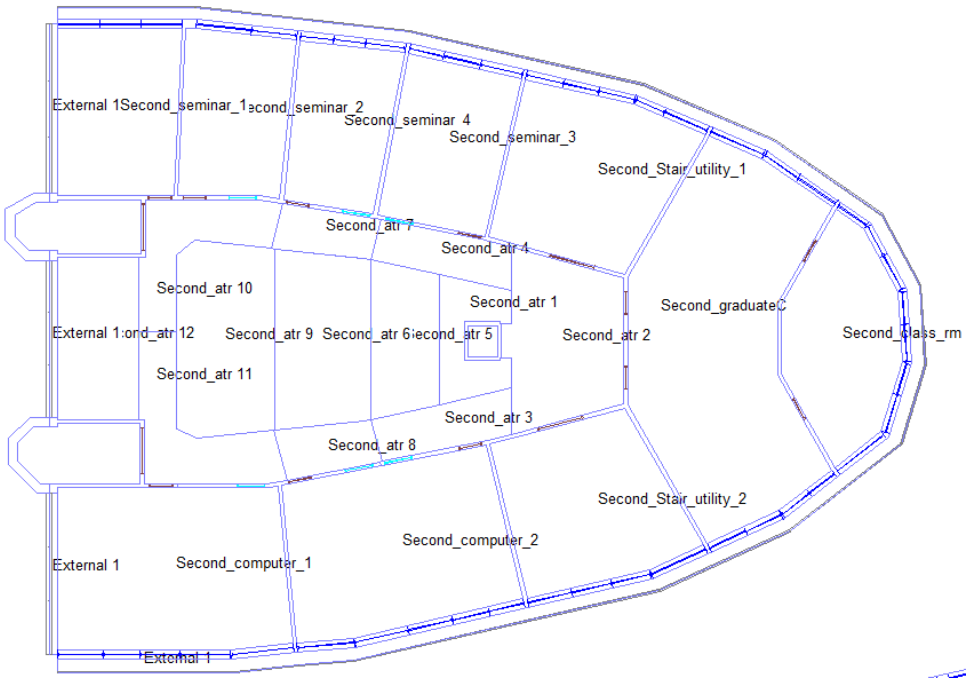
Figure 7-10 presents the simulation model plan showing functional zones located on the ground floor, first floor and second floor of the Engineering and Science Learning Centre.



(a) Ground floor



(b) First floor (Figure 7-10 continued in the next page)



(c) Second floor

Figure 7-10: Zoning of (a) Ground floor, (b) First floor, (c) second floor of Engineering and Science Learning Centre

7.8 Specifications of building fabrics in simulation models

7.8.1 Nottingham High School

Façade properties other than ETFE-foil was obtained from the building management system of Nottingham High School. Thermal optical properties of the ETFE-foils used in the analysis model of Nottingham High School are listed in Table 7-12. In the Nottingham High School, rain suppression mesh was placed on top of the ETFE-foil cushion roof of the atrium. Moreover, from the investigation results presented in Chapter 5, it was evident that presence of rain mesh on top of ETFE-foil panel reduced solar transmittance by 12%. This reduction in solar transmittance was taken into account while calculating thermal optical properties of ETFE-foil cushion. Table 7-13 presents U-value of building fabrics.

Table 7-12: Properties of ETFE foil cushion

Material properties	ETFE cushion	
	Layer 1 (internal)	Layer 2
	200μm transparent	200μm 75% fritted
Solar transmittance	0.86	0.37
Solar reflectance (External)	0.13	0.11
Solar reflectance (Internal)	0.13	0.55
Light transmittance	0.84	0.38
Light reflectance (External)	0.15	0.13
Light reflectance (Internal)	0.15	0.49
Emissivity (External)	0.82	0.82
Emissivity (Internal)	0.82	0.6

Table 7-13: U-value of building fabrics

Element	U-value (W/m^2°C)
Masonry wall	0.6
Floor	0.95
Window	1.8
Roof (other than ETFE-foil cushion roof)	0.8

7.8.2 Engineering and Science Learning Centre (ESLC)

Thermal optical properties of the ETFE-foil used in the simulation model of the Engineering and Science learning centre is presented in Table 7-14 and U-values of building fabric are presented in Table 7-15.

Table 7-14: Properties of ETFE foil

Material properties	ETFE cushion		
	Layer 1 (internal)	Layer 2 (middle)	Layer 3 (external)
	150μm transparent	150μm transparent	200 μm 65% fritted
Solar transmittance	0.87	0.87	0.49
Solar reflectance (External)	0.13	0.09	0.49
Solar reflectance (Internal)	0.13	0.09	0.49
Light transmittance	0.859	0.859	0.50
Light reflectance (External)	0.14	0.09	0.50
Light reflectance (Internal)	0.14	0.09	0.50
Emissivity (External)	0.82	0.82	0.82
Emissivity (Internal)	0.82	0.82	0.65

Table 7-15: U-value of building fabrics

Element	U- value (W/m^2°C)
Wall	0.23
Floor	0.2
Roof	0.2
Windows, roof windows and roof lights	1.98
Doors	2.19

7.9 Simulation parameters

Accurate and realistic assumptions on input parameters are required to develop the simulation model. Based on the usage information, internal gains from different sources e.g. occupancy, lighting, equipment, ventilation etc. needs to be specified. CIBSE Guide A (CIBSE, 2006, CIBSE, 2015b) provides reliable information on internal gains. But CIBSE guides do not present an occupancy profile that specifies the time schedule of various internal gains.

The Department for Communities and Local Government (DCLG) defined the National Calculation Method (NCM) for the EPDB (Energy Performance of Buildings Directive). The NCM is the procedure for validating compliance with Building Regulations for non-domestic buildings. This validation process is based on calculations that use standard sets of data for different activity areas, construction and service elements. Thus NCM includes the calculation methods as well as the standard data set (DCLG, 2015). However, the NCM profiles may be more suitable for new buildings to check compliance rather than apply in existing buildings where occupancy profiles can be identified. Different approved simulation software e.g. EDSL TAS comprises NCM profile database for occupancy, internal gains and usage patterns of equipment. The following section discusses the selection of input parameters for the simulation models.

7.9.1 Nottingham High School

Simulation parameters:

This section presents simulation parameters used in the model. These parameters were based on data collection, observation and personal communication with the building manager.

- Calendar

Summer period was considered from 1st May to 30th September and winter period considered from 1st October to 30th April. School holidays and weekends were specified in the calendar.

- Weather data

Data collected from different sources to create weather file are listed in Table 7-1.

- Internal gain

Table 7-16 presents internal gains obtained from the NCM database.

- Natural ventilation

Windows located on the west façade were operable only. Detail of window opening used in TAS analysis model and Building Simulator is presented in Table 7-17. According to information provided by the building management system, these windows operate as the air temperature of the second floor reaches 25°C.

- Infiltration for occupied spaces was 0.35ach and unoccupied spaces was 0.3ach.
- Ventilation rate set to 12.5 l/s/p (occupied hours only).
- Profile

The occupancy profile used in the TAS building simulator for different spaces is listed in Table 7-18. Occupied time was considered to be between 8.00am and 6.00pm. Occupancy of each space is represented by factor 0 (unoccupied) to 1 (fully occupied).

- Heating and cooling were not considered.

Table 7-16: NCM Activities_v5.2.4 (Part L 2010) followed (EDLS TAS Version 9.3.3.b)

Space type	Source	Sensible gain (W/m^2)	Latent gain (W/m^2)
Teaching space	Occupant	38.663	38.663
	Equipment	4.7	
	Lighting	10.5	
IT	Occupant	15.98	10.217
	Equipment	30	
	Lighting	11.25	
Lecture room	Occupant	18.644	11.92
	Equipment	2	
	Lighting	11.25	
Office	Occupant	7.519	5.15
	Equipment	11.9	
	Lighting	15	
Communal area	Occupant	6.964	4.452
	Equipment	5.27	
	Lighting	7.8	
Kitchen	Occupant	5.941	11.033
	Equipment	27.2	12.8
	Lighting	26	
Class room	Occupant	14.24	14.24
	Equipment	4.74	
	Lighting	11.25	
Atrium ground floor and first floor	Occupant	10.889	6.962
	Equipment	20	
	Lighting	7.8	
Atrium second floor	Occupant	21.12	18.15
	Equipment	15.25	
	Lighting	19.05	

Table 7-17: Window opening details, function used in analysis model and TAS building simulator

Description	Width (m)	Height (m)	Area (m^2)	Frame (m)	Opening percentage (factor)	value	Function
High Window	1.10	1	1.10	0.05	0.25	Hourly	Air temperature =/> 25°C
Internal doors	0.9	2.1	1.89	0.05	1	Hourly (8.00am-16.00pm	

Table 7-18: Occupancy, lighting and equipment schedule

Time (hour)	1-7	8	9	10	11	12	13	14	15	16	17	18	19-23
Teaching space	0	0.1	0.25	0.75	1	1	0.5	0.5	1	1	0.5	0.5	0
Lecture room		0.1	0.25	0.75	1	1	0.5	0.5	1	1	0.5	0.5	
Class room													
Library		0.1	0.25	0.75	1	1	0.5	0.5	0.5	0.25	0		
Office		0.1	0.25	0.75	1	1	0.5	0.5	1	1	0.5	0.5	
Common room		0.25	0.25	0.5	0.5	1	1	0.5	0.25	0.25	0.25	0.5	
Ground floor atrium		0.25	1	0.25	0.1	1	1	1	0.5	0.25	0.1	0.1	
First floor atrium		0.1	0.25	0.1	0.1	1	1	1	0.25	0.1	0.1	0.1	
Second floor atrium		0.1	0.25	0.25	0.5	1	1	1	0.5	0.1	0.1	0.1	
Equipment (atrium)	0.046	1	1	1	1	1	1	1	1	1	1	1	0.046
Lighting (atrium)	1	0.25	0.25	0.25	0.25	0.25	0.25	0.25	0.25	0.25	1	1	1

7.9.2 Engineering and Science Learning Centre (ESLC)

Simulation parameters:

This section presents simulation parameters used in the model and based on data collection, observation and personal communication with University of Nottingham, Estate.

- Calendar

Summer period was considered from 1st May to 30th September and winter period considered from 1st October to 30th April. University closure days and weekends were specified in the calendar.

- Weather data

Data collected from different sources to create weather file are listed in Table 7-1

- Internal gain

Table **7-19**Table 7-19 presents internal gains obtained from the NCM database (EDLS TAS Version 9.3.3.b) and used in the simulation model.

- Natural ventilation

Detail of window opening used in TAS analysis model and building simulator is presented in Table 7-20. According to information provided by Estates, these windows operate when the average air temperature of the atrium and outdoor air temperature rises above 25°C and 10°C respectively.

- Infiltration for occupied spaces was 0.35ach and unoccupied spaces were 0.3ach.
- Ventilation rate set to 12.5 l/s/p (occupied hours only).
- Heating and cooling

  Heating and cooling were assumed for predicted model

- Profile

The occupancy profile used in the TAS building simulator for different spaces is listed in Table 7-21. Occupied time was considered to be between 8.00am and 9.00pm. Occupancy of each space is represented by factor 0 (unoccupied) to 1 (fully occupied).

Table 7-19: NCM Activities_v5.2.4 (Part L 2010) followed (EDLS TAS Version 9.3.3.b)

Space type	Source	Sensible gain (W/m^2)	Latent gain (W/m^2)
IT	Occupant	16.927	10.823
	Equipment	27.81	
	Lighting	11.25	
class room	Occupant	14.24	14.24
	Equipment	4.74	
	Lighting	11.25	
Office	Occupant	7.519	5.15
	Equipment	11.9	
	Lighting	15	
Communal area	Occupant	7.453	7.453
	Equipment	1.83	
	Lighting	5.2	
lecture room	Occupant	17.22	11.011
	Equipment	1.83	
	Lighting	11.25	
Cafe	Occupant	14.648	9.365
	Equipment	17.62	
	Lighting	7.8	
Graduate centre	Occupant	13.839	8.48
	Equipment	17.17	
	Lighting	19.05	
Atrium ground floor	Occupant	11.677	11.677
	Equipment	4.3	
	Lighting	23.6	
Atrium first floor	Occupant	7.453	7.453
	Equipment	1.83	
	Lighting	5.2	
Atrium second floor	Occupant	6.964	4.452
	Equipment	5.27	
	Lighting	15.25	

Table 7-20: Window opening details, function used in analysis model and TAS building simulator

Description	Width (m)	Height (m)	Area (m2)	Frame (m)	Opening percentage (factor)	value	Function
High Window	1.15	1	1.15	0.05	0.25	Hourly	Air temperature =/> 25°C
Internal doors	0.9	2.1	1.89	0.05	1	Hourly	
Entry door	1.5	2.5	3.75	0.05	1	Hourly	

Table 7-21: Occupancy, lighting and equipment schedule

Time (hour)	22-7	8	9	10	11	12	13	14	15	16	17	18	19	20	21
IT	0	0.1	0.5	0.75	1	1	0.75	0.75	1	1	1	0.75	0.5	0.5	0.5
Class room	0	0.1	0.25	0.75	1	1	0.5	0.5	1	1	0.5	0.5	0	0	0
Lecture room		0.1	0.25	0.75	1	1	0.5	0.5	1	1	0.5	0.5	0	0	0
Office		0.1	0.25	0.75	1	1	0.5	0.5	1	1	0.5	0.5	0	0	0
Graduate centre		0.25	0.25	0.5	0.5	1	1	0.5	0.25	0.25	0.25	0.5	0.5	0.25	0.25
Ground floor atrium		0.25	1	0.25	0.1	1	1	1	0.5	0.25	0.1	0.1			
First floor atrium		0.1	0.25	0.1	0.1	1	1	1	0.25	0.1	0.1	0.1			
Second floor atrium		0.1	0.25	0.25	0.5	1	1	1	0.5	0.1	0.1	0.1			
Equipment (atrium)	0.055	1	1	1	1	1	1	1	1	1	1	1	0.055	0.055	0.055
Lighting (atrium)	1	0.05	0.05	0.05	0.05	0.05	0.05	0.05	0.05	0.05	0.5	1	1	1	1

7.10 Model Calibration

This section investigates the influence of internal gains, occupancy, window opening, the shape of the roof etc. on the performance of the atrium of Nottingham High School and ESLC. Description of the simulation model and criteria are listed in Table 7-22.

Table 7-22: Model description and parameter

Model description	Simulation parameter	Roof configuration	Purpose
Level 3_NH_Base Case 0	• Internal gains and window opening was not considered	Two way curved	• To examine the impact of external environmental parameters e.g. solar radiation, outdoor ambient temperature etc. on the thermal performance of atrium
Level 3_ESLC_Base Case 0			
Level 3_NH_Base Case 1	• Internal gain, infiltration, occupancy profile included according to • Table 7-16,Table 7-18. • Window opening was considered according to Table 7-17.	Two way curved	• To compare with Base case 0 • To examine impact of input parameter on the thermal performance of atrium
Level 3_ESLC_Base Case 1	• Internal gain, infiltration, occupancy profile included according to • Table 7-19 and Table 7-21. • Window opening was considered according to • Table 7-20		
Level 3_NH_Base Case 2	• Similar to Base case 1	Flat ETFE panel	• To compare with Base case 1 to see the influence of roof configuration on the thermal environment of the atrium
Level 3_ESLC_Base Case 2			

Onsite monitoring results presented in Chapter 6 showed that external environmental parameters e.g. incident solar radiation, outdoor ambient temperature etc. affected the thermal performance of different levels of the atria. It was also evident that among

different floor levels, floor (Level 3) adjacent to ETFE foil cushion roof was affected significantly. In both of the case study buildings, second floor (Level 3) was adjacent to ETFE cushion roof. Therefore, calibration results particularly focused on air temperatures of the second floor of simulation models of the atria.

7.10.1 Calibration results for simulation mode of Nottingham High School

A Base Case 0 was created using the properties of fabric materials listed in Table 7-12 and Table 7-13. In this model occupancy profile, internal gains and window opening profile was not included.

In the next step Base Case 1, was developed by adding occupancy profile (Table 7-18), internal gains (Table 7-16) and window opening (see Table 7-17) in Base Case 0. The rationale for developing Base Case 0 and Base Case 1 is stated in Table 7-22. Figure 7-11 presents temperature difference of Level 3_NH_Base Case 1 and Level 3_NH_Base Case 0.

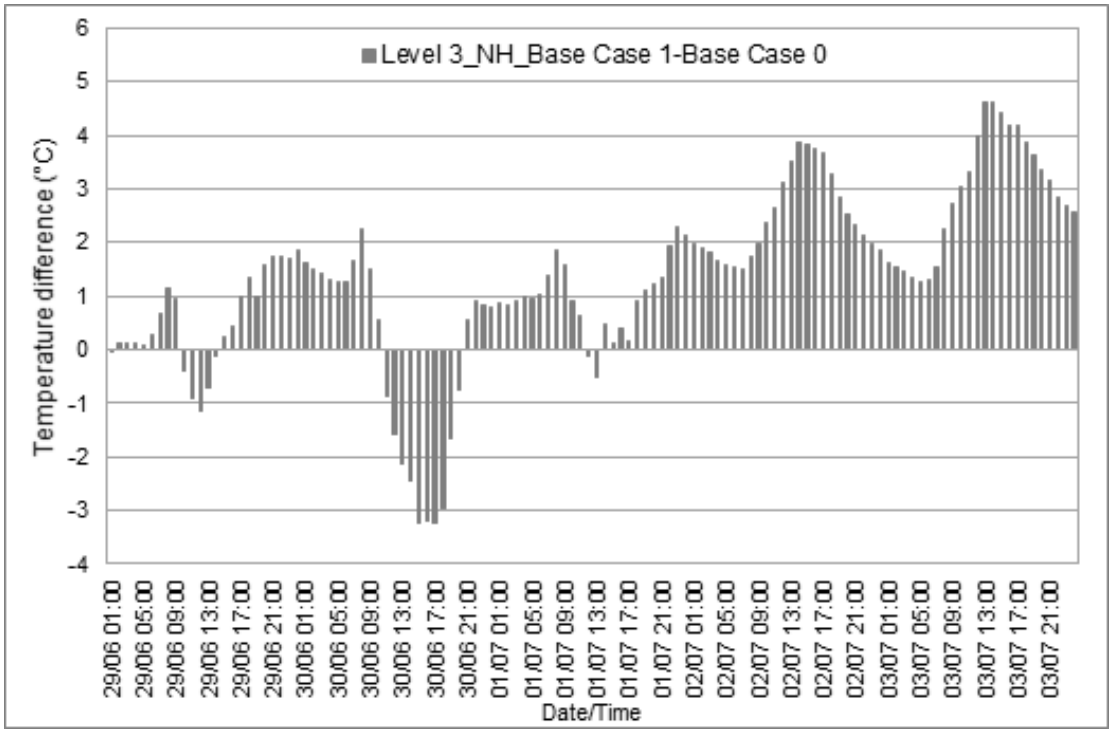


Figure 7-11: Base Case 1 air temperature relative to Base-Case 0

From Figure 7-11 it is evident that internal gains, window opening and occupancy had a significant impact on air temperatures of Level 3 (second floor) of the atrium. At this level, air temperature of Base Case 1 showed a maximum deviation of 4.5°C from that of Base Case 0. Thus, the selection of input parameters on the basis of building operation is important to avoid discrepancy in predicted results. Among the different input parameters - window opening, internal gains and occupancy schedule etc., were

found to have a considerable impact on the simulation results. Furthermore, the calibration process might be challenging if one of these parameters is unknown. These findings are also consistent with the previous study carried by Lomas et al. (1997), Westphal and Lamberts (2005), Pellegrino et al. (2016).

In this study standard values of occupancy profile and internal gains were used in Base Case 1 whereas a window opening schedule was assumed on the basis of personal observation and information from building management. Therefore, in the next step, a different window opening percentage was simulated using Base Case 1 where internal gains, window opening and occupancy schedule was not changed. The results of this variable window opening and its impact on air temperature is presented in Figure 7-12.

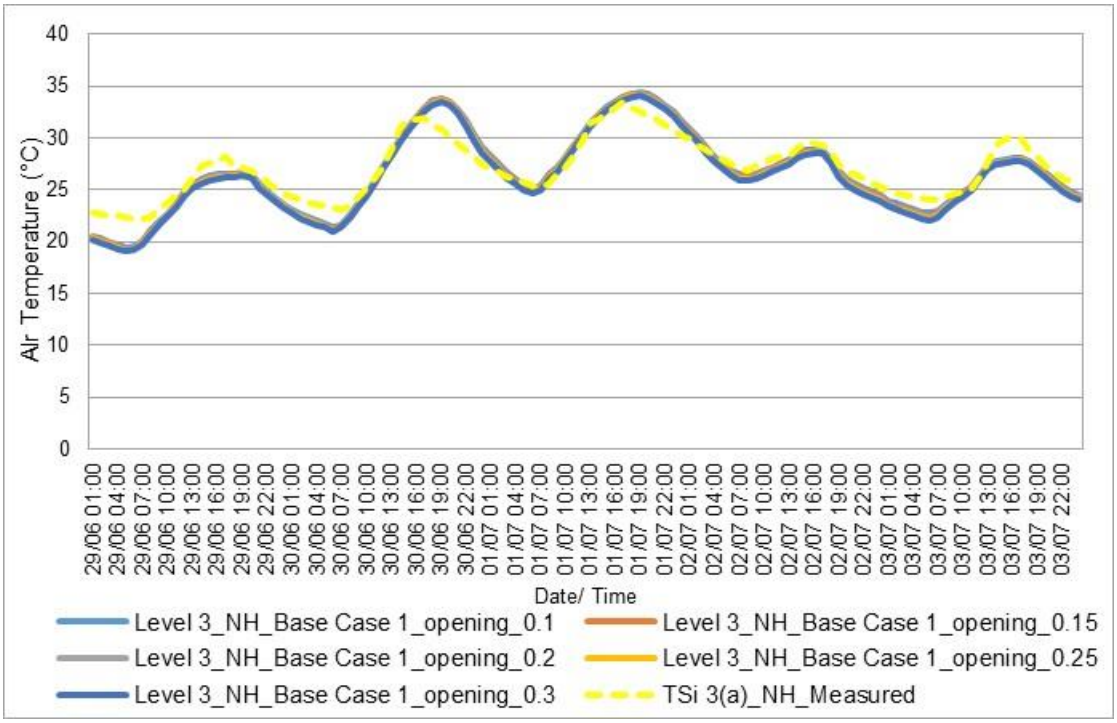


Figure 7-12: Simulated air temperatures of the second floor of the atrium with various window opening percentage and comparison with measured data

From the results presented in Figure 7-12, it can be seen that air temperatures of the second floor of the atrium did not vary significantly as opening percentage was changed from 0.1 to 0.3. Besides, the opening percentage of 0.25 was suggested by school management. Therefore, this Base Case 1 opening was set to 0.25 and this model was selected for further analysis.

The ETFE-foil cushion roof of Base Case 1 was modelled in a way that (approximately) represented the doubly curved roof configuration. To see the impact of roof configuration on the atrium air temperatures, another model with flat ETFE-foil panels was created and named as Base Case 2. The difference between simulated air

temperature of Base Case 1, Base Case 2, and the measured air temperature are presented in Figure 7-13. From the result, it can be seen that the maximum difference between measured and Base Case 2 air temperature was 9.6°C and on average this difference was 4.6°C. On the other hand, the maximum difference between measured and Base Case 1 air temperature was 3°C, which varied on an average by 0.5°C during the study period (29th June to 3rd July 2015). From this result, it can be demonstrated that modelling ETFE-foil cushion as flat ETFE-foil panel could cause significant error in predicted results.

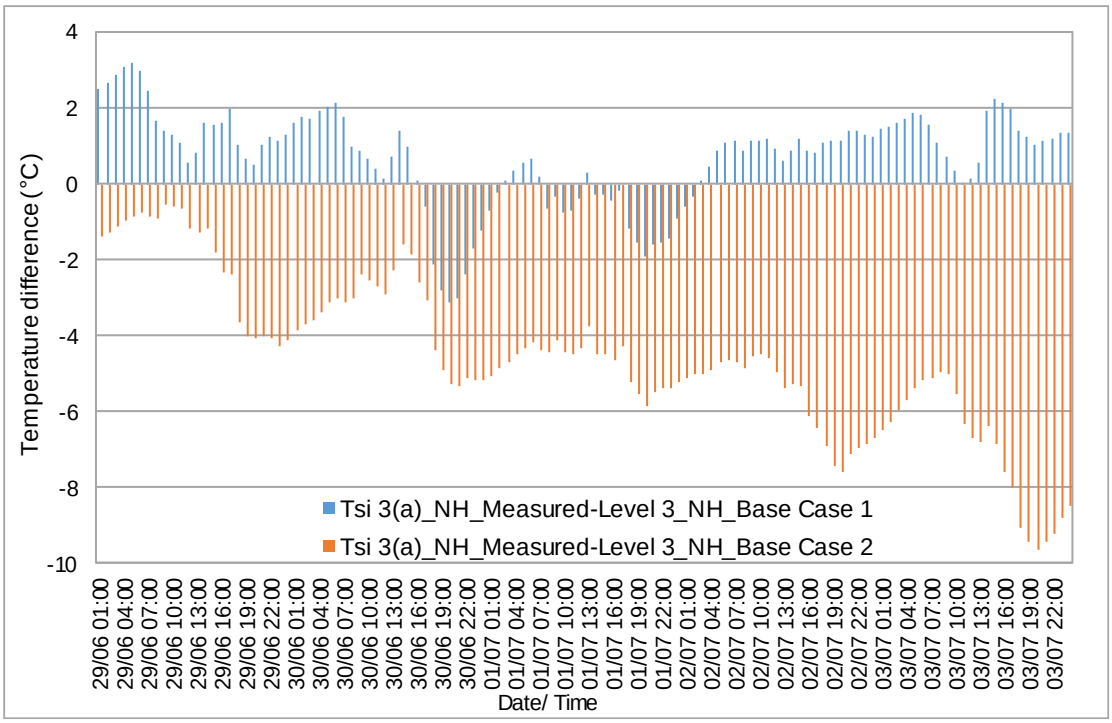


Figure 7-13: Base model 1 and Base model 2 air temperature relative to measured data

A comparative Pearson correlation analysis was done to show the variation between measured data and predicted results for both Base Case 1 and Base Case 2. The results showed that the correlation coefficient of Base Case 1 and measured data was 0.966. However, this value was 0.7 when comparison was made between measured data and the Base Case 2 results. This also showed, simulation results of base case 1 was in close agreement with measured data.

7.10.2 Calibration results for ESLC simulation model

Base Case 0 and Base Case 1 of ESLC was created using the fabric properties presented in Table 7-14 and Table 7-15. Description of the simulation models, parameters and aim of the simulations are stated in Table 7-22.

Figure 7-14 illustrates temperature difference between air temperature of Base Case 1 and Base Case 0. The results showed significant deviation (6.3°C) of air temperature between Base Case 1 and Base Case 0. This deviation resulted from input parameters, such as internal gains, occupancy profile, window opening etc.

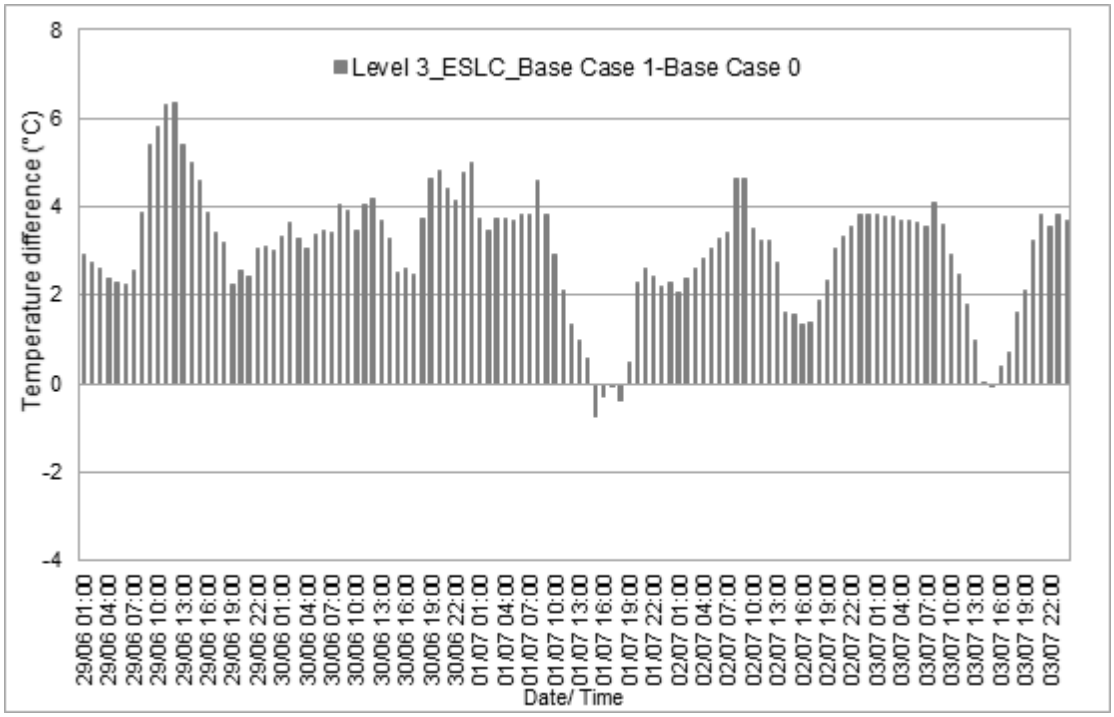


Figure 7-14: Base model 1 air temperature relative to Base model 0

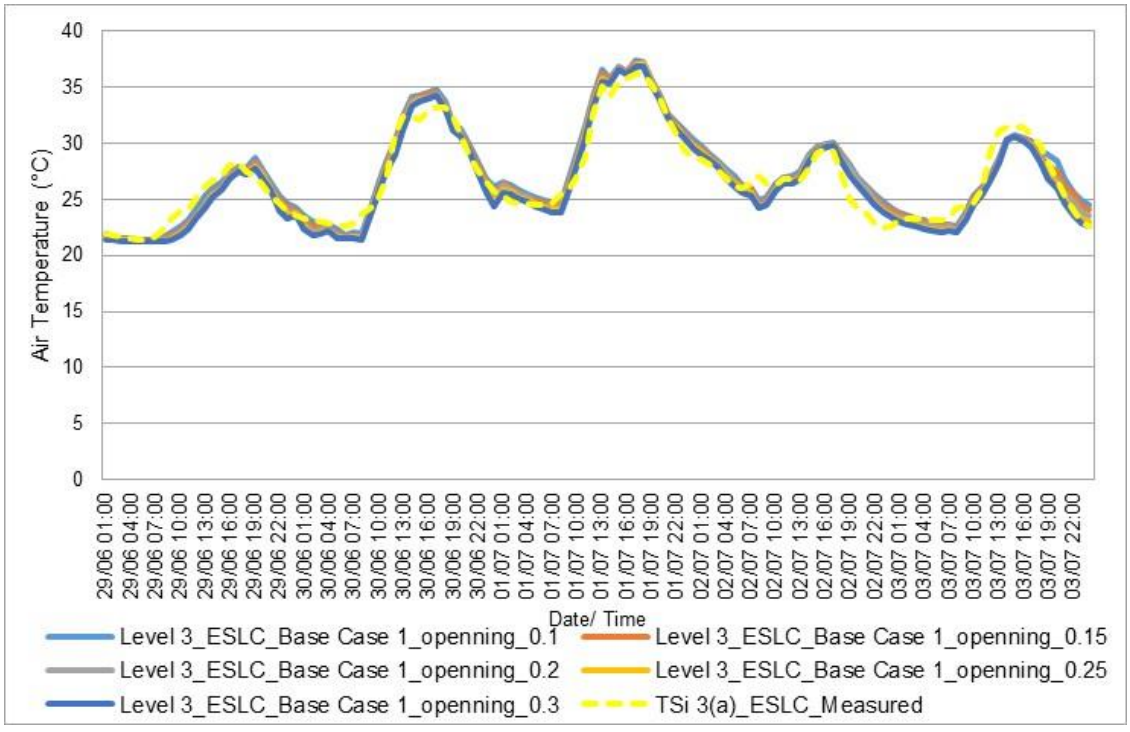


Figure 7-15: Simulated air temperatures of the second floor of the atrium with various window opening percentage and comparison with measured data

Figure 7-15 presents variations of air temperatures obtained from simulation, by varying window opening percentage from 0.1 to 0.3 in Base Case 1. The results showed that variation in window opening percentage from 0.1 to 0.3 had little impact on predicted air temperatures. Finally, window opening 0.3 was selected and included in Base Case 1 model for further analysis.

In Base Case 0 and Base Case 1 the ETFE-foil roof was modelled as a double curved shape. It was decided to model the ETFE-foil cushion roof as a flat three layer ETFE-foil panel also. This was done in Base Case 2. All input parameters of Base Case 1 and Base Case 2 were identical. Relative air temperature of Base Case 1 and Base Case 2 with respect to measured data is presented in Figure 7-16. The results demonstrated that if the ETFE-foil roof is modelled as a flat ETFE-foil panel then average temperature difference between predicted and measured air temperature was 4.25°C whereas if this roof is modelled in doubly curved shape this average reduced to 0.3°C. The maximum difference found between measured and Base Case 2 air temperature was 6.4°C. Therefore, the modelling configuration of three layer ETFE-foil cushion roof had a considerable impact on the predicted result. This was also evident while calculated Pearson coefficient. Pearson coefficient was 0.95 when compared with Base Case 1 and measured data. But Pearson coefficient was 0.75 while comparison was made between Base Case 2 and measured data. This Base Case 1 was considered for further analysis which is presented in the subsequent section where Base Case 1 was named as Predicted model.

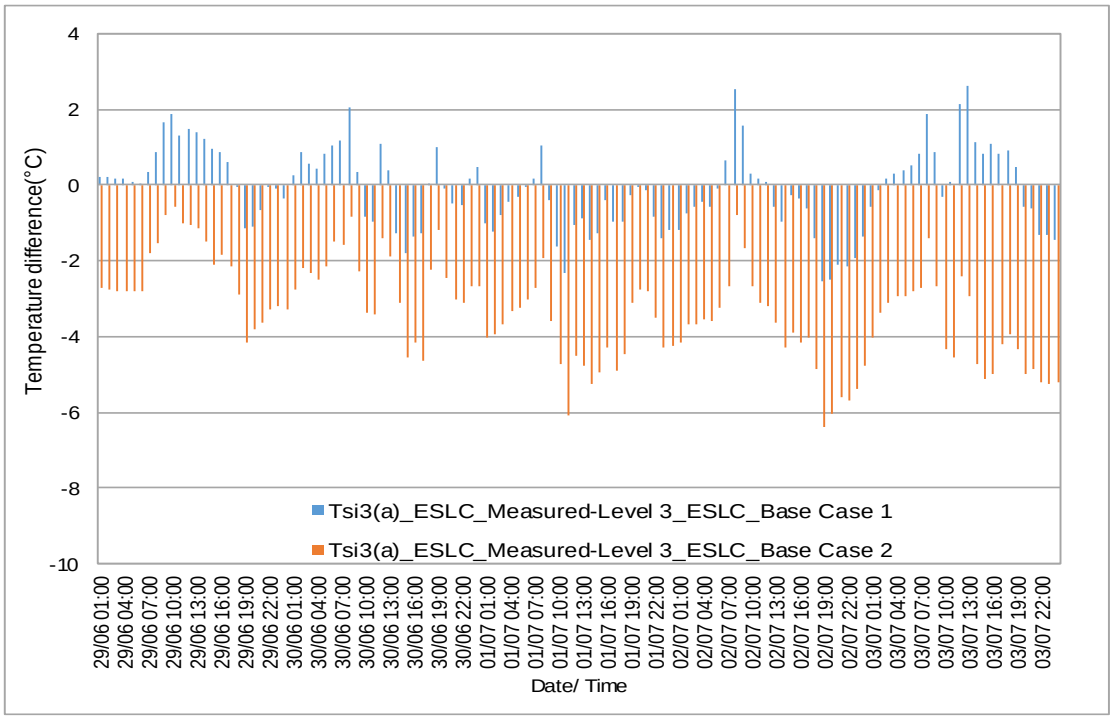


Figure 7-16: Base model 1 and Base model 2 air temperature relative to measured data

7.11 Strategies to improve thermal performance of space

The results of monitoring presented in Chapter 5 showed that both of the buildings-Nottingham High School and ESLC overheated during summer 2015. This was the result of increase in outdoor temperature, solar radiation transmission through the ETFE-foil cushion roof, increase of mean radiant temperature of occupied levels due to increase in surface temperatures of the ETFE-foil cushions, inadequate ventilation system, opening area with respect to atrium floor area etc. The peak summer period was observed between 29th June and 3rd July 2015. Therefore, for detailed simulation, this particular period was selected.

Studies carried by Modirrousta and Boostani (2016), He and Hoyano (2009), Wang. X. et al. (2011), Moosavi et al. (2015), also demonstrated that solar radiation and inadequate ventilation systems are the major factors that can cause overheating in atria with large glazed roofs. Thus, previous investigation results were consistent with the finding of this study. Therefore, to improve thermal comfort conditions of the atria, different strategies were applied in the simulation model. These strategies included solar radiation control by modifying solar and light transmittance of the ETFE-foil and change of opening percentage. Solar and light transmittance of the ETFE-foil cushions were based on the results presented in Chapter 4. Moreover, opening percentage of existing windows located adjacent to the ETFE-foil cushion roof were modified and investigated. The fundamental aim of this simulation was to examine whether modification of optical properties of ETFE foil and/or opening percentage could improve thermal comfort of the monitored spaces by eliminating overheating.

7.11.1 Strategies applied for the Nottingham High School and ESLC simulation model

The following section discusses the application of strategies in the simulation models for the Nottingham High School and Engineering and Science Learning Centre (ESLC). It was mentioned in section 7.10.1 and 7.10.2 that the Base model 1 was selected to carry out further investigation. This Base model 1 is described as Predicted model in the following analysis.

i. Criteria 1

Thermal optical properties of the ETFE foil cushions of Nottingham High School and ESLC were presented in Table 7-12 and Table 7-14 respectively. Thermal optical properties of the external layer of the ETFE-foil cushion were modified exclusively in

the simulation Cases as described in Table 7-23. These properties of ETFE-foil are based on the results presented in Chapter 4.

Table 7-23: Thermal optical properties of the external layer of ETFE foil cushion

Simulation number	Case 1	Case 2	Case 3	Case 4	Case 5	Case 6	Case 7
Silver (Pigment) type	Light	Medium	Medium	Medium	Dark	Dark	Dark
Fritting percentage	89%	65%	75%	89%	65%	75%	89%
Solar transmittance	0.31	0.255	0.225	0.127	0.225	0.187	0.0833
Solar reflectance (External)	0.11	0.11	0.11	0.11	0.11	0.11	0.11
Solar reflectance (Internal)	0.628	0.68	0.726	0.83	0.72	0.764	0.88
Light transmittance	0.318	0.2516	0.219	0.126	0.217	0.1784	0.082
Light reflectance (External)	0.13	0.13	0.13	0.13	0.13	0.13	0.13
Light reflectance (Internal)	0.62	0.69	0.732	0.839	0.73	0.769	0.883
Emissivity of layer 2 (External)	0.82	0.82	0.82	0.82	0.82	0.82	0.82
Emissivity of layer 2 (Internal)	0.6	0.6	0.6	0.6	0.6	0.6	0.6

ii. Criteria 2

Thermal optical properties of the external and internal layer were modified and presented in Table 7-24.

Table 7-24: Thermal optical properties of external and internal layer of ETFE foil cushion

Simulation Case number	**Case 8**		**Case 9**		**Case 10**		**Case 11**		**Case 12**		**Case 13**		**Case 14**	
Location	Int.	Ext.	Int.	Ext.	Int.	Ext.	Int.	Ext.	Int.	Ext.	Int.	Ext.	Int.	Ext.
Silver (pigment) type	Light	Med-ium	Light	Med-ium	Light	Dark	Light	Dark	Light	Med-ium	Light	Dark	Med-ium	Dark
Fritting percentage	25%	25%	25%	50%	25%	25%	25%	50%	50%	50%	50%	50%	25%	25%
Solar transmittance	0.72	0.58	0.72	0.405	0.72	0.567	0.72	0.378	0.58	0.405	0.58	0.3784	0.66	0.566
Solar reflectance (External)	0.13	0.11	0.13	0.11	0.13	0.11	0.13	0.11	0.13	0.11	0.13	0.11	0.13	0.11
Solar reflectance (Internal)	0.278	0.33	0.278	0.53	0.278	0.35	0.278	0.55	0.415	0.53	0.415	0.55	0.33	0.35
Light transmittance	0.708	0.563	0.708	0.45	0.708	0.63	0.708	0.42	0.578	0.45	0.578	0.42	0.64	0.63
Light reflectance (External)	0.15	0.13	0.15	0.13	0.15	0.13	0.15	0.13	0.15	0.13	0.15	0.13	0.15	0.13
Light reflectance (Internal)	0.289	0.35	0.289	0.54	0.289	0.36	0.289	0.56	0.42	0.54	0.42	0.35	0.35	0.36
Emissivity of layer 1& 2 (External)	0.82	0.82	0.82	0.82	0.82	0.82	0.82	0.82	0.82	0.82	0.82	0.82	0.82	0.82
Emissivity of layer 1 & 2 (Internal)	0.6	0.55	0.6	0.55	0.6	0.5	0.6	0.5	0.6	0.55	0.6	0.5	0.55	0.5

iii. Criteria 3

The internal emissivity of the external layer of ETFE-foil cushion was modified. Different emissivity considered in the simulation are presented in Table 7-25.

Table 7-25: Emissivity of ETFE foil

Emissivity	Original	Case 15	Case 16	Case 17	Case 18	Case 19
External emissivity of layer 2	0.82	0.82	0.82	0.82	0.82	0.82
Internal emissivity of layer 2	0.6	0.5	0.4	0.3	0.2	0.1

iv. Criteria 4

The indoor thermal performance of the spaces is influenced by the window opening profile. In order to investigate this, opening area and percentage of existing windows located on the second floor of the atrium were modified in the simulation. In addition, variable indoor air temperature thresholds were applied to modulate window opening profiles (e.g. window was open when the indoor air temperature was above 21°C, 22°C, 23°C and 25°C). However, the results identified no significant impact for these variable threshold scenarios on indoor thermal performance. The findings are similar for both the Nottingham High School and ESLC. These simulation cases were not presented here. Options that were examined in the Nottingham High School and ESCL simulation models are presented in Table 7-26 and Table 7-27.

Table 7-26: Window opening and associated air temperature of atrium second floor, Nottingham High School

Case no.	North windows	South windows	East windows	West windows
Case 20	-	Open (factor= 0.25), 24hr	-	Open (factor= 0.25), 24hr
Case 21	Open (factor= 0.25), 24hr	Open (factor= 0.25), 24hr	-	Open (factor= 0.25), 24hr
Case 22	-	Open (factor= 0.25), 24hr	Open (factor= 0.25), 24hr	Open (factor= 0.25), 24hr
Case 23	Open (factor= 0.25), 24hr	Open (factor= 0.25), 24hr	Open (factor= 0.25), 24hr	Open (factor= 0.25), 24hr
Case 24	Open (factor= 0.5), 24hr	Open (factor= 0.5), 24hr	Open (factor= 0.5), 24hr	Open (factor= 0.5), 24hr
Case 25	Open (factor= 0.75), 24hr	Open (factor= 0.75), 24hr	Open (factor= 0.75), 24hr	Open (factor= 0.75), 24hr
Case 26	Open (factor= 1), 24hr	Open (factor= 1), 24hr	Open (factor= 1), 24hr	Open (factor= 1), 24hr

Table 7-27: Window opening and associated air temperature of atrium second floor, Engineering and Science Learning Centre

Case no.	North East windows	South East windows	West windows
Case 20		Open (factor= 0.25), 24hr	Open (factor= 0.25), 24hr
Case 22	Open (factor= 0.25), 24hr		Open (factor= 0.25), 24hr
Case 23	Open (factor= 0.25), 24hr	Open (factor= 0.25), 24hr	Open (factor= 0.25), 24hr
Case 24	Open (factor= 0.5), 24hr	Open (factor= 0.5), 24hr	Open (factor= 0.5), 24hr
Case 25	Open (factor= 0.75), 24hr	Open (factor= 0.75), 24hr	Open (factor= 0.75), 24hr
Case 26	Open (factor= 1), 24hr	Open (factor= 1), 24hr	Open (factor= 1), 24hr

The time period selected for simulation is presented in Table 7-28, this period also represents the hottest period of summer 2015.

Table 7-28: Period selected for simulation in summer 2015

Time period	Nottingham High School	ESLC
29th June to 3rd July	5 days	5 days
Number of occupied hours simulated	40 hours	45hours
Percentage of time covered	8.33% (480 occupied hours)	6.1% (738 occupied hours)

7.11.2 Results of implication of simulation criteria

Figure 7-17 presents air temperature difference between Case 24, Case 25, Case 26, and predicted model of Nottingham High School.

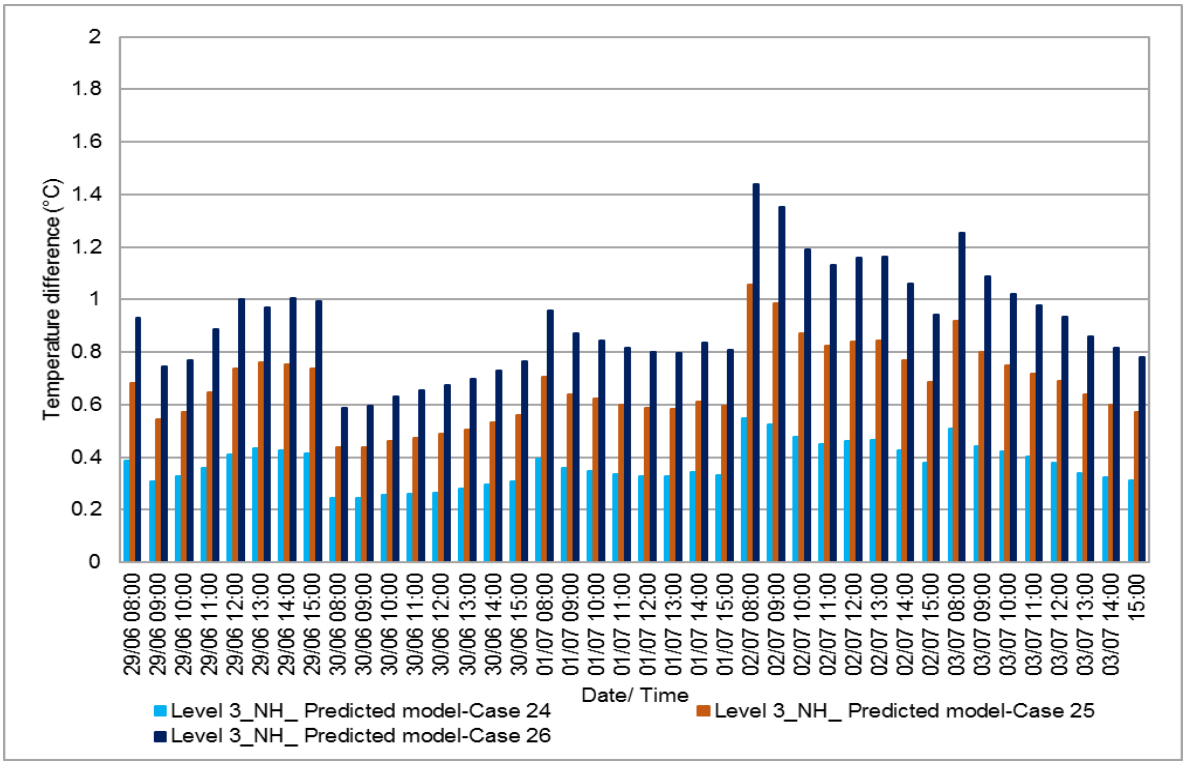


Figure 7-17: Temperature differences between case 24, 25, 26 and Predicted model air temperatures during occupied hours (Nottingham High School)

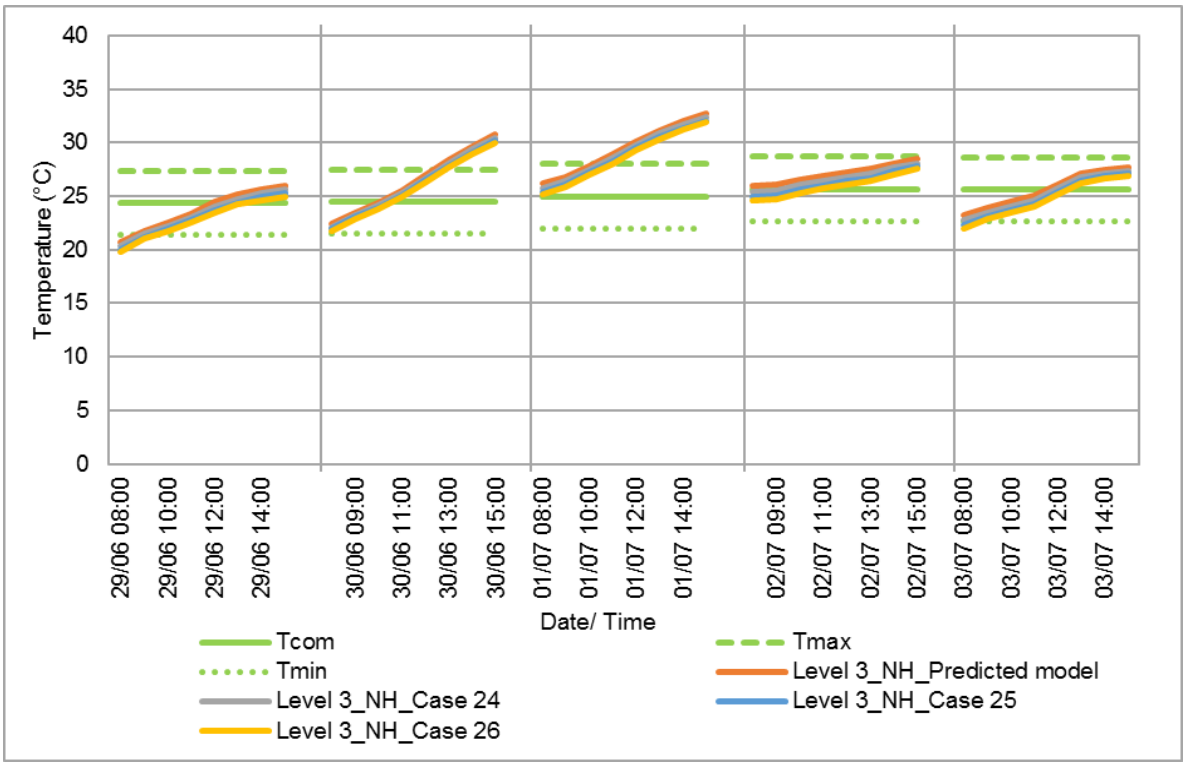


Figure 7-18: Air temperatures of Predicted, Case 24, Case 25, Case 26 model; maximum, minimum and comfort temperature (Nottingham High School)

From the results illustrated in Figure 7-17, it can be demonstrated that among different simulation cases, air temperature maximum dropped by 1.44°C in Case 26 during 2nd July. In this case, windows were 100% open during the occupied hours. The results

obtained during the hottest days showed that this model was only able to reduce air temperature on average by 0.67°C (in 30th June) and 0.84°C (in 1st July) even if windows were 100% open. Nevertheless, this reduction is not sufficient to ease overheating occurring during the peak summer period. This is reflected in the following discussion on thermal comfort assessment.

Figure 7-18 presents air temperature obtained from the Predicted model, Cases 24, 26 and 27 as well as comfort temperature, maximum and minimum acceptable temperature between 29th June and 3rd July 15. Detailed description and calculation procedure for comfort temperature, maximum and minimum acceptable temperature range can be found in Chapter 6.

The results presented in Figure 7-18 showed that during 30th June and 1st July the air temperature of the Predicted model, Case 24, 25 and 26 rose above the maximum acceptable temperature and for 15% of occupied hours the air temperature of the second floor of the atrium (Case 26) stayed above T_{max}. Although this was less than that occurred in the base Predicted model (where 20% of occupied hours predicted model air temperature was above T_{max}).

In Case 26 of the simulated model of the ESLC (Figure 7-19), air temperature of the second floor of the atrium maximum was reduced by 1.77°C during 3rd July. In this model, windows were also 100% open. During the peak period observed on 30th June and 1st July, average air temperature of this model reduced by 0.9°C and 0.85°C respectively. Similarly to Case 26 of Nottingham High School, this model did not provide any substantial variation in air temperature from that of the predicted model, particularly during 30th June and 1st July.

Comfort temperature, maximum and minimum acceptable temperature range and air temperature of Case 24, 25, 26 are stated in Figure 7-20. From Figure 7-20 it is evident that air temperature of the Predicted model, Case 24, 25 and 26 rose significantly above the maximum acceptable temperature, particularly in 30th June and 1st July 2015. Therefore the overheated condition observed in on-site monitoring was not possible to eliminate with the scenarios investigated, even if existing windows were 100% open. It was also apparent that for 40% of the occupied hours air temperature of predicted model was above Tmax, which was less in Case 26 (31%), Case 25 (33.33%) and Case (35.55%).

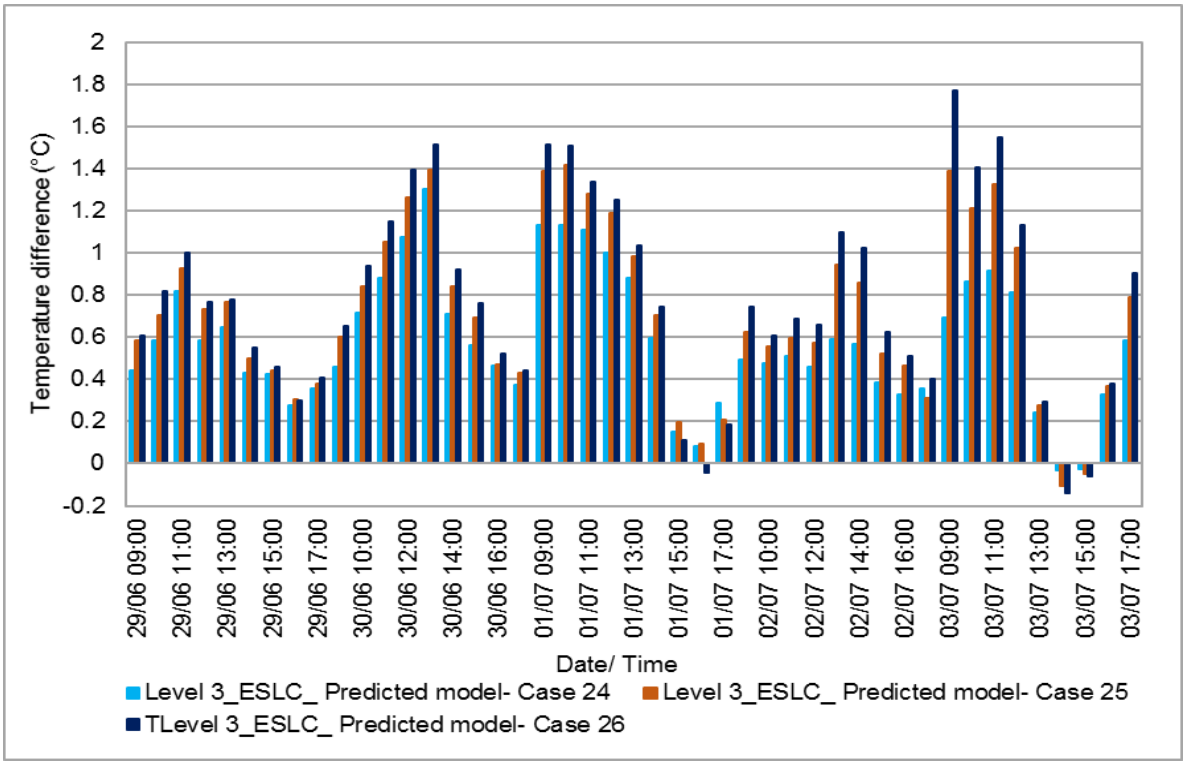


Figure 7-19: Temperature differences between case 24, 25, and 26 and predicted air temperatures during occupied hours (ESLC)

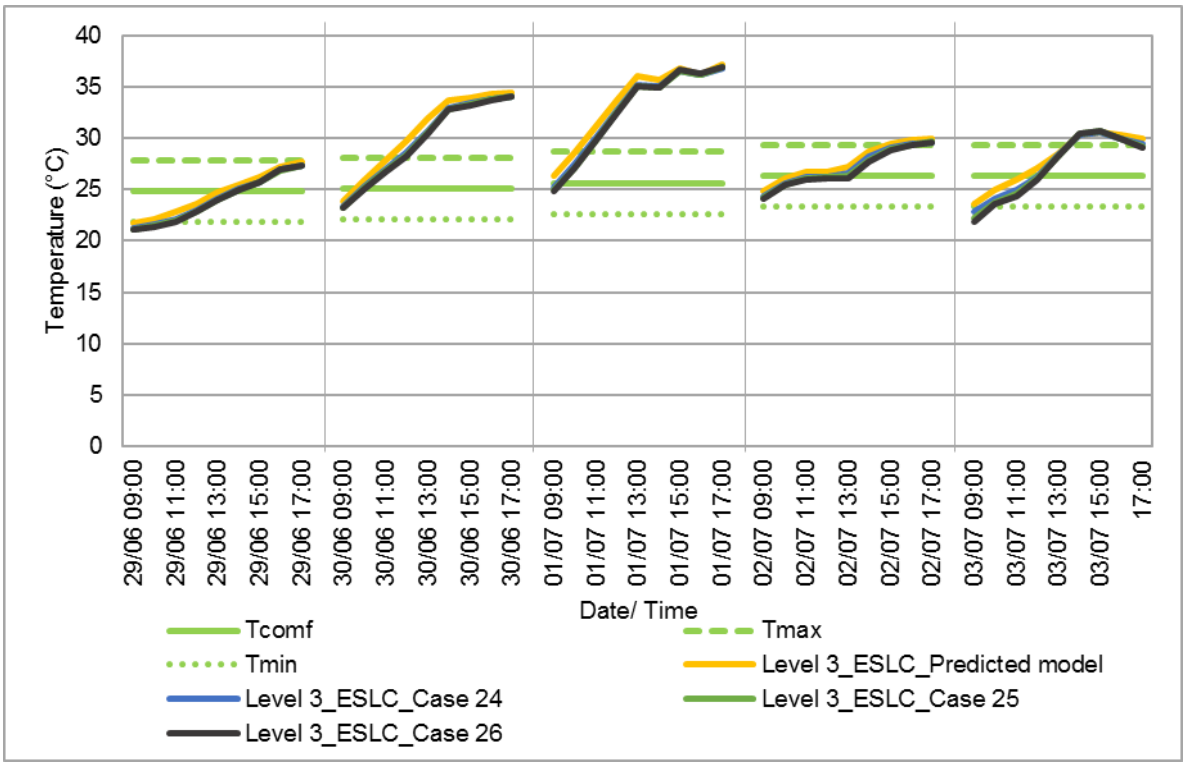


Figure 7-20: Air temperatures of Predicted, Case 24, Case 25, Case 26 model maximum, minimum and comfort temperature (ESLC)

The results obtained from simulation cases of Nottingham High School and ESLC is summarised in Table 7-29.

Table 7-29: Results and remarks on simulation criteria

Simulation Cases	Result	Remark on Nottingham High School	Consideration	Remark on ESLC	Consideration
Case 1 - 7	No variation was observed between Predicted and Case 1-7	In an ETFE cushion roof, change of optical properties of top layer of ETFE foil had no impact on internal air temperature	Decided to modify properties of top and bottom layer	Similar to Nottingham High School	Decided to modify properties of top and bottom layer
Case 8-14	No variation was observed between Predicted and Case 8-14	In an ETFE cushion roof, variation in optical properties of top and bottom layer of ETFE foil had no significant impact on internal air temperature	To modify emissivity of ETFE foil	Similar to Nottingham High School	To modify emissivity of ETFE foil
Case 15-19	No variation was observed between Predicted and Case 15-19	Variation in emissivity of ETFE foil had no significant impact on internal air temperature	To change opening area, by operating existing windows those were fixed in existing building	Similar to Nottingham High School	To change opening area, by operating existing windows those were fixed in existing building
Case 20	No variation observed	Windows open in south and west façade had no noticeable impact on air temperature	To operate windows located in north facade	Windows open in south-east and west façade had no significant impact on air temperature	To operate windows located in north-east and west facade
Case 21	No variation observed	Windows open in north, south and west façade had no substantial impact on air temperature	To operate windows located in east and west facade	Not applicable	Not applicable
Case 22	No variation observed	No noticeable variation in air temperature even if windows located in south, east and west were operable	To operate all the windows and opening factor 0.25	Windows open in north-east and west façade had no considerable impact on air temperature	To operate all the windows and opening factor 0.25

(Table 7-29 continued)

Case 23	No significant variation observed	Even if the all the windows were 25% open, this had no significant impact on air temperature of the second floor	Increase opening factor to 0.5.	Condition observed was similar to that of Nottingham High School atrium	Increase opening factor to 0.5.
Case 24	Air temperature was on average 0.5°C~0.6°C lower than predicted air temperature Maximum reduction 0.7°C	17.5% of occupied hour air temperature was above maximum acceptable temperature (Tmax) [20% of hour occupied hour predicted air temperature was hotter than Tmax]	Did not fulfil comfort criteria stated in CIBSE TM52, CIBSE TM57. To increase opening factor to 0.75.	35.33% of occupied hour air temperature was above maximum acceptable temperature (Tmax) [42% of hours occupied hour predicted air temperature was hotter than Tmax]	Did not fulfil comfort criteria stated in CIBSE TM52, CIBSE TM57. To increase opening factor to 0.75.
Case 25	On average air temperature reduced by 0.6°C ~0.9°C from predicted model Maximum reduction 1 °C	Similar to Case 24	Did not fulfil comfort criteria stated in CIBSE TM52, CIBSE TM57. To increase opening factor to 1.	33.33% of occupied hour air temperature was above maximum acceptable temperature	Did not fulfil comfort criteria stated in CIBSE TM52, CIBSE TM57. To increase opening factor to 1.
Case 26	Air temperature reduced by 0.8°C ~1.2°C, maximum 1.44°C reduced from predicted air temperature	15% of occupied hour air temperature above maximum acceptable temperature (Tmax)	Even if all the windows opened 100%, air temperature of the second floor of the atrium did not fulfil comfort criteria stated in CIBSE TM52, CIBSE TM57.	31% of occupied hour air temperature was above maximum acceptable temperature	Even if all the windows opened 100%, air temperature of second floor of the atrium did not fulfil comfort criteria stated in CIBSE TM52, CIBSE TM57.

7.12 Comparison with glass roof

This section presents a comparison of the thermal performance of atria enclosed with an ETFE-foil cushion roof and polycarbonate and glass roofs. To do that, ETFE-foil cushion roof of the Predicted model of the Nottingham High School and ESLC was replaced with a polycarbonate or glass roof. Various single and double glazing units were used to roof Predicted model. Specifications of these gazing units can be found from Table 7-2.

7.12.1 Comparison of thermal performance of ETFE foil cushion and glass

Thermal performance of the atria roofed with ETFE cushion, polycarbonate and glass was evaluated based on overheating criteria stated in CIBSE TM52 for Category II buildings (CIBSE, 2013b) and CIBSE guide A (CIBSE, 2006, CIBSE, 2015b). This calculation was performed for the time period stated in Table 7-28. The results are presented in Table 7-30 and Table 7-31.

Table 7-30: Percentage of Hours air temperature of Predicted simulation models enclosed with ETFE cushion roof and different type of glazing above T_{max} during Peak period

Roof material	Criterion 1	Criterion 2	Criterion 3	CIBSE guide A
Two layer ETFE-foil cushion roof 75% fritted top layer and Transparent bottom layer. Cushion covered with rain mesh externally	Fail Percentage of hour air temperature > Tmax =20%	Fail We = 13	Fail ΔT= 5K	Fail Maximum temperature =33.2° C
Glazing type 1	Fail Percentage of hour air temperature > Tmax =75%	Fail We = 40	Fail ΔT= 7K	Fail Maximum temperature =35.3° C
Glazing type 2	Fail Percentage of hour air temperature > Tmax =62.5%	Fail We = 28	Fail ΔT= 6K	Fail Maximum temperature =34.25° C
Glazing type 3	Fail Percentage of hour air temperature > Tmax =90%	Fail We = 65	Fail ΔT= 12K	Fail Maximum temperature =39.9° C
Glazing type 4	Fail Percentage of hour air temperature > Tmax =88%	Fail We = 60	Fail ΔT= 12K	Fail Maximum temperature =39.7° C
Glazing type 7	Fail Percentage of hour air temperature > Tmax =65%	Fail We = 29	Fail ΔT= 7K	Fail Maximum temperature =35° C

Table 7-31: Percentage of Hours air temperature of Predicted simulation models enclosed with ETFE cushion roof and different type of glazing above T_{max} during Peak period

Roof material	Criterion 1	Criterion 2	Criterion 3	CIBSE guide A
ETFE cushion roof Three layer ETFE-foil cushion with 65% fritted top layer, transparent bottom and middle layers	Fail Percentage of hour air temperature > Tmax =42%	Fail We = 45	Fail ΔT= 8K	Fail Maximum temperature =37° C
Glazing type 1	Fail Percentage of hour air temperature > Tmax =46.67%	Fail We = 43	Fail ΔT= 8K	Fail Maximum temperature =37° C
Glazing type 2	Fail Percentage of hour air temperature > Tmax =46.67%	Fail We = 42	Fail ΔT= 8K	Fail Maximum temperature =37° C
Glazing type 3	Percentage of hour air temperature > Tmax =60%	Fail We = 65	Fail ΔT= 11K	Fail Maximum temperature =39.5° C
Glazing type 4	Fail Percentage of hour air temperature > Tmax =58%	Fail We = 63	Fail ΔT= 11K	Fail Maximum temperature =39.8° C
Glazing type 7	Fail Percentage of hour air temperature > Tmax =46.67%	Fail We = 48	Fail ΔT= 9K	Fail Maximum temperature =37.5° C

The results showed that all of the simulation models with two-layer and three-layer ETFE foil cushion roof, polycarbonate and glass roofs failed to meet the criteria stated in CIBSE TM52 and CIBSE guide A. Therefore, the model roofed two-layer and three-layer ETFE foil cushion roof, polycarbonate and glass roofs were overheated.

7.12.2 Comparison of energy consumption of ETFE foil cushions, polycarbonate and glass

During the selected period stated in Table 7-28 cooling loads were calculated for the atrium spaces covered with two-layer and three-layer ETFE-foil cushion roofs, polycarbonate and glass roofs. The results showed that cooling load of the predicted model of the ESLC (roofed with three-layer ETFE foil cushion) was higher than that of the Nottingham High School (roofed with two-layer ETFE foil cushion). Figure 7-21 presents cooling loads of the predicted model of the Nottingham High School and cooling load of this same model when covered with Glazing type 1, 2 and 3. Whereas Figure 7-22 states cooling load of the predicted model of the ESLC and cooling load

of this same model when it was roofed with Glazing type 1, 2 and 3. The results, demonstrated that during peak periods the cooling load of the Nottingham High School model when enclosed with two-layer ETFE-foil cushion roof, was up to 42.5% less than that of the same model when enclosed with a glazed roofs. During this period, the cooling load of the predicted model of the ESLC enclosed with ETFE roof was also less (up to 14.5%) than that of model enclosed with glazed roofs, Glazing type 3 roof in particular.

Insulation properties of three-layer the ETFE-foil cushion roof compared to the two-layer ETFE-foil was better due to the extra layer of air and ETFE-foil. Moreover, fritting and rain mesh reduced solar gain by creating shading in the model enclosed with the two-layer ETFE-foil cushion roof. As a result, cooling load of the model enclosed with three-layer ETFE-foil cushion roof was higher than the two-layer ETFE-foil cushion roof. However, a glazing panel with low- E coating also caused a significant rise in air temperature of the spaces and, due to the presence of the low-E coating which limits heat exchange between warm indoor towards relatively cold outdoor, increased the cooling load of the spaces.

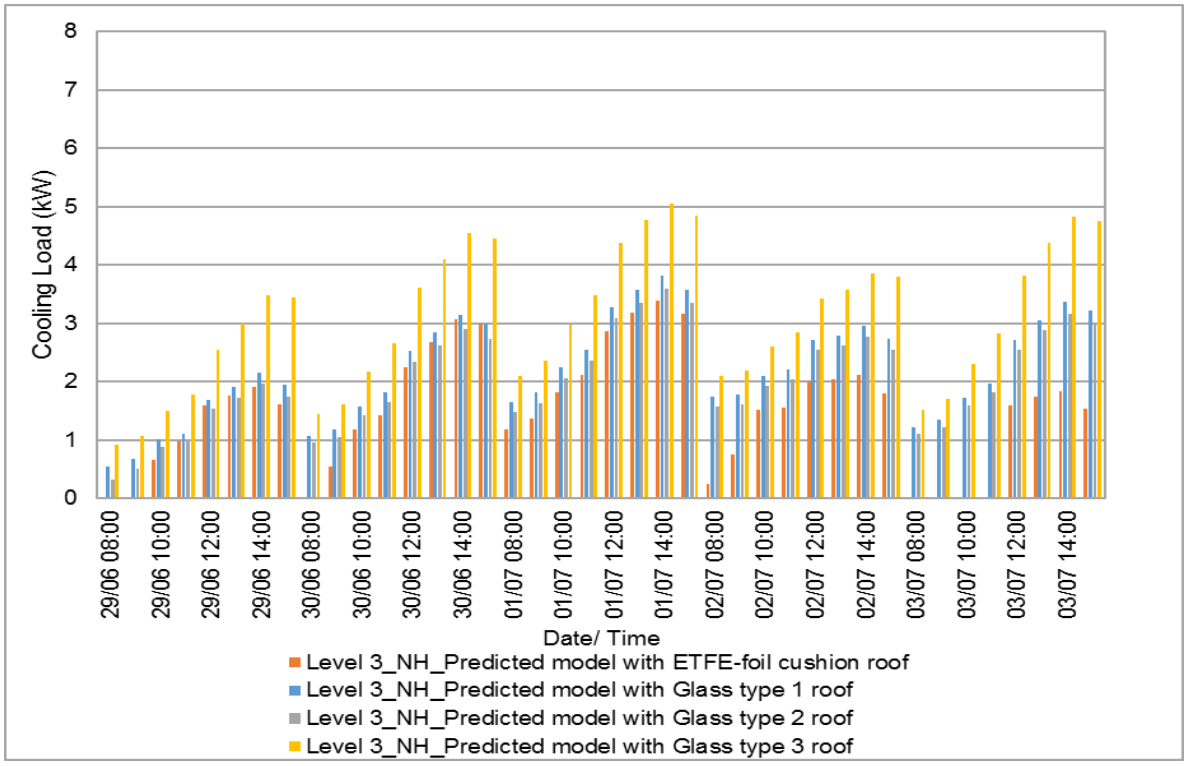


Figure 7-21: Cooling load in Predicted model of Nottingham High School, roofed with two layer ETFE cushion and Glass type 1, 2, 3

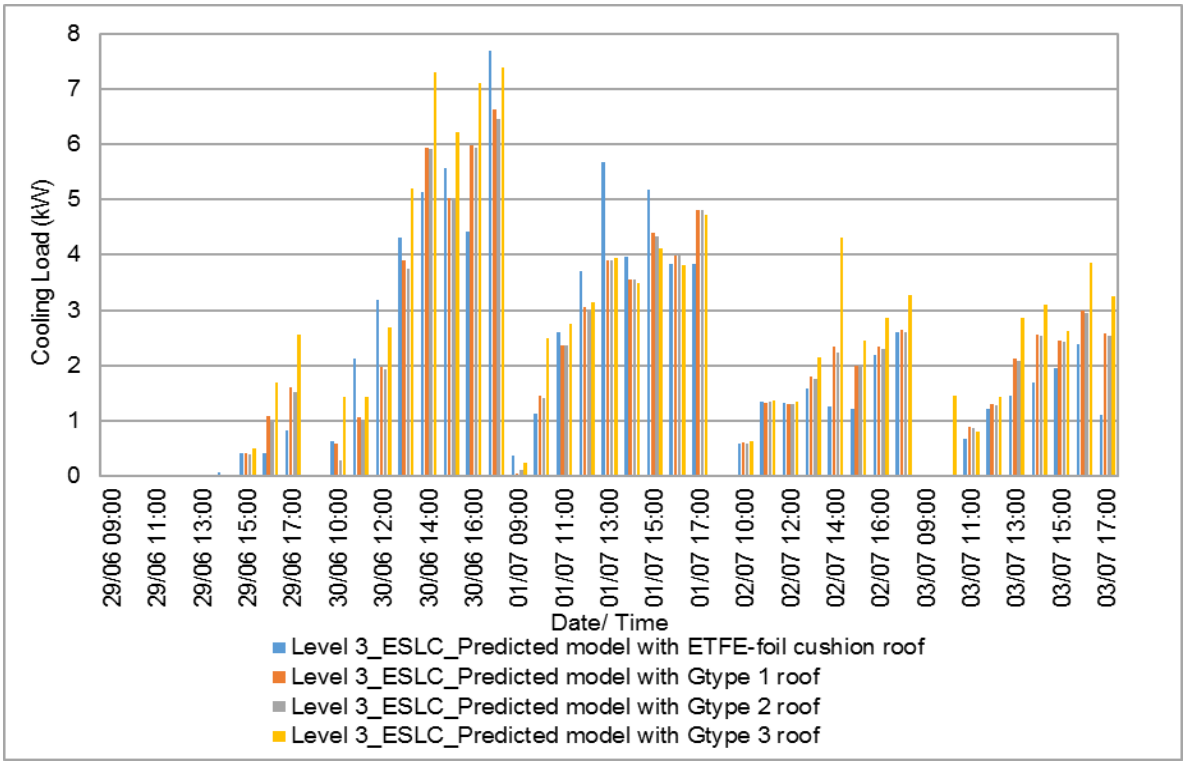


Figure 7-22: Cooling load in Predicted model of ESLC, roofed with three layer ETFE cushion and Glass type 1, 2, 3

7.13 Future weather data

A simulation approach was used to investigate the thermal performance of the atria of Nottingham High School and the ESLC in 2050 and 2080 using UKCIP climate change scenarios.

The objective of this section is to investigate the performance of the Nottingham High School and the ESLC in 2050 and 2080 to see how these models will perform in future. This was done by changing the weather file while all other input parameters of the simulation were similar to the Predicted models of both of the buildings.

7.13.1 The result

Table 7-32 presents percentage of occupied hours when the air temperature of the second floor (Level 3) of the atrium was hotter than the maximum acceptable temperature (T_{max}) during 2015, 2050 and 2080. This maximum acceptable temperature (T_{max}) was calculated based on outdoor air temperature which was obtained from the weather file for the year 2050 and 2080.

Table 7-32: Projected Scenario of the predicted model of the Nottingham High School and ESLC

Period	Nottingham High School	ESLC
Time period considered in simulation	Between 18th June and 3rd July	
Number of occupied hours	96	108
Atrium level	Level 3 (Second floor)	
2015	8% of occupied hours > T_{max}	17.6% of occupied hours > T_{max}
2050	16.67% of occupied hours > T_{max}	37.2% of occupied hours > T_{max}
2080	21.88% of occupied hours > T_{max}	48.5% of occupied hours > T_{max}

The result of the simulation showed that both of these atria will also face the overheating problems in 2050 and 2080. Nevertheless, the extent of overheating will be higher than that observed in the recent time (2015).

7.14 Summary

This chapter presented simulation-based analysis to evaluate and compare the thermal performance of the atria enclosed with ETFE-foil cushion, polycarbonate and glass roofs with a view to identifying the specific influence of these construction materials may induce.

To represent doubly curved surfaces in the simulation was a difficult task. Therefore, a procedure was developed to represent the roof configuration of ETFE-foil cushions in the simulation model. Using this roof configuration, simulation of atria enclosed with ETFE-foil cushion roofs was completed. Simulation models were calibrated by validating results with the measured data and the results agreed well. The calibration process indicated that occupancy profile, window opening, internal gains, and roof shape etc., impact air temperature of both of the atria.

It was also identified that modelling the doubly curved surface of an ETFE-foil cushion roof as flat panels could impact the accuracy of the predicted models. This was evident in both of the atria.

The results from on-site monitoring identified that the atria overheated in summer 2015, detailed findings were presented in Chapter 6. Therefore, an initiative was made to apply alternative approaches to mitigate this overheating problem from both of the atria. The results showed that by varying thermal optical properties of ETFE-foil cushion, it was not possible to eliminate existing overheating problems. However, in both of the atria, by opening existing windows 100% for 24 hours, it was possible to

reduce the number of hours when indoor air temperatures were below the maximum acceptable temperature T_{max}. Thus, window opening influenced indoor thermal environment. This result was consistent with Moosavi et al. (2014). However, this criterion was not able to fulfil the criteria stated in CIBSE TM52 to mitigate overheating. Besides it may not be a realistic solution that windows will be open 100% for 24 hours.

The results of the study also showed that indoor air temperature of the modelled test-rig enclosed with two-layer and three-layer ETFE-foil panels was hotter than when covered with a double glazing unit constructed of polycarbonate (e.g. Glazing type 1 and 2). The results further show that indoor air temperature of spaces (replicated model of the test- rig and both atria) configured with double glazing panels with low-E coating was hotter when enclosed with two and three-layer ETFE-foil flat panels as well as cushions.

Comparison of air temperature of atria covered with two-layer and three-layer ETFE-foil cushion, polycarbonate and glass roofs showed that atria covered with glazed roofs were also overheated. Moreover, the extent of overheating was higher in the atria when enclosed with a glass roof than ETFE-foil cushion roof.

The simulation also measured the energy consumption for both of the atria. The results showed that cooling load of the predicted model of the ESLC (roofed with three-layer ETFE foil cushion) was higher than that of the Nottingham High School (roofed with two-layer ETFE foil cushion). The results also showed that atria with double glazing with low-E coating increased cooling load compared with an ETFE-foil cushion roof (both two-layer and three-layer).

The thermal environment is largely influenced by solar gain, internal gains, ventilation opportunities and construction U-values of the space; roof configuration may have an impact on the internal thermal environment as well. The insulation properties were improved for three-layer ETFE-foil cushions (used in the ESLC) compared to two-layer ETFE-foil cushions (used in Nottingham High School) may cause to stabilise the high temperature for longer period. Also, fritting and rain mesh (used in Nottingham High School) may reduce direct solar gain by creating shading in the space enclosed with two-layer the ETFE-foil cushion roof. As a result, cooling load of the model enclosed with the three-layer ETFE-foil cushion roof was higher than the two-layer ETFE-foil cushion roof. However, a glazing panel with low-E coating also caused a significant rise in the indoor air temperature, this may be because the presence of low-E coating limits heat exchange between warm indoor towards relatively cold outdoor, therefore increased required cooling load.

Simulation performed using projected climate scenarios showed that both of the atria will be overheated in 2050 and 2080, however it is expected that the extent of overheating will be higher than that observed in this study.

Chapter 8

8 Discussion and Conclusions

8.1 Introduction

This chapter summarises the findings from previous chapters and draws conclusions. The results are analysed critically and correlated to obtain the collective outcome of the empirical research. At the beginning, the chapter presents a summary of results gathered through experimental investigation of ETFE-foil material properties; data collection and analysis from onsite monitoring; and simulation. This chapter also evaluates the research methods adopted to conduct the research. A set of design recommendations are proposed on the basis of theoretical knowledge and findings obtained from the empirical studies. Finally, the chapter discusses the fulfilment of research aim and objectives. Novelty of the study and contribution to the knowledge are discussed with limitations and future research.

8.2 Summary of findings

8.2.1 Investigation of thermal-optical properties

Experimental investigations were carried out to determine the thermal-optical properties of ETFE-foils. ETFE-foil samples were selected which are typically used in the construction of building envelopes. On the basis of measured thermal-optical properties of foil samples, properties of single, two- and three-layer ETFE-foils were calculated. Thermal-optical behaviour was identified for a range of combinations of single, two- and three-layer ETFE-foil panels. A list of various combinations is presented in Table 8-1 and a summary of identified thermal-optical properties of these combinations are presented Table 8-2. Detailed descriptions of foil types and combinations, and methods used in these investigations were presented in Chapter 4.

Thermal-optical properties of single, two- and three-layer foils developed knowledge on solar and light transmittance of different types of ETFE-foil and combination of ETFE-foils which was one of the barriers in the development of ETFE-foil and its building integration, particularly for the fritted foil types. This information about properties will enable designers to select ETFE-foils to integrate in building envelopes in the form of cushions or panels, depending on the functional requirement of the spaces.

Thermal transmittance of a two layer ETFE-foil cushion was also determined using a steady-state method. Detail methodological descriptions are discussed in Chapter 4 (section 4.7). The results summarised that thermal transmittance (U-value) of a single cushion varied at different cross sections (see Figure 4-13). This variation was due to the influence of air conductance that varies in the same cushion due to curvature. As a result, the thermal transmittance of the middle of the cushion (highest point in the camber) was less than near the edge. Thermal transmittance is also influenced by emissivity, such that the thermal transmittance of ETFE-foil cushion decreases as the emissivity of foil layers' increases. This was the result of the reduction in radiation conductance in the ETFE-foil cushion due to the increase of emissivity of ETFE-foil layers.

Table 8-1: List of properties, and combination of single, two and three-layer ETFE-foils

Properties of Single Layer ETFE-foils					Combination of Two Layer ETFE-foil panels			Combination of Three Layer ETFE-foil panels			
Type (single layer)	**Thick-ness**	**Transparent part**	**Fritted part**	**Colour of fritting (density of pigment)**	**Combi-nation**	**Layer 1 (single layer type)**	**Layer 2 (single layer type)**	**Combi-nation**	**Layer 1 (singles layer type)**	**Layer 2 (single layer type)**	**Layer 3 (single layer type)**
Type 1	100µm	100%	-	-	Combination 1	Type 3	Type 6.1	Combination 16	Type 3	Type 1	Type 6.1
Type 2	150µm	100%	-	-	Combination 2	Type 3	Type 6.2	Combination 17	Type 3	Type 1	Type 6.2
Type 3	200µm	100%	-	-	Combination 3	Type 3	Type 6.3	Combination 18	Type 3	Type 1	Type 6.3
Type 4	300µm	100%	-	-	Combination 4	Type 3	Type 6.4	Combination 19	Type 3	Type 1	Type 6.4
Type 5	500µm	100%	-	-	Combination 5	Type 3	Type 6.5	Combination 20	Type 3	Type 1	Type 6.5
Type 6.1	200µm	75%	25%	25% silver (translucent)	Combination 6	Type 3	Type 7.1	Combination 21	Type 3	Type 1	Type 7.1
Type 6.2	200µm	50%	50%	25% silver (translucent)	Combination 7	Type 3	Type 7.2	Combination 22	Type 3	Type 1	Type 7.2
Type 6.3	200µm	35%	65%	25% silver (translucent)	Combination 8	Type 3	Type 7.3	Combination 23	Type 3	Type 1	Type 7.3
Type 6.4	200µm	25%	75%	25% silver (translucent)	Combination 9	Type 3	Type 7.4	Combination 24	Type 3	Type 1	Type 7.4
Type 6.5	200µm	11%	89%	25% silver (translucent)	Combination 10	Type 3	Type 7.5	Combination 25	Type 3	Type 1	Type 7.5
Type 7.1	200µm	75%	25%	50% silver (translucent)	Combination 11	Type 3	Type 8.1	Combination 26	Type 3	Type 1	Type 8.1

(Table 8-1 continued)

Properties of Single Layer ETFE-foils					Combination of Two Layer ETFE-foil panels			Combination of Three Layer ETFE-foil panels			
Type (single layer)	**Thick-ness**	**Transparent part**	**Fritted part**	**Colour of fritting (density of pigment)**	**Combi-nation**	**Layer 1 (single layer type)**	**Layer 2 (single layer type)**	**Combi-nation**	**Layer 1 (singles layer type)**	**Layer 2 (single layer type)**	**Layer 3 (single layer type)**
Type 7.2	200µm	50%	50%	50% silver (translucent)	Combination 12	Type 3	Type 8.2	Combination 27	Type 3	Type 1	Type 8.2
Type 7.3	200µm	35%	65%	50% silver (translucent)	Combination 13	Type 3	Type 8.3	Combination 28	Type 3	Type 1	Type 8.3
Type 7.4	200µm	25%	75%	50% silver (translucent)	Combination 14	Type 3	Type 8.4	Combination 29	Type 3	Type 1	Type 8.4
Type 7.5	200µm	11%	89%	50% silver (translucent)	Combination 15	Type 3	Type 8.5	Combination 30	Type 3	Type 1	Type 8.5
Type 8.1	200µm	75%	25%	100% silver (opaque)							
Type 8.2	200µm	50%	50%	100% silver (opaque)							
Type 8.3	200µm	35%	65%	100% silver (opaque)							
Type 8.4	200µm	25%	75%	100% silver (opaque)							
Type 8.5	200µm	11%	89%	100% silver (opaque)							

Table 8-2: Thermal optical properties of single, two- and three-layer ETFE-foils

Single layer			Double layer			Three layer		
Type (single layer)	**Solar transmittance**	**Light transmittance**	**Combination**	**Solar transmittance**	**Light transmittance**	**Type (three Layer)**	**Solar transmittance**	**Light transmittance**
Type 1	0.91	0.905	Combination 1	0.644	0.62	Combination 16	0.6	0.586
Type 2	0.87	0.859	Combination 2	0.53	0.52	Combination 17	0.5	0.494
Type 3	0.86	0.84	Combination 3	0.46	0.456	Combination 18	0.44	0.435
Type 4	0.794	0.763	Combination 4	0.436	0.434	Combination 19	0.42	0.415
Type 5	0.76	0.724	Combination 5	0.345	0.349	Combination 20	0.33	0.336
Type 6.1	0.719	0.708	Combination 6	0.594	0.574	Combination 21	0.56	0.542
Type 6.2	0.582	0.578	Combination 7	0.43	0.415	Combination 22	0.41	0.398
Type 6.3	0.499	0.5	Combination 8	0.325	0.314	Combination 23	0.31	0.304
Type 6.4	0.472	0.4739	Combination 9	0.289	0.28	Combination 24	0.28	0.272
Type 6.5	0.367	0.375	Combination 10	0.15	0.145	Combination 25	0.148	0.143
Type 7.1	0.66	0.645	Combination 11	0.58	0.562	Combination 26	0.55	0.53
Type 7.2	0.464	0.45	Combination 12	0.4	0.389	Combination 27	0.385	0.374
Type 7.3	0.346	0.335	Combination 13	0.286	0.28	Combination 28	0.277	0.2715
Type 7.4	0.307	0.304	Combination 14	0.25	0.24	Combination 29	0.243	0.236
Type 7.5	0.157	0.149	Combination 15	0.1	0.094	Combination 30	0.096	0.093
Type 8.1	0.645	0.63						
Type 8.2	0.434	0.422						
Type 8.3	0.307	0.296						
Type 8.4	0.265	0.255						
Type 8.5	0.1044	0.096						

The steady-state method was employed here to calculate thermal transmittance of two layer ETFE-foil cushion. This derived value was 93% (3.12 W/m^{2}K, middle of the cushion) to 82% (3.55 W/m^{2}K, edge of the cushion) of the value (see Table 4-6) presented in Poirazis et al. (2009). Therefore, using the method stated in BS 6993: Part 1 (BSI 1989), it is possible to generate U-values. However, these values need to be verified using other established methods such as Hot-Box testing. On the basis of the results obtained on thermal transmittance, a number of assumptions can be made which might impact the thermal performance of ETFE-foil cushion and spaces enclosed with ETFE-foil cushion envelope by allowing or limiting exchange of heat with the external thermal environment.

8.2.2 Summary of findings from test-rig experiment

This study analysed the thermal performance of single, two- and three- layer ETFE-foil panels in an experimental environment in two phases.

In the first phase of the experiment, solar transmittance of single, two- and three- layer ETFE-foil panels were measured through on-site monitoring in test-rigs placed in the outdoor environment. The results obtained from this experiment demonstrated that under actual outdoor environment, solar transmittance of ETFE-foil panels varied during different times of the day depending on the position of the sun.

In the second phase of the experiment the thermal performance of the single, two- and three- layer ETFE-foil panels were evaluated though on-site monitoring using test-rigs in the outdoor environment. The results showed that-

- Surface temperature of the ETFE-foil and the thermal environment of the test-rig changed rapidly as a result of the variations in the outdoor conditions e.g. solar radiation, outdoor temperature etc.
- Under the same external condition, heat was better preserved in the test-rig enclosed with three-layer ETFE-foil panel system, than with the two-layer ETFE-foil panel system.
- Density of fritting also influenced thermal environment enclosed with ETFE-foil panel by reducing solar gain.
- Thermal environment of the test-rigs were affected by the variations in the surface temperatures of ETFE-foils and, the air temperature of the air-volume enclosed with ETFE-foils, by convective and radiative heat transfer mechanism.

- During the day this heat transfer was dominated by short-wave radiation and increased mean radiant temperature of the adjacent air. Whereas at night, due to the impact of long-wave radiation exchange between the surface of ETFE-foil and cold night sky, foil surface temperature decreased, this, in turn, reduced heat transfers in air and ETFE-foil layers, and also reduced mean radiant temperature of the air adjacent to it.
- In this experiment impact of rain-mesh on the test-rigs' air temperatures were evident in (Figure 5-33). The shading created by rain-mesh reduced foil surfaces temperatures as well as air temperatures inside the test-rig.

8.2.3 Summary of findings from on-site monitoring of actual buildings

Environmental data was collected from two different atria with different configurations of ETFE-foil cushion roof.

8.2.3.1 Thermal behaviour of spaces enclosed with ETFE-foil cushion roof

Thermal behaviour was studied based on clear sky conditions and overcast sky conditions.

Thermal environment, on a typical sunny day was particularly influenced by the surface temperature of ETFE-foil cushion, radiant temperature, solar gain into the enclosure and, outdoor air temperature. Typically, during an overcast day, this thermal environment was more stable with relatively uniform temperature distribution.

The roof demonstrated more extreme thermal behavior under clear sky conditions where both direct solar and long-wave infrared radiation appeared to govern the fluctuations of the ETFE-foil surface temperatures.

It was apparent that, outdoor temperatures, as well as transmitted solar radiation, had a strong positive relationship with the indoor air temperatures of occupied levels and, level adjacent to ETFE-foil cushion roof, while the surface temperatures of ETFE-foil cushion were strongly related with adjacent mean radiant temperature (Correlation coefficient R^2 value ranged from 0.952 to 0.984).

The thermal environment observed in both of the atria on overcast days in summer was similar. However, on hot summer days during the day the extent of stratification was more significant in the ESLC atrium (enclosed with three-layer cushion) than the Nottingham High School atrium (enclosed with two-layer cushion). Whereas, at night air temperature of the ESLC atrium was on average 2°C less than the average air temperature of the Nottingham High School atrium. Table 8-3 and Table 8-4

respectively present maximum, minimum, average and standard deviation of air temperature, and comparison of stratification of air temperatures on an extremely hot day (1st July 2015). The results indicated that maximum air temperature as well as maximum temperature stratification occurred in the ESLC atrium. Possible reason of this variation could be the peripheral masonry wall (U value 0.6 W/m^{2}K), ETFE-foil cushion covered with rain noise suppression mesh and, percentage of fritted part (75% fritting) of top ETFE-foil layer that reduces surface temperature and solar gain by creating shading in the Nottingham High School atrium. Whereas the higher level of thermal insulation provided by the 3-layer cushion roof, wall (0.23 W/m^{2}K) and floor (0.2 W/m^{2}K) of ESLC atrium resulted in the increase of average air temperature during the day. However, at night longwave radiation losses were pronounced in the ETFE-foil cushion roof with 65% fritted top layer, which resulted in the decrease of average air temperature of the atrium. Transparency of ETFE-foils to longwave radiation was apparent in the results presented in Chapter 4 and Poirazis et al. (2009). Moreover, at night this variation of air temperatures between these two atria also indicated that, longwave radiation losses through ETFE-foil cushion roof was less when the ETFE-foil cushion was covered with rain-mesh. At night the surface temperature of ETFE-foil dropped below the outdoor temperature but the rain suppression mesh temperature stayed above, or similar to, the outdoor air temperature, and above the external surface temperature of the ETFE-foil cushion. This was evident at Nottingham High School and also in the test-rig experiment (chapter 5).

Table 8-3: Summary of air temperature (°C) at different levels of the atria on 1st July 2015

Air temperature	**Case Study A: Nottingham Boys High School**			**Case Study B: Engineering and Science Learning center (ESLC)**		
	Level 1	Level 2	Level 3	Level 1	Level 2	Level 3
Maximum	29.89	31.17	33.86	28.85	32.55	36.8
Minimum	23.08	24.64	25.13	23.71	24.47	24.42
Diurnal average	27.13	28.06	29.25	25.98	27.7	29.79
Standard deviation	1.27	1.47	1.418	1.1	1.16	1.58

Table 8-4: Comparison of extreme temperature differences (thermal stratification) between different levels in the monitored atria (1st July 2015)

	Case Study A: Nottingham Boys High School (Level 3-Level 1)	**Case Study B: Engineering and Science Learning centre (Level 3-Level 1)**
Maximum	4.24°C	9.64°C
Minimum	0.99°C	0.34°C
Diurnal average	2.13°C	3.81°C
	Case Study A: Nottingham Boys High School (Level 4-Level 3) **Height difference between level 4 and 3 was 7.5 metres**	**Case Study B: Engineering and Science Learning centre (Level 4-Level 3)** **Height difference between level 4 and 3 was 3.25 metres**
Maximum	8.15°C	5.75°C
Minimum	-1.2°C	0.06°C
Diurnal average	2.76°C	1.38°C

Table 8-5: Comparison of temperature difference (°C) between individual atrium levels and outdoor air temperature

Air temperature	**Case Study A: Nottingham Boys High School**			**Case Study B: Engineering and Science Learning center (ESLC)**		
	Level 1-OAT	Level 2-OAT	Level 3-OAT	Level 1-OAT	Level 2-OAT	Level 3-OAT
Maximum	6.85	7.42	8.06	5.84	6.23	6.5
Minimum	-4.09	-3.12	-1.45	-9.73	-7.04	-2.49
Diurnal average	0.98	1.92	3.11	-2.19	-0.44	1.62

On an extremely hot day, 1st July 2015, in both of the case study atria, a significant rise of air temperature was evident. On that day, for 1.6% to 2.9% of occupied hours the air temperature of Level 3 exceeded 32°C. This significant rise in air temperatures, as well as the duration, could have considerable effects on the thermal comfort of the occupants. Therefore, guides and standards were used to evaluate thermal comfort of both atria.

8.2.3.2 CIBSE (Guide A and TM52) and BB101 performance of existing spaces enclosed with ETFE-foil cushion roof

Thermal comfort assessment of the Nottingham High School and ESLC atria during summer 2014 and 2015 was done on the basis of the criteria stated in CIBSE temperature benchmark, CIBSE TM52 and BB101. The results are presented in Table 6-6.

Thermal comfort assessment showed that, Level 3 of the Nottingham High School atrium 2.5% of occupied hours in summer, the air temperature went above 28°C. Even during occupied hours, the air temperature at this level stayed above 32°C between 12.30pm and 15.00pm on 1st July 2015. Whereas for Level 3 of the ESLC atrium, for 3.17% (location a) and 7.35% (location b) of occupied hours the air temperature went above 28°C. Moreover, the air temperature of location b of Level 3 of this atrium also failed to comply with the CIBSE temperature benchmark during 2014 (Table 6-6), as for 2.28% of occupied hours the temperature of this location went above 28°C.

In Nottingham High School atrium the Level 2 and 3 air temperature exceeded the maximum acceptable temperature (T_{max}) for 2.29% and 10.63% of occupied hours respectively, whereas the daily weighted exceedance (W_e) was at a maximum of 7 (Level 2) and 13 (Level 3). Also for Level 3 the temperature difference (difference between air temperature and T_{max}) went above 4K for 1.67% of occupied hours. Therefore, Level 2 and 3 of Nottingham High School atrium failed to comply with the criteria stated in CIBSE TM52 (CIBSE, 2013b).

In the ESLC atrium, the Level 3 air temperature was above T_{max} for 7.58% (location a) and 9.75% (location b) of occupied hours, and the weighted exceedance was a maximum of 36 (location a) and 42 (location b). Also for 0.94% (location a) and 1.49% (location b) of occupied hours the temperature difference (difference between air temperature and T_{max}) went above 4K. Furthermore, the Level 2 air temperature (location a) was above T_{max} for 3.38% of occupied hours, and the weighted exceedance was a maximum of 36. Thus, Level 3 and Level 2 of the ESLC atrium failed to meet the criteria stated in CIBSE TM52 during 2015. Besides, location b of Level 3 also failed to comply with the criteria during 2014, as for 4.9% of occupied hours the air temperature of this location went above T_{max} and the daily weighted exceedance (W_e) was a maximum of 7. Thus, this level 3 (location b) also failed to meet the criteria during summer 2014.

Again, in the Nottingham High School atrium the temperature difference between Level 3 and outdoor air temperature was above 5°C for 445 hours and Level 3 air temperature went above 32°C, thus this level of the atrium also failed to comply with the criteria stated in BB101.

Thus, the above results showed that in both of the atria (both Levels 2 and 3) overheated during summer 2015. In the ESCL atrium, Location b of Level 3 also overheated during summer 2014.

In the Nottingham High School, it was observed air conditioning systems were installed on Level 3 of the atrium during August 2015. This might be one of the initiatives of the school management to ease the excessive air temperatures experienced throughout the summers of 2014 and 2015.

8.2.4 Summary of findings from modelling and simulation

The simulation based analysis evaluated the thermal performance of ETFE-foil panels/cushions of two test-rigs and two case study buildings. The test-rigs were covered with single, two- and three- layer ETFE-foil panels, and detailed descriptions were presented in Chapter 5. The simulation model of the test-rig was also used to investigate various glass panels to compare their thermal performance with that of the ETFE-foil panels.

The results showed that-

- Internal air temperatures of the test-rig with two-layer and three-layer ETFE-foil panels were hotter than the notional glazing unit constructed of polycarbonate (e.g. Gtype 1 and 2). Between the ETFE-foil panels and the glazing panel constructed with polycarbonate, the solar transmittance of polycarbonate (0.203) was less than that of the two-layer and three-layer ETFE-foil panels. However, the presence of air-volume in the ETFE-foil panels might also have an impact on this temperature difference when compared with different glazing types (Glass type 1, 2 and 7).
- It was also evident that the internal air temperatures of test-rig, roofed with a double glazing [Glass type 3 (see Table 7.2)] unit with low-E coating were hotter than both of the above two-layer and three-layer ETFE-foil panels. Also the high solar transmittance of the double glazing unit (0.566) compared to ETFE-foil panels (75% fritted two-layer solar transmittance was 0.42), while low thermal transmittance (1.55 W/m^2K) of glazing panels with low-E coating reduced heat exchange between the interior and exterior, thus increased the internal air temperature of simulation model.

Simulation based analysis was also conducted to evaluate alternative strategies to improve thermal performance under current and projected climatic scenarios for the two case study buildings. The thermal environment of the two existing atria covered with different compositions of ETFE-foil cushion roof were evaluated. The two case study buildings were the Nottingham High School (atrium roof configured with two-layer ETFE-foil cushion), and Engineering and Science Learning Centre (atrium roof

configured with three-layer ETFE-foil cushion). These atria were investigated with various strategies (e.g. by changing the thermal optical properties, the emissivity of ETFE-foil cushion roof etc.) to improve their performance under current and UKCIP projected climate scenarios. Finally, glass panels were applied instead of ETFE-foil cushions for the atrium spaces of these two buildings and a comparative simulation analysis is presented using current climate scenarios.

The simulation results agreed well with the monitored data for both of the atria and indicated that:-

- With various alternative thermal optical properties of the ETFE-foil cushion studied, it was not possible to overcome the existing overheating problem under current scenarios in both of the simulated atria.
- Adequate ventilation through atria would be effective to mitigate overheating. However, with the existing opening area in the two atria studied, it was not possible to eliminate overheating from the large scale atria under current scenarios.
- Both of the atria have a high risk of overheating under current and, projected climate scenarios (2050, 2080). However, the extent of overheating will be higher in future than that observed under current scenarios.

Comparison of air temperature of atria covered with ETFE-foil cushion and glass roof under current scenarios showed that:-

- The extent of overheating was a maximum of 70% higher in the atria when enclosed with a glass roof than an ETFE-foil cushion roof (model roofed with double layer ETFE-foil cushion with 75% fritted top layer and rain mesh, similar to the Nottingham High School atrium roof).
- Both of the atria modelled with two-layer and three-layer ETFE-foil cushion and glass roofs failed to meet the criteria stated in CIBSE temperature benchmark and CIBSE TM52. The results are presented in Table 7-30. As a consequence, atria with glass roofs had increased cooling load in summer compared to ETFE-foil cushion roof.
- During the peak period (a day with extreme outdoor temperature- 1st July 2015) in summer the average cooling load of the atrium enclosed with three layer ETFE-foil cushion roof was similar to (or slightly higher than) that with glass panels. However, two-layer ETFE-foil cushion performed better than glass panels.

- Therefore, ETFE-foil can be applied in the building envelope as an effective alternative to a glass roof (double glazing). This not only improved the thermal environment but also reduced energy consumption by 36.4% on the peak summer day observed during 2015, 1st July.

8.3 Evaluation of methodology

To conduct the empirical research a mixed approach was adopted. Research methods included experimental investigations in the laboratory, onsite monitoring of a test-rig and actual buildings, and computer simulation.

Thermal-optical properties of ETFE-foils were determined by laboratory experiment using the appropriate British Standard. During the experiment, a Biochrom Libra S22 spectrometer and a Fourier Transform Infrared spectrometer IFS 66v/s were used to get the accurate results. The results obtained were validated by comparing with results from previous similar studies. In a number of studies, a similar approach was applied and found effective in determining thermal optical properties of ETFE-foils.

The steady-state method was used to calculate thermal transmittance of an ETFE-foil cushion. This method required various input parameter such as conductance of air, heat transfer co-efficient between exterior to interior, etc. Careful selection of data was important to get the accurate results for this purpose.

The thermal performance of single, two and three layer ETFE-foil panels were analysed by conducting a test-rig experiment. Transparent foils of different thickness and two different percentages of fritted (75% and 25% fritted) ETFE-foils were used. This method was challenging because the experimental setup had to be installed in an exposed outdoor environment with a range of sensors and data-loggers installed in the correct manner. This was a bespoke designed experimental setting considering the above mentioned issues. Moreover, it was necessary to ensure that the ETFE- foil panels could be fitted firmly to withstand extreme weather and could also be replaced easily when required.

The experimental setup included data loggers, pyranometers, etc. Necessary measures were taken to ensure security, such as the data logger being secured in a box with a padlock; and the test-rig containing a pyranometer inside was secured with ETFE-foil panels using padlocks, etc. The safety issue was considered for the users of the adjacent space. Test-rigs were fixed to the roof paving, panels were clamped to the test-rigs to protect them from being blown away by strong winds, etc. This experimental study was completed in two phases. The first phase measured thermal

properties of single, two- and three- layer ETFE-foil using a test-rig under actual outdoor conditions. The approach applied was similar to the method stated in ASTM (1986b) with slight alteration. ASTM (1986b) specified use of the same experimental box, with and without the test specimen, such that the solar transmittance will be the ratio of average solar radiation transmitted through specimen (measured by a pyranomteer), and the average solar radiation measured by the same pyranometer without the specimen. However, in this study two separate test-rigs were placed side by side (Test-rig 1 and Test-rig 2) with dedicated pyronameters for each. Test-rig 1 was capped with ETFE-foil panels whereas Test-rig 2 was without a cap to obtain unobstructed solar radiation. Thus, the solar transmittance was obtained from the ratio of the average solar radiation transmitted through ETFE-foil in Test rig 1, and the average solar radiation incident in Test rig 2. This method was found more accurate than method stated in ASTM (1986b) to measure the solar transmittance for single, two- and three-layer ETFE-foil panels because in both of the test-rigs, the pyranometer location was identical. Using this method, it was possible to determine solar transmittance of the ETFE-foil panels under actual outdoor conditions. The results obtained were validated with solar transmittance obtained from the laboratory experiment, and accuracy was 88.2%-97%. Therefore, if the pyranometers are properly calibrated as readings with and without the specimen are taken simultaneously, under exactly the same weather conditions this method can be applied to measure solar transmittance of ETFE-foil panels of different configurations.

The second phase of the experiment evaluated and compared thermal behaviour of single, two- and three- layer ETFE-foil panels by measuring environmental data (e.g. temperature, humidity, etc.) in a time series inside the test-rigs. Selection of foil layers to construct ETFE-foil panels was completed carefully to ensure they were adequate to meet the objective.

The thermal performance of spaces enclosed with a ETFE-foil cushion envelope was investigated by conducting on-site monitoring of indoor environmental parameters from two case study buildings. This was another challenging method in this study, that required direct access to a school building and another institutional building, and collection of data for a long period (two years approximately). Equipment to monitor these buildings was carefully selected to meet research objectives while meeting the budget constraints. It was also challenging to find appropriate locations to install sensors and data logger. While identifying suitable locations for sensors and data loggers the following issues were considered: safety for school users (particularly pupils) and the researcher, ease of accessibility for regular maintenance purposes

(e.g. data download, etc.) and locations closer to the ETFE-foil cushion roof where required. The method was verified by reviewing similar previous studies (Harvie, 1996, Devulder, 2004, Croome and Moseley, 1984a, Wu et al., 1984) and it was identified that a similar approach was effective to assess the thermal behaviour of spaces enclosed with other light-weight envelopes.

To evaluate and compare the thermal performance of the spaces enclosed with ETFE-foil cushions and glass roofs, simulation-based analysis was undertaken. The selection of dynamic simulation software was validated by reviewing acceptability and validity of the software by recognised institutions (e.g. CIBSE). To select the appropriate approach for calibration of simulation models, various methods were reviewed. The simulation models were calibrated using a systematic procedure described in Chapter 7. The calibration ensured the validity of the simulation model and developed confidence with the final results.

8.4 Recommendations

It was identified from the onsite monitoring of actual spaces that the thermal performance of the spaces is influenced by the surface temperatures of ETFE-foil and temperature stratification during summer. Solar radiation and outdoor air temperature affected the thermal environment significantly. Therefore, it is necessary to develop approaches to reduce the impact of surface temperatures and extent of temperature stratification. Furthermore, simulation results indicated that by varying thermal optical properties of the ETFE-foil cushion roof it was not possible to eliminate overheating from large scale atria with currently available material under current climatic scenarios. The simulation also demonstrated that adequate ventilation through atria would be effective to mitigate overheating. However, within the available opening area in both of the atria studied, it was not possible to eliminate overheating in current and future climatic scenarios. Improvement of the ventilation system was not included in the scope of this research and should be considered in future research. This could be done by applying alternative ventilation techniques such as cross ventilation, stack ventilation, modification of inlet and outlet size located at lower and upper level of the atrium etc. Controllable ventilation flaps can be incorporated in ETFE-foil cushion roofs to potentially eliminate hot air zones at roof level. However, in-depth analysis is necessary to determine the ventilation strategies that could be used in the existing spaces to improve the indoor thermal environment.

It was evident from the study that rain suppression mesh reduced solar gain thus reduced ETFE-foil surface temperature and internal air temperature by creating

shading. Similar to rain suppression mesh, a sun shading effect can be created with partially opaque top and/or middle layers in a multilayer ETFE-foil cushion system. This type of envelope has been used in building façades already and presented in Knippers et al. (2011). However, further investigations are required to evaluate the performance of spaces with this type of envelope systems. Solar shading can also be provided by operable high-level solar blinds. Nevertheless, it is necessary to identify that these shading systems should not absorb heat and contribute to increasing radiant temperature of adjacent spaces.

It is also necessary to consider alternative design and construction strategies to lower the internal surface temperatures of the ETFE-foil cushion, which, in turn, will reduce mean radiant temperature in the enclosed spaces. Use of a water spray on a vertical ETFE-foil panel was investigated by Mainini et al. (2016), and found effective in reducing surface and air temperatures. However, it can be challenging to drain water from cushions in the horizontal position, used in the roofs and also imposes high load on the foil, possibly causing failure. Besides, water may be an expensive resource in urban context.

It is necessary to assess different strategies to improve the performance of an ETFE-foil cushion roof before implementation. This assessment can be done by using building simulation or following data collection from an experimental setup or from existing buildings where similar design strategies are already implemented. Simulation based analysis has now become a widely recognised method to identify design strategies for buildings. However, discrepancies between predicted and actual performance may be wide, because output from simulation models is limited by the assumptions made in the model, which do not always represent the actual use. This may be exacerbated because dynamic simulation software e.g. EDSL Tas, IES VE etc. do not currently include material templates for ETFE-foils. Without appropriate material properties, it is not possible to accurately represent the actual building envelope in simulation and could generate results with a high level of uncertainty. Thus, without accurate information on thermal/optical properties of ETFE-foils, the simulation-based approach cannot be used to achieve an effective solution. This area needs further development. Alternatively, data collected from actual buildings measure the true performance and may identify specific problems or risks. Nowadays, building management systems (BMS) have become an integral part of new buildings and, therefore, environmental data (e.g. air temperature, humidity, etc.) from existing buildings are technically available. In this study, a part of data was collected from sensors associated with the BMS system of ESLC, which represented location b (see

Figure 3-17) of the atrium. However, in Nottingham High School because of limited access, it was not possible to obtain data from BMS system.

New design strategies can also be tested in small scale using an experimental set-up under the actual outdoor conditions to understand its actual performance prior to large scale application.

The constructed building should be assessed by post-occupancy evaluation (POE), and/or monitoring of energy and environmental data. Hence the overall procedures of establishing an efficient structure can be divided into two primary stages: design stage and evaluation stage. Figure 8-1 presents fundamental steps to be considered at design and evaluation stages.

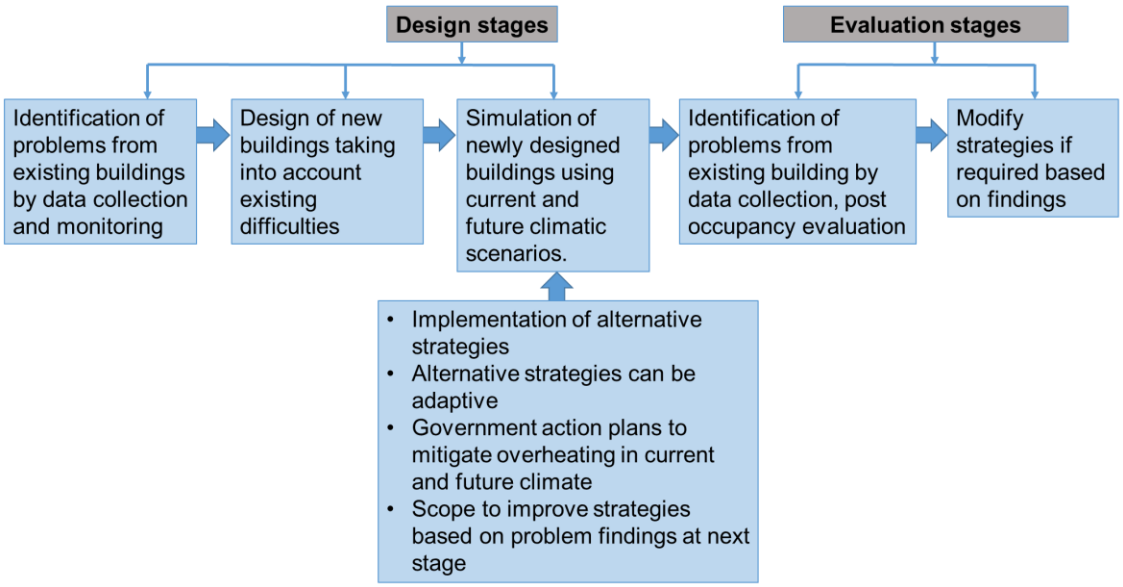


Figure 8-1: Design and evaluation stages for building performance analysis

Thus, this process will allow designers to identify the problems before implementation and will increase the opportunity to manage the building's design at an earlier stage to overcome difficulties such as the occurrence of overheating.

Moreover, nowadays with the rapid change in climatic scenarios it is not sufficient to rely on just one strategy. Different strategies should be considered to make the buildings more adaptive to climatic variations. However, installing different strategies might incur additional design and construction costs. Nevertheless, it is the designer's responsibility to raise awareness among their clients, to make buildings resilient to current and future climate.

Current legislation (HMGovernment, 2010c, NARM, 2010) only specified the energy conservation of roof lights. But for large transparent envelopes, solar radiation

significantly affects thermal performance of the spaces they enclose. Therefore, it would be desirable to improve legislation to provide specific guidelines to limiting solar gain.

BS EN 410:2011 (BSI, 2011), was developed for luminous and solar characteristics of glazing, therefore, only considered flat panels. Whereas, nowadays, ETFE-foil cushions with double-curved surfaces are widely applied in building envelopes. Thus it requires a standard method that can be used to determine overall thermal optical properties of ETFE-foil cushions considering multiple reflections (Knippers et al., 2011) occurring at the ETFE-foil cushion surfaces due to their curvature.

Simulation based analysis indicated that the thermal performance of ETFE-foil cushion roofs was similar to or in some cases better than glass roofs. Although the space enclosed with both ETFE-foil cushion and glass roofs was found to overheat during summer, the extent of overheating was higher in the space enclosed with a glass roof with a higher energy consumption (cooling load). This was apparent when comparing the air temperature and cooling load of the atrium model, roofed with two-layer ETFE-foil cushion with 75% fritted top layer and rain mesh, and glass roofs. Although the solar transmittance of ETFE-foils (200μm transparent foil - 0.86) are higher than for glasses considered (e.g. Glass type 3 - 0.566), but use of fritting and an additional layer of ETFE-foil in the two-layer cushion system reduced solar transmittance to (0.436). Moreover, rain mesh also reduced the internal air temperature by creating shading (as was evident in the test rig experiment). Thus, use of a fritted layer and rain mesh reduced the internal air temperature of the model with ETFE-foil cushion roof when compared to the glass roof. Therefore, ETFE-foil with fritting and rain mesh can be used as an effective alternative to glass. However, the field of application of ETFE-foil requires further research to develop innovative systems that can be used to reduce foil surface temperature as well as solar gain in ETFE-foil cushion enclosures. It is required to take initiatives to improve the performance of ETFE-foil covered enclosures to gain confidence in its field of application.

8.5 Conclusions and fulfillment of aim and objectives

8.5.1 Objective one

Objective one was to develop a knowledge base on properties of ETFE-foils and ETFE-foil cushion construction; identify the thermal behaviour of fabric membranes and spaces enclosed with fabric membrane envelope. To achieve this objective an extensive literature review was conducted on related areas. The literature review

provided understanding about the topic and helped to narrow down the required information to progress with the empirical study.

8.5.2 Objective two

Objective two was to determine thermal-optical properties of ETFE-foil, which was achieved by conducting laboratory experiments and using the appropriate methodology recommended by BS EN 410 (BSI 2011).

The novelty of this study was to be able to independently determine thermal optical properties of single, two- and three- layer ETFE-foil panels including combinations of transparent and fritted foils of different fritting percentage.

Results obtained compared well with previous studies, to develop confidence about the thermal optical properties of ETFE-foil and multilayer cushions. However, further studies are required.

8.5.3 Objective three

The objective three was to evaluate the thermal performance of single, two- and three-layer ETFE-foil panels achieved by measuring thermal properties of test-rigs installed in exposed outdoor environment. The results provided useful insight into the thermal performance of different combinations of single, two- and three-layer foil panels under actual outdoor conditions.

Conclusions:

The results obtained in the first phase of the test-rig experiment agreed reasonably well (88.2% to 97%) with measured and calculated thermal properties (solar transmittance) obtained from the laboratory experiment and BS EN 410. Thus, to determine thermal properties (solar transmittance) of ETFE-foil panels the method was useful.

In the lab it was only possible to measure thermal optical properties of single layer ETFE-foil samples and difficulties arose while measuring these properties for fritted foils. Therefore, the method incorporating test-rigs provided an opportunity to measure directly the thermal properties (solar transmittance) of single, two- and three- layer ETFE-foil panel of different combinations of fritted and transparent foils. Using this method, the solar transmittance was measured over the range of sensitivity of the pyranometer that covered ultra-violet to infra-red wavelength, which also covered the total wavelength required to measure solar transmittance using BSI (2011). Thus,

depending on the sensitivity of the pyranometer, this method can be used to determine the properties of multilayer systems and for future research.

The results obtained in the second phase showed how the number of foil layers and air layers influenced the thermal performance of ETFE-foil panels by increasing (or decreasing) the internal air temperature of the test-rig it enclosed. The effect of fritting of various proportions and covering of the ETFE-foil panels with rain suppression mesh on the rate of radiative and convective heat transfers between the foils and intermediate air layers, and the influence this variation has on the enclosed air temperature of the test-rig, was demonstrated for a number of commonly applied multilayer systems. However, further studies in this area are required to gain confidence about the developed methods.

8.5.4 Objective four

The objective four was to evaluate the thermal performance of occupied spaces enclosed with an ETFE-foil cushion envelope, which was achieved by conducting on-site monitoring of indoor environment parameters from two case study buildings. This study was being able to evaluate thermal performance on the basis of overheating assessment criteria and also presented a comparative analysis of thermal environment of two different atria covered with different compositions of ETFE-foil cushion roof. The novelty of this objective was it evaluated thermal performance of two separate atria covered with two types of ETFE-foil cushion roof (two layer and three layer) and presented a comparative study.

Conclusions:

The indoor thermal environment was found to vary depending on the type of envelope system. Both buildings which have large transparent/ translucent ETFE-foil cushion roofs were found to be at high risk of overheating in summer according to commonly used assessment criteria - CIBSE temperature benchmark, CIBSE TM52, Building Bulletin 101. Further studies are required in the field to develop more confidence about the results.

8.5.5 Objective five

Objective five was to evaluate and compare thermal performance between the spaces enclosed with ETFE-foil cushions and glass roofs using building simulation.

Conclusions:

A novel approach of modelling and simulating ETFE-foil cushion roofs was developed. The approach was validated by comparing with actual measurements.

Comparative analysis of indoor air temperature distribution between similar enclosures covered with either ETFE-foil cushions or glass panels demonstrated very similar results. Both the simulated atrium spaces were found to overheat in current climate scenarios.

The extent of overheating was higher in the atria when enclosed with a glass roof compared to two-layer ETFE foil cushions. Results also demonstrated that atria with a glass roof increased cooling load in summer. However, during a day with extreme outdoor temperature in summer the average cooling load of the atrium enclosed with three layer ETFE-foil cushion roof was similar to the glass roof.

Simulation of the test-rigs showed that the model with two- layer (with 75% fritted top layer, 200 μm bottom layer) and three-layer ETFE-foil panel (with 25% fritted top layer, 100 μm middle and 200 μm bottom layer), and notional glazing unit constructed of poly carbonate (e.g. Gtype 1 and 2) performed better than a typical double glazing unit with low-E coating under summer conditions.

The low-E coated double glazing roof system was found to be more efficient in winter. However, in summer, the thermal performance and energy consumption was better in the simulation model enclosed with ETFE-foil cushion roofs.

8.5.6 Objective six

Objective six was to identify strategies to improve the thermal performance (overheating) of spaces in current and projected climate scenarios. The objective was achieved by applying alternative strategies in simulation to improve the thermal performance of existing spaces enclosed with ETFE-foil cushion roofs under current and projected climatic scenarios. Strategies were selected carefully to ensure they were suitable to meet the anticipated objective.

Conclusions:

It was concluded that by varying thermal optical properties of the ETFE-foil cushion roofs studied it was not possible to eliminate overheating in the studied enclosures under current or projected climate scenarios, using currently available materials.

It was demonstrated that appropriately designed ventilation through the studied atria would be effective to mitigate overheating under current and projected scenarios.

8.5.7 Objective seven

Objective seven was to identify implications of the research for designers and develop design recommendations of ETFE-foil panels and spaces enclosed with ETFE-foil cushion envelope. This objective was achieved by synthesizing theoretical knowledge and findings from the empirical studies.

Conclusions:

Design recommendations for ETFE-foil covered enclosures were presented in section 8.5, based on:-

- reducing solar gain by shading, such as use of fritted layers and rain mesh to actively reduce internal air temperature and foil surface temperature of the ETFE-foil cushion
- updating of material libraries of current dynamic simulation software by adding material templates for ETFE-foils based on this research to provide more accurate simulations.
- application of improved and adequate ventilation strategies determined by simulation
- consideration of projected as well as current climate scenarios in simulations
- collection of energy and environmental data, and post occupancy evaluation in completed buildings covered with ETFE-foil to determine any health and safety risks resulting from unexpected indoor environmental factors (e.g. overheating, excessive glare, etc.).
- revision of legislation to take into account energy conservation characteristics of the light-weight envelope like ETFE-foil cushions.

8.6 Novelty and contribution to the knowledge

The novelty of this study was to be able to accurately determine thermal optical properties of single, two-, and three- layer ETFE-foil panels, including combinations of transparent and fritted foils. In this study this information was incorporated into the material template of EDSL TAS version 9.3.3 b and applied in the simulations. These thermal optical properties of ETFE-foil can be used in future research to do similar investigations.

This study also developed new evidence base of environmental performance of actual buildings configured with ETFE-foil cushion. The study evaluated the thermal performance of actual spaces enclosed with ETFE-foil cushion roofs and also presented a comparative analysis of the thermal environment of two different atria covered with different compositions of ETFE-foil cushion roof. Thus, an evidence base was developed and this knowledge can be used in future research on ETFE-foil and glass covered enclosures.

Using the custom designed test-rigs located in an outdoor environment, the study assessed the thermal performance of single, two- and three- layer ETFE-foil panels. This particular study was unique in its character as previous studies using test-rigs were in controlled chambers rather than exposed to an actual outdoor setting. This was a novel approach in this study and knowledge generated through this research can also be used as an evidence base for future research. This study also measured thermal properties of ETFE-foil (e.g. solar transmittance) in an actual outdoor condition. Data was validated with the same properties measured in the laboratory. Thus, the study was able to generate new knowledge on solar transmittance of single, two- and three-layer foil. This method can be used in future research to investigate thermal properties of ETFE-foil under actual outdoor conditions.

This study also investigated the thermal performance of spaces enclosed with ETFE-foil cushion roofs under current and future climatic scenarios. It also applied alternative strategies to improve the thermal performance under current and future climatic conditions. The novelty was to be able to evaluate thermal performance under current and future scenarios and compare the performance of spaces with alternative approaches.

This study assessed and compared the thermal performance of ETFE-foil panels and glass panels in simulation using replicate model of the test-rig; it also evaluated the thermal performance of spaces enclosed with ETFE-foil cushions and glass roofs in simulation using replicate models of Nottingham High School and the Engineering and Science Learning Centre, under current and projected climate scenarios. A comparative analysis between these two materials is limited in existing literature. Also the validity of simulations models was based on data measured from the on-site monitoring of the test-rig, Nottingham High School and ESLC, thus findings from this study are original and strengthen the current knowledge base.

This study also developed a novel method of modelling doubly curved surfaces of the ETFE-foil cushion roof. This approach was validated by comparing with measured data

and found effective in evaluating spaces configured with ETFE-foil cushions. A similar approach can be applied to model ETFE-foil cushion roofs in further research.

8.7 Limitations of the study

- ETFE-foil samples were obtained from off cut samples provided by the supplier, some of them were scratched and dusty, measures were taken to remove dust as possible however it was not possible to remove scratches from ETFE-foil surface. Nevertheless, these type of foil samples gave more realistic properties for foil in normal use.
- BS EN 410: 2011 was used to determine thermal optical properties of ETFE foils. This standard is particularly used for glazing panels. Therefore, these derived optical properties represent thermal optical properties of ETFE-foil panels of different combinations of parallel foil layers, rather than ETFE cushions which usually consist of doubly-curved surfaces.
- This is the limitation of British Standard that only considered flat panels, while nowadays ETFE-foil cushions are widely applied in the building envelopes. Thus, it requires a standard method that can be used to determine overall thermal optical properties of ETFE-foil cushion considering multiple reflections occurring at ETFE-foil cushion surface.
- Equipment to measure the thermal transmittance of horizontal façade element was limited, thus it was not possible to measure the thermal transmittance of an ETFE-foil cushion in an actual test condition.
- The method used to determine solar transmittance of ETFE-foil panels using a test rig in an outdoor environment, sometimes required days with clear sky and with no cloud. However, in a country such as the UK, it is very rare to find sky without any cloud cover.

8.8 Future research

- Direct measurement of thermal transmittance of ETFE-foil cushions (e.g. double layer, three layers, etc.) taking into account variation in U-value at different cross sections of a cushion.
- Investigation of angular thermal-optical properties of different colour ETFE-foils.
- Lack of evidence base for building with ETFE-foil cushion envelopes is apparent. Therefore, it is necessary to get further evidence from different other buildings where ETFE-foil cushion envelopes are incorporated.

- Focus can be given to the ventilation system of the buildings constructed with ETFE-foil cushion envelope. This can include both natural and mechanical ventilation. Both summer and winter weather should be considered while investigating the ventilation system.
- The cost of improving ventilation system can be considered and analysed.
- Cost analysis of the implementation of alternative strategies to improve the thermal performance of spaces enclosed with ETFE-foil cushion envelopes in summer and winter.
- Based on knowledge developed in this research, different strategies can be applied to improve performance of existing and new spaces enclosed with ETFE-foil cushion roofs
- Intelligent envelope systems using ETFE-foils were already applied in different buildings, however, it is important to assess the performance of innovative envelope systems.

References

Afrin, S., Chilton, J. & Lau, B. 2015. Evaluation and Comparison of Thermal Environment of Atria Enclosed with ETFE Foil Cushion Envelope. *Energy Procedia,* 78**,** 477 – 482.

Antretter, F., Haupt, W. & Holm, A. 2008. Thermal Transfer through Membrane Cushions Analyzed by Computational Fluid Dynamics. *In:* Rode, C., ed. Proceedings of the 8th Symposium on Building Physics in the Nordic Countries, June 16-18 2008 Dept. of Civil Engineering, Technical University of Denmark. Copenhagen: Kgs. Lyngby, 347- 354.

Asdrubali, F. & Baldinelli, G. 2011. Thermal transmittance measurements with the hot box method: Calibration, experimental procedures, and uncertainty analyses of three different approaches. *Energy and Buildings,* 43**,** 1618-1626.

ASHRAE 2009. ASHRAE Handbook: Fundamentals SI. Atlanta, GA: ASHRAE.

ASHRAE 2013. ASHRAE Handbook Fundamentals. Atlanta: ASHRAE.

ASTM 1986a. Annual Book of ASTM Standards. *ASTM E 424-71: Standard Test Methods for Solar Energy Transmittance and Reflectance (Terrestrial) of Sheet Materials.* U. S. A: ASTM.

ASTM 1986b. Annual Book of ASTM Standards. *Standard Test Method for Solar Absorptance, Reflectance, and Transmittance of Materials Using Integrating Spheres.* U. S. A: Easton, MD.

ASTM 1991. ASTM E 1084-86: Standard Test Method for Solar Transmittance (Terrestrial) of Sheet Materials Using Sunlight. U. S. A: ASTM.

ASTM 2014. C1363-11: Standard Test Method for Thermal Performance of Building Materials and Envelope Assemblies by Means of a Hot Box Apparatus. United States: ASTM International.

Badescu., V. 2008. *Modelling Solar Radiation at the Earth's Surface,* Berlin, Springer.

Baille, A., Lo´pez, J., C & Bonachela, S. 2006. Night energy balance in a heated low-cost plastic greenhouse. *Agriculture and Forest Meteorology,* 137**,** 107-118.

Bauer, G. 1965. *Measurement of Optical Radiations: The detection of electromagnetic radiation from ultra-violet to infra-red,* London, The Focal Press.

BSEN15251 2007. Indoor environmental input parameters for design and assessment of energy performance of buildings addressing indoor air quality, thermal environment, lighting and acoustics. UK: BSI.

BSI 1989. BS 6993: Part 1: Thermal and radiometric properties of glazing. United Kingdom: BSI.

BSI 2005. BS EN ISO 7730: Ergonomics of the thermal environment. Analytical determination and interpretation of thermal comfort using calculation of the PMV and PPD indices and local thermal comfort criteria UK: BSI.

BSI 2007. BS EN ISO 6946: Building components and building elements. Thermal resistance and thermal transmittance. Calculation method United Kingdom: BSI.

BSI 2011. Glass in building Determination of luminous and solar characteristics of glazing. UK: BSI.

Callister, W., D. 2011. *Materials Science and Engineering,* Chichester, GB, John Wiley and Sons Ltd.

Chilton, J., C. 2013. Lightweight envelopes: ethylene tetra-fluoro-ethylene foil in architecture *Proceedings of the ICE - Construction Materials,* 166**,** 343-357.

Chilton, J., Pezeshkzadeh, S., A. & Afrin, S. 2013a. Embodied energy in ETFE foil construction. *Tensinet Ssymposium 2013- [RE]THINKING lightweight structures.* Mimar Sinan Fina-Art University, Istanbul.

Chilton, J., Pezeshkzadeh, S. & Afrin, S. EFFECT OF CUSHION GEOMETRY AND CONFIGURATION ON THE EMBODIED ENERGY OF ETFE FOIL CONSTRUCTION. VI International Conference on Textile Composites and Inflatable Structures, STRUCTURAL MEMBRANES 2013, 9-11 October 2013 2013b Munich.

CIBSE 2006. CIBSE Guide A - Environmental Design Great Britain: CIBSE.

CIBSE 2013a. The limits of thermal comfort : avoiding overheating in European buildings. London, UK.

CIBSE 2013b. TM52: The limits of thermal comfort: avoiding overheating in European buildings. *Predicting discomfort.* London: Page Bros. (Norwich) Ltd.

CIBSE 2015a. Applications Manual AM11: Building performance modelling. London, UK.

CIBSE 2015b. CIBSE GUIDE A: ENVIRONMENTAL DESIGN 2015. Great Britain: CIBSE.

CIBSE 2015c. CIBSE Journal. April 2015 ed.: CIBSE.

CIBSE 2015d. TM57: Integrated school design. Norwich: Page Bros. (Norwich) Ltd.

Clarke, J. A., Strachan, P., A., & C., P. 1993. An approach to the calibration of building energy simulation models. *ASHRAE Transactions,* 99**,** 917-927.

Cremers, J. 2010. Research in Architectural Engineering : Future Envelope 3 : Facades : The Making Of. *In:* Klein, T. & Knaack, U. (eds.). Amsterdam, NLD IOS Press.

Croome, D. & Moseley, P. Energy and thermal performance of airhouses. Proceedings of conference The design of air-supported structures, 1984a Bristol. the Institution of Structural Engineers, London, 223-237.

Croome, D. & Moseley, P. Temperature Prediction Methods for Lightweight Structures. The design of air- supported structures, 1984b London. The Institute of Structural Engineers, 247-260.

DCLG 2015. UK's National Calculation Method for Non Domestic Buildings BRE.

de Dear, R., Brager, G. & Berkeley, U., C. 1998. Developing an adaptive model of thermal comfort and preference. *ASHRAE RP- 884,* 104**,** 1-18.

Desmarais, G., C.,, Ratti, C. & Raghavan, G., S. 1999. Heat transfer modelling of screenhouse. *Solar Energy,* 65**,** 271-284.

DETR 2003. DETR sponsord research project: ETFE Foil Cushions as an alternative to glass for roofs and atria. Department of the Environment, Transport and the Regions.

Devulder, T. 2004. *The Thermal Response of Textile membrane Constructions.* PhD Thesis, University of Nottingham.

Devulder, T., Wilson, R. & Chilton, J. 2007. The thermal behaviour of buildings incorporating single skin tensile membrane structures. *International Journal of Low Carbon Technologies,* 2**,** 195-213.

Dimitriadou, E. 2015. *Experimental Assessment and Thermal Characterisation of Lightweight Co-Polymer Building Envelope Materials.* Doctor of Philosophy, University of Bath.

Eames 2009. Multi-foil Insulation BD2768. United Kingdom.

Elmahdy, A. H. & Haddad, K. 2000. Experimental procedure and uncertainty analysis of a guarded hot box method to determine the thermal transmission coefficient of skylights and sloped glazing. *ASHRAE Transactions,* 106**,** 601-613.

EPD 2014. ENVIRONMENTAL PRODUCT DECLARATION. 06/05/2014 ed.: Institut Bauen und Umwelt e.V. (IBU).

Fanger, M., O. 1967. Calculation of Thermal Comfort: Introduction of a Basic Comfort Equation. *ASHRAE Transactions,* 73.

Gómez-González, A., Neila, J. & Monjo, J. 2011. Pneumatic Skins in Architecture. Sustainable Trends in Low Positive Pressure Inflatable Systems. *Procedia Engineering,* 21**,** 125-132.

Harvie, G. 1996. *An investigation into the thermal behaviour of spaces enclosed by fabric membranes.* PhD Thesis, Cardiff University.

Harvie, G. 2015. Thermal behaviour in architectural fabric structures. *In:* Llorens, J. (ed.) *Fabric Structures in Architecture.* Cambridge: Woodhead Publishing.

He, J. & Hoyano, A. 2009. Measurement and simulation of the thermal environment in the built space under a membrane structure. *Building and Environment,* 44**,** 1119-1127.

He, J. & Hoyano, A. 2010. Measurement and evaluation of the summer microclimate in the semi-enclosed space under a membrane structure. *Building and Environment,* 46**,** 230-242.

HMGovernment 2010a. Approved Document F1: Means of ventilation. England: Online Version.

HMGovernment 2010b. Approved Document L2A: Conservation of fuel and power in new buildings other than dwellings. England: Online Version.

HMGovernment 2010c. Approved document L2B: Conservation of fuel and power in exsiting buildings other than dwellings. England: Online version.

Hopfe, C., J. & Hensen, J., L., M. 2011. Uncertainty analysis in building performance simulation for design support. . *Energy and Buildings,* 43**,** 2798-2805.

Hu, J., Chen, W., Yang, D., Zhao, B., Song, H. & Ge, B. 2016. Energy performance of ETFE cushion roof integrated photovoltaic/thermal system on hot and cold days. *Applied Energy,* 173**,** 40-51.

IEATask12 1996. Atrium Models for the Analysis of Thermal Comfort and Energy Use. *In:* Bryn, I. & Schiefloe, P. (eds.) *A Report of Task 12: Building Energy Analysis and*

Design Tools for Solar Applicationa. SINTEF Energy, Norway: International Energy Agency.

Incropera, F., Dewitt, D., Bergman, T. & Lavine, A. 2013. *Principles of Heat and Mass Transfer,* Asia, John Wiley & Sons Singapore Pte. Ltd.

ISO 2003. ISO 9050: Glass in building- Determination of light transmittance, solar direct transmittance, total solar energy transmittance, ultraviolet transmittance and related glazing factors. Geneva: ISO.

Kasten, F., Kok, C., J. & Justus, C., G. 1989. Technical Report on Solar Spectral Irradiance. Vienna, AUSTRIA: THE INTERNATIONAL COMISSION ON ILLUMINATION.

Kim, Y. & Park, C. 2016. Stepwise deterministic and stochastic calibration of an energy simulation model for an existing building. *Energy and Buildings,* 133**,** 455-468.

Kipp&Zonen. 2016. *Theoretical Information* [Online]. Available: http://www.kippzonen.com/Knowledge-Center/Theoretical-info [Accessed 02/10/2016].

Knippers, J., Cremers, J., Gabler, M. & Lienhard, J. 2011. *Construction manual for Polymers + Membranes,* Basel, Switzerland, Birkhauser.

LeCuyer, A. 2008. *ETFE Technology and Design,* Germany, Birkhauser.

Libby, P., A.,, Olfe, D., B., & Atta, C., W. Proceedings of the 1967 Heat Transfer abd Fluid Mechanics Institue. Heat Transfer abd Fluid Mechanics Institue, 1967 University of California, Sandiego. Stanford University Press, 123-129.

Lomas, K., J & Giridharan, R. 2012. Thermal comfort standards, measured internal temperatures and thermal resilience to climate change of free-running buildings: A case-study of hospital wards. *Building and Environment,* 55**,** 57-72.

Lomas, K., J. & Eppel., H. 1992. Sensitivity analysis techniques for building thermal simulation programs. *Building and Environment,* 19**,** 21-44.

Lomas, K. J., Eppel, H., Martin, C. J. & Bloomfield, D., P. 1997. Empirical validation of building energy simulation programs. *Energy and Buildings,* 26**,** 253-275.

Macdonald, I. & Strachan, P. 2001. Practical application of uncertainty analysis. *Building and Environment,* 33**,** 219-227.

Mainini, A., Poli, T., Paolini, R., Zinzi, M. & Vercesi, L. 2014. Transparent multilayer ETFE panels for building envelope: thermal transmittance evaluation and assessment

of optical and solar performance decay due to soiling. *Energy Procedia* 48**,** 1302 – 1310.

Mainini, A., Speroni, A., Zani, A. & Poli, T. 2016. The effect of water spray systems on thermal and solar performance of an ETFE panel for building envelope *Procedia Engineering,* 155**,** 352-360.

Max, J. F. J., Reisinger, G., Hofmann, T., Hinken, J., Tantau, H., Ulbrich, A., Lambrecht, S., Elsner, B. & Schurr, U. 2012. Glass–film-combination: Opto-physical properties and energy saving potential of a novel greenhouse glazing system. *Energy and Buildings,* 50**,** 298-307.

McAdams, W. H. 1954. *Heat Transmission,* New York, McGraw Hill.

Minamisawa, R. A., Abidzina, V., de Almeida, A., Budak, S., Tereshko, I., Elkin, I. & Ila, D. 2007. Radiation effects on ETFE polymer exposed to glow discharge. *Nuclear Instruments and Methods in Physics Research Section B: Beam Interactions with Materials and Atoms,* 261**,** 715-718.

Modirrousta, S. & Boostani, H. Analysis of Atrium Pattern, Trombe Wall and Solar Greenhouse on Energy Efficiency. International Conference on Sustainable Design, Engineering and Construction, 2016. Procedia Engineering 145, 1549-1556.

Monticelli, C., Campioli, A. & Zanelli, A. Evolution and Trends in Design, Analysis and Construction of Shell and Spatial Structures. Symposium of the IASS, 28 September 09 – 2 October 09 2009 Valencia. 200-202.

Moosavi, L., Mahyuddin, N. & Ghafar, N. 2014. Thermal performanceofatria: An overview of natural ventilation effective designs. *Renewable and Sustainable Energy Reviews,* 34**,** 654-670.

Moosavi, L., Mahyuddin, N. & Ghafar, N. 2015. Atrium cooling performance in a low energy office building in the Tropics, a field study. *Building and Environment,* 94**,** 384-394.

Moritz, K. 2007. *ETFE -Foile als Tragelement.* PhD, Technical University of Munich.

Moritz, K. & Hafner, A. Transparency carried by air-pneumatic ETFE-foil cushion technology. Proceedings of the structures congress, 2010. 2518-2529.

NARM 2010. Assessment of thermal performance of out-of-plane rooflights. United Kingdom: NARM.

Nicol, F., Humphreys, M. & Roaf, S. 2012. *Adaptive Thermal Comfort: Principles and practice,* Great Britain, Routledge.

NREL 2015. Building Technologies Office: EnergyPlus Energy Simulation Software. *Energy Efficiency and Renewable Energy.*

NREL 2016. OpenStudio SketchUp Plug-in Interface Guide. *User Documentation.*

Paliouras. P., Matzaflaras. N., Peuhkuri, R. H. & Kolarik, J. 2015. Using measured indoor environment parameters for calibration of building simulation model- a passive house case study. *6th International Building Physics Conference.* Elsevier Ltd.

Parsons, K. C. 2003. *Human Thermal Environments: The effects of hot, moderate and cold environments on human health comfort and performance. The principles and the practice,* London, Taylor & Francis Ltd.

Pellegrino, M., Simonetti, M. & Chiesa, G. 2016. Reducing thermal discomfort and energy consumption of Indian residential buildings: Model validation by in-field measurements and simulation of low-cost interventions. *Energy and Buildings,* 113**,** 145-158.

Pérez-Lombard, L., Ortiz, J. & Pout, C. 2008. A review on buildings energy consumption information. *Energy and Buildings,* 40**,** 394-398.

Poirazis, H., Kragh, M. & Hogg, C. Energy modelling of ETFE membranes in building application. Eleventh International IBPSA Conference, 27-30 July 2009 Glasgow, Scotland.

Reddy, T. 2007. Calibrating detailed building energy simulation programs with measured data—part I: general methodology (RP-1051). *ASHRAE Transactions,* 13**,** 221-241.

Robinson-Gayle, S. 2003. *Environmental Impact And Perfromance Of Transparent Building Envelope Materials And Systems.* Doctor of Engineering, Brunel University.

Robinson-Gayle, S., Kolokotroni, M., Cripps, A. & Tanno, S. 2001. ETFE foil cushions in roofs and atria. *Construction and Building Materials,* 15**,** 323-327.

Schiemann, L. & Moritz, K. 2010. Polymer foils used in construction. *In:* Pohl, G. (ed.) *Textiles, polymers and composites for buildings.* Cambridge: Woodhead Publishing.

Schöne, L. 2007. Bauen mit ETFE-Folien – Ein Praxisbericht. *Stahlbau,* 76**,** 305-313.

British Standards 2008. BS EN 15251:2007 Indoor environmental input parameters for design and assessment of energy performance of buildings addressing indoor air quality, thermal environment, lighting and acoustics.

Szokolay, S. V. 2008. *Introduction to architectural science: the basis of sustainable design,* Oxford Elsevier Architectural Press.

Tamburrini, M., Palmer, D. & Macdonald, I. 2003. Calibrating models for simulation use in design practices. . *8th International IBPSA Conference.* Eiendhoven: IBPSA.

Toyoda, M. & Takahashi, D. 2013. Reduction of rain noise from Ethylene/TetraFluoroEthylene membrane structures. *Applied Acoustics,* 74**,** 1309-1314.

TRNSYS 2016. Transient System Simulation Tool.

Turrin, M., Ham, V., Kilian, A. & Sariyildiz, S. Proceedings of the International Conference on Computing in Civil and Building Engineering. *In:* Tizani, W., ed. iccbe, 2010 Nottingham University. Nottingham University Press.

Turrin, M., Von Buelow, P., Kilian, A. & Stouffs, R. 2012. Performative skins for passive climatic comfort. *Automation in Construction,* 22**,** 36-50.

UKGOV 2014. Building Bulletin 101: Ventilation of School Buildings. UK: Education Funding Agency.

Vector-foiltec. 2013. The TEXLON System. Available: http://www.vector-foiltec.com/en/downloads/brochures.html [Accessed 20/04/2013].

Wang. X., Kendrick. C., Ogden, R., Walliman, N. & Baiche, B. 2011. A case study on energy consumption and overheating for a UK industrial building with rooflights. *Applied Energy,* 104**,** 337-344.

Ward, T. I. & Doran, S. M. 2005. The thermal performance of multi-foil insulation. United Kingdom: BRE.

Westphal, F. S. & Lamberts, R. 2005. Building Simulation Calibration Using Sensitivity Analysis. *9Th International IBPSA Conference.* Montreal: IBPSA.

Wu, H., Boonyatikarn, S. & Engen, B. The stratification in fabric roof structures: a strategy of energy conservation and system design. International Symposium on Architectural Fabric Structures, AFSF, 1984. 192-196.

Wu, M., Wu, Y. & Kim, J.-Y. 2011. ETFE foil spring cushion structure and its analytical method. *Thin-Walled Structures,* 49**,** 1184-1190.

APPENDIX A: List of Publications





Available online at www.sciencedirect.com

ScienceDirect

Energy Procedia 78 (2015) 477 – 482

Energy Procedia

6th International Building Physics Conference, IBPC 2015

Evaluation and Comparison of Thermal Environment of Atria Enclosed with ETFE Foil Cushion Envelope

Sabrina Afrin, John Chilton* and Benson Lau

Department of Architecture & Built Environment, University of Nottingham, University Park, Nottingham, NG7 2RD, United Kingdom

Abstract

This paper presents results of on-site monitoring of foil surface temperatures and the thermal environment within two different atria covered with different compositions of ETFE foil cushion roof (one two-layer, the other three-layer) and differing ventilation regimes. Results of the study show strong vertical stratification in both atria. Foil surface temperatures respond rapidly to high solar radiation with the internal layer being hotter than both the external layer and the adjacent internal air. At night the surface temperature of external foil follows the ambient external temperature closely whilst the internal layer temperature follows approximately the mean of adjacent internal temperature in the atria and external temperature.

© 2015 The Authors. Published by Elsevier Ltd. This is an open access article under the CC BY-NC-ND license (http://creativecommons.org/licenses/by-nc-nd/4.0/).
Peer-review under responsibility of the CENTRO CONGRESSI INTERNAZIONALE SRL

Keywords: ETFE cushion envelope, building performance, building continuous monitoring, thermal environment, solar radiation transmission

1. Introduction

Afrin S., Chilton J. and Lau B. Evaluation and Comparison of Thermal Environment of Atria Enclosed with ETFE Foil Cushion Envelope, In 6th International Building Physics Conference, IBPC 2015, *Energy Procedia*.

Afrin S., Chilton J. and Lau B. (2014). Thermal Environment of an atrium enclosed by an ethylene-tetrafluoro-ethylene (ETFE) foil roof, In Shells, Membranes and Spatial Structures Footprints, Proceedings of the International Association for Shell and Spatial Structures (IASS)-SLTE Symposium 2014 (Reyolando M.L.R.F. and Ruy M.O. (eds.)). Brasilia, Brazil.

Afrin S., Chilton J. and Lau B. Thermal Environment of an Atrium enclosed with ETFE Foil Cushion Envelope, In 14th International Conference on Sustainable Energy Technologies – SET 2015, August 2015, Nottingham, UK.

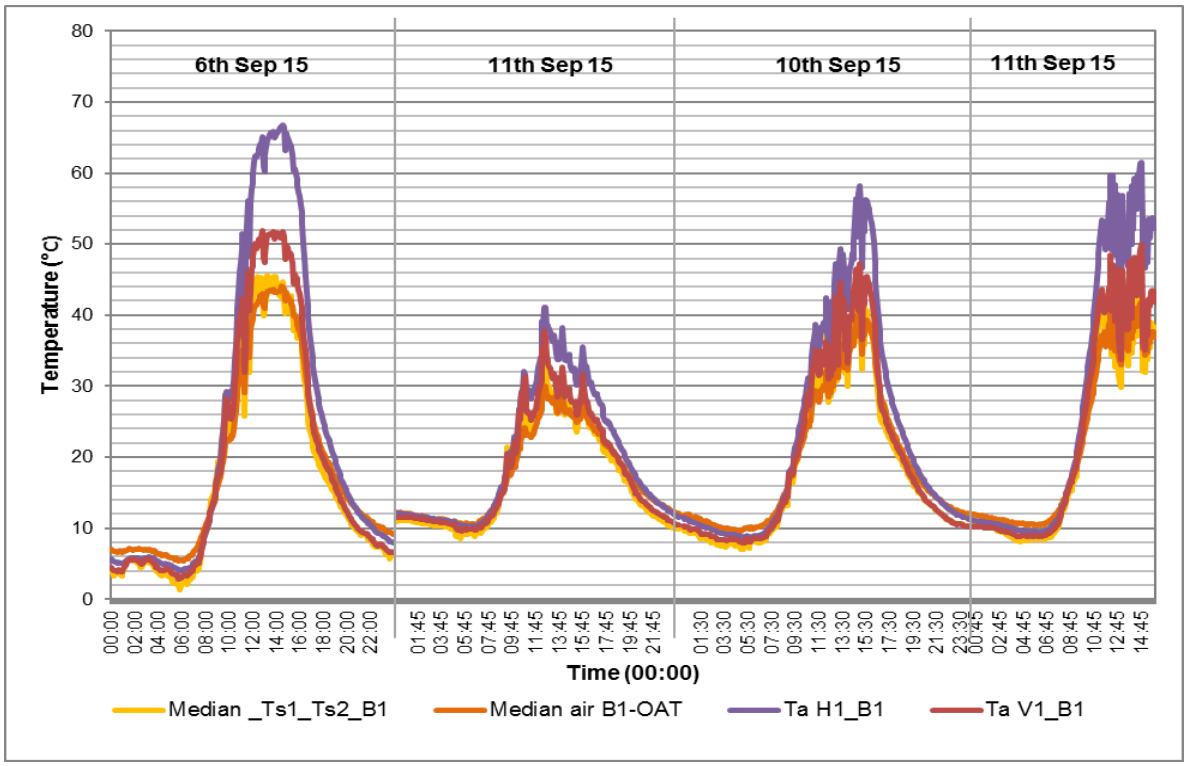
Afrin S., Chilton J. and Lau B. MEASUREMENT AND SIMULATION OF SUMMER THERMAL ENVIRONMENT OF AN ATRIUM ENCLOSED WITH ETFE FOIL, In VI

International Conference on Textile Composites and Inflatable Structures, STRUCTURAL MEMBRANES 2015. E. Oñate, K. U. Bletzinger, and B. Kröplin (Eds) Spain, Barcelona.

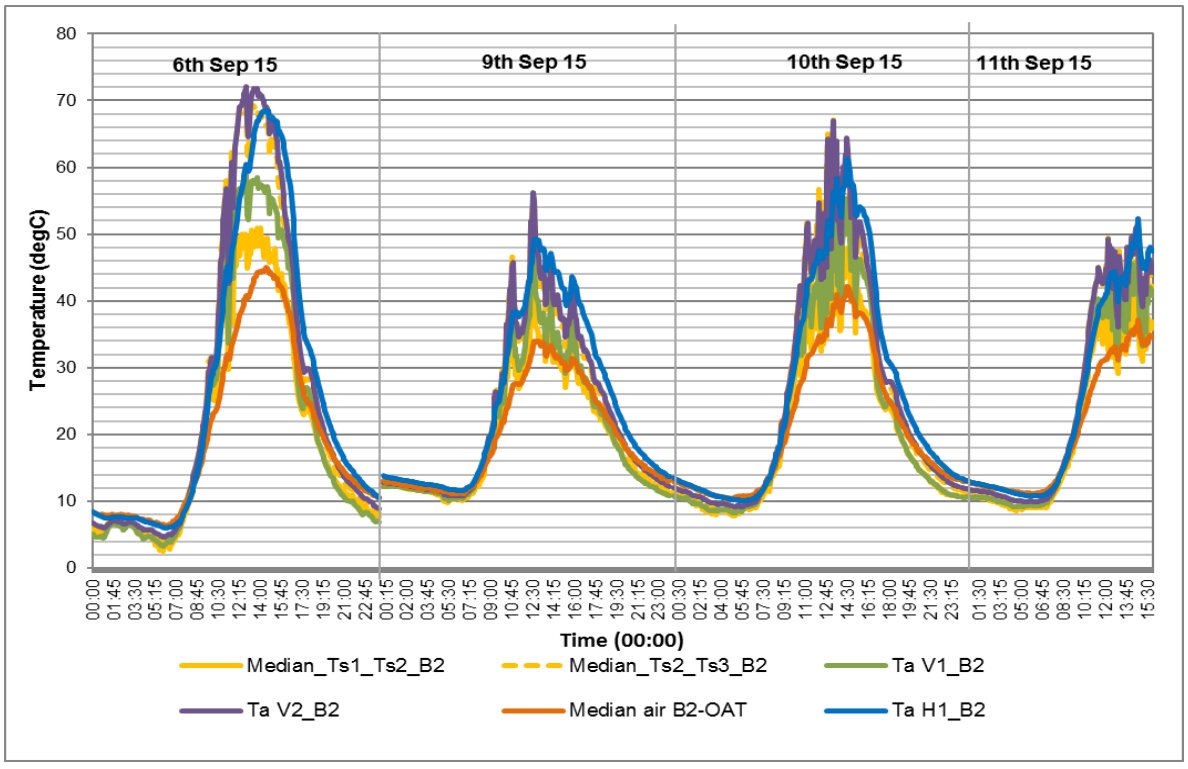
Chilton J., Pezeshkzadeh S., and **Afrin S**.,Effect of cushion geometry and configuration on the embodied energy of ETFE foil construction, VI International Conference on Textile Composites and Inflatable Structures, STRUCTURAL MEMBRANES, K.-U.Bletzinger, B. Kröplin and E. Oñate (Eds) 2013.

Chilton J., Pezeshkzadeh S.A. and **Afrin S**. Embodied energy in ETFE foil construction, [RE]THINKING lightweight structures Proc. TensiNet Symposium 2013, (Bögner-Balz H and Mollaert M (eds)). Istanbul, Turkey, (2013) 457-466.

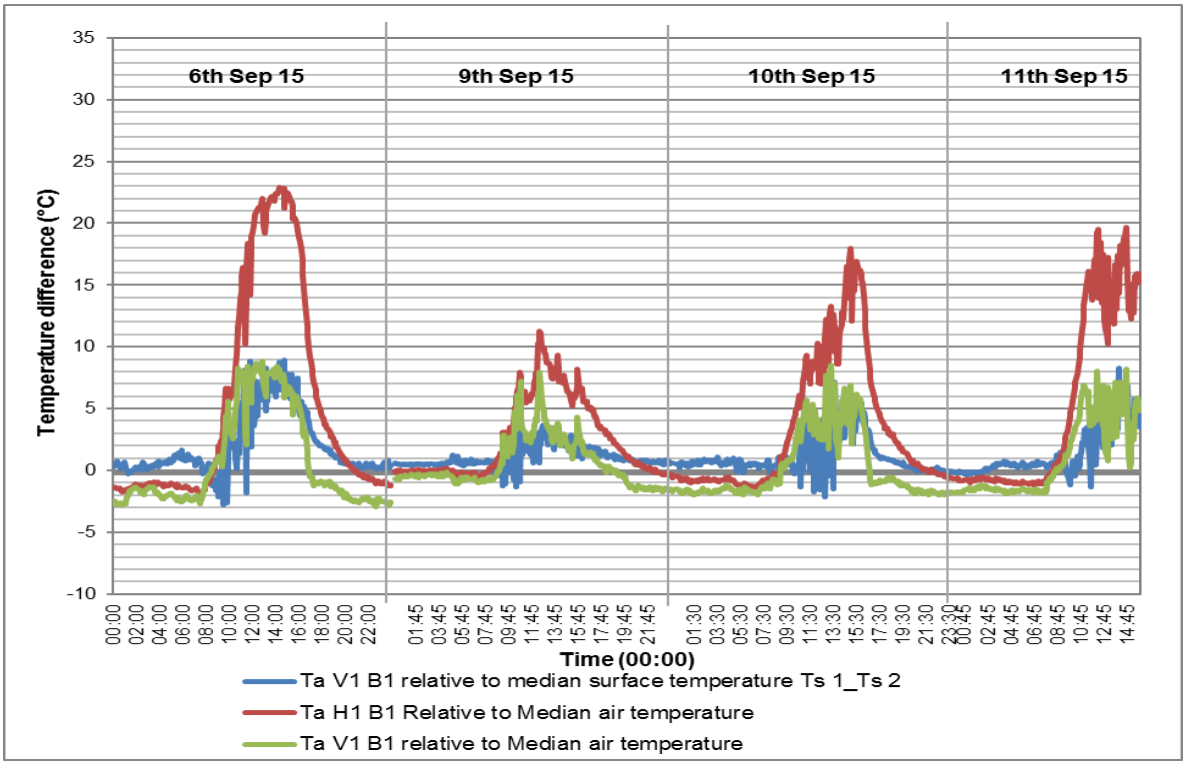
APPENDIX B: Figures and Tables



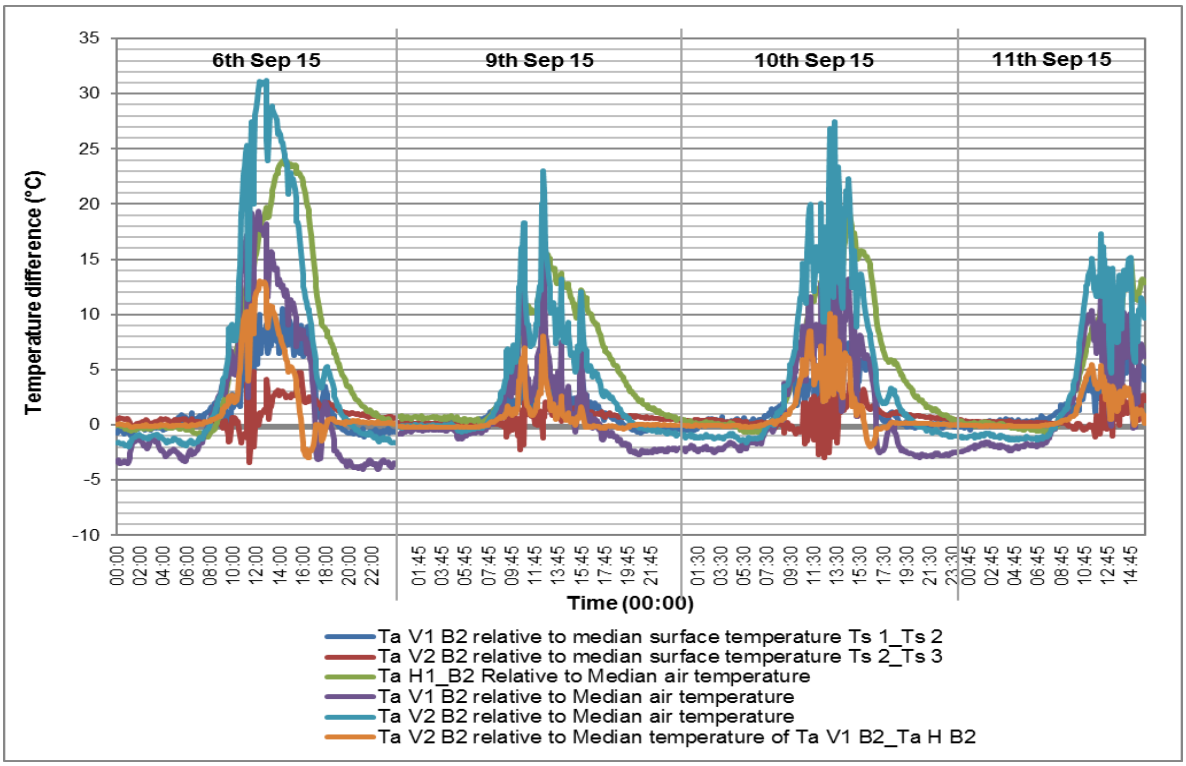
Median surface temperatures, temperature differences between median air temperatures of test rig 1 and OAT, air temperatures of test rig 1 and volume air temperatures



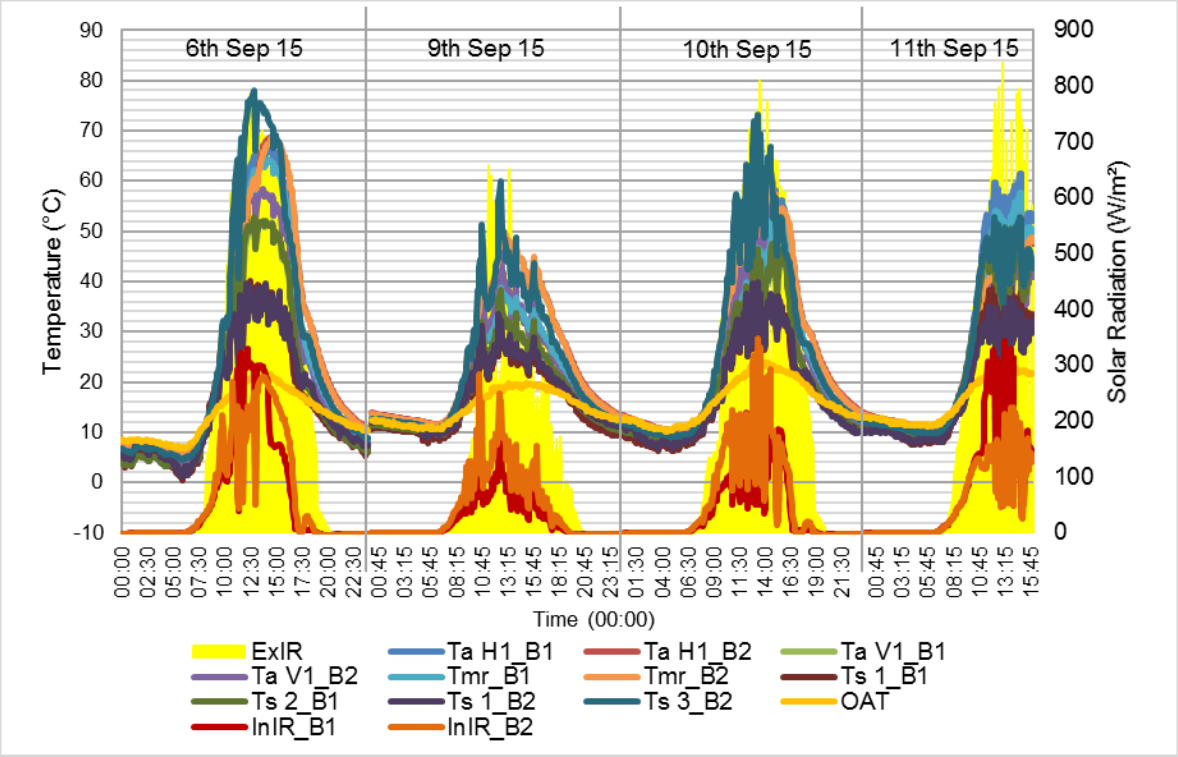
Median surface temperatures, temperature differences between median air temperatures of test rig 1 and OAT, air temperatures of test rig 2 and volume air temperatures



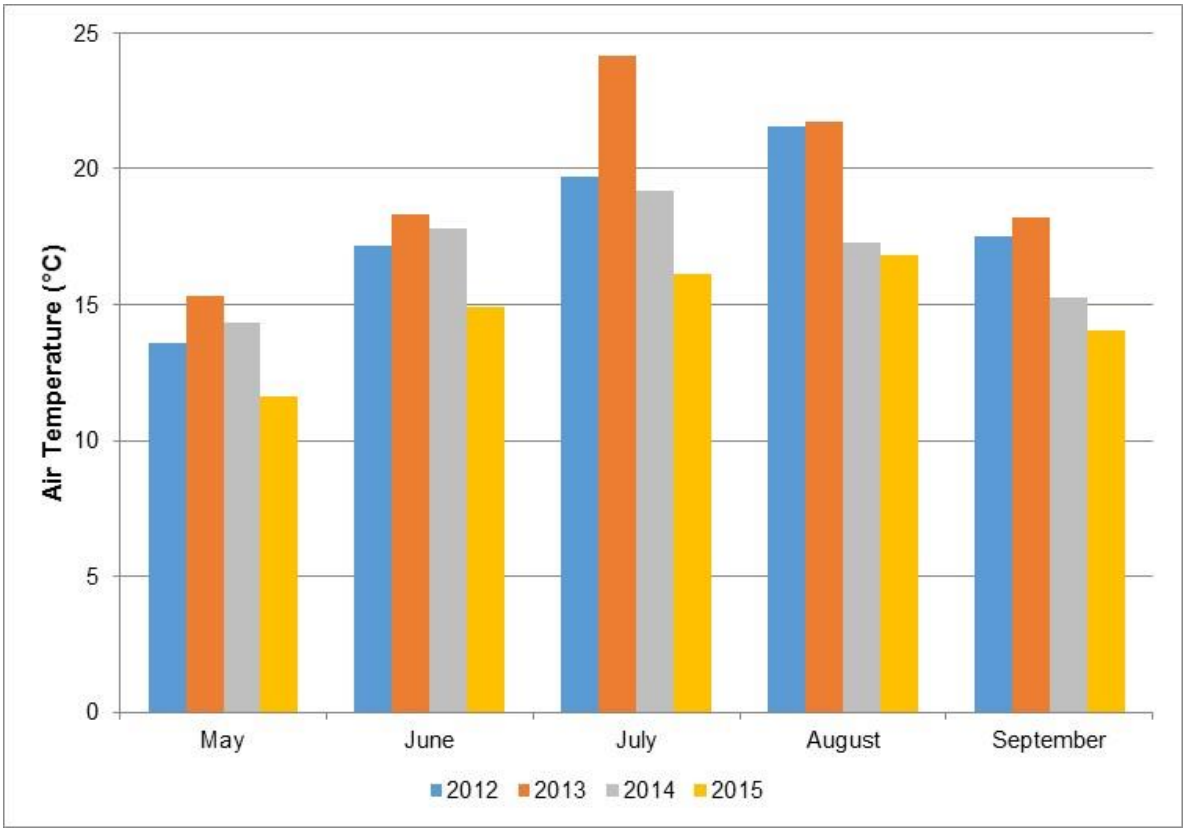
Air volume air temperature relative to surface median temperature, test rig 1 air temperature relative to median air temperature, air volume air temperature relative to median air temperature



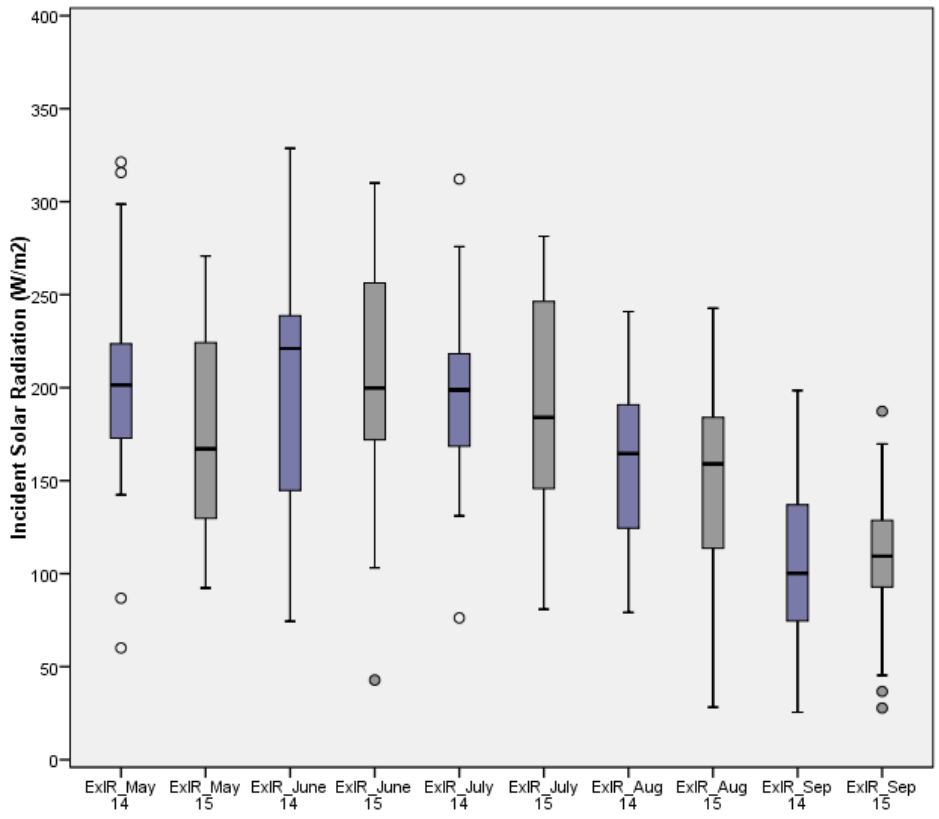
Air volume air temperature relative to surface median temperature, test rig 2 air temperature relative to median air temperature, air volume air temperature relative to median air temperature



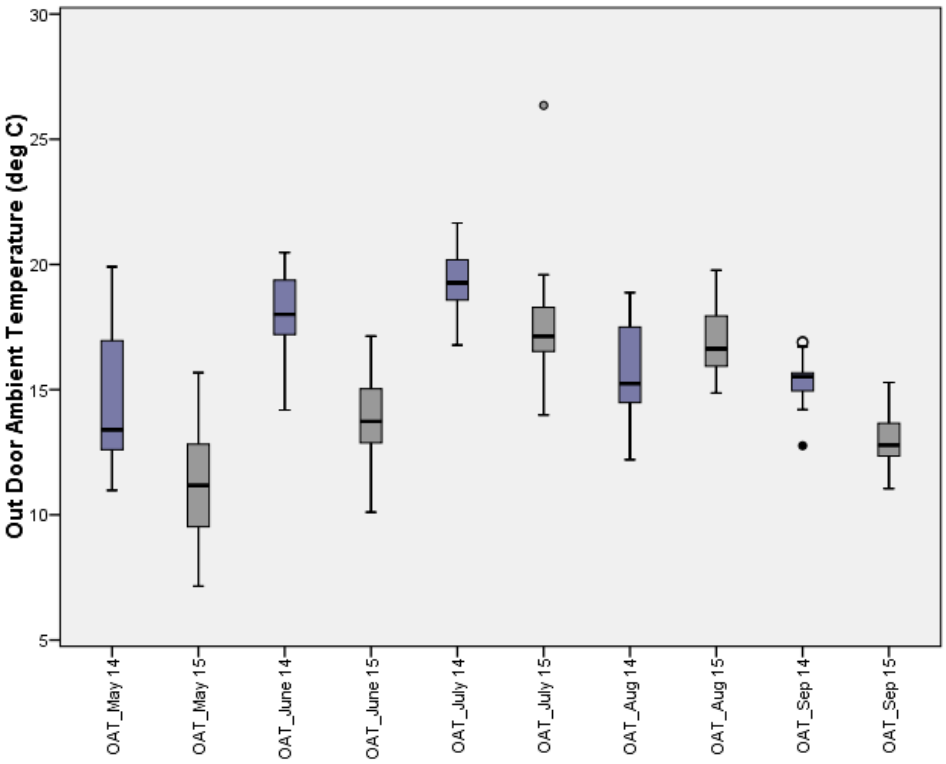
Air temperatures, mean radiant temperature, air volume air temperature, external and internal surface temperatures, incident and transmitted solar radiation recorded in test rig 1 and test rig 2



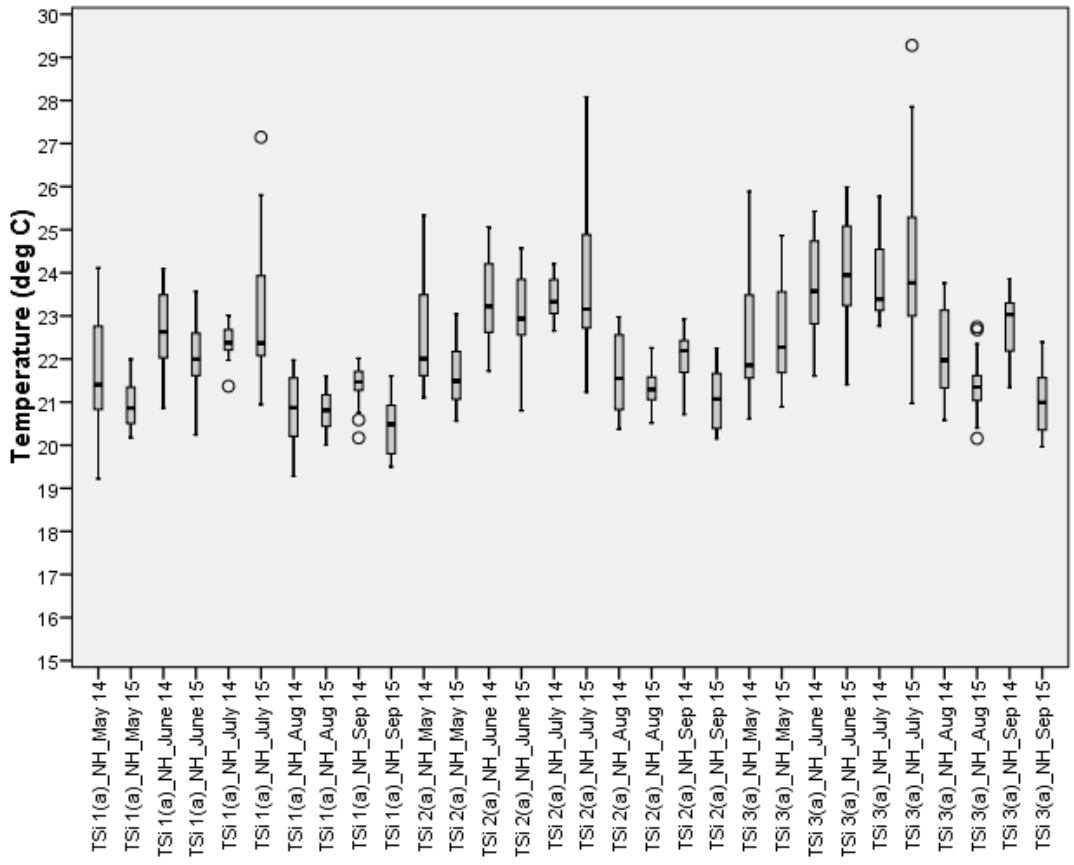
Comparison of outdoor ambient temperature in summer 2012, 2013, 2014 and 2015



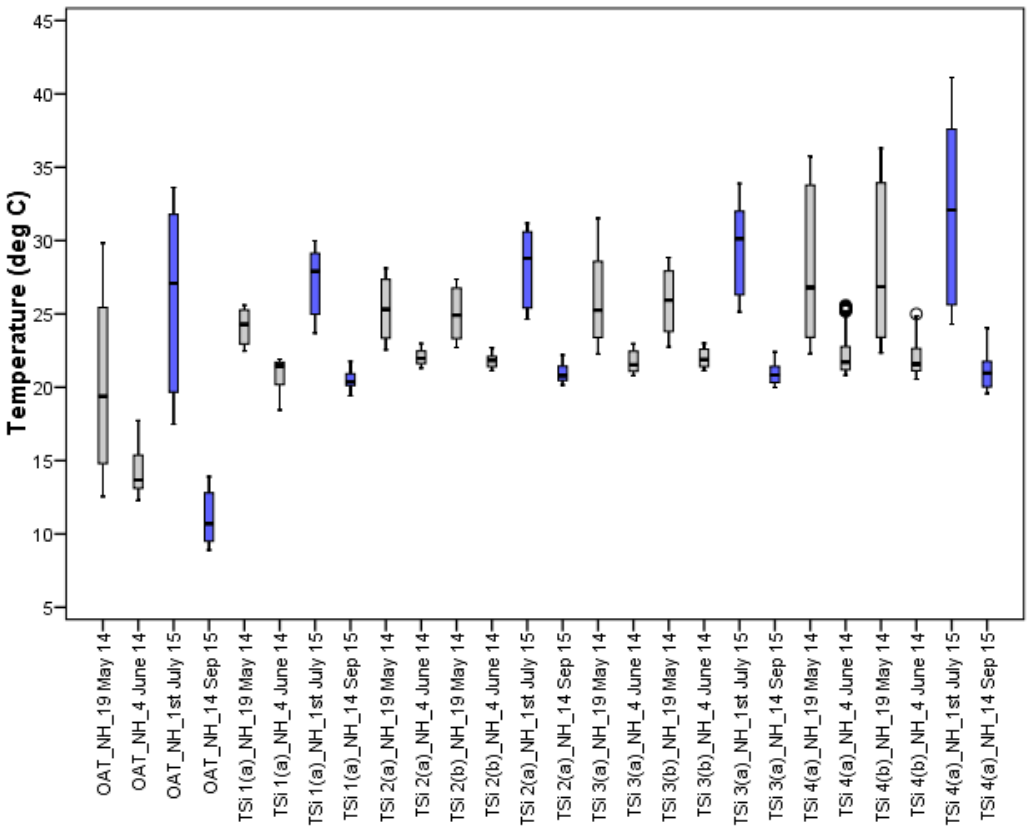
Comparison of ExIR during summer 2014 and 2015 (Incident solar radiation, outdoor ambient temperature)



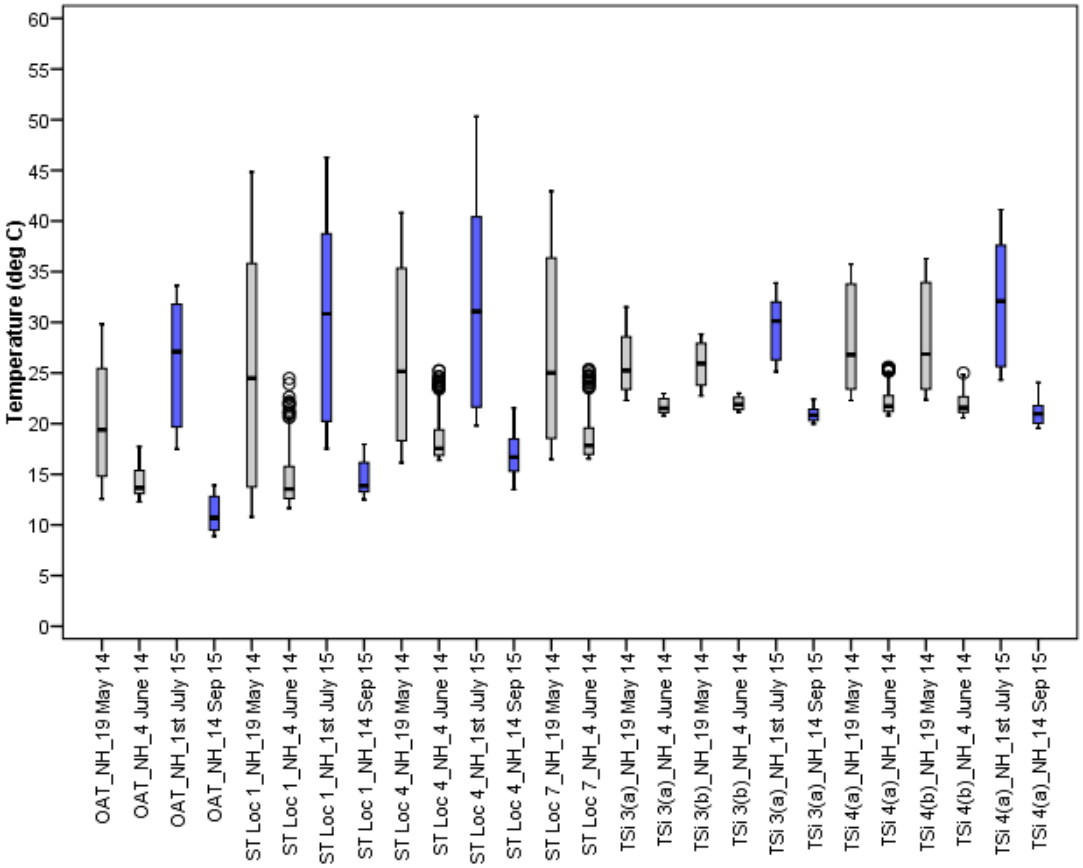
Comparison of OAT during summer 2014 and 2015 (Incident solar radiation, outdoor ambient temperature)



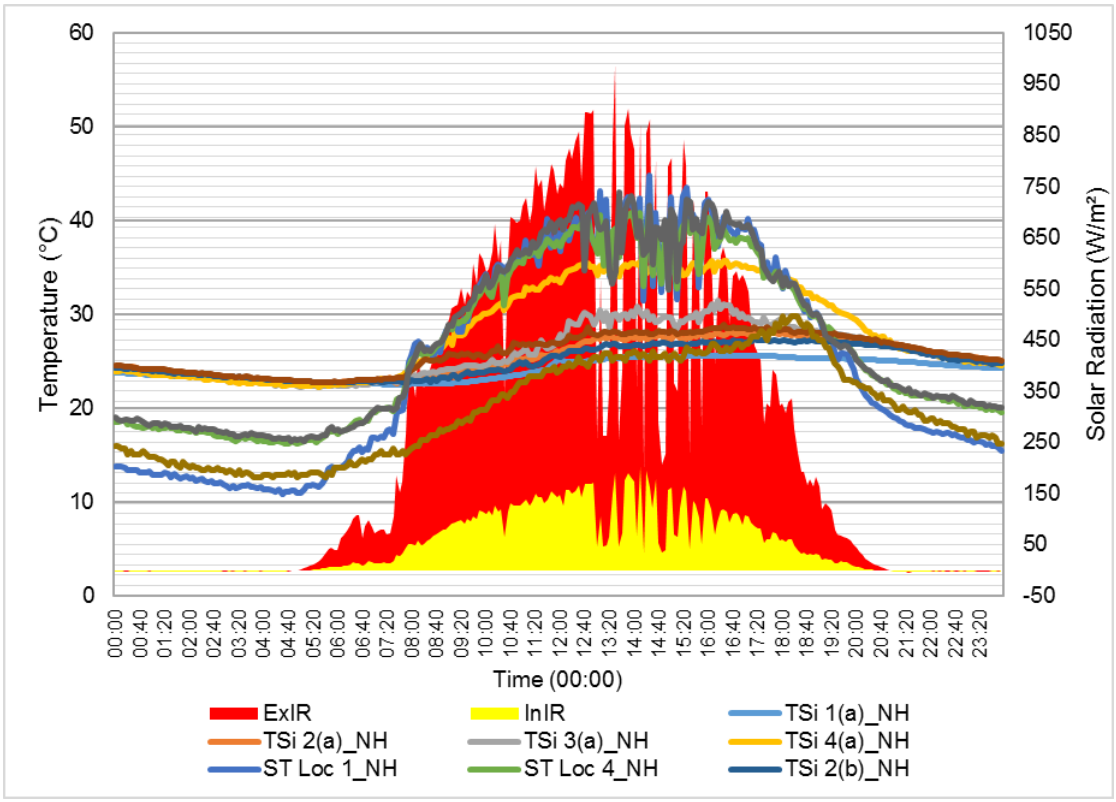
Recorded temperature ranges during occupied hours in all occupied level of the atrium



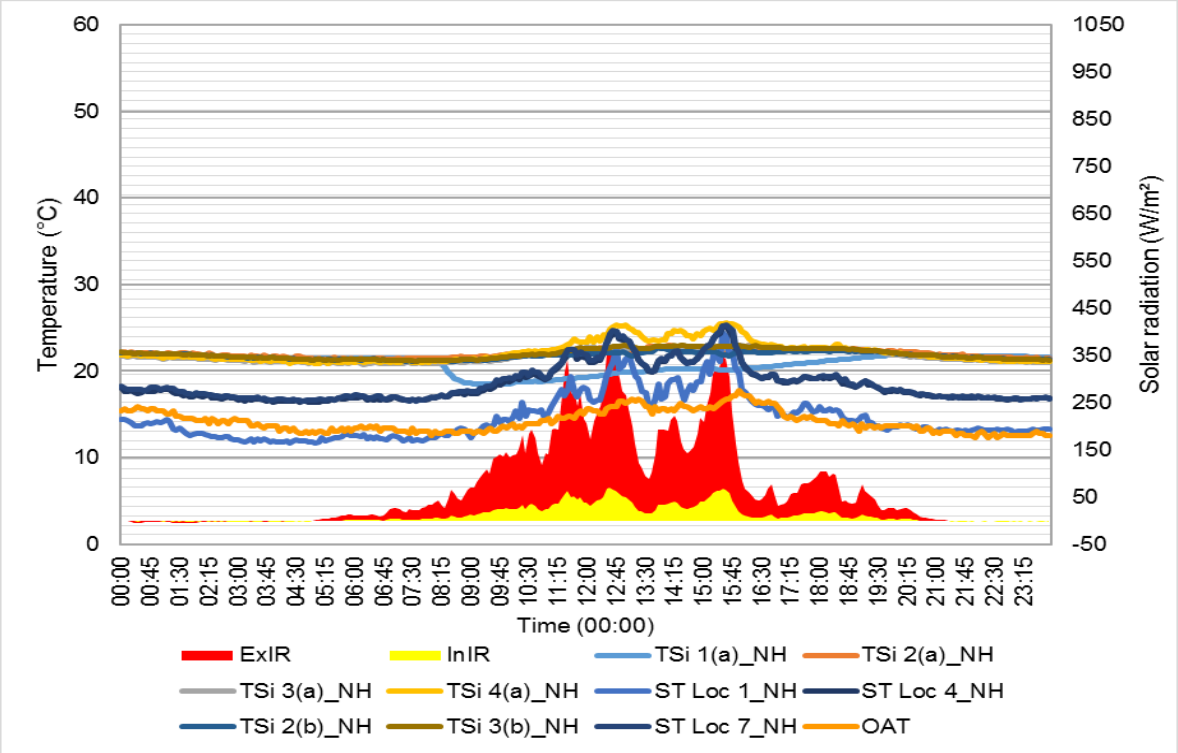
Air temperature range, median of air temperature of different occupied levels denoted by TSi 1(a)_NH, TSi 2(a)_NH, TSi 3(a)_NH and outdoor ambient temperature recorded during 19th May 14, 4th of June 14; 1st July 15 and 14th September 15



Air temperature range, median of air temperature of TSi 3(a)_NH, TSi 4(a)_NH; internal and external surface temperatures, and outdoor ambient temperatures recorded during 19th May 14, 4th of June 14; 1st July 15 and 14th September 15



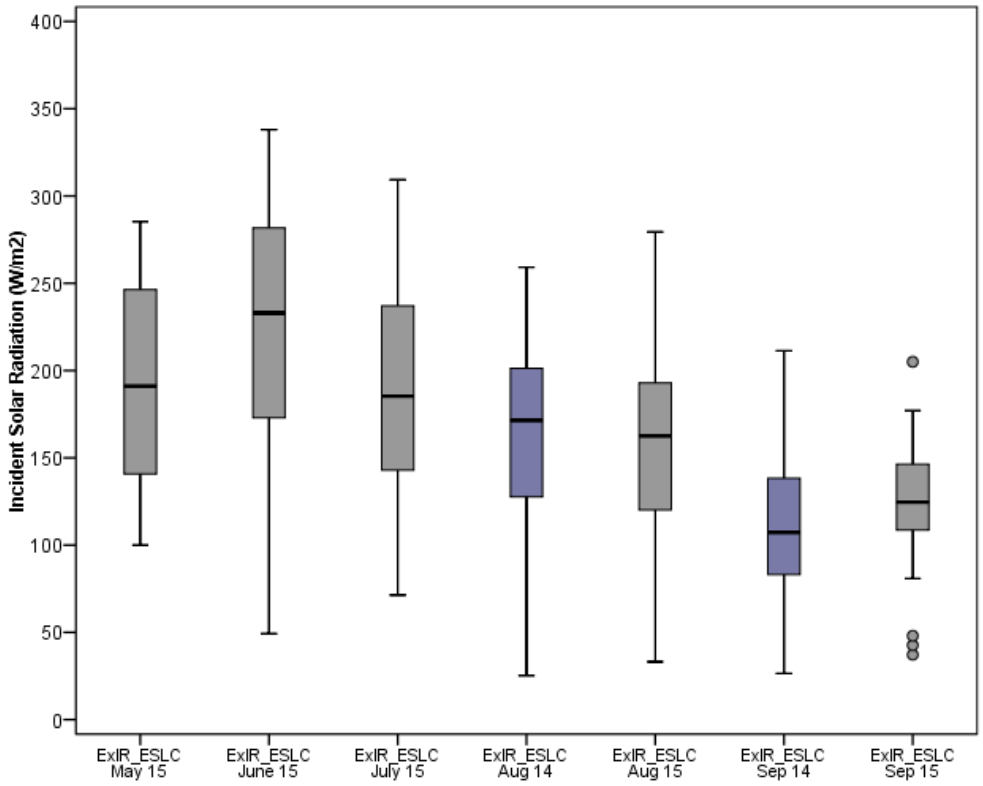
Recorded temperatures and solar radiation for Nottingham High School atrium during 19th May 2014



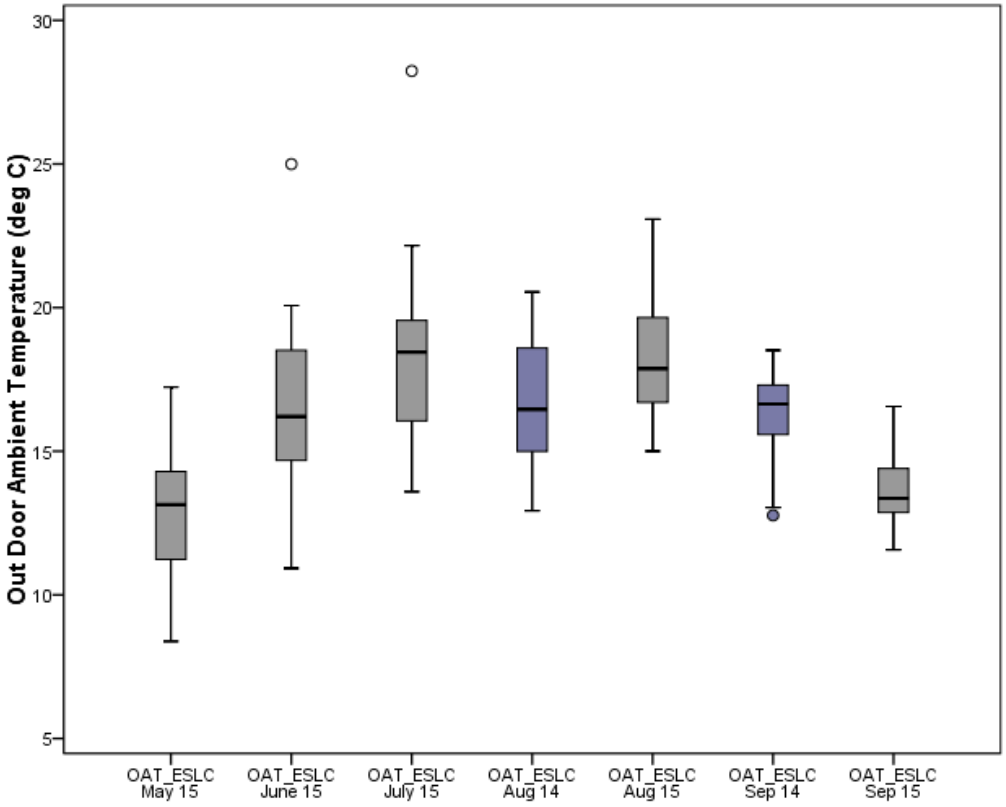
Recorded temperatures and solar radiation for Nottingham High School atrium during 4th June 2014

Mean Outdoor ambient temperature, mean incident solar radiation and relative humidity recorded in 19th May 14, 4th June 14, 30th June 15, 1st July 15, 2nd July 2015 and 14th Sep 15

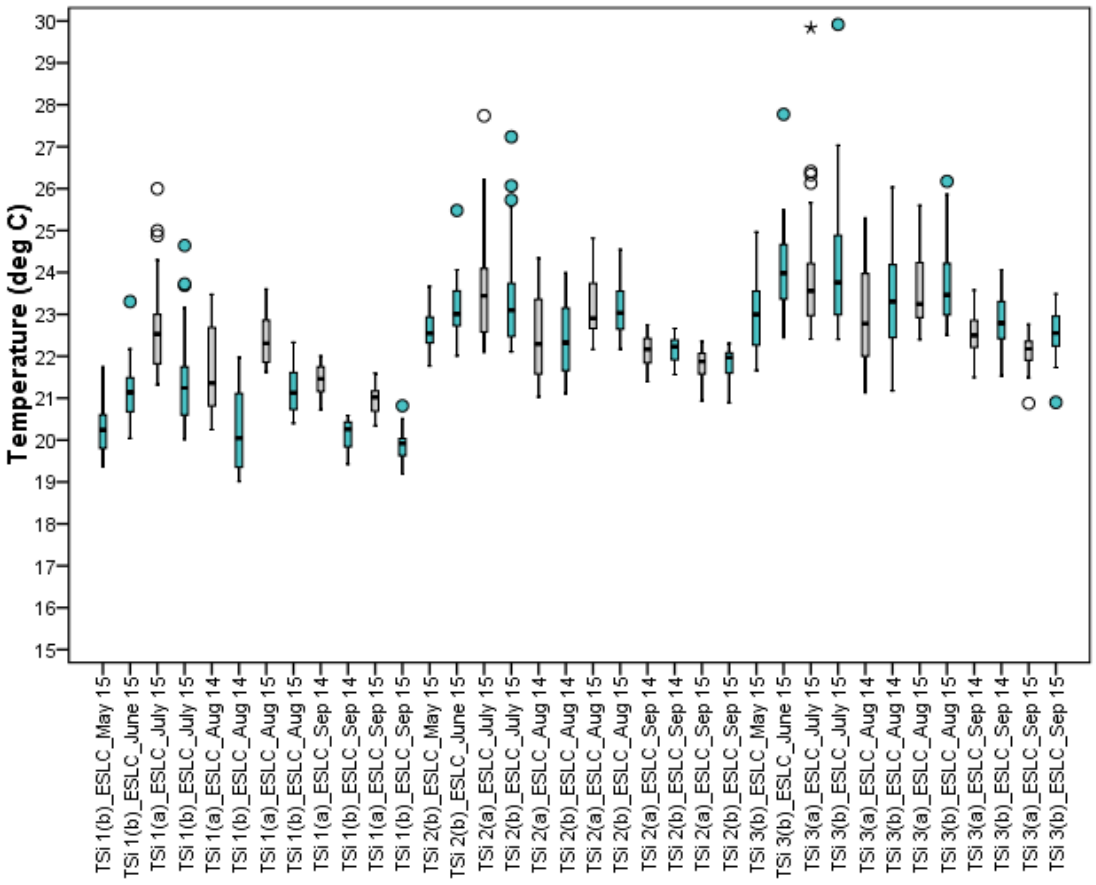
Time of the year	Day type	Mean OAT (24 hr)	S.D OAT	Mean OAT (8.00am-15.00pm)	S.D OAT (8.00am-15.00pm)	Mean ExIR (24 hr)	Mean ExIR (8.00am-15.00pm)	Mean RH (24hr)	Mean RH (8.00am-15.00pm)
		°C	°C	°C	°C	W/m²	W/m²	%	%
19th May 2014	Warm sunny	19.9	5.3	21.4	4.1	266.94	576.76	70.6	66.74
4th June 2014	Cold overcast	14.18	1.3	14.5	1.3	71.3	155.4	93	92.9
30th June 2015	Warm sunny with no cloud cover	22.33	4.8	24.4	2.88	313.4	647.94	12.5	4.7
1st July 2015	Warm sunny with presence of limited cloud cover	26.16	5.8	29.23	4	247.45	519.72	11.5	5.44
2nd July 2015	Cloudy sky with presence of solar radiation for limited period of time	19.5	3.3	20.63	2.11	145.76	322.44	75.6	70.2
14th September 2015	Cold overcast	11.05	1.53	10.56	1.33	36.67	85.4	94.3	99.4



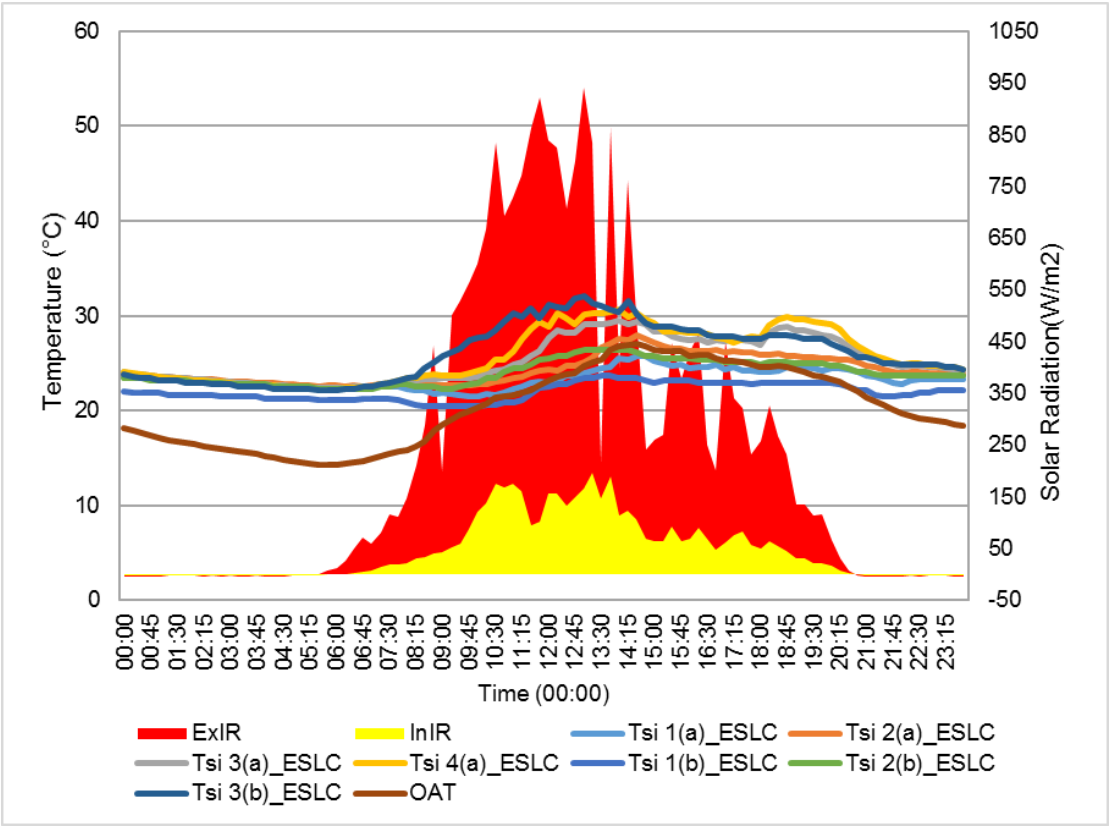
Recorded incident solar radiation in ESLC during summer 2014 and 2015



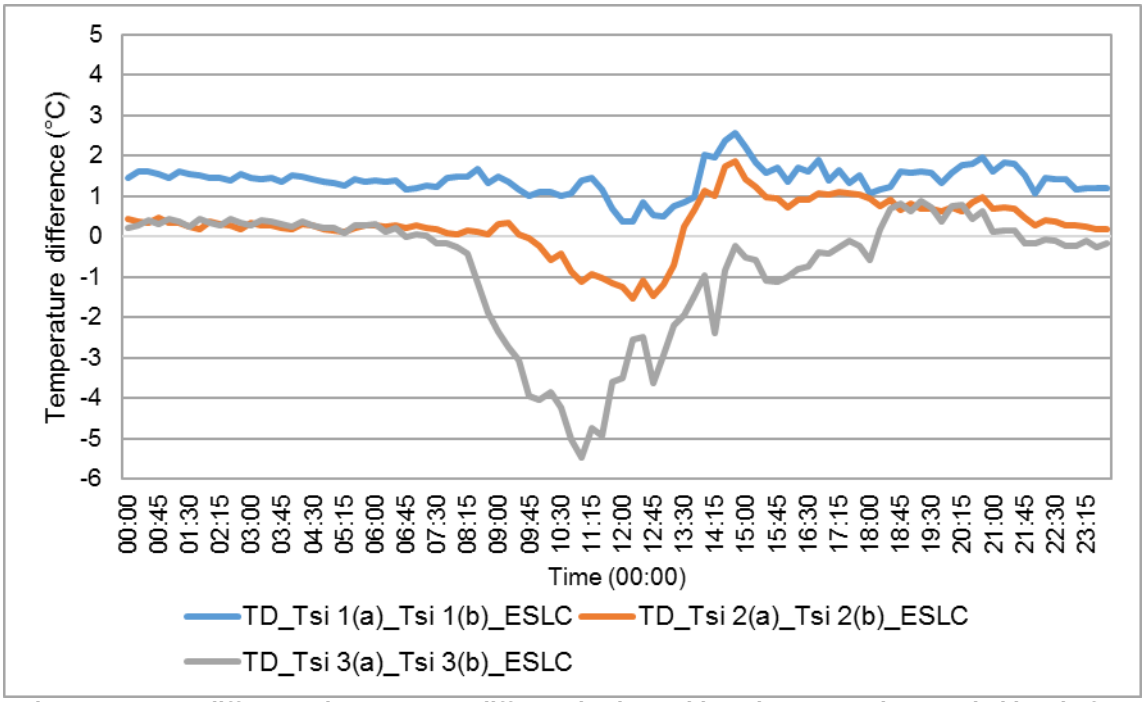
Recorded incident OAT in ESLC during summer 2014 and 2015



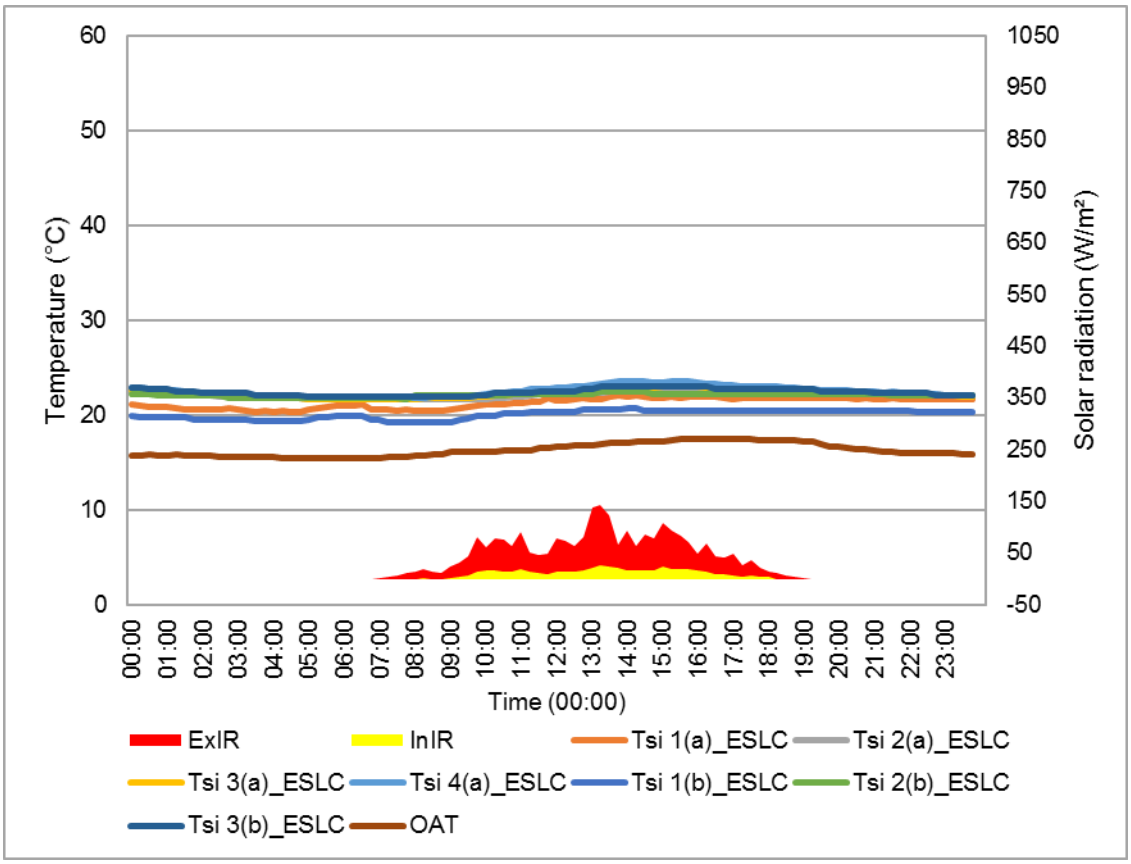
Recorded temperature ranges during occupied hour in all occupied level of the atrium for two different location of the atrium



Recorded temperatures and solar radiation for ESLC atrium during 7th August 2014



Air temperature difference between two different horizontal locations at each occupied level of the atrium 7th August 2014



Recorded temperatures and solar radiation for ESLC atrium during 19th September 2014